The Evolution of Morphological Diversity in Rodents: Patterns of Cranial Ontogeny

---

Dissertation
zur
Erlangung der naturwissenschaftlichen Doktorwürde
(Dr. sc. nat.)
vorgelegt der
Mathematisch-naturwissenschaftlichen Fakultät
der
Universität Zürich

von

Laura A. B. Wilson

aus

United Kingdom

Promotionskomitee
Prof. Dr. Marcelo R. Sánchez-Villagra
(Leiter und Vorsitz der Dissertation)
Prof. Dr. Winand Brinkmann
Prof. Dr. Hugo Bucher (Gutachter)
Dr. Anjali Goswami (Gutachterin)

Zürich, 2010


S H

Die vorliegende Arbeit wurde von der Mathematisch-naturwissenschaftlichen Fakultät der Universität Zürich im Herbst semester 2010 als Dissertation angenommen.
Promotionskomitee:
Prof. Dr. Marcelo R. Sánchez-Villagra (Leiter und Vorsitz der Dissertation)
Prof. Dr. Winand Brinkmann (Gutachter)
Prof. Dr. Hugo Bucher (Gutachter)
Dr. Anjali Goswami (Gutachterin)

This work was accepted as a dissertation by the Mathematics and Natural Sciences Faculty of the University of Zurich in the Autumn semester of 2010.
Members of the PhD-committee:
Prof. Dr. Marcelo Sánchez-Villagra (leader and head of the dissertation)
Prof. Dr. Winand Brinkmann (referee)
Prof. Dr. Hugo Bucher (referee)
Dr. Anjali Goswami (referee)

ISBN: 978-3-905923-06-3
2010 Scidinge Hall Verlag Zürich
www.scidinge-hall-verlag.de

CONTENT

CONTENT

LIST OF TABLES

LIST OF TABLES

ACKNOWLEDGEMENTS

A number of people have contributed to help make doing this PhD and my time in Zürich both rewarding and enjoyable. First, I am extremely grateful for the continual support, patience and encouragement of my advisor, Prof. Dr. Marcelo Sánchez-Villagra, from whom I have learnt a phenomenal amount. Through his unfailing interest and enthusiasm in my work, I have gained much confidence. I appreciate having had the opportunity to visit many museum collections, scientific conferences, and attend several courses during the last three years. These activities have greatly augmented my skill-set and would not have been possible without Marcelo's support.

I am thankful to have Dr. Anjali Goswami as a second supervisor; especially I thank her for enduring the many less-than-coherent explanations I offered regarding my research. I'm also grateful that she always took time to discuss many aspects of my work and provided insightful and constructive comments, and lots of helpful advice during her visits to Zürich. I am grateful to Prof. Dr. Hugo Bucher for stimulating, broadly-scoped discussions and constructive criticisms which helped to improve my scientific thinking.

Dr. Ingmar Werneburg is thanked for being a fantastic office-mate, and for all the science and non-science discussions and fun moments during the last three years. I was most fortunate to have someone who could relate to the hurdles that have presented themselves during the course of my research. For many thoughtful comments on my work, I thank the other members of the research group of Prof. Dr. Marcelo Sánchez-Villagra. Particularly, I am grateful to Dr. Christian Mitgutsch for teaching me clearing and staining methods, and for several useful discussions about Parsimov. I also appreciate all the constructive comments and advice that Dr. Torsten Scheyer provided during lab meetings.

For helping teach me to program, and many other statistical methods, I am thankful to Prof. John Alroy (Macquarie), Dr. Gene Hunt (Smithsonian), Dr. Mark Webster (Chicago), Prof. Pete Wagner (Smithsonian) and Prof. Tom Olszewski (Texas A&M), whose lessons during the Paleobiology Database (PBDB) summer course in Santa Barbara were both exceptional and inspiring. I thank Prof. Norm MacLeod (NHM) for introducing me to geometric morphometrics, and for thought-provoking discussions on various methodological issues during my time in London. For lots of useful advice on eigenshape and tips on coding I thank Dr. Jonathan Krieger (NHM).

For encouraging comments and useful advice at various stages in the past three years, I thank Dr. Janine Ziermann (Leiden), Dr. Vera Weisbecker (Cambridge), Prof. Dr. Lennart Olsson (Jena), Dr. Rob Asher (Cambridge), Dr. Lionel Hautier (Cambridge), Dr. Graeme Smith (Villanova), Dr. Sandrine Ledèveze (Brussels), Prof. Gabriel Marroig (São Paulo), Prof. Dr. Andrea Mess (Berlin) and Dr.

ACKNOWLEDGEMENTS

Renaud Lebrun (Montpellier). Additionally, I thank Daisuke Koyabu (Tokyo) for many enthusiastic discussions on morphology and heterochrony. Karen Bacon (Dublin), Michelle Lawing (Indiana), Emily Lindsey (Berkley), Daniel Thomas (Otago) and Liz Freedman (Montana) are also thanked for various lengthy debates on mathematics and Ph.D. life. I am especially thankful to Dr. Louise Humphrey (NHM) for thoughtful advice which has helped immensely in London and Zürich, and for generally being like a 'mother' to me in the past few years.

I thank all the curators in the many museums I have visited across Europe and S. America for all their help with access to the collections in their charge. Particularly, I wish to thank Dr. Loic Costeur (Basel) and Dr. Marianne Haffner (Zürich) for always granting me access to materials and especially at short notice. For their personal thought, I thank Dr. Morgens Anderson (Copenhagen) for the loan of a bicycle, and Dr. Olavi Grönwall (Stockholm) for inviting me to play badminton. My stay in South America was most productive and enjoyable thanks to Dr. Fredy Carlini (La Plata), who I thank for letting me stay at his place and for all his help with logistical issues and access to materials. I'm also grateful to Fernando Galliari and Dr. Diego Verzi for their help in La Plata, Dr. Andrea Elissamburu and Dr. Alejandro Donda for kindly making me feel welcome at Mar del Plata, and Javier Echevarria for fun memories in La Plata. I also wish to thank Dr. Carsten Schradin (Zürich) and Dr. Hugo Cardoso (Lisbon) for fruitful and supportive collaborations. For always helping in a friendly manner with many financial aspects of my trips abroad, I thank Heike Götzmann (Zürich).

For contributing to making living in Zürich a great experience I thank all members of the Paläontologisches Institut und Museum, who made me feel welcome from the very beginning. I especially wish to mention Jasi Hugi, Kenneth De Baets, Jérôme Gapany, Carlo Romano, Lui Unterrassner, Nico Goudemand, Dr. Severine Urdy, James Neenan, Dr. Christian Klug and David Ware for many fun times. I'm also equally grateful to know Nalini Puliamoorthy, Dr. Massimo Delfino (Florence), Dr. David Berger, Dr. Richard Walters, Ralf Jochmann, Oscar Ramos, Barbara Beck-Wörner, Anna Beck-Wörner, Dr. Erik Postma, Adrian Iten and Olivier Soligo. I am especially thankful to Andrea Spring for many kind thoughts, and for helping with German practice, and to Morana Mihaljević for being a truly great friend. Life outside of work has been most enjoyable thanks to Hauke Koch - I thank him for countless happy times in these last few years.

I thank the Forschungskredit committee (Universität Zürich) for granting me money to support the last two years of my Ph.D. studies. I am also appreciative of travel grants from SYNTHESYS (NHM London), Auslandskurz Mentorate (Universität Zürich), and the VAUZ Tagungsfond (Uni-

ACKNOWLEDGEMENTS

versität Zürich) which have provided monies that have enabled me to visit the museum collections necessary for the acquisition of data included in this dissertation.

Above all, I am indebted to my parents, Enid and Peter, and my brother, Jonathan, for their patience, perseverance, and support throughout my education.

SUMMARY

The role of ontogeny in the generation of adult morphological diversity is poorly understood. The aims of this study are to investigate the developmental bases for the extraordinary level of anatomical and ecological diversity and differing life strategy displayed by hystricognath rodents (e.g. guinea pigs, porcupines, capybaras) compared with muroids (mice and rats). The complementary methodological frameworks of heterochrony and allometry are used as a base to explore patterns of cranial growth at different points in developmental time. Developmental series of 58 rodent species were examined for this work, including prenatal and postnatal specimens.

In one part of this thesis I examine the importance of sequence heterochrony in morphological evolution. Two time windows are investigated: the onset of skeletal formation, beginning prenatally, and the point of suture closure, occurring during the latter part of postnatal growth. Sequence heterochrony was analysed using the Parsimov method. In the first comprehensive assay of heterochronies in cranial suture growth for a mammalian clade, we find that numerous heterochonies in suture closure have occurred in the evolutionary history of hystricognaths. Sutures are of particular interest because they serve as major sites of bone expansion during postnatal craniofacial growth in the vertebrate skull, and we show that their sequence of closure represents an aspect of ontogeny with functional and phylogenetic correlates. In complement, we present the most comprehensive sampling of rodent ossification sequences to date, including data for non-model organisms and several representatives from both muroid and hystricognath clades. This study contributes considerably to improving the amount of data that presently exist on skeletal development across mammalian clades. We find, in contrast to the results for suture closure patterns, that heterochrony is not a common mode of evolutionary change during skeletal formation. We additionally present data on intraspecific variation in cranial, postcranial, and autopodial ossification sequences for *Rhabdomys pumilio*, to further expand the extremely limited literature regarding this topic.

It has been hypothesized that most morphological evolution occurs by allometric differentiation. Hence the second part of this thesis focuses upon the evolution and patterning of ontogenetic allometry in rodents. The evolution of postnatal growth trajectories is examined across major clades; prenatal skull growth is comprehensively recorded morphometrically for the first time for the muroid rodent, *R. pumilio*. Studies directed towards examining the evolution of allometry are few and of small scope. We investigated the influence of phylogenetic relations and ecological factors on the results of the first quantification of allometric disparity among rodents by exploring allometric space, a multivariate morphospace that, in this study, was derived from the ontogenetic trajectories of 17 muroids and 17 hystricognaths. Disparity was quantified using angles between ontogenetic trajectories. We found an overlapping occupation of allometric space for muroids and hystricognaths, indi-

SUMMARY

cating similar abilities to evolve in different directions of phenotypic space. We show changes to covariance structure were common during rodent evolution and anatomic diversity was not found to constrain the labile nature of allometric patterning. Grouping of taxa in allometric space was found to be related to dietary habit; rodents sharing morphological features considered to be associated with the processing of particular dietary materials were found to group most closely with one another, showing the evolution of allometry in rodents has an adaptive basis. Whilst postnatal ontogenetic allometry has been documented for many species, there are very few studies that compare the dynamics of prenatal and postnatal growth. From this standpoint, trends regarding the linearity of prenatal allometry and its association to postnatal growth patterns are relatively unknown. Using a reflex microscope to measure cleared and stained specimens of *R. pumilio*, I performed the first study of prenatal ontogenetic allometry in a rodent, providing a crucial base for future comparative studies. Bivariate and multivariate estimates of allometry were coupled with matrix comparison methods to assess growth trends. The results indicate that prenatal growth is characterized by rapid lengthening of cranial elements. Ontogenetic allometric trends are found to shift between the prenatal and postnatal period, and localized variation in growth relationships occurs among cranial elements.

KEYWORDS: ontogeny, rodent, cranium, heterochrony, allometry, disparity, phenotypic covariance structure, prenatal allometry, suture, skeletogenesis

ZUSAMMENFASSUNG

Die Bedeutung der Ontogenese für die Ausbildung erwachsen morphologischer Diversität ist bisher kaum verstanden. Im Vergleich zu den Muroiden (Mäuse und Ratten) zeigen die hystricognathen Nagetiere (z. B. Meerschweinchen, Stachelschweine, Wasserschweine) einen außergewöhnlichen Grad anatomischer und ökologischer Diversität als auch unterschiedliche Überlebensstrategien. Um die mögliche entwicklungsbiologische Grundlage hierfür zu verstehen, wurde das craniale Wachstum zu verschiedenen Zeitpunkten der Individualentwicklung untersucht. Dazu nutzte die vorliegende Arbeit die sich gegenseitig ergänzenden methodischen Ansätze der Heterochronie und der Allometrie. Prä- und postnatale Individuen einbeziehend, wurden Entwicklungsreihen von 58 Nagetierarten für diese Studien untersucht.

Ein Teil der Arbeit untersucht die Bedeutung der Sequenzheterochronie in der morphologischen Evolution. Zwei Zeitfenster wurden betrachtet: Der pränatal einsetzende Beginn der skeletalen Ossifizierung, sowie die Zeitpunkt des Suturenverschlusses, der in der späten Phase des postnatalen Wachstums auftritt. Sequenzheterochronie wurde mit den Parsimov-Methoden untersucht. In dieser ersten umfassenden Studie zu zeitlichen Verschiebungen cranialen Suturenwachstums in einer Säugetiergruppe konnten wir eine hohe Anzahl von Heterochronien in der Evolution der hystricognathen Nagetiere feststellen. Suturen sind von besonderem Interesse, da sie die Hauptbereiche der Knochenausbreitung darstellen, die während des postnatalen Wachstums im craniofacialen Bereich des Wirbeltierschädels festzustellen ist. Wir konnten zeigen, daß die Sequenz des Suturenverschlusses einen Aspekt der Schädelentwicklung darstellt, der funktionelle und phylogenetische Entsprechungen hat. Zudem legen wir die bisher umfangreichste Sammlung von Ossifikationssequenzen der Nagetiere vor. Dabei sind Daten zu Tieren, die nicht als Modellorganismen gelten, als auch Daten zu weiteren Vertretern der Muroidae und Hystricognathi enthalten. Diese Studie trägt beträchtlich dazu bei, den relativen Mangel an Daten zu verringern, der gegenwärtig zur skeletalen Entwicklung der Säugetiergruppen vorzufinden ist. Im Gegensatz zu den Resultaten des Suturenverschlusses, haben wir feststellt, daß Heterochronie kein allgemeingültiger Mechanismus des evolutionären Wandels während der skeletalen Verknöcherung darstellt. Für ein nicht als Modellorganismus genutztes Tier, *Rhabdomys pumilio,* stellen wir zusätzlich eine Studie zur intraspezifischen Variation in der Sequenz der Schädel-, Körper- und Gliedmaßenverknöcherung vor, um die extrem begrenzte Literatur zu diesem Thema zu erweitern.

Es wurde vorgeschlagen, daß ein Großteil der morphologischen Evolution durch allometrische Differenzierung stattfindet. Der zweite Teil der vorliegenden Arbeit befaßt sich daher mit der Evolution und der Musterbildung ontogenetischer Allometrie bei den Nagetieren. Zum einen wurde die Evolution postnataler Wachstumsrichtungen untersucht, während zum anderen craniale

Wachstum für *Rhabdomys pumilio* umfassend aufgezeichnet wurde. Studien, die sich auf die Erforschung der Evolution von Allometrie zubewegen, sind rar und von geringem Umfang. Wir untersuchten den Einfluß phylogentischer Beziehungen und ökologischer Faktoren auf die – hier zum ersten Mal quantifizierten – allometrischen Unterschiede bei Nagetieren. Dazu definierten wir einen allometrischen Raum, ein multivariabler, morphologischer Raum, der in dieser Studie aus den Entwicklungsrichtungen von je 17 Muroidae und Hystricognathi abgeleitet wurde.

Die Unterschiede wurden mit Hilfe von Winkeln zwischen den Entwicklungsrichtungen quantifiziert. Wir fanden einen sich überlappenden allometrischen Raum der Muroidae und Hystricognathi, was darauf hindeutet, daß beide Gruppen ähnliche Möglichkeiten besitzen, in unterschiedliche phänotypische Räume zu evolvieren. Wir zeigen auf, daß Veränderungen zu Kovarianzstrukturen in der Evolution der Rodentia gleichartig verliefen, und daß anatomische Vielfältigkeit nicht die labile Natur allometrischer Musterbildung beschränkt. Die Gruppierung von Taxa im allometrischen Raum konnte mit dem Freßverhalten in Verbindung gesetzt werden; Nagetiere mit gemeinsamen morphologischen Merkmale, die mit der Verarbeitung bestimmter Nahrungsbestandteile assoziiert werden, gruppieren sich am nächsten zusammen im allometrischen Raum.

Während postnatale Allometrie für viele Arten dokumentiert worden ist, wurden nur sehr wenige Studien vorgestellt, die die Dynamik prä- und postnatalen Wachstums miteinander vergleichen. Von diesem Standpunkt aus sind die Trends, die die Linearität pränataler Allometrie und ihrer Verbindung zu Mustern postnatalen Wachstums betreffen, relativ unbekannt. Mit Hilfe eines Reflex-Mikroskops habe ich die erste Studie zur pränatalen ontogenetischen Allometrie eines Nagetieres durchgeführt, das nicht als Modell-Organismus gilt. Dazu wurden die Knochen aufgehellter Embryonen von *Rhabdomys pumilio* gemessen. Mit dieser Untersuchung ist eine wichtige Basis für zukünftige vergleichende Studien gelegt. Bi- und multivariate Allometrie-Bewertungen wurden mit Methoden von Matrix-Vergleichen gekoppelt, um Wachstumstrends festzustellen. Die Resultate weisen darauf hin, daß pränatales Wachstum durch eine rasante Verlängerung cranialer Elemente charakterisiert ist. Es wurde festgestellt, daß die Trends ontogentischer Allometrie zwischen prä- und postnataler Periode verschoben sind und daß lokale Variationen in den Wachstumbeziehungen zwischen den cranialen Elementen auftreten.

AUTHOR CONTRIBUTIONS

All the chapters and appendices included in this thesis are either published, accepted for publication, or under review at the time of submission.

CHAPTER 1

Authors: Wilson LAB, Sánchez-Villagra MR

Publication: 2009, *Journal of Anatomy*, 214: 339-354

Contributions: designed research (LABW, MRS-V), data analysis and collection (LABW), wrote paper (LABW)

CHAPTER 2

Authors: Wilson LAB, Sánchez-Villagra MR

Publication: 2010, *Proceedings of the Royal Society B Biological Sciences*, 277: 1227-1234

Contributions: designed research (LABW, MRS-V), data analysis and collection (LABW), wrote paper (LABW)

CHAPTER 3

Authors: Wilson LAB, Schradin C, Mitgutsch C, Galliari FC, Mess A, Sánchez-Villagra MR

Publication: 2010, *Organisms, Diversity and Evolution*, 10: 243-258

Contributions: designed research (LABW, MRS-V), data collection (LABW, FCG), data analysis (LABW, CM), contributed materials (CS, AM), photographed collection material (CM), wrote paper (LABW)

CHAPTER 4

Authors: Wilson LAB

Submitted to: *Journal of Mammalogy*

Contributions: designed research, data analysis and collection, wrote paper (LABW)

AUTHOR CONTRIBUTIONS

APPENDIX I

Authors: Wilson LAB, Sánchez-Villagra MR

Publication: *Journal of Experimental Zoology Part B* in press

Contributions: designed research (MRS-V, LABW), data collection (MRS-V, LABW), data analysis (LABW), wrote paper (LABW)

APPENDIX II

Authors: Wilson LAB, Cardoso HFV, Humphrey LT

Publication: 2010, *Forensic Science International* in press

Contributions: designed research (LABW), data collection (LABW, HFVC, LTH), data analysis (LABW), wrote paper (LABW), comments to manuscript and provision of historical information (HFVC, LTH)

CO-AUTHOR AFFILIATIONS (outside Paläontologisches Institut)

Cardoso Hugo FV (Appendix II)

Departamento de Zoologia e Antropologia, Museu Nacional de História Natural & Centro de Biologia Ambiental, Universidade de Lisboa, Lisbon, Portugal

Galliari Fernando C (Chapter 4)

Departmento Cíentifico de Paleontología de Vertebrados, Facultad de Ciencias Naturales y Museo, Universidad Naciaonal de la Plata, La Plata, Argentina

Humphrey Louise T (Appendix II)

Department of Palaeontology, Natural History Museum, London, United Kingdom

Mess Andrea (Chapter 4)

Museum für Naturkunde Leibniz-Institüt für Evolutions - und Biodiversitätsforschung and der Humboldt-Universität zu Berlin, Berlin, Germany

Schradin Carsten (Chapter 4)

Zoological Institute, Department of Animal Behaviour, University of Zürich, Zürich, Switzerland / School of Animal, Plant and Environmental Sciences, University of the Witwatersrand, Wits, South Africa

CHAPTER 1

Introduction

Evolution and Development - a connection

Largely inspired by the work of Darwin (1859) and of Ernst Haeckel (1866), who created the terms 'heterochrony' and 'heterotopy' to account for the temporal and spatial exceptions that interfered with his theory of recapitulation, scientific thought has been generally propelled towards connecting evolution and development. Resting upon the notion that adult morphology represents the endpoint of development along an ontogenetic trajectory, evolutionary developmental biology is concerned most fundamentally with the idea that ontogenies evolve, and through these changes adult morphological diversity is generated. Spearheaded most famously by de Beer (1930, 1958), who first created a general, broad definition of heterochrony as a change in developmental timing of an organ in a descendant compared to the same organ in an ancestor, and later by Gould (1977), who proposed that heterochrony plays a fundamental mechanistic role in the evolution of changes in morphological form, the study of heterochrony has been cited to be one of the most persistent themes in evolutionary developmental biology (Raff 1996).

A revival in the idea of connecting evolution and development has, in the latter portion of the 20th Century, been sparked in the Anglo-Saxon literature most markedly by Gould (1977) who, through the pages of his book *Ontogeny and Phylogeny*, synthesized and assessed many ideas that instigated attention from a wide audience of evolutionary biologists. Gould (1977) recognised the adaptive value of life history parameters as causal agents in generating morphological variability, and thus in part built upon Haeckel's (1866) theory of recapitulation, which was bound in an adaptational framework. Most significantly, Gould (1977) created a measurable, clock model and with this he proposed that heterochrony represented a dissociation between ontogenetic events, such that differences between an ancestor and descendant could be explained as the result of perturbations in any, or all, of three variables: size (growth), shape (development) and age (Fig. 1.1). Besides recognising the mosaic nature of evolution, one key feature of this model was the separation of heterochrony as a process compared with heterochrony as a result (Cubo et al. 2000; Richardson et al. 2009). This distinction represents an important thought for the multitude of multi-disciplinary approaches to investigating ontogeny, often including the fields of palaeontology, biology and ecology. It is necessary to remember that heterochronies may be present at any window of developmental time, and since ontogeny progresses temporally, processes other than heterochrony that also act along the timeline of ontogeny are also present, thus heterochronic processes may not produce

heterochronic results and heterochronic results may occur as a consequence of nonheterochronic processes. Bearing importantly upon this matter are both the level of study and in turn the level of causal explanation sought, which in each case differ among fields of inquiry. For instance, for a palaeontologist the opportunity to study heterochrony may only be possible through the examination of a pattern that remains from the remnants of an incomplete record (see Sánchez-Villagra 2010). Gould's treatment acted as a base for a later formalization by Alberch et al. (1979) which further addressed heterochronic shifts in the timing of onsets of developmental sequences. Whilst reaching a quantifiable concept of heterochrony, these two models also identified growth to be an important factor in evolutionary analyses and hence provided a theoretical underpinning that encouraged an approach focused upon measuring traits (e.g. McKinney and Schoch 1985; McNamara 1988; Rice 1997). The latter resulted in a foray into 'allometric heterochrony' (McKinney 1986; Shea 1988; McKinney and McNamara 1991), a term collectively applied to studies whereby size was used as a proxy for age and the direct examination of growth dynamics were interpreted in terms of heterochronic processes; an idea that has been discounted on numerous occasions for lacking coherency and for an incompatibility with age-based heterochronic processes

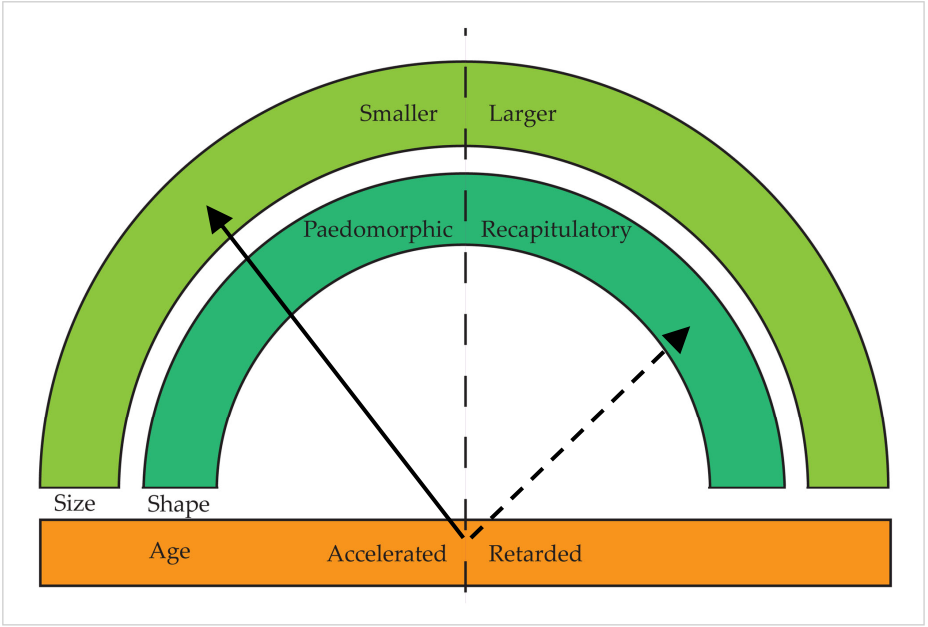

Figure 1.1: The clock model of Gould (1977). Size is represented on the outer scale and indicated with the solid arrow whilst shape is represented on the inner scale and indicated with the dashed arrow. The horizontal bar represents age, indicated by amount of shading. The central, dashed line represents identical ancestor and descendent values.

(e.g. Emerson 1986; Blackstone and Yund 1989; Klingenberg and Spence 1993; Godfrey and Sunderland 1996). Although 'allometric heterochrony' resulted in the unfortunate entanglement of allometry and heterochrony in the literature, it serves at least to highlight the close link between the two investigative tools. Indeed, heterochrony and allometry are complementary since ontogeny can be described by the allometric trajectory of an organism and the rate at which it proceeds along the trajectory, both of which, in turn, may be altered by heterochronic changes. Hence, the study of allometry presents a rich avenue of research for the understanding of how ontogenies evolve. First coined by Julian Huxley and Georges Tessier (1936a,b), the term allometry refers to the pattern of covariation among morphological traits or between measures of size and shape, and thus, unlike heterochrony, a temporal aspect is not considered explicitly. Stemming from the early works of Dubois (1897) and Lapique (1907) that examined relationships between brain weight and body weight in mammals, allometry studies have a long history in the literature, and have more recently begun to be examined from a mechanistic perspective, as evolutionary developmental biology has focused more sharply on indentifying specific genes and developmental pathways that are responsible for the evolution of ontogenies (West and Brown 2005; Li et al. 2007; Sears et al. 2007).

The advent and application of geometric morphometrics, the statistical analysis of Cartesian geometric coordinates (Bookstein 1991; Dryden and Mardia 1998), has reformed the ways in which morphological form can be described. Through this revolution, which has been aided significantly by technological advances in data acquisition methods, the univariate consideration of shape under the models of Gould (1977) and Alberch et al. (1979) has been translated to a multivariate framework. This has permitted intuitive visualisations of ontogenetic trajectories as vectors in multivariate morphospace (e.g. O'Higgins 2000; Ponce de León and Zollikofer 2001; Monnet et al. 2009; Urdy et al. 2010a,b), commonly through the application of principal components analysis (PCA).

Framed, for instance, by phylogenetic, ecological, or functional hypotheses, the exploration of morphospace occupation and structure, in a comparative context, has offered many insights into morphological evolution. The integration of ontogenetic data to create developmental morphospaces has great potential to yield a wealth of results comparable to those currently documented by the studies of adult form, which at present dominate the literature. With an extensive tool-kit of geometric morphometric techniques at the disposal of present-day researchers (Lawing and Polly

2009; Mitteroecker and Gunz 2009), it is possible to examine the ontogenetic changes that create diversity and how the evolution of ontogenies across lineages contributes to the patterning of clade diversity. Ontogenetic trajectories are commonly represented using the major axis of covariance, and consequently through the exploration of developmental morphospaces, the extent and patterning of modification to covariance structure can be revealed, reflecting the possibilities that remain for the functional or developmental differentiation of integrated phenotypes (Eble 2004).

The skull - the study system

Anatomists and functional morphologists have studied the cranium over the course of the past two centuries, and have contributed a wealth of knowledge to understanding this complex structure. Since the skull houses the brain, the major sensory organs and the masticatory apparatus, it serves a crucial functional role and provides a platform to explore hypotheses relating to adaptation and constraint (Hanken and Hall 1993). As a form, the skull presents the opportunity to record and compare a suite of homologous, quantifiable traits. Moreover, it is also represented well in the mammalian fossil record, and particularly in the case of rodents, for which ontogenetic series of several species are also known (Fig. 1.2; Vassallo and Mora 2007; Verzi 2008).

Figure 1.2: Growth series of the Pliocene fossil rodent *Actenomys priscus*. Specimens from Museo de Ciencias Naturales "Lorenzo Scaglia", Mar del Plata, Argentina (Wilson, unpub.). Scale: 2cm.

Rodents - the study subject

The earliest known rodents appear in the later Paleocene of North America and the earliest Eocene of Europe (Wood 1959), which presents at least the beginning of an astonishing adaptive radiation throughout the Cenozoic, leading to their current taxonomic diversity of 2277 species, representing almost half of

all living mammalian species (Wilson and Reeder 2005). Their unparalleled taxonomic success among mammals, coupled with phenomenal levels of morphological diversity and a rich fossil record, make rodents a prime example taxon for the study of morphological evolution.

Together with their sister group the lagomorphs (rabbits, hares and pikas), rodents make up the Glires clade and along with relatives Primates, Scandentia (tree shrews) and Dermoptera (flying lemurs) these form the 'superorder' Eurarchonglires (Murphy et al. 2001; Asher et al. 2009) (Figure 1.3). The elucidation of the phylogenetic relationships between rodent taxa has been confounded by the extensive amount of convergence among morphological characters within the group (Jaeger 1988). Morphological characters have been used to identify either two or three divisions among rodents. Towards the middle of the 19th Century, Waterhouse (1839) proposed that rodents could be classified into two main groups: the rabbits, and all others. The collective "all others" were further subdivided, on the basis of masseter muscle origin and insertion, to belong to three groups, identified by the following features: 1) an enlarged masseter muscle passes through an enlarged infraorbital formen to originate on the side of the rostrum, 2) a portion of the masseter muscle arises in front of the orbit and descends to insert on the lower jaw, and 3) a combination of conditions (1) and (2). These categories were later named by Brandt (1855) as 1) hystricomorpha 2) sciuromorpha and 3) myomorpha, whilst the condition found in rabbits was assigned the term lagomorpha. These divisions, though, as suggested by Woods (1965) and later confirmed through molecular phylogenetic analyses (Huchon et al. 2002; Adkins et al. 2003) are based on homoplastic characters and cannot be used for the subordinal classification of rodents. More common is the subdivision of Rodentia into Sciurognathi and Hystricognathi (Tullberg 1899; Carleton 1984), based upon the position of the angular process of the jaw relative to the plane of the incisors. In sciurognaths, the angular process of the jaw is in the same plane as the root of the incisors, whilst among hystricognaths, because of a widened bony shelf for jaw muscle attachment, the angular process falls outside the plane formed by the root of the incisors. At present, molecular analyses support the identification of seven major clades within rodents and these are clustered into three main lineages (Figure 1.4) (Huchon et al. 2002, 2007; DeBry 2003; Montgelard et al. 2008; Blanga-Kanfi et al. 2009).

Within rodents there are two groups with contrasting levels of morphologic and taxonomic diversity. Comprising less than 13% of the taxonomic diversity of rodents (290 species), but including animals that span over

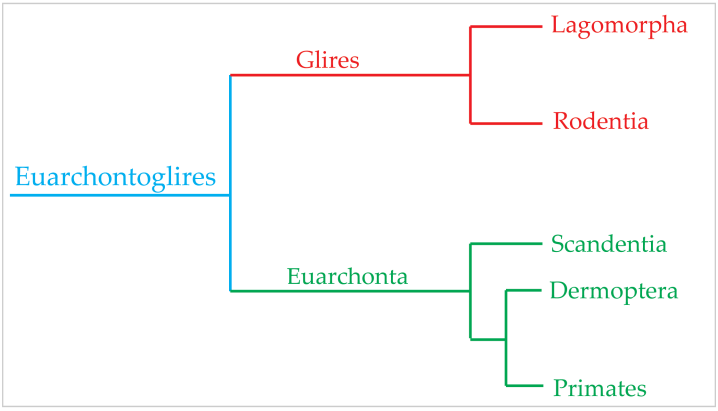

Figure 1.3: The Eurarchontoglires clade. One of the four major clades in placental mammal phylogeny (Asher et al. 2009).

three orders of magnitude of body mass from the tuco tuco (~200g) to the largest living rodent, the capybara (50-60kg), and that give birth to few, well developed young (precocial) which mature slowly, the hystricognaths present an interesting case. These rodents, found mainly in South America (Caviomorpha), but also Africa (Phiomorpha), adopt semi-aquatic, terrestrial, arboreal and fossorial lifestyles, and present a contrast to muroid rodents (mice and rats) – a taxonomically diverse (1518 species) group that show a comparatively diminished level of morphological diversity and typically give birth to many, poorly developed (altricial) young after short intervals.

Aims and overview

From an evolutionary perspective, the polarization between hystricognaths and muroids leads to the question: why are some lineages more morphologically diverse than others? To investigate this question, a broad-scale comparison is required. Although the literature contains many studies of rodents, not least due to their geographically cosmopolitan distribution and their application in biomedical fields as model organ systems, attention has not been directed towards examining the basis for the discordant levels of morphological diversity among these two groups. This thesis adopts an approach focused upon investigating the role that ontogeny plays in the generation of morphological diversity. To encapsulate the widest possible morphological, ecological and phylogenetic breadth, the results of this study are based upon the examination of developmental series for 58 species. In the subsequent four chapters of this thesis (2-5), differing windows of developmental time are examined using the interrelated analytical frameworks of heterochrony, allometry and disparity, to test fundamental hypotheses relating to the evolution and modification of developmental pathways, their phylogenetic signal and functional correlates.

In chapter 2 the first comprehensive as-

say of heterochronies in cranial suture growth is documented for a mammalian clade. Bones of the face and cranial vault meet at sutural boundaries, which are important for craniofacial growth. Suture formation in mammals has been linked to functional and phylogenetic patterns, and a conserved pattern has been proposed based on the study of hominoids. We compared the sequence and timing of closure for 35 cranial sutures across 31 rodent species, including 26 hystricognaths. Using the Parsimov method (Jeffrey et al. 2005) to analyze sequence heterochrony, we show numerous heterochronies in suture closure have occurred in the evolution of this diverse clade of rodents. Differing life history and locomotory strategies

Figure 1.4: Within Rodentia, recent molecular analyses suggest that rodents are divided into seven well-supported clades: 1-Anomaluromorpha (scaly-tailed flying squirrels, springhares), 2-Castoridae (beavers), 3-Ctenohystrica (gundi, porcupines, guinea-pigs), 4-Geomyoidea (pocket gophers, pocket mice), 5-Gliridae (dormice), 6-Myodonta (rats, mice, jerboas), and 7-Sciuroidea (mountain beavers, squirrels, woodchucks) (Blanga-Kanfi et al. 2009).

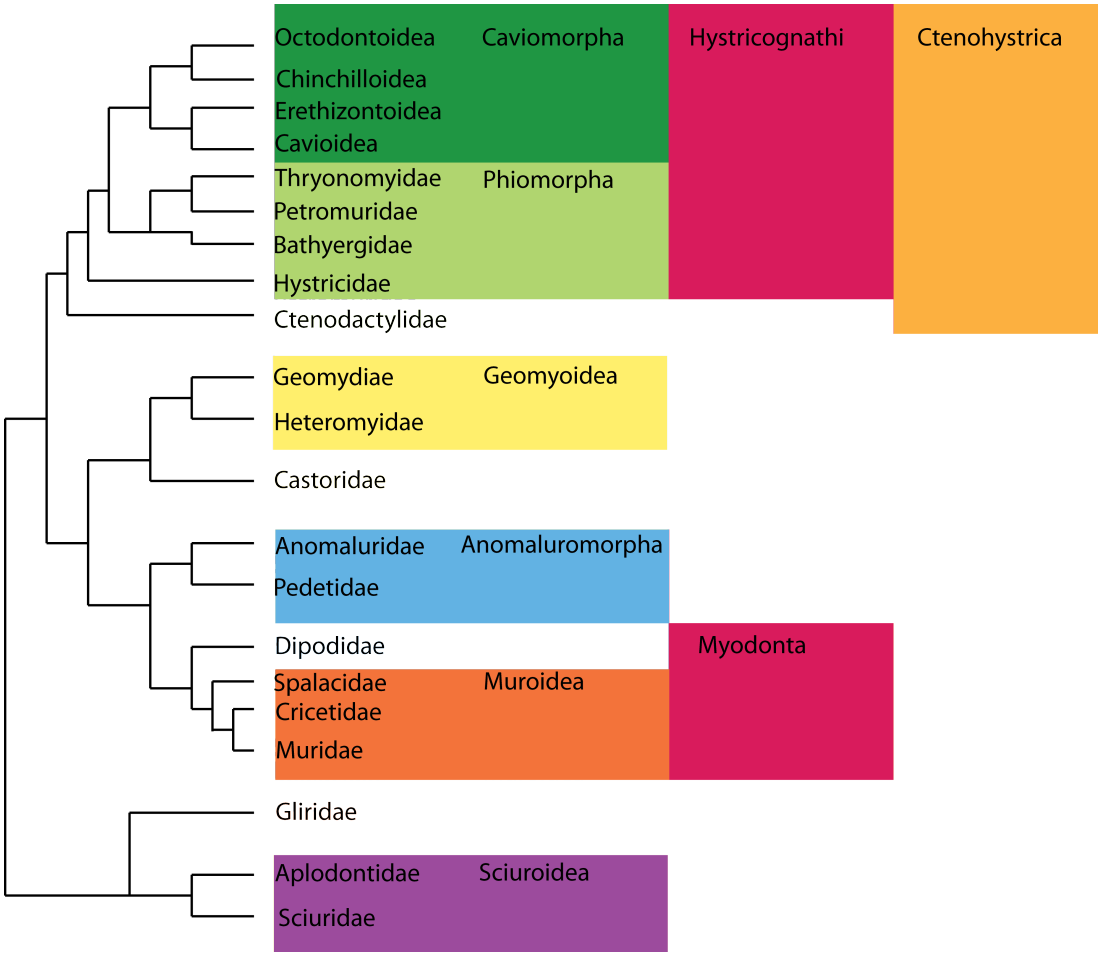

are, in part, shown to be coupled with the degree and pattern of suture closure.

It has been hypothesized that most morphological evolution occurs by allometric differentiation, however studies directed towards examining the evolution of allometry are few and of small scope. In chapter 3 we investigate the influence of phylogenetic relations and ecological factors on allometric evolution by comparing the postnatal growth trajectories of 17 muroid and 17 hystricognath species. This study uses the framework of disparity – the quantitative description of the empirical distribution of taxa in morphospace. Rather than a summarization of morphological distributions through ordination, the goal is to produce state space summaries that represent the average spread and spacing of forms in morphospace. Derived from, and encapsulating all of, the ontogenetic trajectories of the 34 species examined, a multivariate, 'allometric space' was produced to enable the appraisal of developmental dynamics in rodent evolution. This is the first study of its kind for rodents, and we show that changes to covariance structure are common in rodent evolution. Anatomical diversity does not constrain allometric patterning in rodents, but rather that the morphological features which enable efficient processing of food serve to group rodents in allometric space. Our results highlight the importance of convergent evolution, rather than shared evolutionary history, in the generation of allometric patterns.

Chapter 4 considers an earlier point in skeletal development; the onset of skeletal formation. At present there is a relative dearth of data on skeletal development across mammalian clades, and, for Rodentia this shortcoming is particularly marked, since it is species-rich in comparison to other mammalian 'orders'. We present the most comprehensive sampling of rodent ossification sequences to date, including improvements in resolution for several taxa previously studied, and data from two non-model species with representatives from both muroid and hystricognath clades. Data on cranial and postcranial ossification sequences were analysed using the Parsimov method. Additionally, we provided a detailed documentation of skeletogenesis in the African striped mouse (*Rhabdomys pumilio*) including data on the sequence of ossification for the autopods and a comparison of intraspecific variability in ossification sequence. In complement to the results of chapter 2, we find that sequence heterochrony is not pivotal or prevalent during early skeletal formation in rodents. This mirrors a similar general result for Laurasiatherian placental mammals (Sánchez-Villagra et al. 2008).

Chapter 5 focuses upon *Rhabdomys pumilio*, this time through the comparison of prenatal and postnatal ontogenetic allometry.

The difficulty in obtaining a developmental series for any mammal has restricted the documentation of prenatal allometry, and the relation between prenatal and postnatal ontogenetic trajectories is thus poorly known. In this study I use bivariate and multivariate methods for estimating allometry, and, additionally, compare the prenatal and postnatal matrices using common principal components (Flury 1988) and random skewers methods (Cheverud 1996) to detect differences in covariance structure. I show the prenatal period is characterized by rapid bone growth and that growth dynamics shift for several cranial elements, indicating a non-linearity of ontogenetic allometry with respect to birth.

The two documents appended to this thesis represent additional publications (Appendix I – in press; Appendix II – in press) on areas of my research work which further illustrate or discuss methodological aspects treated in the main chapters of this thesis.

The efficacy of morphological versus molecular data is a topic of contention in vertebrate systematics, and the exploration of ontogenetic data to address phylogenetic questions remains limited in spite of its purported significance. In Appendix I we focus on examining the evolution of growth trajectories in 10 species of chelid turtles, with a particular emphasis upon assessing the role of ontogenetic data in contributing to the debated phylogenetic interrelationships of this group, which are represented by differing hypotheses based upon morphological and molecular data. We find scaling patterns among cranial characters are most similar between the geographically separated (Australasia vs. South America) clades promoted by molecular data. This result favours the hypothesis that the long neck exhibited by many chelid species, originated independently in South American and Australasian taxa. Most importantly, we showed that ontogenetic trajectory data contain phylogenetic signal, arguing for similar studies for other taxa and issues.

Appendix II compares the ontogeny of sexual dimorphism in two modern human populations, from the U.K. and Portugal, and addresses the ability of outline-based geometric morphometric methods (eigenshape) to reliably identify the sex of juvenile postcranial remains. Our results demonstrate that a technique previously developed by Wilson et al. (2008) can be used to successfully document dimorphism in another sample. Significant differences between male and female iliac morphology are revealed at early stages in ontogeny, suggesting differences between the sexes are at least present from birth, and continue to remain distinct during later ontogeny.

REFERENCES

Alberch P, Gould SJ, Oster GF, Wake DB. 1979.

Size and shape in ontogeny and phylogeny. *Paleobiology* 5: 296-317.

Asher RJ, Bennett N, Lehmann T. 2009. The new framework for understanding placental mammal evolution. *Biology Letters* 31: 853-864.

Blackstone NW, Yund PO. 1989. Morphological variation in a colonial marine hydroid: a comparison of size-based and age-based heterochrony. *Paleobiology* 15: 1-10.

Bookstein FL. 1991. *Morphometric Tools for Landmark Data: Geometry and Biology*. Cambridge University Press, Cambridge.

Cheverud JM. 1996. Quantitative genetic analysis of cranial morphology in the cotton-top (*Saguinus oedipus*) and saddle-back (*S. fuscicollis*) tamarins. *J. Evol. Biol.* 9: 5–42.

Cubo J, Fouces V, González-Martín, Pedrocchi V, Ruiz X. 2000. Nonheterochronic developmental changes underlie morphological heterochrony in the evolution of Ardeidae. *J. Evol. Biol.* 13: 269-276.

de Beer GR. 1930. *Embryology and Evolution*. Clarendon Press, Oxford.

de Beer GR. 1958. *Embryos and Ancestors*. Third Edition. Clarendon Press, Oxford.

DeBry RW. 2003. Identifying conflicting signal in a multigene analysis reveals a highly resolved tree: The phylogeny of Rodentia (Mammalia). *Syst. Biol*. 52(5): 604-617.

Darwin C. 1859. *On the origin of species by means of natural selection, or the preservation of favoured races in the struggle for life*, 1st Edition. John Murray, London.

Dryden IL, Mardia KV. 1998. *Statistical Shape Analysis*. Jon Wiley and Sons, New York.

Dubois E. 1897. Sur le rapport de l'encéphale avec la grandeur du corps chez les Mammifères. *Bull. Soc. anthropol. Paris, 4e série* 8: 337–374.

Eble GJ. 2004. The Macroevolution of phenotypic integration. In *Phenotypic Integration* (eds. M Pigliucci, K Preston), pp. 253-273. Oxford University Press, New York.

Emerson SB. 1986. Heterochrony and frogs: the relationship of a life history trait to morphological form. *Am. Nat.* 127: 167-183.

Flury BD. 1988. *Common principal components and related multivariate models*. Wiley, New York.

Godfrey LR, Sutherland MR. 1996. Paradox of peramorphic paedomorphosis: heterochrony and human evolution. *Am. J. Phys. Anthropol*. 99: 17-42.

Gould SJ. 1977. *Ontogeny and Phylogeny*. Harvard University Press, Cambridge (Mass.).

Haeckel E. 1866. *Generelle Morphologie der Organismen*. Georg Reimer, Berlin.

Hanken J, Hall BK. 1993. *The Skull*. The Univer-

sity of Chicago Press, Chicago, Illinois USA. Pp 460.

Huchon D, Chevret P, Jordan U, Kilpatrick CW, Ranwez V, Jenkins PD, Brosius J, Schmitz J. 2007. Multiple molecular evidences for a living mammalian fossil**.** *Proc. Natl. Acad. Sci. U.S.A.* 104(18): 7495-7499.

Huchon D, Madsen O, Sibbald MJJB, Ament K, Stanhope M, Catzeflis F, De Jong WW, Douzery EJP. 2002. Rodent phylogeny and a timescale for the evolution of glires: evidence from an extensive taxon sampling using three nuclear genes**.** *Mol. Biol. Evol.* 19(7): 1053-1065.

Huxley JS, Teissier G. 1936a. Terminology of relative growth. *Nature* 137: 780-781.

Huxley JS, Teissier G. 1936b. Terminologie et notation dans la description de la croissance relative. *Comptes rendus séances soc. biol. fil.* 121: 934–937.

Jaeger J-J. 1988. Rodent phylogeny: new data and old problems**.** In *The phylogeny and classification of the Tetrapods Volume 2*. (ed. MJ Benton), pp. 177-193. Clarendon Press, Oxford.

Jeffery JE, Bininda-Emonds ORP, Coates MI, Richardson MK. 2005. A new technique for identifying sequence heterochrony. *Syst. Biol.* 54: 230-240.

Klingenberg CP, Spence JR. 1993. Heterochrony and allometry: lessons from the water strider genus *Limnoporus*. *Evolution* 47: 1834-1853.

Lapicque L. 1907. Tableau général des poids somatiques et encéphaliques dans les espèces animales. *Bull. Soc. anthropol. Paris, 5e série* 9:248–269.

Lawing AM, Polly PD. 2010 Geometric morphometrics: recent applications to the study of evolution and development. *J. Zool.* 280: 1–7.

Li H, Huang Z, Gai J, Wu S, Zeng Y, Li Q, Wu R. 2007. A Conceptual Framework for Mapping Quantitative Trait Loci Regulating Ontogenetic Allometry. *PLoS ONE* 2(11): e1245.

Mitteroecker P, Gunz P. 2009. Advances in geometric morphometrics. *Evol. Biol.* 36: 235-247.

McKinney ML. 1986. Ecological causation of heterochrony: a test and implications for evolutionary theory. *Paleobiology* 12: 282-289.

McKinney ML, McNamara KJ. 1991. *Heterochrony: the Evolution of Ontogeny*. Plenum Press, New York.

McKinney ML, Schoch RM. 1985. Titanothere allometry, heterochrony, and biometrics: revising an evolutionary classic. *Evolution* 39: 1352-1363.

McNamara KJ. 1988. The abundance of heterochrony in the fossil record. In *Heterochrony in Evolution: A Multidisciplinary*

Approach (ed. ML McKinney), pp. 287-325. Plenum Press, New York.

Monnet C, Zollikofer C, Bucher H, Goudemand N. 2009. Three-dimensional morphometric ontogeny of mollusc shells by micro-computed tomography and geometric analysis. *Paleontologica Electronica* 12(3): 12A.

Montgelard C, Forty E, Arnal V, Matthee CA. 2008. Suprafamilial relationships among Rodentia and the phylogenetic effect of removing fast-evolving nucleotides in mitochondrial, exon and intron fragments. *BMC Evol. Biol*. 8: 321.

Murphy WJ, Eizirik E, Johnson WE, Zhang YP, Ryder OA, O'Brien SJ. 2001: Molecular phylogenetics and the origins of placental mammals. *Nature* 409: 614-618.

O'Higgins P. 2000. *Quantitative Approaches to the Study of Craniofacial Growth and Evolution: Advances in Morphometric Techniques: Development, Growth and Evolution*. Academic Press, San Diego.

Ponce de Léon MS, Zollikofer CP. 2001. Neanderthal cranial ontogeny and its implications for late hominid diversity. *Nature* 412: 534–538.

Raff RA. 1996. *The Shape of Life: Genes, Development, and the Evolution of Animal Form*. University of Chicago Press, Chicago.

Richardson MK, Gobes SMH, Van Leeuwen AC, Polman JAE, Pieau C, Sánchez-Villagra MR. 2009. Heterochrony in limb evolution: developmental mechanisms and natural selection. *J. Exp. Zool.* 312 (6): 639-664.

Rice SH. 1997. The analysis of ontogenetic trajectories: when a change in size or shape is not heterochrony *Proc. Natl. Acad. Sci. U.S.A*. 94: 907-912.

Sánchez-Villagra MR. 2010. Developmental palaeontology in synapsids: the fossil record of ontogeny in mammals and their closest relatives. *Proc. R. Soc. B.* 277: 1139-1147.

Sánchez-Villagra MR, Goswami A, Weisbecker V, Mock O, Kuratani S. 2008. Conserved relative timing of cranial ossification patterns in early mammalian evolution. *Evol. Dev.* 10(5): 519-530.

Sears KE, Goswami A, Flynn JJ, Niswander LA. 2007. The correlated evolution of *Runx2* tandem repeats, transcriptional activity, and facial length in Carnivora. *Evol. Dev.* 9(6): 555-565.

Shea BT. 1988. Heterochrony in primates. In *Heterochrony in Evolution* (ed. M. L. McKinney), pp. 237-266. Plenum Press, New York.

Urdy S, Goudemand N, Bucher H, Chirat R. 2010a. Allometries and the morphogenesis of the molluscan shell: a quantitative and theoretical model. *J. Exp. Zool.* 314 (4): 280-302.

Urdy S, Goudemand N, Bucher H, Chirat R. 2010b. Growth-dependent phenotypic variation of molluscan shells: implications for allometric data interpretation. *J. Exp. Zool.* 314(4): 303-326.

Vassallo AI, Mora MS. 2007. Interspecific scaling and ontogenetic growth patterns of the skull in living and fossil ctenomyid and octodontid rodents (Caviomorpha: Octodontoidea). In *The Quintessential Naturalist. Honoring the life and legacy of Oliver P. Pearson.* (Eds. DA Kelt, EP Lessa, J Salzar-Bravo, JL. Patton), pp. 945-968. University of California Publications in Zoology.

Verzi DH. 2008. Phylogeny and adaptive diversity of rodents of the family Ctenomyidae (Caviomorpha): delimiting line ages and genera in the fossil record. *J. Zool.* 274: 386-394.

West, GB, Brown JH. 2005. The origin of allometric scaling laws in biology from genomes to ecosystems: towards a quantitative unifying theory of biological structure and organization. *J. Exp. Biol.* 208: 1575-1592.

Wilson LA, MacLeod N, Humphrey LT. 2008. Morphometric criteria for sexing juvenile human skeletons using the ilium. *J. Forensic Sci*. 53(2): 269-278.

Wood AE. 1959. Eocene radiation and phylogeny of the rodents. *Evolution* 13(3): 354-361.

CHAPTER 2

Heterochrony and patterns of cranial suture closure in hystricognath rodents

CHAPTER 2
Heterochrony and patterns of cranial suture closure in hystricognath rodents

Article submitted to *Journal of Anatomy* on 7th July 2008, accepted for publication on 6th November 2008

Reference: **Wilson LAB**, Sánchez-Villagra MR. 2009. Heterochrony and patterns of cranial suture closure in hystricognath rodents. *J. Anat.* **214**: 339-354

Abstract

Sutures, joints that allow one bone to articulate with another through intervening fibrous connective tissue, serve as major sites of bone expansion during postnatal craniofacial growth in the vertebrate skull and represent an aspect of cranial ontogeny which may exhibit functional and phylogenetic correlates. Suture evolution among hystricognath rodents, an ecologically diverse group represented here by 26 species, is examined using sequence heterochrony methods, i.e. event pairing and Parsimov. Although minor nuances in suture closure sequence exist between species, the overall sequence was found to be conserved both across the hystricognath group and, to an increasing degree, within selected clades. At species level suture closure pattern exhibited a significant positive correlation with patterns previously reported for hominoids. Patterns for most clades revealed the first sutures to close are those contacting the exoccipital, interparietal, and palatine bones. Heterochronic shifts were found along 19 out of 35 branches within the hystricognath phylogeny. The number of shifts per node ranged from one to seven events and, overall, involved 21 out of 34 suture sites. The topology generated by parsimony analyses of the event pair matrix yielded only one grouping that was congruent with the evolutionary relationships, compiled from morphological and molecular studies, taken as framework. Sutures contacting the exoccipital displayed the highest levels of most complete closure across all species. Level of suture closure is negatively correlated with cranial length ($p < 0.05$). Differing life history and locomotory strategies are coupled in part with differing suture closure patterns among several species.

KEYWORDS**:** suture; skull; heterochrony; development; Rodentia; Hystricognathi

INTRODUCTION

The relation between ontogenetic and phylogenetic change has commonly been addressed using an analytical framework constructed from the quantification and exploration of size and shape change (Klingenberg, 1998), with a focus on heterochrony or changes in developmental rate or timing. Although organismal form is innately a multivariate concept and thus may be expressed by size and shape, some aspects of development are best studied with other approaches. The study of sequence heterochrony (Smith, 2001) provides a methodology to study changes in the timing of developmental events. Earlier studies of sequence heterochrony within mammals have concentrated upon differences between marsupial and placental mammal ossification sequences (Smith, 1997; Nunn & Smith, 1998; Sánchez-Villagra, 2002; Bininda-Emonds et al. 2003; Goswami, 2007; Sánchez-Villagra et al. 2008; Weisbecker et al. 2008). The present study considers the influence of heterochronic processes and developmental conservatism in the generation of diversity within a single clade of placentals and a later aspect of skeletal development: sutures in hystricognath rodents.

Rodents are the most abundant and taxonomically diverse order of living mammals, with 2,277 members representing almost half of all living species (Wilson & Reeder, 2005). Living rodents inhabit all continents except Antarctica, and are found in almost every terrestrial habitat throughout their geographic range, playing integral roles in the ecosystems they inhabit. Within Rodentia a polarization exists which pivots upon Hystricognathi. This monophyletic clade, which includes Old World phiomorphs and New World caviomorphs (Adkins et al. 2001, 2003), contains less than 13% of all rodent species (Wilson & Reeder, 2005). Nevertheless extant hysticognaths show ranges in body size and ecological diversity (Fig. 2.1, Table 2.1) that exceed those observed for any other group of rodents (Nowak, 1999; Sánchez-Villagra et al. 2003): members of the clade possess different life history strategies, locomotion styles and reproductive strategies thereby providing a potentially relevant subject to investigate developmental mechanisms intrinsic to the evolution of diversity (e.g. Mess, 2003). From this precept, we concentrate upon the cranium and specifically one element that mediates its growth: suture closure.

Sutures are joints in the vertebrate skull that have two bone fronts interposed with fibrous connective tissue (Rice, 1999; Depew et al. 2008). The vertebrate skull may be segmented into the bones surrounding the skull, the neurocranium, and the bones that form the face, the viscerocranium. The neurocranium has two subdivisions; the base, formed by endochondral ossification, and the calvaria or

cranial vault, formed from membrane bones and primarily composed of five elements: paired frontals, paired parietals and an interparietal (Rice, 1999). During early development an increase in intracranial volume is achieved primarily by sutural growth (Henderson et al. 2004). In response to signals transmitted through the dura mater, new bone is produced perpendicularly to the orientation of the suture, at the bone fronts of the sutural margins. Sutures maintain an approximately similar width while the cranial vault expands to accommodate the developing brain (Opperman, 2000; Morriss-Kay & Wilkie, 2005). Sutures must remain patent in order to function; premature closure (craniosynostosis) results in growth constraint at the site of the affected suture and can lead to deformity. The genetic etiology of craniosynostosis has been studied extensively revealing sutural biology to be intimately linked with transforming growth factors (TGFβs), fibroblast growth factors (FGFs) and bone morphogenetic proteins (BMPs) (Rice, 1999; Ogle et al. 2004). Critical for the maintenance of normal cranial sutures, these factors must interact in the presence of dura mater (Opperman et al. 1993).

Topological correspondence is an important component of the invocation of homology between two elements (Hall, 1994; Depew et al. 2008). Cranial elements are bounded by sutures and thus in definition the suture becomes a prime unit in the identification of homology between elements. Nonetheless past study has focussed upon elements: their cellular, molecular and functional characteristics, and not the sutural boundary that constrains their topological relation with other structures.

Early studies of cranial suture closure in humans focussed upon the forensic application of quantifying suture synostosis: an extensive study by Todd & Lyon (1924, 1925a, 1925b, 1925c) concluded that suture closure exhibited a definite periodicity and as such could be used to estimate skeletal age at death. Patterns of suture closure were investigated in hominoids by Krogman (1930) who described a reference pattern of suture closure that was considered to be of general application to mammals (Chopra, 1957; Herring, 1993). The sequence is commonly given as follows: vault, base, circum-meatal, palatal, facial, and craniofacial (Fig. 2.2). Work by Schultz (1940; 1941; 1942) concerning apes and by Chopra (1957) who studied 10 genera of Old and New World monkeys, further corroborated this pattern.

Herring (1972, 1974) attributed differences in endocranial suture fusion pattern among pigs and peccaries to cranial stresses. Sutures are more compliant than the bones they join and thus are able to absorb tensile and compressive forces. In particular, peccaries exhibited an early fusion of sutures associated with the palatal and facial regions, which

Herring (1974) noted to be a marked contrast to Krogman's (1930) pattern and proposed to be directly related to stress in these regions of the skull. Several studies have suggested a functional relationship between suture complexity and forces associated with mastication (Sun et al. 2004; Wu et al. 2007). Indeed the work of Herring (1972) on pigs, Dolan (1971) on ceboid monkeys and Giannini et al. (2006) on a fruitbat indicated suture closure pattern to be species specific. Recently, Cray et al. (2008) reported that *Gorilla gorilla* exhibits a unique pattern of ectocranial vault suture closure, further substantiating this notion. Moreover for a sample of Rhesus monkeys (*Macaca mulatta*) of known age and sex, Wang et al. (2006) detected familial groupings in suture patterns, suggesting variation may be heritable.

A comprehensive assay of heterochronies in cranial suture growth has not previously been conducted for any clade of mammals. The available methods to study sequence heterochrony (Smith, 1997; Jeffery et al. 2005) provide the opportunity to evaluate evolutionary changes in sutural timing patterns. Presently we address these issues by examining hystricognaths, an ecologically diverse clade of rodents. Several hypotheses are tested: (i) Hystricognathi is defined by a specific pattern of suture closure; (ii) heterochronic shifts in suture closure events characterise monophyletic clades within Hystricognathi; (iii) suture closure patterns for the species examined here are similar to patterns for hominoids (Krogman, 1930); (iv) event pair data accurately reflects evolutionary relationships; (v) level of suture closure is correlated with cranial dimension.

MATERIALS AND METHODS

Data collection

The study sample comprised 628 crania from a total of 31 species. The sample included 26 species of Hystricognathi spanning a taxonomic and ecological breadth; additionally the out-group consisted of three species of Myomorpha and one species each of Sciuromorpha and Castorimorpha (Table 2.1). Data were collected from specimens at the following Institutions: Palaeontologisches Institut und Museum der Universität Zürich, Naturhistorisches Museum Bern, Naturhistorisches Museum Basel, Museum für Naturkunde (Humboldt-Universität zu Berlin), Zoologische Staatssammlung München, National Museum of Natural History (Naturalis) Leiden, Muséum national d'Histoire naturelle Paris, and Naturhistorisches Museum Wien. A total of 34 suture sites were coded for each cranium (Fig. 2.3 and Table 2.2). Sutures were scored as either open (score 1), ¼ closed (score 2), ½ closed (score 3) or completely closed (score 4) (see Fig. 2.4). Crania exhibiting gross pathology were excluded from the sample. The

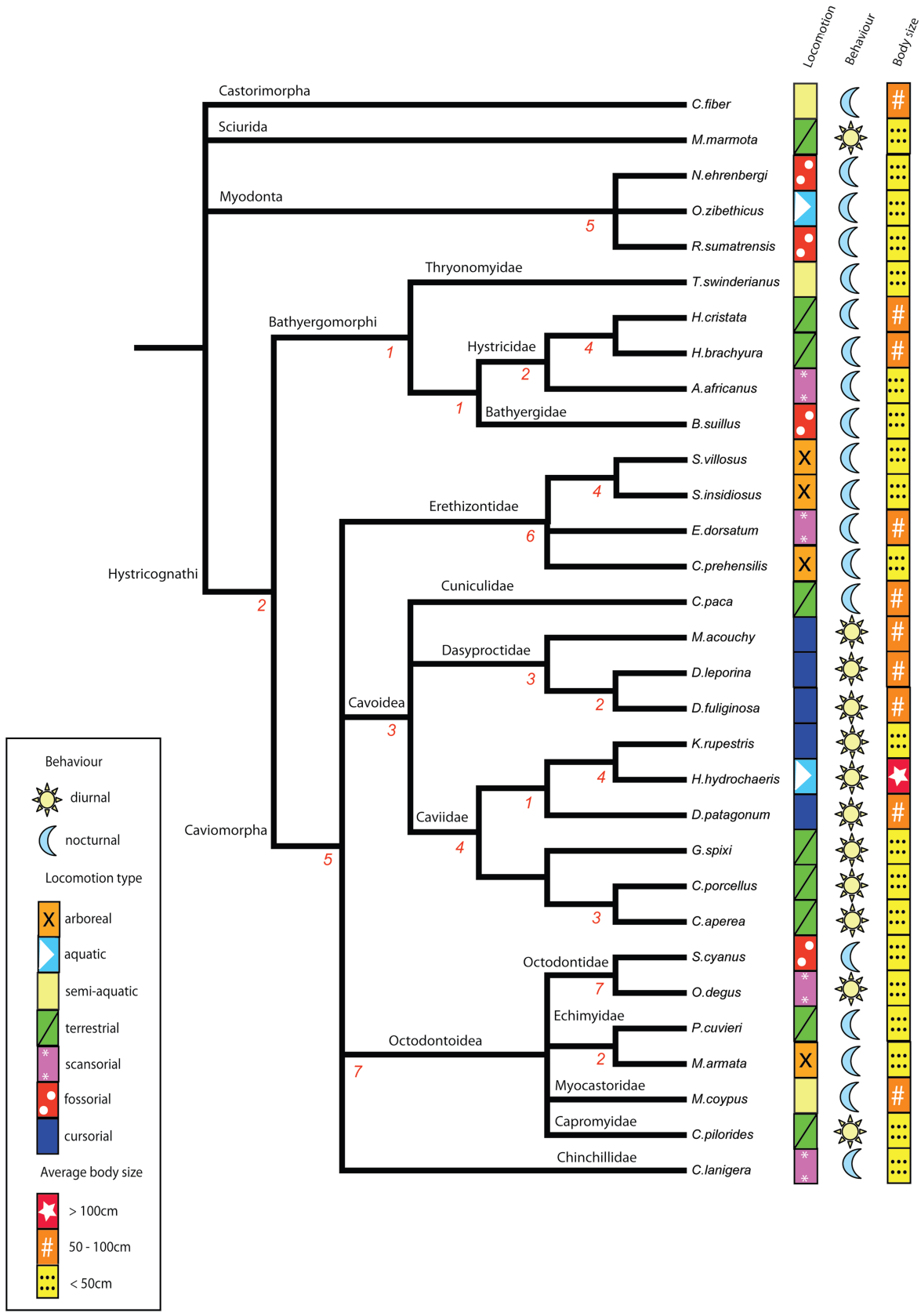

Figure 2.1: Compound phylogeny featuring species investigated: 26 Hystricognath taxa and five outgroup species selected from Myodonta, Sciurida and Castorimorpha. Number of recorded heterochronic shifts, or changes in timing of suture closure events following the consensus approach of Parsimov denoted under each branch.

length of each cranium was measured and crania were specifically chosen such that the sample for each species resembled a growth series (Fig. 2.5). Species that exhibited fewer than 5 different suture closure events were considered to provide inadequate resolution and hence removed before final analyses. All specimens were coded by LABW; to control for error a subset was re-coded at the end of the data collection period.

Phylogenetic framework

Evolutionary relationships among the hystricognaths were reconstructed from several literature sources, as there is no comprehensive phylogenetic study that includes all taxa studied. The clades used here are indicated in the phylogenetic framework depicted in Figure 2.1. Relationships between Old World hystricognaths, Cavoidea, Erethizontoidae, Chinchillidae, and Octodontoidea follow Huchon & Douzery (2001). Within Octodontoidea, relationships follow the molecular work of Honeycutt et al. (2003). Relations among the Echimyidae follow Galewski et al. (2005), and the systematics of Hystricidae are based on the classification by McKenna & Bell (1997).

Analyses of suture pattern conservation

The pattern of suture closure was determined for Bathyergomorphi and Caviomorpha

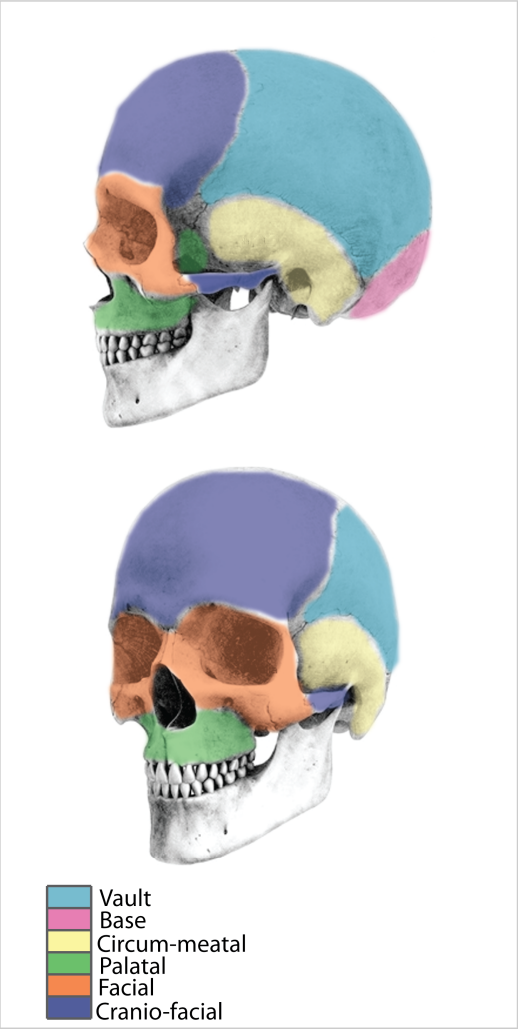

Figure 2.2: Illustration of divisions within the pattern of suture closure proposed for hominoids (Krogman, 1930). The sequence is considered to be generally applicable to mammals and is as follows: valut, base, circum-meatal, palatal, facial, cranio-facial.

and also for Hystricognathi as a whole. The raw closure scores for each species, for each suture site were totalled and the suture sites were then ranked by descending numerical value, reflecting the first to last incidence of suture closure. Kendall's Coefficient of Concordance (Kendall's W) was calculated, using the

ranked raw closure scores, for Bathyergomorphi and Caviomorpha and then for Hystricognathi as a whole, to determine the relative conservation of suture closure pattern. Kendall's W is a non-parametric statistic that may be applied to ordinal data to evaluate the degree to which several judges (*p*) concur when ranking a given set of objects (n): here the judges are replaced by species and the objects are the suture sites. The null hypothesis of Kendall's W states that the judges produce rankings that are independent of one another, hence the different species do not share any identifiable pattern of suture closure. Kendall's W statistic initially calculates a sum-of-squares statistic (*S*) computed from row marginal sums of ranks (R_i) received by the suture sites (Equation 1.0). The *S* statistic is then utilised to obtain the coefficient value (Equation 1.1). Thus the variance present in the row sums of ranks is evaluated in the context of the maximum possible value the variance may have, which is equal to all species exhibiting identical suture closure patterns. Therefore $0 \leq W \leq 1$ (Zar, 1999) where 0 reflects total independence of suture closure pattern between species and 1 represents identical patterns between species.

$$S = \sum_{i=1}^{n} (R_i - \overline{R})^2 \qquad (1.0)$$

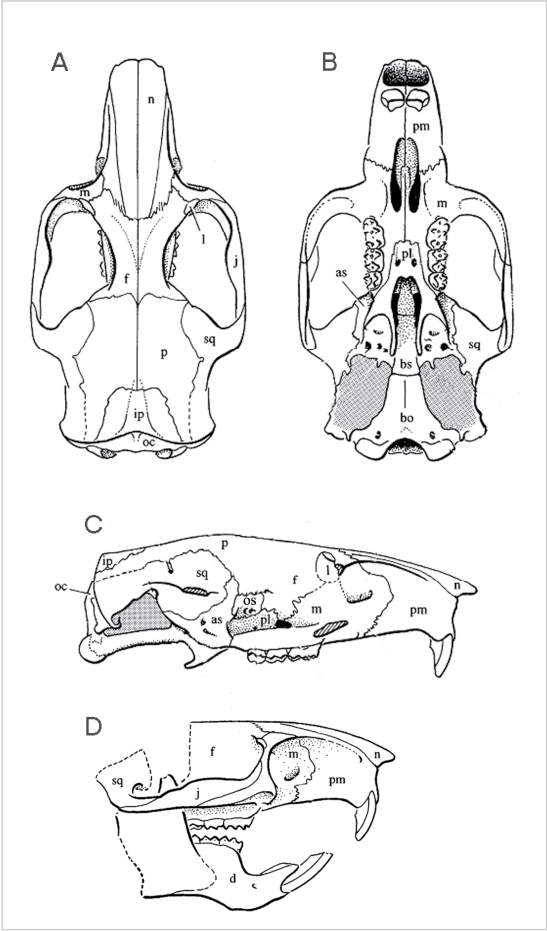

Figure 2.3: Sutural contact of cranial bones viewed in dorsal (A), ventral (B) and lateral (C, D) orientation. The zygomatic arch was removed from the lateral view (c) to illuminate the sutures surrounding the orbit: bones contacting the lacrimal or orbitosphenoid. Cranial bones: nasal (n), maxillary (m), jugal (j), lacrimal (l), frontal (f), parietal (p), squamosal (sq), interparietal (ip), occipital (o), premaxillary (pm), palatine (pl), alisphenoid (as), basisphenoid (bs), basioccipital (bo), dentary (d), (os) orbitosphenoid. Scale = 1cm. Modified after Carrasco & Wahlert (1999).

$$W = \frac{12\,S}{p^2(n^3 - n) - pT} \qquad (1.1)$$

$\overline{R}$ is the mean of R_i and T is a correction factor to account for tied values between ranks.

Kendall's W statistic is related to the Friedman chi-square χ^2_r and thus W may be converted to its equivalent χ^2_r value (Equation 1.2) to determine whether the Kendall's W statistic produced from a sample represents an association different from zero within the sample population.

$$\chi^2 = p(n-1)W \tag{1.2}$$

A Kendall's tau (τ) rank correlation was computed to assess the correspondence of suture closure pattern between each species and the general pattern proposed by Krogman (1930). Kendall's τ (Equation 1.3) measures cross tabulation associations between two rankings. A rank was created to represent the order of suture closure that would be expected following the pattern suggested by Krogman (1930) such that a number was assigned to each suture site reflecting the spatial divisions, and order of these divisions as follows: vault sutures (1), base sutures (2), circum-meatal sutures (3), palatal sutures (4), facial sutures (5), and craniofacial sutures (6). The suture closure pattern for each species was re-ranked using this scheme to enable comparison with Krogman's (1930) sequence. Kendall's tau-b statistic was chosen to enable adjustments to be made for ties within the rankings and is defined as:

$$tau-b = \frac{(P-Q)}{\sqrt{\left[(P+Q+Y_0)(P+Q+X_0)\right]}} \tag{1.3}$$

Where the number of concordant (P) over discordant (Q) pairs is divided by the geometric mean of the number of tied events for the first suture sequence (Y_0) and the number of tied events for the second suture sequence (X_0).

All statistical analyses were performed using SPSS version 16.0 (SPSS Inc, 2007).

Heterochrony analysis

Thirty four events were identified, representing each site of sutural contact between two cranial bones. To identify heterochronies within the pattern of suture closure between the 31 different taxa, the timing of each of these events was assessed by comparing the relative timing of pairs of elements. An event pair matrix was constructed for each taxon in which the timing of each of the 34 events relative to each other event could be expressed: a given event was coded to have occurred earlier than (score 0), simultaneously with (score 1), or later than (score 2) each of the other events in turn (Smith, 1997). The resultant matrix contained 561 event pairs. Event pairs were mapped onto the composite phylogeny using PAUP*4.0b10 (Swofford, 2002) to reconstruct apomorphic character state changes. Parsimov (Jeffery et al. 2005), a parsimony-based computer program, was used to implement event pairing analysis.

The Parsimov method derives a solution that accounts for all the possible event pair changes along a given branch that may be explained by the least number of event movements (Jeffery et al. 2005). Data were optimized using ACCTRAN and DELTRAN criteria to consider ambiguous character-state reconstructions. For situations where a character state change offers equally parsimonious explanations an ACCTRAN optimization will imply the character state originated early within the phylogenetic framework and subsequently a reversal occurred at a later stage. In reverse a DELTRAN optimization delays a change resulting in the occurrence of parallel origination at a later stage. Jeffery et al. (2005) proposed a conservative approach (Sánchez-Villagra et al. 2008), adopted here, using the consensus of ACCTRAN and DELTRAN optimizations thus only unambiguous changes are inferred to be heterochronic.

Event pairs for phylogenetic reconstruction

Event pair data were analysed with PAUP*4.0b10 (Swofford, 2002) using maximum parsimony methods, notwithstanding the limitations of this approach (see Discussion). A heuristic search was performed with tree bisection-reconnection (TBR) branch-swapping on all most parsimonious trees (MPT's). The resulting topology was compared with the composite phylogeny (Fig. 2.1) to assess the utility of event pairs in the context of phylogenetic reconstruction.

Relationship between level of sutural closure and cranial dimension within and between species

To quantify the level of suture closure per species across the 34 examined sutural contact sites the raw scores for each site were averaged and the total number of completely open (score 1) and completely closed (score 4) sites was recorded as a percentage of total sites. To illuminate the typical closure trend for a species the overall amount of closure was defined as a percentage of complete closure: Σ site 1-34/(34*4). The same method was also applied to quantify the level of suture closure per site across the 31 species examined.

To examine the relationship between cranial dimension and level of suture closure, cranial length was recorded for each specimen using callipers. Cranial length measurements, and maximum raw suture closure scores were averaged for each species and between species. Spearmans rank correlation coefficient was used to test the significance of the relationship between cranial length and level of suture closure for both within species and between species data.

RESULTS

Scientific name	N	Adult body length (cm)	Adult body mass (kg)	Age to maturity (months)
*Marmota marmota**	20	30 - 60	3 – 7.5	24
*Castor fiber**	24	60 - 80	12 – 25	18 - 24
*Ondatra zibethicus**	30	22.9 – 32.5	0.68 – 1.8	1.5 - 2
*Nannospalax ehrenbergi**	21	28 - 65	0.1 – 0.22	24
*Rhizomys sumatrensis**	13	23 - 48	1 - 4	5
Thryonomys swinderianus	31	35 – 61	4 – 7	12
Hystrix cristata	20	60 – 93	10 – 30	8 – 18
Hystrix brachyura	14	60 – 93	10 – 30	8 – 18
Atherurus africanus	10	36.5 - 57	1.5 – 4	24
Bathyergus suillus	10	8 – 33	0.64 – 0.93	12
Sphiggurus villosus	23	28 – 65	0.5 – 1.34	19
Sphiggurus insidiosus	11	28 – 65	0.5 – 1.34	19
Erethizon dorsatum	19	64.5 – 80	3.5 – 7	30
Coendou prehensilis	26	30 – 60	0.9 – 5	19
Cuniculus paca	30	50 – 77	7 -12	12
Myoprocta acouchy	13	45 – 70	0.6 – 1.3	12
Dasyprocta leporina	31	41.5 – 62	1.3 – 4	6.5
Dasyprocta fuliginosa	9	41.5 – 62	1.3 – 4	6.5
Kerodon rupestris	16	38	1	5
Hydrochoerus hydrochaeris	35	106 – 134	35 – 66	15
Dolichotis patagonum	32	69 - 75	8 - 9	8
Galea spixii	17	15 – 20	0.3 – 0.6	2 - 3
Cavia porcellus	37	22 – 36	0.7 – 1.2	2 – 3
Cavia aperea	16	22 – 36	0.4 – 0.6	2 – 3
Spalacopus cyanus	8	11.5 – 16	0.06 -0.12	8
Octodon degus	16	12.5 – 19	0.17 – 0.3	6
Proechimys cuvieri	24	26 – 30	0.3 -0.38	5
Makalata armata	11	17 - 24	0.15 – 0.4	?
Myocastor coypus	32	43 – 63.5	5 – 10	3 – 7
Capromys pilorides	9	33 – 45	1 – 2	10
Chinchilla lanigera	20	22.5 – 38	0.5 – 0.8	8

Table 2.1: Ecological and reproductive data for 26 investigated Hystricognath species and the five outgroups (marked with an asterisk *); number of specimens sampled (N). Data from Sherman et al. (1991), Nowak (1999), Lacey et al. (2000), Grzimek (2004), and Mess (2007).

Suture closure quantification between sites and species

Suture sites remained completely open among 195 specimens (31%) while only 25 specimens (4%) displayed any completely closed sutures (Table 2.3a). Indeed 21 out of 34 suture sites remained open in all species: the least amount of overall closure (26-28%) was observed for the mandibular symphysis, premaxillo-maxillary (v), maxillo-jugal, premaxillo-maxillary (f), and naso-frontal sutures (Fig. 2.6). Conversely, the interpalatine, interparietal, exoccipito-supraoccipital, and exoccipito-basioccipital sutures displayed the highest amount of closure (81-87%). Overall closure at

a site averaged 43% (Table 2.5a).

For all species studied, per cranium an average of 12 sites (35%) remained completely open and 1 site (4%) displayed complete closure (Table 2.3b). *Bathyergus suillus* and *Spalacopus cyanus* exhibited the highest number of completely closed sutures (29% and 13% respectively) and the highest overall closure (52-75%) was observed in *Nannospalax ehrenbergi*, *Sphiggurus villosus*, *Sphiggurus insidiosus*, *C. prehensilis*, and *Makalata armata*. Several taxa did not exhibit any completely open sutures (*C. prehensilis*, *S. insidiosus*, *Hystrix brachyura*, and *Marmota marmota*) whereas 61-68% of suture sites remained open among specimens belonging to *Dasyprocta fuliginosa* and *H. hydrochaeris*: representatives for both species included individuals with cranial lengths above 100mm; especially, some *H. hydrochaeris* crania spanned 245mm (Fig 2.7).

Suture closure pattern for Hystricognathi

Kendall's Coefficient of Concordance and supporting Friedman's χ^2_r values indicate suture closure pattern is conserved across Hystricognathi (Table 2.4) with correlation between ranks varying from 0.57 to 0.90. Related critical values for Friedman's chi square χ^2_r ranged between $p < 0.025$ and $p < 0.001$. The highest degree of correlation was displayed by clades comprising the least number of taxa.

Cranial suture site
Mandibular symphysis
Interpremaxillary
Premaxillo-maxillary (v)
Intermaxillary
Maxillo-Palatine (v)
Interpalatine
Pterygo-palate
Palate-alisphenoid
Basispheno-basioccipital
Basispheno-presphenoid
Alispheno-squamosal
Alispheno-orbitosphenoid
Orbitospheno-frontal
Palato-orbitosphenoid
Maxillo-lacrimal (o)
Jugo-squamosal
Lacrimo-frontal (o)
Lacrimo-frontal (f)
Jugo-frontal
Maxillo-jugal
Premaxillo-maxillary (f)
Premaxillo-nasal
Internasal
Naso-frontal
Interfrontal
Fronto-parietal
Interparietal
Fronto-squamosal
Parieto-squamosal
Supraoccipito-parietal
Supraoccipito-squamosal
Exoccipito-squamosal
Exoccipito-supraoccipital
Exoccipito-basioccipital

Table 2.2: Cranial sites representing sutural contact with each bone of the skull. Sutures denoted to be visible from orbital (o), frontal (f) and ventral (v) positions where applicable.

Nevertheless W = 0.67 for the six taxa representing Octodontoidea, reflecting a marginal decrease compared to W = 0.71 for the 10 taxa incorporated within Cavoidea. Equally, Kendall's W for Hystricidae (0.70) is considerably lower than that for the members of *Dasyprocta* (0.86) despite each clade being represented by three different species. This discrepancy likely reflects the differing number of total specimens within the two clades (Table 2.1) and additionally the unequal distribution of specimens across the three species within the clade.

Heterochronic shifts in suture closure pattern

Heterochronic shifts were found along 19 out of 35 branches in the composite phylogeny (Fig. 2.1). The number of heterochronic shifts per node ranged from one to seven events and, overall, involved 21 out of 34 investigated suture sites (62%). In total 65 consensus heterochronic events were identified (Fig. 2.1); of these events, 50 shifts occurred within Caviomorpha, eight shifts occurred within Bathyergomorphi and two shifts were found to characterise Hystricognathi: early closure of the fronto-parietal and late closure of the alisphenoid-squamosal.

Heterochronies in the Caviomorpha

Caviomorpha was characterised by relatively early closure of vault sutures (supraoccipital-parietal and supraoccipital-squamosal) relative to palatal sutures and a relatively late closure of the internasal suture (Fig. 2.6A) in relation to suture contact between the nasal and premaxillary or frontal. Within Caviomorpha, the octodontids exhibited the greatest number of shifts per branch; particularly Octodontidae, represented by *Spalacopus cyanus* and *Octodon degus*, showed seven shifts and was the only group to display closure of the jugo-squamosal (Fig. 2.6B), which was identified to be delayed relative to facial suture closure. Members of Echimyidae shared an early closure of cranial base sutures (basisphenoid-basioccipital and basisphenoid-presphenoid) compared to closure of the maxillo-palatine. Both Octodontoidea and Cavoidea exhibited early closure of the parieto-squamosal suture (Fig. 2.6A) whereas Cavoidea was distinguished from Octodontoidea by the late closure of the mandibular symphysis, shared by both species of *Cavia* (*C. porcellus* and *C. aperea*), in relation to sutures associated with the jugal. Additionally, five out of 16 heterochronic shifts (31%) occurring within Octodontoidea were characterised by a relative late event shift compared to 14 out of 27 instances (52%) in Cavoidea. Members of Dasyproctidae, within Cavoidea, exhibited early closure of the maxillo-palatine and palate-alisphenoid in relation to more than 10 other sutures associated with lacrimal, jugal and nasal elements. Differently, Caviidae was characterised by relatively

Cranial suture site	% open (score 1)	% closed (score 4)	% closure
Mandibular symphysis	62	0	27
Interpremaxillary	48	0	32
Premaxillo-maxillary (v)	55	0	28
Intermaxillary	19	3	40
Maxillo-Palatine (v)	19	0	41
Interpalatine	0	13	81
Pterygo-palate	45	0	34
Palate-alisphenoid	26	0	41
Basispheno-basioccipital	10	0	43
Basispheno-presphenoid	6	3	66
Alispheno-squamosal	22	0	37
Alispheno-orbitosphenoid	3	0	52
Orbitospheno-frontal	6	0	43
Palato-orbitosphenoid	0	13	68
Maxillo-lacrimal (o)	16	16	55
Jugo-squamosal	68	0	27
Lacrimo-frontal (o)	23	3	49
Lacrimo-frontal (f)	46	3	41
Jugo-frontal	42	3	42
Maxillo-jugal	74	0	28
Premaxillo-maxillary (f)	45	0	29
Premaxillo-nasal	81	0	26
Internasal	52	0	30
Naso-frontal	71	0	28
Interfrontal	3	3	46
Fronto-parietal	26	0	37
Interparietal	0	29	86
Fronto-squamosal	26	0	38
Parieto-squamosal	45	0	35
Supraoccipito-parietal	32	0	39
Supraoccipito-squamosal	45	0	34
Exoccipito-squamosal	49	0	34
Exoccipito-supraoccipital	0	19	84
Exoccipito-basioccipital	0	26	87

Table 2.3a: Quantification of closure per suture site for all crania studied. Percentage of crania scoring 1 (open) or 4 (closed) for each suture and evaluation of overall closure exhibited at a given site.

early closure of the maxillo-lacrimal, shared by members of both Caviinae and Hydrochoerinae. All lacrimal contacting sutures closed late, relative to the sutural margins of the alisphenoid, within the New World porcupines (Erethizontidae) reflecting a marked contrast to the early closure of selected lacrimal sutures amongst other members of Caviomorpha, especially Octodontidae and Caviinae.

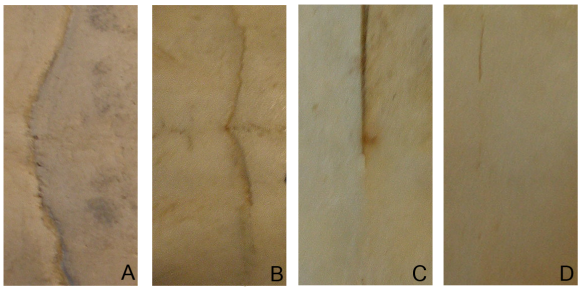

Figure 2.4: Illustration of suture sites displaying varying levels of closure: completely open - score 1 (A), 1/4 closed - score 2 (B), 1/2 closed - score 3 (C) and completely closed - score 4(D).

Heterochronies in the Bathyergomorphi

The maxillo-palatine suture closed relatively late amongst members of Bathyergomorphi, though this suture was also found to close late amongst Erethizontidae, specifically *Sphiggurus* and, in reverse, comparatively early within Dasyproctidae. Species belonging to Hystricidae were characterised by late closure of supraoccipital sutures relative to sutures joining the frontal and maxillary to the lacrimal. Similarly the late closure of the naso-frontal relative to sutures linked with the maxillary was also observed within Hystricidae.

Figure 2.5: Growth series of *Dasyprocta leporina* from the Naturhistorisches Museum Basel (from left to right NHMBa-8409, 6955, 7647, 6645). Scale = 2cm.

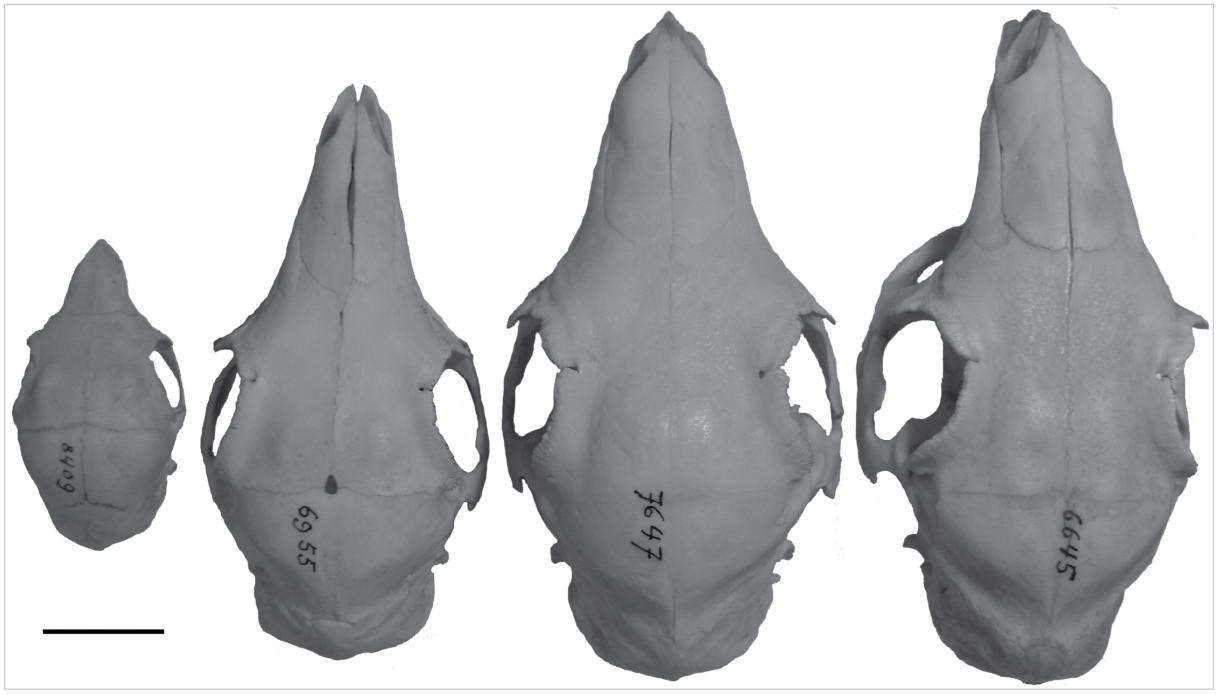

Species	% open (score 1)	% closed (score 4)	% closure
*Marmota marmota**	0	0	43
*Castor fiber**	42	0	34
*Ondatra zibethicus**	23	10	54
*Nannospalax ehrenbergi**	3	6	75
*Rhizomys sumatrensis**	39	0	49
Thryonomys swinderianus	52	0	34
Hystrix cristata	26	0	40
Hystrix brachyura	0	3	44
Atherurus africanus	39	3	39
Bathyergus suillus	42	29	56
Sphiggurus villosus	13	0	52
Sphiggurus insidiosus	0	10	60
Erethizon dorsatum	29	3	49
Coendou prehensilis	0	10	55
Cuniculus paca	52	0	35
Myoprocta acouchy	52	10	38
Dasyprocta leporina	45	0	36
Dasyprocta fuliginosa	61	3	38
Kerodon rupestris	52	3	44
Hydrochoerus hydrochaeris	68	0	33
Dolichotis patagonum	42	0	37
Galea spixii	55	3	40
Cavia porcellus	42	0	40
Cavia aperea	39	6	43
Spalacopus cyanus	52	13	46
Octodon degus	42	0	43
Proechimys cuvieri	32	0	42
Makalata armata	32	10	54
Myocastor coypus	32	0	40
Capromys pilorides	35	3	40
Chinchilla lanigera	29	0	41

Table 2.3b: Quantification of closure per species, including outgroup taxa (*), for all crania studied. Percentage of suture sites scoring 1 (open) or 4 (closed) for each species and evaluation of overall closure exhibited by a given species.

Comparison of suture closure pattern with previous pattern suggested for hominoids

When compared with Krogman's (1930) pattern, the suture closure patterns for sampled species revealed τ correlations between -0.08 and 0.49 (Table 2.5a). A significant positive relationship ($p < 0.05$) with Krogman's (1930) pattern existed among ten of the 31 species analysed, ranging from $\tau = 0.28$ to $\tau = 0.43$. Particularly, all representatives of *Hystrix* and *Dasyprocta* exhibited a significant relationship to Krogman's (1930) pattern while the highest level of significance was displayed by *Cuniculus paca* ($p<0.001$, $\tau = 0.49$). Notably, the five largest average cranial lengths belonged to those species that exhibited a suture pattern which significantly correlated with Krogman's: ranging from 129mm for *C. paca* to 96mm for *Dasyprocta leporina* (Table 2.5a). With the exception of Bathyergomorphi ($t = 0.23$, $p <0.05$), the τ correlations for monophyletic clades were weakly positive. When examining the patterns closely (Table 2.5b) this may be evidenced by the relatively late closure of facial sutures (premaxillo-maxillary, naso-frontal, maxillo-jugal, jugo-squamosal and premaxillo-nasal) that characterises each clade. Sutures within the facial division were penultimate to close within Krogman's (1930) pattern.

Event pairs for phylogenetic reconstruction

The topology generated from PAUP*-4.0b10 (Swofford, 2002) analyses of the event pair matrix (Fig. 2.8) yielded only one grouping that was congruent with the evolutionary relationships taken from the literature (Fig. 2.1).

Correlation of suture closure with cranial length

Level of suture closure displayed a significant negative correlation with cranial length within species for 11 out of 31 species (Table 2.6). The most significant relationship between these two variables was exhibited by *C. paca*, and *N. ehrenbergi* ($p <0.01$). Four of the remaining 20 species displayed a marginally insignificant ($p = 0.06$-0.07) correlation between level of suture closure and cranial length.

Level of suture closure also displayed a significant correlation with cranial length between species (Fig. 2.9). A trend to a decrease in level of closure is coupled with an increase in cranial length, evidenced by a correlation coefficient of -0.45 ($p <0.05$).

DISCUSSION

Although minor differences in suture closure sequence existed between species, the overall sequence was conserved both across the group and, to an increasing degree, within selected clades (Table 2.3). For several species and selected clades (Table 4a) this pattern correlated significantly with that found in

hominoids (Krogman, 1930) and hyaenas (Schweikher, 1930). The application of sequence heterochrony methods to investigate suture closure revealed unique patterns occur among several clades but equally numerous closure events are characterised in part by parallelism.

Suture closure pattern quantification between sites and species

The capybara (*Hydrochoerus hydrochaeris*) had the greatest percentage of sutures remaining fully open (68%). The pattern of suture closure exhibited by this species also correlated significantly with Krogman's (1930) pattern (p<0.05). In contrast none of the species that displayed the highest levels of overall suture closure (54-75%) exhibited a significant correlation to the pattern proposed by Krogman (1930); these species actually displayed the lowest levels of significance (p<0.75) and included two subterranean rodents (*B.suillus* and *N.ehrenbergi*) in addition to three out of four members of New World porcupines (Erethizontidae). The anomalous species within Erethizontidae was *Erethizon dorsatum*: specimens belonging to this species exhibited marginally less overall suture closure (49%) and an increased amount of complete patency (29%) compared to other group members. Contrasting with the other representative members of Erethizontidae, *E. dorsatum* adopts a scansorial, not arboreal, mode of life and is a larger animal: the lowest average body mass for *E. dorsatum* is more than twice the highest value for either *Sphiggurus* or *Coendou* whilst, similarly, ranges in body length between the latter two genera and the former species barely overlap (Table 2.1).

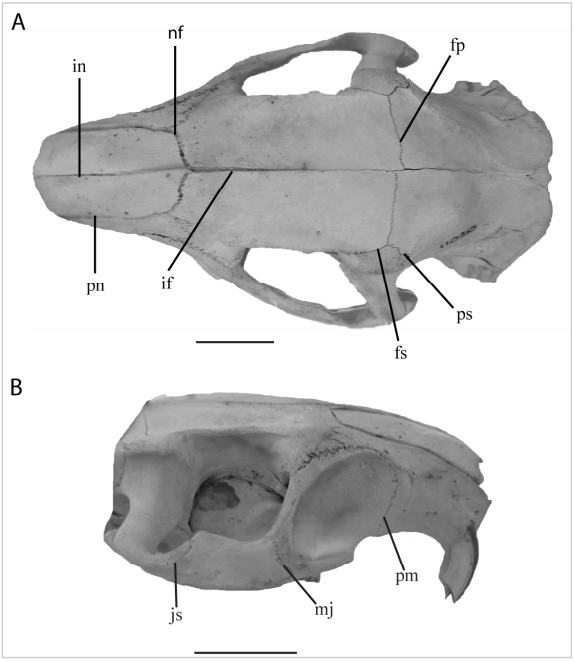

Figure 2.6: Dorsal (A) and lateral (B) view of *Myocastor coypus*. Open (score 1) cranial sutures indicated as follows: interfrontal (if), premaxillo-nasal (pn), internasal (in), fronto-parietal (fp), fronto-squamosal (fs), parieto-squamosal (ps), naso-frontal (nf), jugo-squamosal (js), maxillo-jugal (mj), premaxillo-maxillary (pm). Scale bar represents 2cm.

Sutures displaying the highest levels of closure across all sampled species were the exoccipito-basioccipital (87%), interparietal (86%), exoccipito-supraoccipital (84%), and the interpalatine (81%) (Table 2.3a). Herring (1972)

proposed the early fusion of palatal sutures in peccaries was directly related to high levels of palatal stress. A similar pattern was not demonstrated here: the interpalatine was the only suture within the palatal division (Krogman, 1930) to exhibit a high degree of overall closure, other sutures within this division include the intermaxillary (40% overall closure) and interpremaxillary (32%). Expectedly the palatal sutures did not cluster together within the closure pattern sequence (Table 2.5b) whereas, in comparison, the facial sutures, previously implicated in cranial stress mitigation, all exhibit an analogous degree of overall closure (26-30%).

Chopra (1957) found high intraspecific and intrageneric variability in suture closure of monkeys but noted that each genus had a regular sequence. The number of specimens per species within our study ranged from nine to 37 (Table 2.1), and within species the range in cranial length varied from 13mm for *Galea spixii* to 204mm for *H. hydrochaeris* (Fig. 2.7), hence differing degrees of intraspecific variation are not completely comparable across the studied sample. Intraspecific variation was low for *Capromys pilorides*, *C. paca*, *M. marmota*, *N. ehrenbergi*, and *S. cyanus* whereas *C. prehensilis* and *M. coypus* exhibited a comparatively higher level of intraspecific variability. The species with the highest range of measured cranial length and the greatest overall cranial size (*H. hydrochaeris*) did not exhibit a high level of intraspecific variability perhaps indicating the limited effect of differing cranial size.

Heterochronic shifts in suture pattern

Heterochronies recorded within Hystricognathi exhibit considerable parallelism, evidenced in part by the reconstruction of evolutionary relationships using event pairs (Fig. 2.8). A late closure of the lacrimal-associated

Clade	N	N_s	Kendall's W (0 – 1)	Friedman χ^2_r
Hystricognathi	26	520	0.57	$p < 0.001$
Caviomorpha	21	435	0.64	$p < 0.001$
Caviidae	6	153	0.79	$p < 0.001$
Caviinae	3	70	0.84	$p < 0.001$
Cavoidea	10	236	0.71	$p < 0.001$
Dasyproctidae	3	53	0.86	$p < 0.001$
Echimyidae	2	35	0.89	$p < 0.025$
Erethizontidae	4	79	0.83	$p < 0.001$
Hystricidae	3	44	0.70	$p < 0.001$
Octodontidae	2	24	0.90	$p < 0.025$
Octodontoidea	6	100	0.67	$p < 0.001$

Table 2.4: Kendall's Coefficient of Concordance (Kendall's W statistic) and Friedman's chi square for selected clades: number of taxa (N) and number of specimens (N_s) detailed for each clade. W = 1 indicates identical suture closure sequence among clade members. Critical values based on (n -1) degrees of freedom.

Species	τ	*p*	Average cranial length recorded (mm)
*Marmota marmota**	0.43	<0.01	56.7
*Castor fiber**	0.33	<0.05	77.6
*Ondatra zibethicus**	-0.01	<0.75	66.7
*Nannospalax ehrenbergi**	-0.05	<0.75	59.4
*Rhizomys sumatrensis**	0.19	<0.25	65.2
Thryonomys swinderianus	0.39	<0.01	80.1
Hystrix cristata	0.34	<0.05	125.4
Hystrix brachyura	0.39	<0.01	99.7
Atherurus africanus	0.26	<0.10	90.5
Bathyergus suillus	0.01	<0.75	72.2
Sphiggurus villosus	0.12	<0.50	66.1
Sphiggurus insidiosus	-0.04	<0.75	65.5
Erethizon dorsatum	0.20	<0.25	82.9
Coendou prehensilis	0.15	<0.50	75.7
Cuniculus paca	0.49	<0.001	128.8
Myoprocta acouchy	0.40	<0.01	71.1
Dasyprocta leporina	0.37	<0.01	96.1
Dasyprocta fuliginosa	0.45	<0.01	74.7
Kerodon rupestris	0.18	<0.25	71.4
Hydrochoerus hydrochaeris	0.28	<0.05	117.3
Dolichotis patagonum	0.41	<0.10	95.4
Galea spixii	0.25	<0.10	56.0
Cavia porcellus	0.22	<0.25	59.8
Cavia aperea	0.20	<0.25	60.2
Spalacopus cyanus	0.21	<0.25	44.0
Octodon degus	0.19	<0.25	47.6
Proechimys cuvieri	-0.08	<0.75	58.9
Makalata armata	0.01	<0.75	46.8
Myocastor coypus	0.03	<0.75	90.6
Capromys pilorides	0.29	<0.05	84.1
Chinchilla lanigera	0.28	<0.10	58.27

Table 2.5a: Correlation, using Kendall's tau (t) rank, of suture pattern per species in relation to the classical paradigm (Krogman, 1930), outgroups marked with an asterisk (*).

sutures relative to alisphenoid sutural boundaries was found to distinguish Erethizontidae. This shift also occurred within Muroidea, though only three out of four lacrimal sutures closed late. Nonetheless within the reconstructed tree (Fig. 2.8) *N. ehrenbergi* clusters amongst the erethizontids and when evaluating the position of the lacrimal sutures within the suture sequence for each of the three representatives of Muriodea, *N. ehrenbergi* was found to display the latest occurrence of lacrimal suture closure. The correct reconstruction of sister species *D. leporina* and *D. fuliginosa* reflects the early closure of the maxillo-palatine and palate-alisphenoid shared by these two species: the palate-alisphenoid closes later for all other taxa.

Octodontids are characterised by the greatest amount of heterochronic shifts per branch. This group was represented by six taxa and 100 specimens, the increased number of heterochronic shifts likely reflects the divergent nature of the closure sequences for each of the species within the group: the Kendall's W for Octodontoidea was 0.67, which, in the context of the observed trend to an increased level of correspondence coupled with a decreased number of inclusive taxa, is comparatively low.

Ecological correlates with suture closure pattern

Although cranial sutures form in the absence of muscle activity, research directed to understanding the biomechanical role of sutures (e.g. Jaslow, 1990; Rafferty et al. 2003) has supported experimental evidence that the fine details of suture morphology are secondary responses to extrinsic forces (Moss, 1957). Sutures associated with the facial region of the skull in pigs have been implicated in a protective role for the facial bones they join (Rafferty et al. 2003). Specifically the premaxillary and internasal bones of pigs are subject to a high degree of strain during mastication, and deformation within these sutures is considered to circumvent high levels of strain in the delicate facial bones (Rafferty et al. 2003; Sun et al. 2004). From their study of hominoid ectocranial sutures, Cray et al. (2008) noted that sutures subject to the influence of masticatory forces exhibit the least amount of interspecific variation in degree of closure. For all species studied here, the highest level of patency was exhibited by the seven, representative, facial division sutures: 45-81% of specimens displayed completely open sutures at these sites (Table 2.3a). Moreover inspection of suture patterns for individual species indicated no fewer than four out of seven facial sites were last to close while sutures that belonged to other divisions did not share repeated associations between species, perhaps indicating suture closure pattern conservatism reflects the occurrence of stress related constraint within the facial region.

Nevertheless, in mammals the muscles of mastication are complex and while the same terminology is used for each muscle, these references relate not to function, but location of bone attachment. Hence rodents have an anteriorly directed, fascially subdivided masseter muscle, modified to strengthen propalinal jaw movement, that has little resemblance in function to the vertical, unitary masseter muscle in humans (Ball & Roth, 1995; Herring, 2007) making difficult a direct comparison of the strain loading environment that may influence suture patency within these two groups. Interestingly, the facial sutures also closed last among *B. suillus, Rhizomys sumatrensis* and *N. ehrenbergi*; these rodents exhibit osteological modifications for their fossorial mode of life (Fig. 2.1), several of which impact upon jaw musculature (Topachevskii, 1976; Stein, 2000). Among hystricognaths the anterior masseter medialis muscle, originating largely on the rostrum, passes through an enlarged infraorbital foramen before descending to insert on the lower jaw (Moore, 1981). Subterranean rodents typically have reduced, degenerate eyes; this is coupled with a migration in site of origin of the jaw musculature; moreover most bathyergids (*B. suillus*) possess a small infraorbital foramen that is not penetrated by the masseter muscle. Instead the zygomatic arches are posteriorly widened to accommodate the enlarged jaw muscles making the skull appear wedge-shaped, a feature especially prominent in *Nannospalax* (Stein, 2000). The aforementioned cranial features of subterranean rodents, compared with species that adopt a non-fossorial

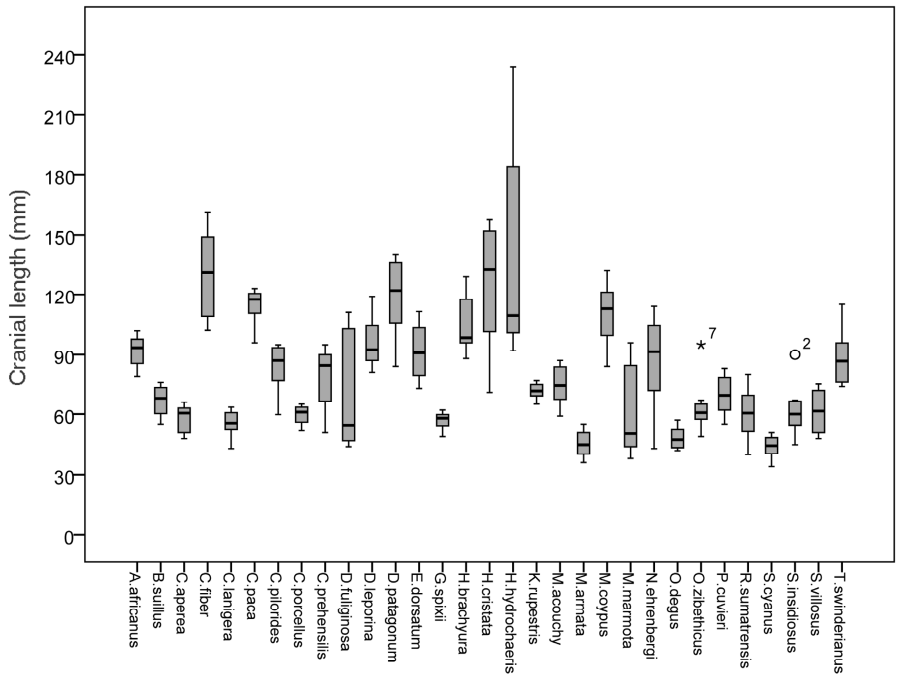

Figure 2.7: Box plot illustrating cranial size variation among specimens studied.

habit, likely create differing levels of strain on analogous cranial elements which may in turn be realised by heterochronies in suture closure pattern, since sutures have been shown to exhibit varying degrees of tension in response to local muscle contractions (Herring & Teng, 2000).

Nevertheless, an exact causal relationship between a specific heterochronic event (e.g. relative late closure of the naso-frontal suture) and an ecological factor cannot be established without a considerable degree of speculation. Further elucidation is beyond the scope of this work, and could be achieved in part by a comparative study, directly extending the methods applied herein. Indeed, morphofunctional analyses of postcranial elements have indicated ecomorphological factors are correlated with, though not a major determinant of, variation in the scapular shape of caviomorph rodents (Morgan, 2009).

Comparison of suture closure pattern with previous pattern suggested for hominoids

Examination of the suture closure pattern across Hystricognathi revealed sutures located at the cranial base and vault, including the exoccipito-basioccipital, exoccipito-supraoccipital, and basisphenoid-presphenoid were the first to close (Table 2.5b). Indeed sutures contacting the exoccipital displayed the highest levels of closure across all species

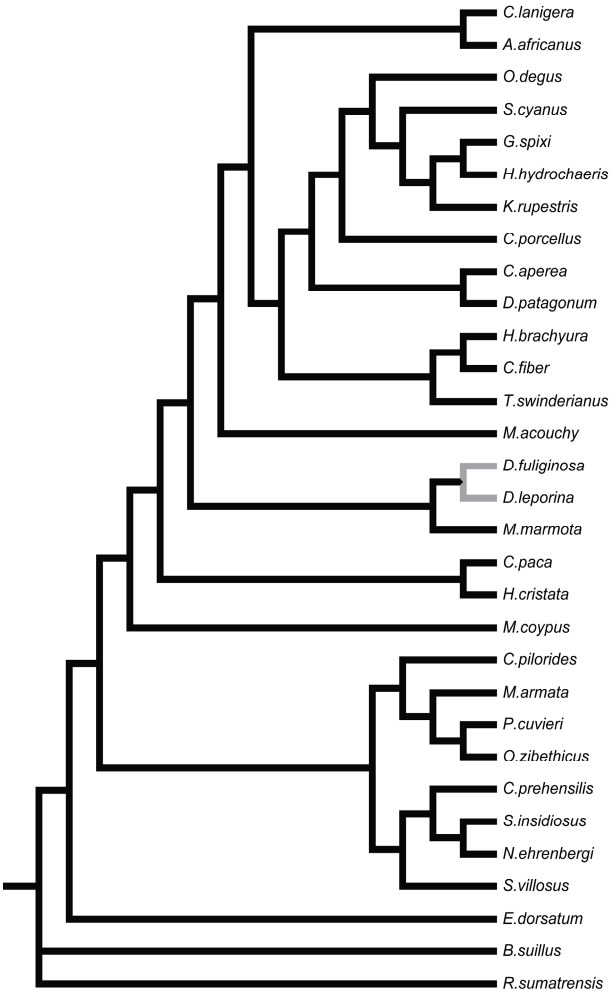

Figure 2.8: Most-parsimonious tree generated using PAUP*4.0b10 (Swofford, 2002) from parsimony analysis of event pair character matrix (3432 steps, CI=0.26, RI=0.39). The only sister group relationship preserved from the composite tree topology (see Fig. 2.1) is highlighted in grey.

(Table 2.3a). This finding compares positively with the order Krogman (1930) identified, and is supported, though not to a significant level, by a positive τ value of 0.19. Suture closure was similarly conserved towards the latter stages of the pattern reported for Hystricog-

nathi (Table 2.5b). The last seven sutures to close were all located in the facial region of the skull. In contrast Krogman (1930), and also Schweikher (1930), found the facial division closed before the cranio-facial division (alisphenoid-orbitosphenoid, lacrimal-frontal, orbitosphenoid-frontal). Towards the earlier, compared with the latter, stages of the closure pattern, hystricognaths were found to exhibit a

Table 2.5b: Suture closure patterns for Hystricognathi (26 taxa), Caviomorpha (21 taxa) and Bathyergomorphi (5 taxa) beginning with the first closure event. Simultaneously occuring events are shaded grey.

Hystricognathi	Caviomorpha	Bathyergomorphi
Interparietal	Interparietal	Exoccipito-supraoccipital
Exoccipito-basioccipital	Interpalatine	Interparietal
Exoccipito-supraoccipital	Exoccipito-basioccipital	Exoccipito-basioccipital
Interpalatine	Exoccipito-supraoccipital	Interpalatine
Basisphenoid-presphenoid	Basisphenoid-presphenoid	Palato-orbitosphenoid
Palato-orbitosphenoid	Palato-orbitosphenoid	Basisphenoid-presphenoid
Maxillo-lacrimal (o)	Maxillo-lacrimal (o)	Intermaxillary
Alispheno-orbitosphenoid	Alispheno-orbitosphenoid	Maxillo-Palatine (v)
Lacrimo-frontal (o)	Lacrimo-frontal (o)	Interfrontal
Basisphenoid-basioccipital	Basisphenoid-basioccipital	Maxillo-lacrimal (o)
Interfrontal	Orbitospheno-frontal	Alispheno-orbitosphenoid
Orbitospheno-frontal	Interfrontal	Supraoccipito-parietal
Maxillo-Palatine (v)	Palate-alisphenoid	Lacrimo-frontal (f)
Maxillo-lacrimal (f)	Maxillo-Palatine (v)	Maxillo-lacrimal (f)
Intermaxillary	Maxillo-lacrimal (f)	Basisphenoid-basioccipital
Palate-alisphenoid	Alispheno-squamosal	Lacrimo-frontal (o)
Lacrimo-frontal (f)	Lacrimo-frontal (f)	Fronto-parietal
Supraoccipito-parietal	Supraoccipito-parietal	Orbitospheno-frontal
Alispheno-squamosal	Intermaxillary	Fronto-squamosal
Fronto-squamosal	Pterygo-palatine (v)	Parieto-squamosal
Fronto-parietal	Fronto-squamosal	Alispheno-squamosal
Pterygo-palatine (v)	Fronto-parietal	Internasal
Parieto-squamosal	Supraoccipito-squamosal	Palate-alisphenoid
Exoccipito-squamosal	Exoccipito-squamosal	Interpremaxillary
Supraoccipito-squamosal	Parieto-squamosal	Exoccipito-squamosal
Interpremaxillary	Interpremaxillary	Naso-frontal
Premaxillo-maxillary (f)	Premaxillo-maxillary (f)	Premaxillo-maxillary (f)
Internasal	Premaxillo-maxillary (v)	Supraoccipito-squamosal
Premaxillo-maxillary (v)	Mandibular symphysis	Maxillo-jugal
Mandibular symphysis	Naso-frontal	Pterygo-palatine (v)
Naso-frontal	Internasal	Premaxillo-maxillary (v)
Maxillo-jugal	Maxillo-jugal	Mandibular symphysis
Jugo-squamosal	Jugo-squamosal	Jugo-squamosal
Premaxillo-nasal	Premaxillo-nasal	Premaxillo-nasal

relatively random closure of the craniofacial sutures (Table 2.5b).

When considering suture closure pattern at a specific level Kendall's τ values supported a positive correlation with Krogman's (1930) pattern; 11 out of 31 species displayed a significant correlation and five of these species exhibited the largest average cranial lengths from the total sampled species (Table 2.5a). All members of Dasyproctidae (Fig. 2.1, Table 2.5a) were found to display a significant relationship to the closure pattern previously proposed for hominoids (Krogman, 1930); members of this group exhibited average cranial lengths between 71-96mm (Fig. 2.6). Sister group Cuniculidae, represented by *C. paca* (Fig 2.1), also exhibited a similar, significant relationship (Table 2.5a) and had the largest average cranial length (129mm) of all species studied. This shared similarity in suture pattern supports close association between these two families, recently sustained by molecular analyses (Rowe & Honeycutt, 2002).

Utility of event pair data for phylogenetic reconstruction

The non-independence of event pair data makes their application to phylogenetic analyses potentially inappropriate (Binninda-Emonds et al. 2002, Schulmeister & Wheeler, 2004; Harrison & Larsson, 2008); similar to recent investigation of mammalian cranial

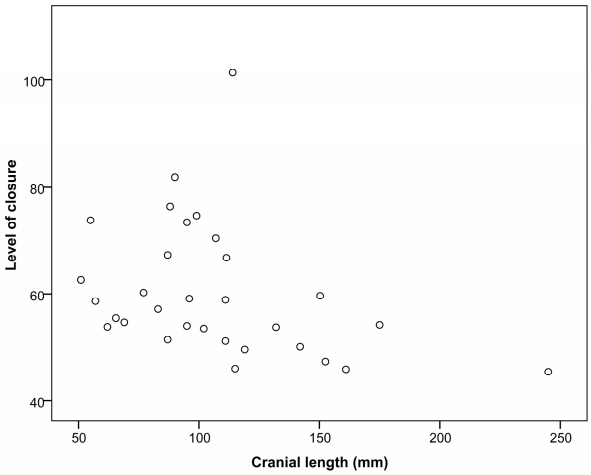

Figure 2.9: Relationship between measured cranial length and level of suture closure, based upon raw closure scores, for each of the 31 sampled species (Spearman's Correlation Coefficient, -0.45, $p < 0.05$).

(Sánchez-Villagra et al. 2008) and postcranial ossification sequences (Weisbecker et al. 2008), the topology reconstructed from event pair data here retains few congruent groups with the phylogenetic framework taken from morphological and molecular analyses of these taxa.

Correlation of suture closure with cranial length

Cranial size was found to display a significant relationship with level of suture closure within species, for 11 of the 31 species sampled (Table 2.6). The use of suture closure as a guide to skeletal age for humans has been unequivocally revoked by several authors who report the erratic nature makes accurate age estimations difficult (Stewart, 1934; Singer, 1953; Powers, 1962; Sahni et al. 2005).

Species	Correlation coefficient	*p*
*Marmota marmota**	-0.38	0.07
*Castor fiber**	-0.46	0.05
*Ondatra zibethicus**	-0.19	0.31
*Nannospalax ehrenbergi**	-0.77	<0.01
*Rhizomys sumatrensis**	-0.57	0.07
Thryonomys swinderianus	-0.41	<0.05
Hystrix cristata	-0.54	0.05
Hystrix brachyura	0.17	0.56
Atherurus africanus	0.17	0.65
Bathyergus suillus	-0.52	0.10
Sphiggurus villosus	-0.42	<0.05
Sphiggurus insidiosus	-0.57	<0.05
Erethizon dorsatum	-0.03	0.91
Coendou prehensilis	-0.50	0.01
Cuniculus paca	-0.48	<0.01
Myoprocta acouchy	0.26	0.36
Dasyprocta leporina	-0.54	0.01
Dasyprocta fuliginosa	-0.73	<0.05
Kerodon rupestris	0.22	0.42
Hydrochoerus hydrochaeris	-0.13	0.47
Dolichotis patagonum	0.16	0.35
Galea spixii	0.33	0.19
Cavia porcellus	0.31	0.06
Cavia aperea	0.22	0.42
Spalacopus cyanus	0.11	0.79
Octodon degus	0.25	0.34
Proechimys cuvieri	-0.37	0.07
Makalata armata	0.24	0.48
Myocastor coypus	0.42	0.05
Capromys pilorides	0.43	0.24
Chinchilla lanigera	0.14	0.62

Table 2.6: Spearmans rank correlation coefficient and associated significance values (*p*) for the relationship between cranial length and level of suture closure. Outgroups marked with an asterisk (*).

Although cranial size was found to correlate weakly with level of suture closure for many species, an increased percentage of completely patent sutures (score 1, Table 2.3b) appears to couple with large body (>1kg mass) measurements, evidenced for *H. hydrochaeris* and *C. paca* and moreover within Dasyproctidae and Hystricidae, excepting *H. brachyura* for which the size range of representative specimens was diminished compared to sister *H. cristata* (Fig. 2.7). In correspondence, when examined between species, cranial length and level of suture closure are negatively correlated ($p > 0.05$) (Fig. 2.9).

CONCLUSIONS

Numerous heterochronies in ectocranial suture closure have occurred in the evolution of a diverse clade of mammals, the Hystricognathi. The overall pattern is similar but not equal to the scheme previously suggested to be characteristic for mammals (Krogman, 1930). Differing life history and locomotory strategies appear, in part, to be coupled with differing degrees of suture closure and pattern among several species; some heterochronic transformations in suture patterns do provide diagnostic features for clades of hystricognaths at different taxonomic levels.

The study of late growth using newly developed techniques to analyse sequence heterochrony is potentially a rich avenue of research to address the question 'is sequence heterochrony an important evolutionary mechanism in mammals?' (Bininda-Emonds et al. 2003, p. 335). As exemplified here, this question has different answers depending on the taxonomic level and the organ system or window of developmental timing examined.

ACKNOWLEDGEMENTS

This work was supported by the Swiss National Fond (3100A0-116013) to MRS-V and by a Forschungskredit of the Universität Zürich (Nr 3771) to LABW. We thank A. Ziems, W. Etter, M. Haffner, F. Mayer, S. Hertwig, H. van-Grouw, M. Hiermeier, R. Kraft, J. Cuisin, and B. Herzig for providing access to the collections in their charge. We also thank Anjali Goswami and Ingmar Werneburg for helpful discussion during the preparation of this manuscript, Janine Ziermann for guidance with analyses, and two anonymous reviewers for their useful comments on an earlier version of this paper.

REFERENCES

Adkins RM, Gelke EL, Rowe D, et al. (2001) Molecular phylogeny and divergence time estimates for major rodent groups: Evidence from multiple genes. *Mol Biol Evo* **18**, 777-791.

Adkins RM, Walton AH, Honeycutt RL (2003) Higher level systematics of rodents and

divergence time estimates based on two highly congruent nuclear genes. *Mol Phylogenet Evo* **26**, 409-420.

Ball SS, Roth VL (1995) Jaw muscles of New World squirrels. *J Morphol* **224**, 265-291.

Bininda-Emonds ORP, Jeffery JE, Richardson MK (2003) Is sequence heterochrony an important evolutionary mechanism in mammals? *J Mammal Evol* **10**, 335-361.

Carrasco MA, Wahlert JH (1999) The cranial anatomy of *Cricetops dormitor*, an Oligocene fossil rodent from Mongolia. *Amer Mus Novitat* **3275**, 1-14.

Chopra SRK (1957) The cranial suture closure in monkeys. *Proc Zool Soc Lond* **128**, 67-112**.**

Cray J Jr, Meindl RS, Sherwood CC et al. (2008) Ectocranial suture closure in *Pan troglodytes* and *Gorilla gorilla*: Pattern and phylogeny. *Am J Phys Anthropol* **136(4)**, 394-399

Depew MJ, Compagnucci C, Griffin J (2008) Suture neontology and paleontology: the bases for where, when and how boundaries between bones have been established and have evolved. In *Craniofacial sutures: Development, Disease and Treatment* (eds Rice D), pp. 57-78. Basel: Karger Press.

Dolan KJ (1971) Cranial suture closure in two species of South American monkeys. *Am J Phys Anthropol* **35**, 109-118.

Galewski T, Mauffrey J-F, Leite YLR, et al. (2005) Ecomorphological diversification among South American spiny rats (Rodentia; Echimyidae): a phylogenetic and chronological approach. *Mol Phylogenet Evol* **34**, 601-615.

Giannini NP, Wible JR, Simmons NB (2006) On the cranial osteology of Chiroptera. I. *Pteropus* (Megachiroptera: Pteropodidae). *Bull Amer Mus Nat Hist* **295**, 1-134.

Goswami A (2007) Modularity and sequence heterochrony in the mammalian skull. *Evol Dev* **9**, 291-299.

Hall BK (1994) *Homology: the Hierarchical Basis of Comparative Biology*. San Diego: Academic Press.

Harrison LB, Larsson HCE (2008) Estimating evolution of temporal sequence changes: A practical approach to inferring ancestral developmental sequences and sequence heterochrony. *Syst Bio* **57**, 378-387.

Henderson JH, Longaker MT, Carter DR (2004) Sutural bone deposition rate and strain magnitude during cranial development. *Bone* **34**, 271-280.

Herring SW (1972) Sutures – a tool in functional cranial analysis. *Acta Anat*. **83**, 222-247.

Herring SW (1974) A biometric study of suture fusion and skull growth in peccaries. *Anat Embryol* **146**, 167-180.

Herring SW (1993) Epigenetic and functional influences on skull growth. In *The Skull Vol 1* (eds Hanken J, Hall BK), pp. 153-206.

Chicago: University of Chicago Press.

Herring SW (2007) Masticatory muscles and the skull: a comparative perspective. *Arch Oral Biol* **52**, 296–299

Honeycutt RL, Rowe DL, Gallardo MH (2003) Molecular systematics of South American caviomorph rodents: relationships among species and genera in the family Octodontidae. *Mol Phylogenet Evol* **26**, 476–489.

Huchon D, Douzery EPJ (2001) From the Old World to the New World: a molecular chronicle of the phylogeny and biogeography of hystricognath rodents. *Mol Phylogenet Evol* **20**, 238–251.

Jaslow CR (1990) Mechanical properties of cranial sutures. *J. Biomech*. **23**, 313-321.

Jeffery JE, Bininda-Emonds ORP, Coates MI, et al. (2005) A new technique for identifying sequence heterochrony. *Syst Biol* **54**, 230-240.

Klingenberg CP (1998) Heterochrony and allometry: the analysis of evolutionary change in ontogeny. *Biol Rev* **73**, 79-123.

Krogman WM (1930) Studies in growth changes in the skull and face of anthropoids: Ectocranial and endocranial suture closure in anthropoids and Old World apes. *Am J Phys Anthropol* **46**, 315-353.

McKenna MC, Bell SK (1997) *Classification of Mammals above the Species Level*. New York: Columbia University Press.

Mess A (2003) Evolutionary transformations of chorioallantoic placental characters in Rodentia with special reference to hystricognath species. *J Exp Zool Comp Exp Biol* **299A**, 78-98.

Mess A (2007) Development of the chorioallantoic placenta in *Octodon degus* – a model for growth processes in caviomorph rodents? *J Exp Zool Mol Devel Evol* **308B**, 371-383.

Moore WJ (1981) *The Mammalian Skull (Biological structure and function 8)*. Cambridge: Cambridge: University Press.

Morgan CC (2009) Geometric morphometrics of the scapula of South American caviomorph rodents (Rodentia: Hystricognathi): form, function and phylogeny. *Mamm Biol* **74**, 497-506.

Morriss-Kay GM, Wilkie AOM (2005) Growth of the normal skull vault and its alteration in craniosynostosis: insights from human genetics and experimental studies. *J Anat* **207**, 637-653.

Moss ML (1957) Experimental alteration of sutural area morphology. *Anat Rec* **127**, 569-590.

Nowak RM (1999) *Walker's Mammals of the World, 6th Edition*. Baltimore: The John Hopkins University Press.

Nunn CL, Smith KK (1998) Statistical analyses of developmental sequences: The craniofacial region in marsupial and placental mammals. *Am Nat* **152**, 82-101.

Ogle RC, Tholpady SS, McGlynn KA, et al.

(2004) Regulation of Cranial Suture Morphogenesis. *Cells Tissues Organs* **176**, 54-66.

Opperman LA (2000) Cranial sutures as intramembranous growth sites. *Dev Dyn* **219**, 472-485.

Opperman LA, Sweeney TM, Redmon J, et al. (1993) Tissue interactions with underlying dura mater inhibit osseous obliteration of developing cranial sutures. *Dev Dyn* **198**, 312–322.

Powers R (1962) The disparity between known age and sex as estimated by cranial suture closure. *Man* **84,** 52-54.

Rafferty KL, Herring SW, Marshall CD (2003) Biomechanics of the rostrum and the role of facial sutures. *J Morphol* **257**, 33-44.

Rice D (1999) *Molecular Mechanisms in Calvarial Bone and Suture Development*. *PhD thesis*. Helsinki: Helsinki University Press.

Rowe DL, Honeycutt RL (2002) Phylogenetic relationships, ecological correlates, and molecular evolution within the Caviodea (Mammalia, Rodentia). *Mol Biol Evol* **19**, 263-277.

Sahni D, Jit I, Sanjeev N (2005) Time of closure of cranial sutures in northwest Indian adults. *Forensic Sci Int* **148**, 199-205.

Sánchez-Villagra MR (2002) Comparative patterns of postcranial ontogeny in therian mammals: an analysis of relative timing of ossification events. *J Exp Zool Mol Devel Evol* **294B**, 264-273.

Sánchez-Villagra MR, Aguilera OA, Horovitz I (2003) The anatomy of the world's largest extinct rodent. *Science* **301**, 1708-1710.

Sánchez-Villagra MR, Goswami A, Weisbecker V, et al. (2008) Conserved relative timing of cranial ossification patterns in early mammalian evolution. *Evol Dev* **10**, 519-530.

Schulmeister S, Wheeler WC (2004) Comparative and phylogenetic analysis of developmental sequences. *Evol Dev* **6**, 50-57.

Schultz AH (1940) Growth and development of the chimpanzee. *Contr Embryol Carneg Inst* **170**, 1-63.

Schultz AH (1941) Growth and development of the orang-utan. *Contr Embryol Carneg Inst* **182**, 57-110.

Schultz AH (1942) Growth and development of the proboscis monkey. *Bull Mus Comp Zool Harv* **89**, 277-314.

Schweikher FP (1930) Ectocranial suture closure in hyaenas. *Amer J Anat* **45**, 443-460.

Singer R (1953) Estimation of age from cranial suture closure: a report on its unreliability. *J Foren Med* **1**, 52-59.

Smith KK (1997) Comparative patterns of craniofacial development in eutherian and metatherian mammals. *Evolution* **51**, 1663-1678.

Smith KK (2001) Heterochrony revisited: the evolution of developmental sequences. *Biol*

J Linn Soc **73**, 169-186.

SPSS Inc (2007) *SPSS 16.0 for Windows Release 16.0.1*. Chicago, IL.

Stein BR (2000) Morphology of subterranean rodents. In *Life Underground: the biology of subterranean rodents* (eds Lacey EA, Patton JL, Cameron GN), pp. 19-61. Chicago: Chicago University Press.

Stewart TD (1934) Sequence of epiphyseal union suture closure in Eskimo and American Indians. *Am J Phys Anthropol* **19**, 433-452.

Sun Z, Lee E, Herring SW (2004) Cranial sutures and bones: Growth and fusion in relation to masticatory strain. *Anat Rec* **276A**, 150-161

Swofford DL (2002) PAUP*: Phylogenetic Analysis using Parsimony. Version 4.0b10. Sinauer Associates, Sunderland, MA

Todd TW, Lyon D (1924) Endocranial cranial suture closure: its progress and age relationship I. Adult males of white stock. *Am J Phys Anthropol* **7**, 325-384.

Todd TW, Lyon D (1925a) Cranial suture closure: its progress and age relationship II. Ectocranial closure of males of white stock. *Am J Phys Anthropol* **8**, 23-43.

Todd TW, Lyon D (1925b) Cranial suture closure: its progress and age relationship III. Endocranial suture closure of adult males of Negro stock. *Am J Phys Anthropol* **8**, 47-71.

Todd TW, Lyon D (1924c) Cranial suture closure: its progress and age relationship IV. Ectocranial suture closure of adult males of Negro stock. *Am J Phys Anthropol* **8**, 149-168.

Topachevskii VA (1976) *Fauna of the USSR. Vol 3. Mammals. No 3. Mole rats, Spalacidae*. Leningrad: Nauka Publishers, Leningrad Section.

Wang Q, Strait DS, Dechow PC (2006) Fusion patterns of craniofacial sutures in rhesus monkey skulls of known age and sex from Cayo Santiago. *Am J Phys Anthropol* **131**, 461-485.

Weisbecker V, Goswami A, Wroe S, Sánchez-Villagra MR. (2008) Ossification heterochrony in the therian postcranial skeleton and the marsupial-placental dichotomy. *Evolution* **62**, 2027-2041 (DOI 10.1111/j.1558-5646.2008.00424)

Wilson DE, Reeder DM (2005) *Mammal species of the world: a taxonomic and geographic reference*. Washington DC: Smithsonian Institution Press.

Wu YD, Chien CH, Chao YJ, et al. (2007) Fourier analysis of human sagittal sutures. *Cleft Palate-Cran J* **44**, 482-493.

Zar JH (1999) *Biostatistical analysis 4th Edition.* New Jersey: Prentice Hall.

CHAPTER 3

Diversity trends and their ontogenetic basis: an exploration of allometric disparity in rodents

CHAPTER 3
Diversity trends and their ontogenetic basis: an exploration of allometic disparity in rodents

Article submitted to *Proceedings of the Royal Society B* on 26th October 2009, accepted for publication on 23rd November 2009

Reference: **Wilson LAB**, Sánchez-Villagra MR. 2010. Diversity trends and their ontogenetic basis: an exploration of allometric disparity in rodents. *Proc. R. Soc. B* **277**: 1227-1234

Abstract

It has been hypothesized that most morphological evolution occurs by allometric differentiation. Because rodents encapsulate a phenomenal amount of taxonomic diversity and, among several clades, contrasting levels of morphological diversity, they represent an excellent subject to address the question: how variable are allometric patterns during evolution? We investigated the influence of phylogenetic relations and ecological factors on the results of the first quantification of allometric disparity among rodents by exploring allometric space, a multivariate morphospace here derived from, and encapsulating all, the ontogenetic trajectories of 34 rodent species from two parallel phylogenetic radiations. Disparity was quantified using angles between ontogenetic trajectories for different species and clades. We found an overlapping occupation of allometric space by muroid and hystricognath species, revealing both clades possess similar abilities to evolve in different directions of phenotypic space, and anatomical diversity does not act to constrain the labile nature of allometric patterning. Morphological features to enable efficient processing of food serve to group rodents in allometric space, reflecting the importance of convergent morphology, rather than shared evolutionary history, in the generation of allometric patterns. Our results indicate that the conserved level of morphological integration found among primates cannot simply be extended to all mammals.

KEYWORDS**:** macroevolution; disparity; cranium; ontogeny; diet; phenotypic covariance structure

INTRODUCTION

Between species, populations, and even sexes, morphological traits exhibit an impressive diversity of scaling relationships with body size. Allometric differentiation among morphological traits is thought to drive the evolution of morphology (Frankino et al. 2005). Whilst allometry has long been a focus of study (Huxley 1932; Reeve & Huxley 1945; Jolicoeur 1963), most work has been directed to the consideration of adult morphologies, and it is only recently that methods have been proposed to provide quantification of the variety of ontogenetic trajectories (Gerber et al. 2008) making possible clade-wide comparisons of the role development plays in shaping morphospace occupation and structure.

Stemming from the concept of morphological disparity, a method to quantify the empirical distribution of taxa in morphospace (Foote 1992), and more precisely the associated underlying metrical framework, Gerber et al. (2007, 2008) have recently proposed the notion of "allometric disparity" as a means to quantify the variety of allometric patterns in a clade, that may be displayed in a phenotypic space termed "allometric space". The possibility to compare ontogenetic trajectories derived from the multivariate generalization of allometry, that is the first component of a principal component analysis of all traits for a particular species, was initially referred to by Klingenberg & Froese (1991) in part of their study on fish larvae. The ordination method was further explored in heterochrony and allometry studies on water striders (Klingenberg & Spence 1993; Klingenberg 1996a) but a name was not established. Similarly, previous clade-wide disparity studies have contrasted adult and juvenile disparity using the same principles but without defining a specific metric (e.g. Eble 2002; Zelditch et al. 2003).

Rodents are exceptional mammals both ecologically and taxonomically. Being the most species-rich group, and encapsulating a phenomenal level of morphological diversity, rodents provide an ideal group in which to study the evolution of allometric patterns. One factor promoting the near worldwide spread of rodents is their opportunistic feeding strategies, reflected in an array of dental (Wood 1955, 1959; Evans et al. 2007), muscular (Becht 1953) and cranial specializations (Hautier et al. 2008). Whilst feeding behaviour has been shown to characterize craniodental morphology among ungulates (Janis 1995; Mendoza et al. 2002) and carnivores (e.g. Van Valkenburgh 1989), few studies have addressed the role of dietary habits in shaping rodent cranial morphology (Samuels 2009).

The hystricognaths contrast to other rodent groups (Wilson & Sánchez-Villagra 2009); this monophyletic clade comprises comparatively few species (less than 13% of rodents;

Wilson & Reeder 2005) and yet contains members spanning several orders of magnitude in body size (Nowak 1999) and possessing numerous adaptations to locomotory style (Weisbecker & Schmidt 2007). Hystricognaths, restricted in distribution to South America (caviomorphs) and Africa (phiomorphs), possess attributes which contrast sharply with those of the taxonomically diverse muroid clade (1517 species; Carleton & Musser 2005) whose members show a comparatively diminished level of anatomical diversity (Steppan et al. 2004).

In the present study we provide the first exploration of allometric space for rodents. Allometric patterns among muroids and hystricognaths, two major rodent clades with contrasting attributes, are compared. First we assess to what extent alterations in growth dynamics reflect phylogenetic relationships and ecomorphological diversity encapsulated within each clade, and second whether species distribution in morphospace reflects the convergence of modifications to allometries during evolution as a consequence of shared feeding habits.

MATERIALS AND METHODS

Landmark data were collected from 1113 crania using a Microscribe MX5 Digitizer. Postnatal growth series, including juvenile and adult representatives from the hystricognath (617 specimens) and muroid (496 specimens) clades were chosen, based upon availability of adequate sample size, to cover the widest possible phylogenetic breadth and encapsulate an array of ecological and morphological diversity (Fig. 3.1, see supplementary material Appendix 3.1). Landmark data were recorded for 34 species: 17 from each of the two clades. Measurements for 17 cranial traits were derived from landmark data collected for each species, these are: premaxilla ventral length, premaxilla width at maxilla suture, palatine length, palatine width, occipital condyles width, skull length, nasal length, nasal width, frontal midline length, parietal midline length, jugal length, length of dental diastema, maximum interorbital width, basioccipital length, basioccipital width, basisphenoid length, and basisphenoid width. Following the multivariate generalization of allometry (Jolicoeur 1963), the first principal component represents the line of best fit to the multivariate data (Pearson 1901), whereby size is considered a latent variable that affects all the original variables simultaneously. Hence 34 principal component analyses were performed using log-transformed measurements; one for each species studied. Allometric space was computed for all species from the precept that the distribution of allometric growth can be visualized in the space defined by the normalized vector coefficients (PC1) of the original traits; thus

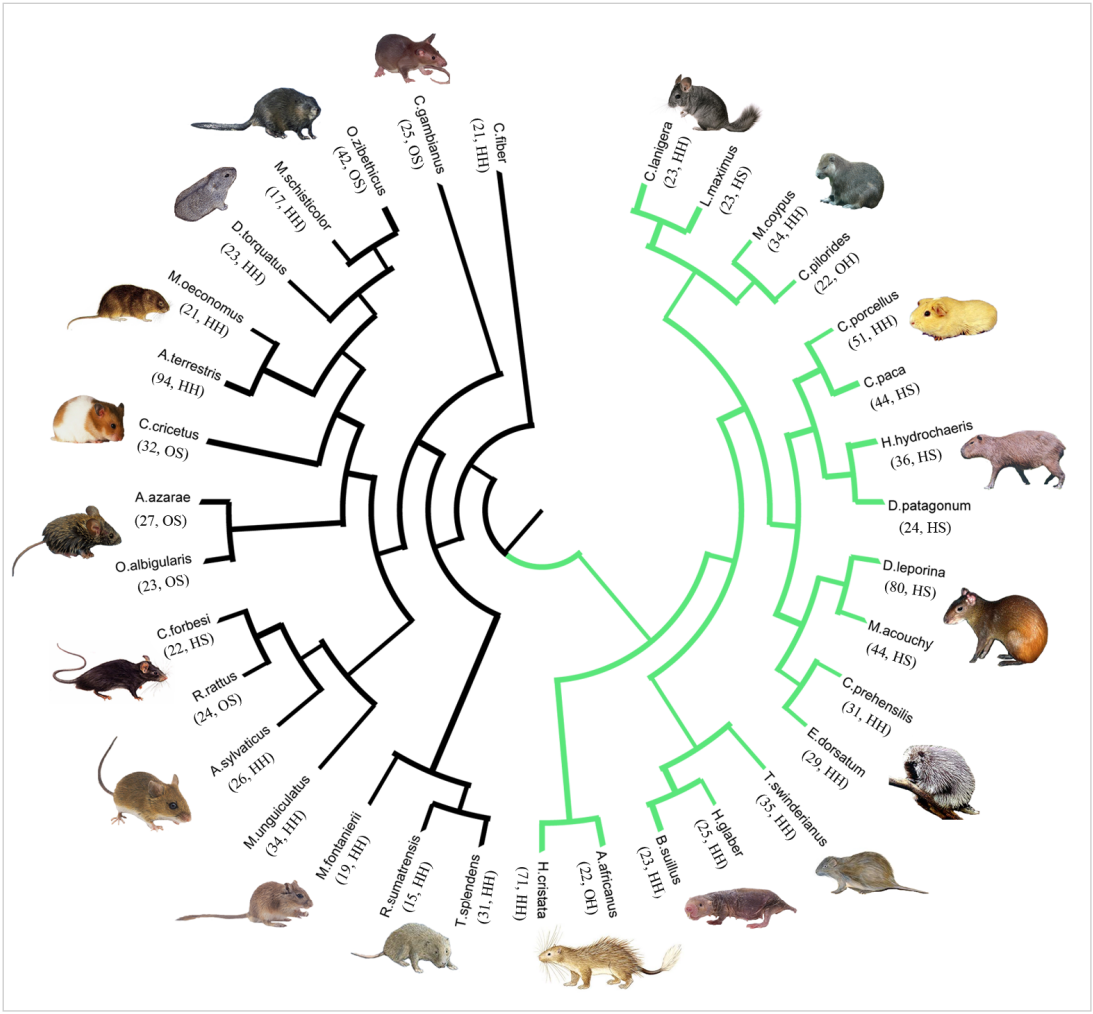

Figure 3.1: Phylogenetic relationships among the rodent species included in this study (see text for reference). Branch colours: black, muroids; green, hystricognaths. Parentheses include number of specimens measured and dietary category (Figure 3.3).

using the 34 originally calculated PC1 vectors as 'observations' for a second principal component analysis. The resultant principal component scores for the first and second axes were plotted to examine species distribution in the coefficient space. Each species is represented in allometric space by a single point which summarizes the allometric trajectory for that particular species.

Because each point in allometric space reflects a normalized vector (PC1), it is possible to quantify the distance in allometric space between any two species as an angle between their directions in the space of log-transformed measurements (e.g. Boitard et al. 1982; Gibson et al. 1984; Solignac et al. 1990). If two PC1 vectors x and y are normalized such that $x'x$ =1 and $y'y$ = 1 then the angle α between the two trajectories is computed as $\alpha = \arccos(x'y)$, the arccosine of the inner product of the two vec-

tors (Klingenberg 1996b). To estimate the standard error (SE) of the PC1 coefficients a bootstrap with replacement was performed for 1000 iterations, for each species. In allometric space, similar to morphospace, the spacing of taxa, also referred to as total variance, can be measured to provide a disparity metric. Total variance, computed as the trace of the covariance matrix of allometric patterns, can be quantified using an average angle between trajectories. Since a group of parallel trajectories would have inter-trajectory angles of zero and total variance would be minimal, the average angle metric provides an indication of spacing in state space. Average angle was used to quantify disparity among all species studied, and separately among muroids and hystricognaths. A vector of length p with all coefficients equal to $p^{-1/2}$ (where p = number of measured variables), termed the isometric vector, was used to assess allometric trends for given trajectories.

Information on dietary habit was compiled from the literature for all rodents studied. Anderson & Jones (1984) and Nowak (1999) were used for general reference, and for several species further details were obtained from a number of works including Gulotta (1971), Woods (1973), Willner et al. (1980) and Pérez (1992). Each species was assigned to one of four dietary categories based upon food materials that were primarily incorporated into

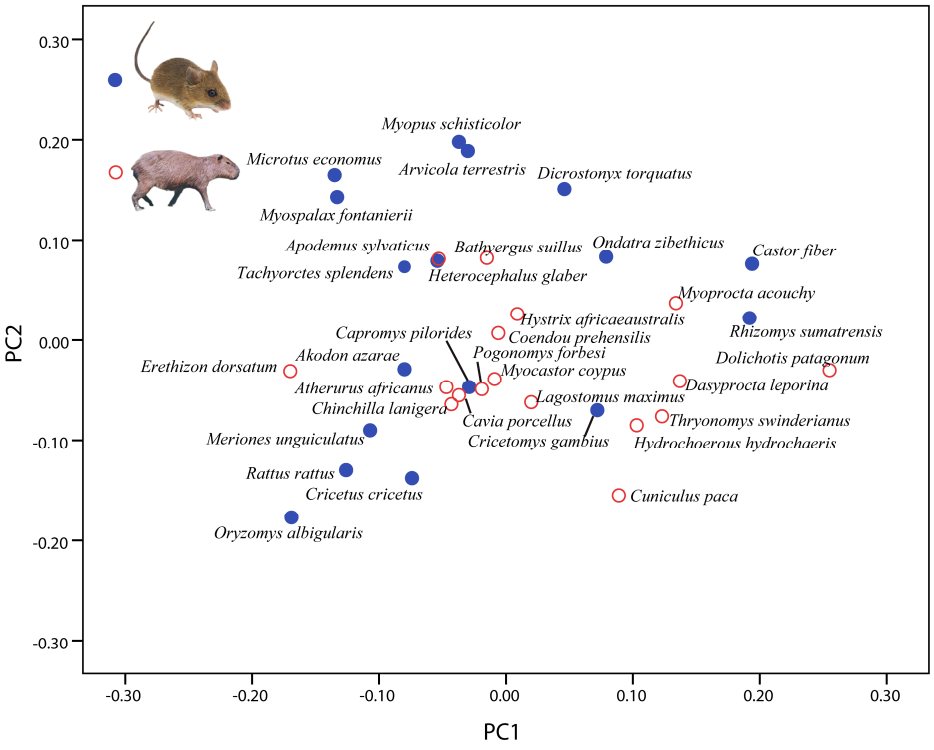

Figure 3.2: Allometric space for 34 rodent species. Clades: closed circels, muroid; open circles, hystricognath.

the diet: herbivore hard (HH), herbivore soft (HS), omnivore soft (OS) or omnivore hard (OH) (Fig. 3.1). These categories are similar to schemes adopted by Williams & Kay (2001) and Samuels (2009): rodents classified as having a hard diet (HH or OH) consistently incorporated roots, tubers, or bark in their diet in contrast to those assigned as having a soft diet (HS or OS), which included species primarily eating fruits, soft leaves, and shoots. Canonical variates analysis (CVA) was performed on the PCA scores accounting for 95% of the variance in allometric space. Based here upon the a priori assignment to one of the four dietary groups, CVA analysis produces a set of canonical variate axes which are expressed as linear combinations of the axes of the original multidimensional (allometric) space. The canonical axes reflect the maximal ratio of between group to within group distance and thus best separate the dietary groups.

Specimens were measured from the following collections: Naturhistorisches Museum Basel, Humboldt-Universität zu Berlin - Museum für Naturkunde, Zoological Museum - Natural History Museum of Denmark, Natural History Museum London, Naturalis Leiden, Zoologische Staatssammlung München, Naturhistoriska Riksmuseet Stockholm, and the Museum and Institute of Zoology—Polish Academy of Sciences, Warsaw.

Evolutionary relationships among rodent species examined here were reconstructed from various studies. For muroids, relationships are based upon the molecular studies of Steppan et al. (2004) and Blanga-Kanfi et al. (2009) and for the arvicolid rodents, Buzan et al. (2008). Relationships among the hystricognaths follow the molecular study of Huchon & Douzery (2001).

RESULTS

For the individual principal component analyses used to construct allometric space, the variance summarized by PC1 ranged across species from 93.1% to 97.3% and for the second component (PC2) variance reduced to between 1.1% and 5.6% across species (supplementary material Table 3.1). Hence, for the species studied here, the multivariate generalization of simple allometry provides an accurate reflection of growth, with PC1 axes representing the direction of growth in the space of log transformed measurements. PC1 coefficients were stable, indicated by associated standard error values ranging between 0.004 and 0.011.

The total variation encompassed within the studied species spans 11 dimensions of space, with the 2-dimensional subspace plotted here accounting for the maximal proportion of variance among the allometric trajectories. The first two dimensions of allometric space (Fig. 3.2) represent 45.7% of the variation among the

species studied with PC1 summarizing 24.5% and PC2 the remaining 21.2%. Examination of the individual principal component analyses reveals that allometric coefficients vary among species in relation to the isometric vector (0.242), a feature tying some species into loose clusters in allometric space. For instance the fossorial rodents *Bathyergus suillus*, *Heterocephalus glaber* and *Tachyorctes splendens* occupy a small cluster, sharing a positive allometry for jugal length. Because the axes in allometric space show the angular deviation from the mean ontogenetic trajectory in respect to the variables associated with the PC axis, large positive or negative values for a given axis represent large positive or negative deviations in ontogenetic growth, respectively. Thus species that have positive scores on PC1 are here characterized by a faster than average relative broadening of the palatal region compared to those species with negative scores for this axis, which would indicate a slower than average growth of the palate. PC2 is associated with relative lengthening of the rostral region (nasal length and premaxilla length) and hence the rostral region lengthens faster than average for species with positive scores on PC2, and slower than average for species with negative scores on this axis.

The occupation of allometric space for the rodent species studied here appears disparate, as indicated by an average angle of 17.1° between PC1 components (range 7.7° to 33.1°). Moreover, species belonging to either the muroid or hystricognath clades do not group exclusively together: each clade occupies an overlapping portion of allometric space. The average angle among PC1 components for hystricognath species is 17.2° whilst the trajectories of species belonging to the muroid clade are separated, on average, by 16.9° (supplementary material Tables 3.1 to 3.3). The trajectories of pairs comprising one species from each clade are, on average, 17.7° apart from one another. The average angle between hystricognaths is not significantly different from that between muroid species (U=8.6E03, $p = 0.32$) and neither clade comprises enough members that are more closely located to one another than they are to members belonging to the other clade to reflect a statistically significant difference (U=1.6E04, $p = 0.15$ for muroids; U = 1.9E04, $p = 0.2$ for hystricognaths). Within the muroid clade, partial relationships are recovered for the arvicolid rodents: species of voles and lemmings included in this study are positioned the furthest along PC2, with the exception of the muskrat *Ondatra zibethicus* located away from the upper portion of space. The PCA for *O. zibethicus*, in contrast to all other species studied, revealed that maximum interorbital width contributed the most to variance along PC1, with this variable exhibiting a positive allometry (0.379+/- 0.004SE, isometric vector = 0.242).

The narrowest angles between trajectories were associated with those species sharing the same dietary habits. Between species classified as hard herbivore (HH), the trajectories of *Apodemus sylvaticus* and *Castor fiber* were 7.7◦ apart, and those of *A. sylvaticus* and *Erethizon dorsatum* were 8.3◦ apart. *Atherurus atherurus* and *Capromys pilorides*, the two species studied here with an omnivorous diet incorporating hard materials (OH), had an inter-trajectory angle of 8.7◦ (see supplementary material Tables 3.4-3.6). The first canonical variate (CV1) accounted for 61.6% of variance and separated the herbivores with diets containing predominantly hard material (HH), typically having negative scores on CV1, from those eating mostly soft materials (HS) with positive CV1 scores (Fig. 3.3). Minor separation of groups occurred along the second canonical variate axis (CV2) which accounted for an additional 24.4% (Fig. 3.3). CVA correctly assigned 94.1% of rodents to their a priori dietary groups, with only two species being misclassified: *Chinchilla lanigera* was misclassified as being an omnivore (OS) instead of having a soft herbivorous diet (HS) and *Akodon azarae*, positioned close to zero on both axes, was classified as HH rather than OS.

DISCUSSION

The developmental basis for the morphological differences observed between

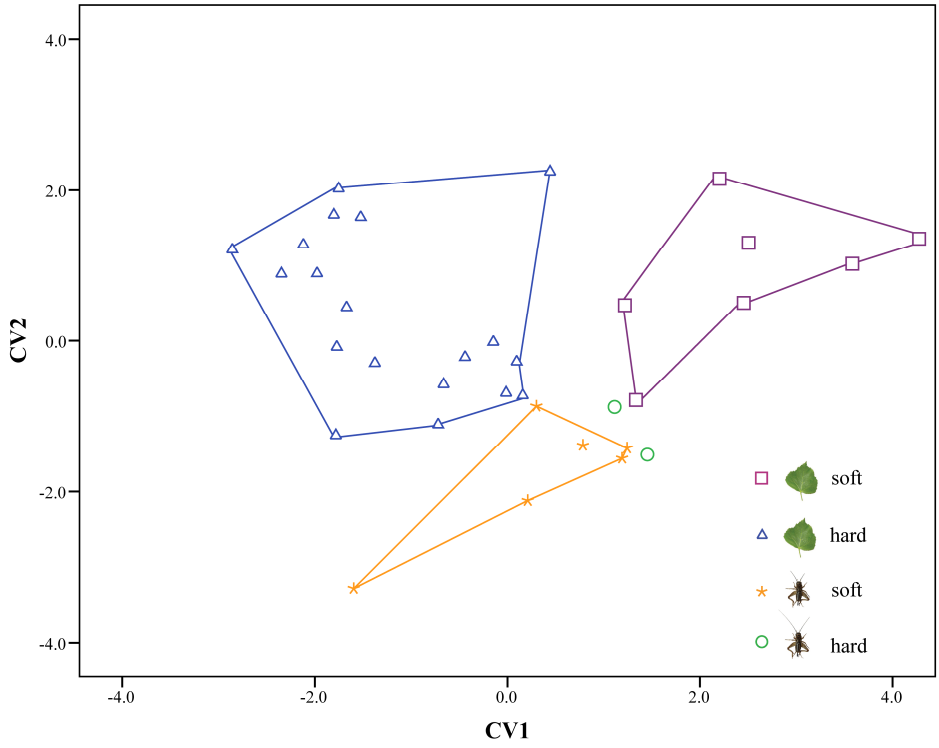

Figure 3.3: CVA of allometric space using predefined habit groups: triangles, herbivore hard (HH); circles, omnivore hard (OH); squares, herbivore soft (HS); asterisks, omnivore soft (OS).

species can be compared in an intuitive, effective manner using allometric space. Examination of the evolutionary modifications to growth trajectories through the quantification of the space encapsulating all realizable patterns provides a suitable stage to consider a large scale comparison of morphological diversity. The overlapping occupation of allometric space by muroids and hystricognaths reveals anatomical diversity does not act to constrain the labile nature of allometric patterning in rodents.

Since the rodents studied here encapsulate aquatic and semi-aquatic, arboreal, fossorial, and scansorial forms, spanning three orders of magnitude from the smallest examined species *Myopus schisticolor* (~26g) to the largest living rodent the capybara *Hydrochoerus hydrochaeris* (50 - 61kg), the diversity of allometries, exemplified by an average inter trajectory disparity of 17.1°, reflects the complex array of modifications possible and consequent within this diverse clade, whose adaptability has led to unparalleled success during the last 55 million years of mammalian evolution (Hartenberger 1985, Huchon et al. 2002). The overlapping and continual distribution within allometric space (Fig. 3.2) for the rodent species examined here is unexpected. Studies of the topology of form space indicate accessibility in morphospace may be anisotropic (Fontana & Schuster 1998, Stadler et al. 2001), and one would conceive that there might be 'gaps' in allometric space that reflect nonfunctional scaling relationships and thus species would be more clustered to reflect the adherence to, and selective forces acting for, the expression of particular allometric patterns such that functional size relationships, obtained by the scaling of traits, are maintained irrespective of genetic or environmental variation. Studies of much smaller scope, particularly the consideration of four crustacean species by Boitard et al (1982) and a study by Klingerberg & Zimermann (1992) investigating nine species of water striders, indicate taxon distribution in space is not continuous, though comparisons must be considered tentatively because the low number of species studied by these authors make difficult the reliable judgment of how real these 'gaps' are. In the latter study, angles between the ontogenetic trajectories of different species averaged 13.4°, while in their study using ten species of Antarctic fishes, Klingenberg & Ekau (1996) reported interspecific trajectory angles of between 2.5° and 8.7°, reflecting greater convergence of allometric patterning among these species than for the rodents studied herein. In contrast, range and absolute magnitude of interspecific trajectory angles reported here are comparatively smaller than those documented by Zelditch et al. (2003) between nine piranha species (22.7° to 76.5°). Thus given the present understanding of differences in allometries

between species, rodents do not appear to lie outside the current documented range of variability.

Because the methods of this work use the major axis of covariance, the results are of direct relation to the evolution of morphological integration and P matrices, the study of which considers trait associations measured through patterns of trait covariation or correlation (Olson & Miller 1958). In macroevolutionary theory, disparity and integration potentially reflect the same concept (Eble 2004), namely one of constraint: strong phenotypic integration may constrain the production of novelties and thus disparity, while conversely comparatively weak integration may make possible the generation of novelties and thus would be associated with an increase in disparity. Further, because functional and developmental constraints are expressed in patterns of integration (e.g. Zelditch et al. 1990), disparity will reflect the possibilities that remain for functional or developmental differentiation of integrated phenotypes. Our results indicate both muroids and hystricognaths possess similar abilities to evolve in different directions of phenotypic space. While broad clade-wide studies of cranial integration are at present lacking for rodents, studies for some other mammals appear to contradict this pattern. Other members of the euarchontoglires clade, particularly primates, have been shown to exhibit conserved patterns of integration, in contrast to the rodents here. Despite a broad range of diversity across the platyrrhine primates, in their extensive analysis Marroig & Cheverud (2001) found a common shared pattern of morphological integration across the whole cranium, independent of phylogenetic history, resulting from common patterns of skull development. Additionally, earlier study (Chevrud 1982, 1989) indicates Old World monkeys share this constrained pattern with their New World relatives, and work comparing living African apes and humans supports the notion that morphological integration is conserved across the entire order (Ackermann 2002, 2005).

Nevertheless, based on her broad study of cranial integration among carnivorans, Goswami (2006) showed that the conserved level of integration found among primates cannot simply be extended to all mammals. Our results further corroborate this finding, and suggest that the similar covariance structure that Steppan (1997) detected among six species of leaf-eared mice (*Phyllotis*) reflects limited genus level sampling. Moreover, when considering non-mammalian clades, a study of six piranha species (Fink & Zelditch 1996) reported labile levels of integration during ontogeny, suggesting rodents are not unusual in their ability to alter covariance structure during evolution. Similarly, studies that explicitly

tested developmental hypotheses in relation to cranial integration have revealed that developmental constraints are transient and flexible in muroid rodents (Zelditch & Carmichael 1989a, 1989b).

Links between dietary habit and dentition, particularly occlusal complexity (Evans et al. 2007), have been found among rodents. Cranial morphology has also been shown to display a significant relationship with differing demands of food processing inherent among varying life habits (Samuels 2009), evidenced here by the successful classification of species to dietary groups based upon their location in allometric space (94.1%, Fig. 3.3). The mechanical effort required to process tough plant materials has been linked with the development of a more massive jaw, larger cheek tooth area and a deeper skull and rostrum to provide an increased area for muscle attachment, thus improving efficiency and power during mastication (Satoh 1997, Michaux et al. 2007). Herbivorous rodents studied here occupy a portion of allometric space associated with allometric patterns reflecting a relative widening of the nasal, lengthening and widening of the premaxilla, and widening of the palate (Fig. 3.3). However, within this portion of space relationships between species exhibiting specialized cranial morphologies, such as mole rats, many of whom burrow primarily using their teeth, are not completely preserved. Several mole rats share a positive allometry for the jugal, a feature reflecting the posterior widening of the zygomatic arch to accommodate the masseter muscle, which among non fossorial rodents passes through an enlarged infraorbital foramen (Moore 1981).

The disparate structure of allometric space indicates that changes in PC slope, which correspond to changes in covariance structure, are common in rodents. The prevalence of slope change among the taxa studied here may be a function of their evolutionary distances from each other. It has been proposed that the more distant the comparison between taxa, in terms of evolutionary relationship, the more likely differences are consequent of slope change rather than changes that conserve the direction of the ontogenetic trajectory (Weston 2003), namely, either an extension or truncation in trajectory (ontogenetic scaling), or a translation in log-transformed space, reflecting a lateral transposition of trajectory; such changes are indicative of an alteration in duration of growth or a change in prenatal development, respectively. Conservation of direction, through lateral transposition or scaling, is considered to be more easily accomplished and thus more likely to occur during morphological evolution (Creighton & Strauss 1986, Gomez 1992). Further work directed to quantifying the capacity of slope change as a mechanism to generate morphological disparity

represents one potentially fruitful future expansion of these methods, considering the evolutionary constraint associated with a conservation of direction and its implications for confounding phylogenetic reconstructions through the promotion of evolutionary convergence.

At a large scale, allometric disparity may be considered a proxy for developmental dynamics; the exploration of allometric space occupation, and its relation with phylogenetic and ecological trends, provides an opportunity to enhance our understanding of factors influencing ontogenetic pathways. The exploration of allometric disparity, and associated correlates, when augmented with clade-wide studies of morphological disparity (e.g. Foote 1991), may reveal yet further clues about morphological macroevolution, addressing the question:*"How has the diversity of organic form, living and extinct, come to be?"* (Foote 1997, p.129).

ACKNOWLEDGEMENTS

Special thanks to Lionel Hautier for thoughtful comments. We also thank all curators for permitting and facilitating access to the specimens in their charge, and Anjali Goswami for discussions. For insightful comments on an earlier version of this paper we thank P. D. Polly and an anonymous reviewer. LABW is supported by a Forschungskredit of Universität Zürich (Nr. 3771) and thanks the Synthesys project, financed by the European Community Research Infrastructure Action under the FP6 Programme, for grants PL-TAF 4504 and SE-TAF 4869. MRS-V is supported by the Swiss National Fond (3100A0-116013).

REFERENCES

Ackermann, R. R. 2002 Patterns of covariation in the hominoid craniofacial skeleton: implications for paleoanthropological models. *J. Hum. Evol.* **43**, 167-187.

Ackermann, R. R. 2005 Ontogenetic integration of the hominoid face. *J. Hum. Evol.* **48**, 175-197.

Anderson, S., & Jones Jr, J. K. 1984 *Orders and families of recent mammals of the world*. New York: John Wiley & Sons.

Becht, G. 1953 Comparative biologic-anatomical researches on mastication in some mammals. *Proceedings Koninklijke Nederlandse Akademie van Wetenschappen, Series C* **564**, 508-526.

Blanga-Kanfi, S., Miranda, H., Penn, O., Pupko, T., DeBry, R. W., & Huchon, D. 2009 Rodent phylogeny revised: analysis of six nuclear genes from all major rodent clades. *BMC Evol. Biol.* **9**, 71 doi:10.1186/1471-2148-9-71.

Boitard, M., Lefebvre, J., & Solignac, M. 1982 Analyse en composantes principales de la variabilité de taille, de croissance et de conformation de espèces du complexe *Jaera*

albrifons (Crustacés Isopodes). *Cahiers de Biologie Marine* **23**, 115-142.

Buzan, E. V., Krystufek, B., Hänfling, B., & Hutchinson, W. F. 2008 Mitochondrial phylogeny of Arvicolinae using comprehensive taxonomic sampling yields new insights. *Biol. J. Linn. Soc.* **94**, 825-835.

Carleton, M., & Musser, G. 2005 Order Rodentia. In *Mammal species of the world* (eds. Wilson, D. E., Reeder, D. M.), pp. 745-752. Washington DC: Smithsonian Institution Press.

Cheverud, J. M. 1982 Phenotypic, genetic, and environmental morphological integration in the cranium. *Evolution* **36**, 499-516.

Cheverud, J. M. 1989 A comparative analysis of morphological variation patterns in the papionins. *Evolution* **43**, 1737-1747.

Creighton, G. K., & Strauss, R. E. 1986 Comparative patterns of growth and development in cricetine rodents and the evolution of ontogeny. *Evolution* **40**, 94-106.

Eble, G. J. 1998 The role of development in evolutionary radiation. In *Biodiversity dynamics: turnover of populations, taxa and communities* (eds. McKinney M. L., & Drake, J. A.), pp. 132-161. New York: Columbia University Press.

Eble, G. J. 2004 The Macroevolution of phenotypic integration. In *Phenotypic Integration* (eds. M. Pigliucci & K. Preston), pp. 253-273. New York: Oxford University Press.

Evans, A. R., Wilson, G. P., Fortelius, M., & Jernvall, J. 2007 High-level similarity of dentitions in carnivorans and rodents. *Nature* **445**, 78-81.

Fink, W. L., & Zelditch, M. L. 1996 Historical patterns of developmental integration in Pirhanas. *Amer. Zool.* **36**, 61-69.

Fontana, W., & Schuster, P. 1998 Continuity in evolution: on the nature of transitions. *Science* **280**, 1451-1455.

Foote, M. 1991 Morphologic and taxonomic diversity in a clade's history: the blastoid record and stochastic simulation: *Univ. Mich. Mus. Paleontol. Contrib.* **28**, 101-140.

Foote, M. 1992 Rarefaction analysis of morphological and taxonomic diversity. *Paleobiology* **19**, 185-204.

Foote, M. 1997 The evolution of morphological diversity. *Ann. Rev. Ecol. Syst.* **28**, 129-152.

Frankino, W. A., Zwaan, B. J., Stern, D. L., & Brakefield, P. M. 2005 Natural selection and developmental constraints in the evolution of allometries. *Science* **307**, 718-720.

Gerber, S., Neige, P., & Eble, G. J. 2007 Combining ontogenetic and evolutionary scales of morphological disparity: a study of Early Jurassic ammonites. *Evol. Dev.* **9**, 472-482.

Gerber, S., Eble, G. J., & Neige, P. 2008 Allometric space and allometric disparity: a developmental perspective in the macroevolutionary analysis of morphological

disparity. *Evolution* **62(6)**, 1450-1457.

Gibson, A. R., Baker, A. J., & Moeed, A. 1984. Morphometric variation in introduced populations of the common myna (*Acridotheres tristis*): An application of the jackknife to principal component analysis. *Syst. Zool.* **33**, 408-421.

Gomez, A. M. 1992 Primitive and derived patterns of relative growth among species of Lorisidae. *J. Hum. Evol.* **23**, 219-233.

Goswami, A. 2006 Morphological integration in the carnivoran skull. *Evolution* **60**, 169-183.

Gulotta, E. F. 1971 *Meriones unguiculatus*. *Mamm. Species* **3**, 5.

Hautier, L., Michaux, J., Marivaux, L., & Vianey-Liaud, M. 2008 The evolution of the zygomasseteric construction in Rodentia, as revealed by a geometric morphometric analysis of the mandible of *Graphiurus* (Rodentia, Gliridae). *Zool. J. Linn. Soc.* **154**, 807-821.

Hartenberger, J. L. 1985 The order Rodentia: major questions on their evolutionary origin, relationships and suprafamilial systematics. In *Evolutionary Relationships among Rodents: A Multidisciplinary Analysis* (eds. Luckett, W. P., & Hartenberger, J. L.), pp. 1-34. New York: Plenum Press.

Huchon, D., & Douzery, E. P. J. 2001 From the Old World to the New World: a molecular chronicle of the phylogeny and biogeography of hystricognath rodents. *Mol. Phylogenet. Evol.* **20**, 238–251.

Huxley, J. S. 1932 *Problems of relative growth*. London: John Hopkins Univ. Press, Methuen.

Janis, C. M. 1995 Correlations between craniodental morphology and feeding behaviour in ungulates: reciprocal illumination between living and fossil taxa. In *Functional morphology in vertebrate paleontology* (ed. J. J. Thomason), pp. 76-98. Cambridge: Cambridge University Press.

Jolicoeur, P. 1963 The multivariate generalization of the allometry equation. *Biometrics* **19**, 497-499.

Klingenberg, C. P. 1996a. Individual variation of ontogenies: a longitudinal study of growth and timing. *Evolution* **50(6)**, 2412-2428.

Klingenberg, C. P. 1996b Multivariate allometry. In *Advances in morphometrics* (eds. L. F. Marcus, M. Corti, A. Loy, D. Slice, G. Naylor), pp. 23-49. New York: Plenum Press.

Klingenberg, C. P., & Ekau, W. 1996 A combined morphometric and phylogenetic analysis of an ecomorphological trend: pelagization in Antarctic fishes (Perciformes: Nototheniidae). *Biol. J. Linn. Soc.* **59**, 143-177.

Klingenberg, C. P., Froese, R. 1991. A multivariate comparison of allometric growth

patterns. *Syst. Zool.* **40**, 410-419.

Klingenberg, C. P., & Spence, J. R. 1993 Heterochrony and allometry: Lessons from the water strider genus *Limnoporus*. *Evolution* **47**, 1834-1853.

Klingenberg, C. P., & Zimmermann, M. 1992 Static, ontogenetic, and evolutionary allometry: A multivariate comparison in nine species of water striders. *Am. Nat.* **140**, 601-620.

Marroig, G., & Cheverud, J. M. 2001 A comparison of phenotypic variation and covariation patterns and the role of phylogeny, ecology, and ontogeny during cranial evolution of New World monkeys. *Evolution* **55**, 2576-2600.

Mendoza, M., Janis, C. M., & Palmqvist, P. 2002 Characterizing complex craniodental patterns related to feeding behaviour in ungulates: a multivariate approach. *J. Zool.* 258, 223-246.

Michaux, J., Chevret, P., & Renaud, S. 2007 Morphological diversity of Old World rats and mice (Rodentia, Muroidae) mandible in relation with phylogeny and adaptation. *J. Zool. Syst. Evol. Res.* **45**, 263-279.

Moore, W.J. 1981 *The Mammalian Skull*. Cambridge: Cambridge: University Press.

Nowak, R. M. 1999 *Walker's mammals of the world*, 6th edn. Baltimore, MD: John Hopkins University Press.

Olson, E. C., & Miller, R. L. 1958 *Morphological Integration*. Chicago: University of Chicago Press.

Pearson, K. 1901 On lines and planes of closest fit to systems of points in space. *Phil. Mag.* **2**, 559-572.

Pérez, E. M. 1992 *Agouti paca*. *Mamm. Species* **9**, 7.

Reeve, E. C. R., & Huxley, J. S. 1945 Some problems in the study of allometric growth. In *Essays on growth and form* (eds. le Gros Clark, W. E., & Medawar, P. B.), pp. 121-156. Oxford: Claredon Press.

Samuels, J. X. 2009 Cranial morphology and dietary habits of rodents. *Zool. J. Linn. Soc.* **156(4)**, 864-888.

Satoh, K. 1997 Comparative functional morphology of mandibular forward movement during mastication of two muroid rodents, *Apodemus speciosus* (Murinae) and *Clethrionomys rufocanus* (Arvicolinae). *J. Morphol.* **231**, 131-142.

Solignac, M., Cariou, M.-L., & Wimitzki, M. 1990 Variability, specificity and evolution of growth gradients in the species complex *Jaera albifrons* (Isopoda, Asellota). *Crustaceana* **59**, 121-145.

Stadler, B. M. R., Stadler, P. F., Wagner, G. P., & Fontana, W. 2001 The topology of the possible: formal spaces underlying patterns of evolutionary change. *J. Theor. Biol.* **213**, 241-274.

Steppan, S. J. 1997 Phylogenetic analysis of

phenotypic covariance structure. II: Reconstructing matrix evolution. *Evolution* **51**, 587-594.

Steppan, S. J., Adkins, R. M., & Anderson, J. 2004 Phylogeny and divergence date estimates of rapid radiations in muroid rodents based on multiple nuclear genes. *Syst. Biol*. **53**, 533-553.

Van Valkenburgh, B. 1989 Carnivore dental adaptations and diet: a study of trophic diversity within guilds. In *Carnivore behaviour ecology, and evolution* (ed. J. L. Gittleman), pp. 410-436. Ithaca, NY: Cornell University Press.

Weisbecker, V., & Schmid, S. 2007 Autopodial skeletal diversity in hystricognath rodents: Functional and phylogenetic aspects. *Mamm. Biol.* **72**, 27-44.

Weston, E. M. 2003 Evolution of ontogeny in the hippopotamus skull: using allometry to dissect developmental change. *Biol. J. Linn. Soc.* **80**, 625-638.

Williams, S. H., & Kay, R. F. 2001 A comparative test of adaptive explanations for hypsodonty in ungulates and rodents. *J. Mamm. Evol.* **8**, 207-229.

Willner, G. R., Dixon, K. R., & Chapman, J. A. 1983 *Ondatra zibethicus. Mamm. Species* **141**, 8.

Wilson, D. E., & Reeder, D. M. 2005 *Mammal species of the world*, 3rd edn. Baltimore: John Hopkins University Press.

Wilson, L. A. B., & Sánchez-Villagra, M. R. 2009 Heterochrony and patterns of cranial suture closure in hystricognath rodents. *J. Anat.* **214**, 339-354.

Wood, A. E. 1955 A revised classification of the rodents. *J. Mammal.* **36**, 165-187.

Wood, A. E. 1959 Eocene radiation and phylogeny of the rodents. *Evolution* **13**, 354-361.

Woods, C. A. 1972 *Erethizon dorsatum*. *Mamm. Species* **29**, 1-6.

Zelditch, M. L, & Carmichael, A. C. 1989a Growth and intensity of integration through postnatal growth in the skull of *Sigmodon fulviventer*. *J. Mammal.* **70**, 477-484.

Zeldtich, M. L., & Carmichael, A. C. 1989b Ontogenetic variation in patterns of developmental and functional integration in skulls of *Sigmodon fulviventer*. *Evolution* **44**, 1738-1747.

Zelditch, M. L., Sheets, D. H., & Fink, W. L. 2003 The ontogenetic dynamics of shape disparity. *Paleobiology* **29**, 139-156.

Zelditch, M. L., Straney, D. O., Swiderski, D. L., & Carmichael, A. C. 1990 Variation in developmental constraints in *Sigmodon*. *Evolution* **44**, 1738-1747.

SUPPLEMENTARY MATERIAL

Supplementary Appendix 3.1
Supplementary Tables 3.1—3.6

Supplementary Appendix 3.1: Cranial length measurements for each specimen used in this study, derived from 3D coordinate landmarks (see Materials and Methods).

Akodon azarae	*Apodemus sylvaticus*	*Arvicola terrestris*		*Atherurus africanus*	*Bathyergus suillus*	*Capromys pilorides*
18.52	23.36	24.10	37.21	49.91	37.12	44.65
23.06	24.71	26.73	37.23	52.24	42.42	55.44
28.65	24.76	28.43	37.26	52.24	46.13	64.68
28.93	25.10	31.67	37.37	58.77	47.72	66.63
29.02	25.54	33.30	37.56	65.30	53.02	70.28
29.74	25.78	33.85	37.57	65.94	56.64	71.84
29.82	25.87	34.26	37.57	79.12	57.36	74.23
29.93	26.13	34.47	37.92	82.54	59.83	76.98
30.04	26.65	34.98	37.93	83.19	60.95	78.09
30.15	26.80	35.02	37.96	83.99	61.08	90.27
30.36	27.04	35.35	38.25	84.94	62.06	92.09
30.51	27.05	35.38	38.31	85.51	62.13	92.40
30.53	27.21	35.38	38.42	88.61	64.54	97.52
30.86	27.22	35.51	38.45	91.74	65.79	98.20
31.03	27.42	35.75	38.49	92.28	65.90	99.09
31.19	27.77	35.93	38.56	93.43	66.42	99.15
31.19	27.98	36.18	38.59	95.88	67.33	99.91
31.22	28.00	36.34	38.62	96.83	70.61	100.27
31.27	28.37	36.36	38.64	101.81	72.02	103.40
31.51	28.51	36.40	38.66	102.12	75.56	104.36
31.97	28.54	36.54	38.74	103.16	75.92	105.84
32.08	28.85	36.57	38.74	118.91	83.51	112.04
32.19	29.80	36.64	38.77		93.38	
32.25	29.81	36.74	38.80			
32.38	31.60	36.88	38.83			
34.90	34.92	36.99	38.85			
35.43		37.02	38.90			
		40.90	38.99			
		41.06	38.99			
		41.43	39.00			
		41.45	39.04			
		41.49	39.40			
		41.57	39.46			
		41.75	39.51			
		43.22	39.59			
		44.05	39.59			
		45.19	39.69			
		48.70	39.76			
		53.95	39.80			
		55.59	39.82			
		40.43	39.96			
		40.52	40.03			
		40.63	40.14			
		40.71	40.17			
		40.86	40.29			
		40.89	40.33			
		40.40	40.40			

Supplementary Appendix 3.1: continued

Castor fiber	*Cavia porcellus*		*Chinchilla lanigera*	*Coendou prehensilis*	*Cricetomys gambius*	*Cricetus cricetus*	*Cunciculus paca*
106.18	32.57	63.17	46.03	48.02	17.13	44.64	81.61
108.09	35.78	63.26	53.07	58.21	19.66	50.09	81.68
113.37	37.34	63.47	55.99	58.64	21.48	50.19	89.85
115.66	37.69	63.92	56.63	64.61	29.01	56.67	94.45
117.28	39.09	64.41	57.28	65.83	30.87	57.57	106.80
122.78	39.78	64.49	57.48	67.47	35.41	59.24	111.51
124.13	40.24	64.51	58.99	68.71	36.50	59.40	111.97
124.90	40.38	65.09	59.07	69.17	36.79	60.50	118.21
129.78	40.46	65.14	59.66	69.65	36.89	62.80	118.25
130.50	40.82	65.19	60.21	70.01	42.63	63.16	119.62
132.39	40.89	65.33	61.11	71.02	43.40	63.69	119.94
132.40	44.33	66.64	61.29	72.18	43.84	63.82	120.26
132.87	45.54	68.33	62.73	73.73	44.12	64.60	120.65
134.74	47.67	68.70	63.26	75.62	44.19	67.63	120.98
137.40	47.91	68.98	63.66	75.94	44.30	67.97	121.15
142.26	54.53	69.17	63.79	76.00	45.14	69.89	121.57
143.00	55.59	71.46	64.15	77.04	47.35	70.54	123.88
151.81	56.23	71.68	65.34	79.61	47.88	70.91	124.22
152.26	57.09	72.06	65.42	80.56	48.11	72.23	124.22
153.19	57.21		65.59	81.02	48.40	75.95	124.55
156.39	57.31		107.75	82.18	49.01	77.61	126.73
	57.83		138.87	83.67	49.14	77.86	127.08
	58.44		167.12	84.78	49.71	79.30	127.13
	58.99			86.42	49.91	79.58	128.23
	60.09			89.90	50.35	95.50	128.34
	60.34			91.55	50.68		128.83
	60.92			93.61	51.82		129.03
	61.56			99.39	52.30		129.25
	62.00			99.60	53.40		130.22
	62.05			101.05	56.08		131.14
	62.10			101.95	58.00		131.23
	62.33				64.08		135.13
							135.30
							136.05
							136.13
							137.57
							140.21
							141.98
							142.14
							142.21
							144.71
							149.25
							151.59
							158.76

Supplementary Appendix 3.1: continued

Dasyprocta leporina		*Dicrostonyx torquatus*	*Dolichotis patagonum*	*Erethizon dorsatum*	*Heterocephalus glaber*	*Hydrochoerous hydrochaeris*	*Hystrix africaeaustralis*	
76.14	110.51	24.57	59.64	51.15	20.39	104.89	57.26	137.32
77.17	110.67	25.33	62.78	52.80	20.87	106.90	59.52	138.72
79.12	110.81	28.64	71.88	52.78	21.03	107.87	63.03	138.80
80.46	111.22	29.12	80.76	55.81	21.51	113.30	64.64	140.53
85.91	111.38	29.48	86.65	57.87	22.64	115.48	74.76	142.00
88.72	111.53	29.96	101.35	78.42	23.03	115.62	80.44	142.51
89.63	111.70	30.93	114.79	88.04	23.07	119.21	82.93	144.19
92.39	111.90	31.14	115.05	88.60	23.17	123.00	88.94	146.50
92.51	112.02	31.47	121.37	88.79	23.21	132.96	95.14	147.31
93.53	112.43	31.54	123.40	90.79	23.43	140.27	95.36	148.38
94.56	112.66	31.65	124.80	93.10	24.47	150.64	97.54	152.07
95.35	112.80	32.39	126.01	93.12	24.71	157.76	97.93	152.40
95.35	113.06	32.72	131.59	93.76	25.04	163.57	101.04	154.41
95.52	113.31	32.87	132.39	95.23	25.11	167.82	103.59	155.16
96.30	114.39	32.92	133.59	95.75	25.12	172.72	104.18	155.38
96.48	115.07	33.31	135.32	96.95	25.22	173.82	107.57	156.26
96.78	117.12	33.59	136.91	98.69	25.24	188.75	111.30	157.59
98.51	117.20	34.65	137.26	99.22	25.35	202.89	111.38	158.33
98.53	117.46	34.82	137.91	99.39	25.49	208.84	114.03	158.55
100.79	118.09	36.38	139.89	99.92	25.51	211.91	115.14	159.64
101.58	118.41	41.78	140.39	102.54	25.64	224.82	116.78	160.87
101.67	118.50	42.83	141.45	103.01	25.68	225.51	117.05	161.45
102.31	119.21	50.16	142.37	104.24	25.96	226.59	118.52	163.03
102.65	119.30		148.85	104.36	27.34	235.72	121.11	163.61
103.36	119.90			106.44	33.68	236.49	125.21	164.85
105.69	120.14			109.43		238.67	125.78	165.53
105.74	121.17			111.02		240.54	127.81	165.82
106.41	122.85			112.02		241.95	127.87	171.30
106.65	125.13			114.43		243.74	128.42	172.36
106.77	126.08					245.73	128.64	
107.56	126.18					247.36	128.89	
108.57	126.63					249.88	129.19	
108.60	147.48					254.01	129.37	
108.70	147.78					260.21	130.68	
108.87	149.04					262.24	131.11	
109.15	154.24					263.13	131.28	
109.57	155.07						132.67	
109.97	158.84						134.20	
109.98							134.35	
110.38							134.40	
110.41							134.69	
110.46							137.02	

Supplementary Appendix 3.1: continued

Lagostomus maximus	*Meriones unguiculatus*	*Microtus economus*	*Myocastor coypus*	*Myoprocta acouchy*	*Myopus schisticolor*	*Myospalax fontanierii*	*Ondatra zibethicus*
48.26	24.77	21.37	43.44	51.02	24.54	30.67	41.81
52.06	26.16	22.30	44.42	56.57	25.32	34.85	45.21
62.14	28.43	26.28	51.37	64.99	26.68	35.20	51.67
72.40	31.53	28.02	74.54	65.98	26.74	36.80	52.92
93.87	32.01	28.74	79.69	67.15	27.05	38.33	54.21
95.27	34.49	29.83	85.94	68.71	27.21	40.00	58.39
98.73	34.56	30.12	86.18	69.22	27.42	40.60	58.78
98.78	35.54	30.15	88.70	69.59	27.98	42.35	60.15
99.60	35.69	30.41	90.58	69.88	28.08	44.72	60.82
103.53	36.60	30.73	94.74	70.17	28.09	45.26	61.77
103.95	36.76	31.03	95.93	73.39	28.20	46.44	62.06
105.15	36.79	31.15	100.24	73.94	28.35	47.94	63.04
105.64	37.39	31.16	102.74	74.38	28.78	48.10	63.49
106.37	38.51	31.24	103.60	74.52	29.17	48.84	64.59
106.97	39.53	31.37	104.89	74.66	29.30	49.27	64.95
120.16	40.32	31.45	107.38	74.73	30.13	51.68	64.97
122.53	40.63	31.55	109.75	74.77	37.41	53.68	65.25
124.29	41.12	31.74	112.59	76.11		63.00	65.32
125.17	41.67	32.15	112.86	76.64		64.42	65.70
127.21	41.87	32.35	114.35	77.14			65.71
129.66	42.36	34.60	114.42	77.27			65.76
145.64	42.99		115.11	77.27			66.32
151.47	42.91		115.68	77.75			66.36
	42.69		115.89	77.92			66.62
	42.57		116.23	77.95			67.11
	42.71		116.59	78.37			67.16
	42.86		117.01	78.59			67.16
	43.00		120.48	79.25			67.16
	43.52		123.36	79.88			67.53
	44.23		123.55	80.20			67.61
	44.89		124.15	80.82			67.79
	47.67		126.06	80.87			67.96
	50.75		126.31	81.04			68.23
			132.99	81.20			69.18
				81.37			69.45
				82.58			69.55
				82.71			69.68
				83.06			70.15
				84.64			70.29
				85.50			71.04
				86.00			72.34
				87.49			82.61
				90.35			
				99.26			

Supplementary Appendix 3.1: continued

Orzyomys albigularis	*Pogonomys forbesi*	*Rattus rattus*	*Rhizomys sumatrensis*	*Tachyorctes splendens*	*Thryonomys swinderianus*
18.99	27.58	21.24	39.10	28.89	49.72
21.59	30.65	24.60	43.01	29.79	55.68
24.53	30.73	26.90	49.19	31.25	55.87
25.22	34.00	27.80	55.91	35.25	64.32
25.62	34.86	30.02	65.98	36.26	74.71
26.68	35.42	31.27	66.09	39.39	75.67
27.40	37.27	33.56	67.26	41.86	77.58
27.47	37.38	33.68	70.38	42.11	77.74
27.77	37.41	36.90	71.85	42.32	78.10
27.82	37.57	37.13	74.82	42.42	78.37
27.86	38.14	41.37	76.15	42.88	78.95
27.90	38.33	42.90	77.44	43.04	80.45
28.08	38.97	43.01	77.68	44.85	80.58
28.86	39.26	43.08	78.41	45.67	81.99
28.93	39.27	43.39	83.77	45.94	83.78
29.37	39.69	45.55		46.04	83.97
30.17	39.84	46.69		46.21	85.78
30.51	40.12	47.55		46.29	87.49
30.81	40.40	49.11		46.69	88.93
36.23	43.93	49.20		46.86	89.20
37.25	49.07	52.01		47.01	89.24
39.95	51.79	52.62		47.07	90.74
41.66		53.63		47.14	91.02
		54.36		47.59	92.93
				48.49	94.50
				48.56	96.97
				48.80	99.92
				49.02	100.35
				50.50	102.01
				59.96	104.28
				63.13	109.59
					113.86
					114.09
					115.26
					117.62

Supplementary Table 3.1: Multivariate patterns of allometry for all rodent species studied. SE = standard error

		Akodon azarae	*Apodemus sylvaticus*	*Arvicola terrestris*	*Atherurus africanus*	*Bathyergus suillus*	*Capromys pilorides*
premaxilla ventral length		0.282	0.224	0.219	0.351	0.248	0.332
SE		0.099	0.006	0.007	0.006	0.006	0.005
premaxilla width at max suture		0.222	0.189	0.203	0.209	0.241	0.258
SE		0.010	0.006	0.007	0.006	0.007	0.005
palatine length		0.237	0.315	0.282	0.270	0.227	0.275
SE		0.011	0.006	0.008	0.006	0.006	0.005
palatine width		0.253	0.311	0.322	0.238	0.288	0.254
SE		0.011	0.006	0.007	0.006	0.007	0.005
occipital condyles width		0.210	0.373	0.255	0.161	0.159	0.170
SE		0.011	0.006	0.007	0.006	0.007	0.005
skull length		0.239	0.231	0.234	0.244	0.243	0.240
SE		0.011	0.005	0.007	0.006	0.006	0.005
nasal length		0.270	0.274	0.200	0.260	0.228	0.238
SE		0.010	0.005	0.007	0.006	0.006	0.005
nasal width		0.286	0.179	0.203	0.190	0.196	0.237
SE		0.010	0.005	0.007	0.006	0.006	0.005
frontal midline length		0.266	0.194	0.177	0.245	0.278	0.214
SE		0.010	0.006	0.007	0.006	0.006	0.005
parietal midline length		0.233	0.193	0.352	0.177	0.312	0.178
SE		0.099	0.006	0.007	0.006	0.006	0.005
jugal length		0.317	0.299	0.274	0.280	0.325	0.303
SE		0.009	0.006	0.007	0.007	0.007	0.005
length of dental diastema		0.226	0.194	0.224	0.248	0.246	0.228
SE		0.009	0.006	0.007	0.006	0.006	0.005
max interorbital width		0.221	0.149	0.163	0.173	0.128	0.232
SE		0.010	0.005	0.007	0.006	0.006	0.005
basioccipital length		0.234	0.224	0.190	0.245	0.198	0.235
SE		0.010	0.006	0.007	0.006	0.006	0.005
basioccipital width		0.225	0.205	0.150	0.222	0.179	0.203
SE		0.010	0.006	0.007	0.006	0.007	0.005
basisphenoid length		0.188	0.158	0.226	0.220	0.232	0.259
SE		0.010	0.006	0.007	0.006	0.006	0.005
basisphenoid width		0.173	0.277	0.331	0.311	0.297	0.211
SE		0.010	0.006	0.007	0.006	0.008	0.005
% Variance	PC1	96.673	93.232	96.237	97.220	97.246	96.563
	PC2	2.224	5.647	2.186	1.023	1.498	1.465

Supplementary Table 3.1: continued

		Castor fiber	*Cavia porcellus*	*Chinchilla lanigera*	*Coendou prehensilis*	*Cricetomys gambius*	*Cricetus cricetus*
premaxilla ventral length		0.190	0.390	0.302	0.299	0.252	0.258
SE		0.010	0.009	0.008	0.006	0.006	0.011
premaxilla width at max suture		0.260	0.177	0.200	0.166	0.297	0.306
SE		0.009	0.009	0.008	0.006	0.006	0.008
palatine length		0.200	0.215	0.401	0.205	0.211	0.245
SE		0.010	0.010	0.008	0.006	0.006	0.008
palatine width		0.472	0.234	0.220	0.286	0.319	0.189
SE		0.009	0.010	0.008	0.006	0.006	0.007
occipital condyles width		0.110	0.137	0.215	0.147	0.115	0.161
SE		0.011	0.010	0.008	0.006	0.007	0.006
skull length		0.244	0.240	0.249	0.251	0.243	0.238
SE		0.010	0.009	0.008	0.006	0.007	0.008
nasal length		0.173	0.282	0.210	0.252	0.273	0.351
SE		0.010	0.009	0.008	0.006	0.007	0.008
nasal width		0.223	0.159	0.190	0.273	0.255	0.212
SE		0.009	0.010	0.008	0.007	0.007	0.006
frontal midline length		0.147	0.147	0.222	0.215	0.209	0.230
SE		0.009	0.009	0.008	0.007	0.006	0.008
parietal midline length		0.275	0.368	0.208	0.310	0.179	0.252
SE		0.010	0.009	0.008	0.006	0.006	0.008
jugal length		0.196	0.224	0.218	0.272	0.265	0.278
SE		0.009	0.010	0.008	0.006	0.006	0.008
length of dental diastema		0.290	0.311	0.251	0.255	0.236	0.300
SE		0.009	0.009	0.008	0.006	0.006	0.008
max interorbital width		0.194	0.106	0.171	0.200	0.249	0.139
SE		0.009	0.009	0.009	0.007	0.007	0.008
basioccipital length		0.268	0.234	0.164	0.198	0.281	0.216
SE		0.009	0.009	0.008	0.006	0.006	0.008
basioccipital width		0.197	0.207	0.288	0.203	0.212	0.161
SE		0.009	0.010	0.008	0.006	0.006	0.010
basisphenoid length		0.223	0.313	0.335	0.312	0.282	0.312
SE		0.010	0.009	0.008	0.006	0.006	0.007
basisphenoid width		0.254	0.155	0.130	0.194	0.151	0.143
SE		0.010	0.009	0.008	0.006	0.007	0.007
% Variance	PC1	94.806	95.079	95.879	95.567	96.985	95.173
	PC2	3.099	3.226	2.094	2.129	1.007	2.632

Supplementary Table 3.1: continued

		Cunciculus paca	*Dasyprocta leporina*	*Dicrostonyx torquatus*	*Dolichotis patagonum*	*Erethizon dorsatum*	*Heterocephalus glaber*
premaxilla ventral length		0.317	0.264	0.211	0.193	0.286	0.257
SE		0.009	0.008	0.007	0.011	0.009	0.009
premaxilla width at max suture		0.229	0.186	0.216	0.150	0.219	0.317
SE		0.009	0.008	0.005	0.011	0.009	0.009
palatine length		0.187	0.299	0.263	0.212	0.127	0.311
SE		0.010	0.009	0.006	0.011	0.009	0.009
palatine width		0.363	0.362	0.380	0.500	0.134	0.316
SE		0.009	0.009	0.006	0.011	0.009	0.009
occipital condyles width		0.197	0.141	0.233	0.197	0.251	0.239
SE		0.009	0.008	0.006	0.010	0.007	0.009
skull length		0.238	0.248	0.256	0.250	0.246	0.246
SE		0.009	0.009	0.006	0.010	0.009	0.009
nasal length		0.256	0.268	0.195	0.263	0.251	0.212
SE		0.007	0.010	0.006	0.011	0.009	0.009
nasal width		0.191	0.197	0.254	0.228	0.219	0.226
SE		0.009	0.009	0.006	0.011	0.009	0.009
frontal midline length		0.185	0.212	0.184	0.179	0.263	0.157
SE		0.009	0.010	0.006	0.089	0.009	0.009
parietal midline length		0.155	0.170	0.319	0.178	0.249	0.138
SE		0.009	0.010	0.006	0.084	0.008	0.009
jugal length		0.301	0.158	0.232	0.217	0.289	0.399
SE		0.009	0.008	0.006	0.011	0.008	0.009
length of dental diastema		0.356	0.234	0.222	0.257	0.272	0.191
SE		0.007	0.009	0.006	0.011	0.008	0.009
max interorbital width		0.178	0.141	0.213	0.160	0.218	0.115
SE		0.008	0.008	0.006	0.011	0.008	0.011
basioccipital length		0.278	0.289	0.230	0.213	0.249	0.158
SE		0.009	0.010	0.006	0.010	0.009	0.008
basioccipital width		0.187	0.225	0.230	0.196	0.262	0.228
SE		0.009	0.009	0.006	0.011	0.009	0.008
basisphenoid length		0.252	0.360	0.224	0.369	0.282	0.235
SE		0.008	0.008	0.006	0.011	0.008	0.011
basisphenoid width		0.169	0.214	0.182	0.173	0.234	0.195
SE		0.007	0.009	0.006	0.011	0.009	0.009
% Variance	PC1	93.070	95.028	95.223	93.826	95.361	94.289
	PC2	4.644	2.369	2.624	4.113	2.419	3.223

Supplementary Table 3.1: continued

		Hydrochoerus hydrochaeris	*Hystrix africaeaustralis*	*Lagostomus maximus*	*Meriones unguiculatus*	*Microtus economus*	*Myocastor coypus*
premaxilla ventral length		0.292	0.202	0.269	0.255	0.201	0.331
SE		0.004	0.005	0.008	0.005	0.011	0.010
premaxilla width at max suture		0.222	0.209	0.207	0.218	0.189	0.204
SE		0.004	0.006	0.007	0.005	0.010	0.010
palatine length		0.253	0.348	0.242	0.215	0.204	0.320
SE		0.004	0.007	0.007	0.006	0.010	0.008
palatine width		0.351	0.176	0.315	0.222	0.209	0.273
SE		0.004	0.006	0.007	0.006	0.010	0.009
occipital condyles width		0.148	0.128	0.212	0.227	0.288	0.175
SE		0.004	0.005	0.007	0.007	0.009	0.010
skull length		0.249	0.256	0.249	0.240	0.239	0.241
SE		0.004	0.006	0.007	0.006	0.009	0.007
nasal length		0.278	0.278	0.304	0.317	0.182	0.257
SE		0.006	0.007	0.007	0.006	0.007	0.007
nasal width		0.228	0.328	0.169	0.164	0.278	0.180
SE		0.004	0.009	0.007	0.006	0.011	0.008
frontal midline length		0.179	0.232	0.237	0.252	0.305	0.216
SE		0.004	0.006	0.007	0.006	0.011	0.010
parietal midline length		0.198	0.261	0.206	0.219	0.367	0.235
SE		0.004	0.007	0.008	0.006	0.011	0.010
jugal length		0.213	0.193	0.233	0.272	0.218	0.230
SE		0.008	0.006	0.010	0.006	0.011	0.011
length of dental diastema		0.306	0.227	0.286	0.258	0.160	0.262
SE		0.008	0.006	0.008	0.006	0.009	0.010
max interorbital width		0.176	0.208	0.180	0.331	0.179	0.205
SE		0.006	0.006	0.007	0.006	0.010	0.011
basioccipital length		0.237	0.276	0.220	0.220	0.290	0.218
SE		0.005	0.006	0.007	0.006	0.010	0.009
basioccipital width		0.226	0.221	0.218	0.235	0.264	0.219
SE		0.004	0.006	0.007	0.004	0.010	0.009
basisphenoid length		0.314	0.278	0.302	0.200	0.268	0.262
SE		0.005	0.006	0.007	0.006	0.009	0.009
basisphenoid width		0.133	0.199	0.211	0.225	0.170	0.233
SE		0.004	0.006	0.007	0.006	0.007	0.007
% Variance	PC1	96.415	95.688	95.617	95.939	94.533	95.610
	PC2	1.570	2.744	2.466	1.475	3.414	2.228

Supplementary Table 3.1: continued

		Myoprocta acouchy	*Myopus schisticolor*	*Myospalax fontanierii*	*Ondatra zibethicus*	*Orzyomys albigularis*	*Pogonomys forbesi*
premaxilla ventral length		0.323	0.254	0.252	0.156	0.267	0.420
SE		0.010	0.010	0.009	0.009	0.009	0.011
premaxilla width at max suture		0.252	0.232	0.188	0.234	0.191	0.212
SE		0.010	0.011	0.010	0.008	0.008	0.011
palatine length		0.165	0.130	0.236	0.266	0.383	0.235
SE		0.010	0.011	0.009	0.008	0.009	0.011
palatine width		0.392	0.291	0.216	0.353	0.135	0.248
SE		0.010	0.009	0.009	0.008	0.009	0.011
occipital condyles width		0.165	0.209	0.201	0.162	0.181	0.236
SE		0.010	0.009	0.007	0.008	0.008	0.011
skull length		0.245	0.249	0.248	0.250	0.241	0.244
SE		0.010	0.009	0.010	0.008	0.009	0.010
nasal length		0.220	0.186	0.215	0.191	0.322	0.251
SE		0.009	0.009	0.010	0.010	0.009	0.010
nasal width		0.222	0.323	0.232	0.233	0.184	0.266
SE		0.010	0.009	0.010	0.007	0.010	0.010
frontal midline length		0.152	0.195	0.234	0.190	0.261	0.210
SE		0.010	0.010	0.009	0.009	0.008	0.010
parietal midline length		0.166	0.370	0.426	0.210	0.233	0.178
SE		0.011	0.010	0.009	0.009	0.009	0.010
jugal length		0.230	0.233	0.267	0.219	0.291	0.225
SE		0.008	0.008	0.009	0.009	0.009	0.010
length of dental diastema		0.203	0.204	0.202	0.198	0.280	0.240
SE		0.009	0.008	0.010	0.008	0.009	0.007
max interorbital width		0.195	0.191	0.148	0.379	0.241	0.214
SE		0.010	0.009	0.010	0.004	0.008	0.008
basioccipital length		0.176	0.181	0.207	0.177	0.199	0.204
SE		0.010	0.010	0.010	0.008	0.009	0.011
basioccipital width		0.245	0.285	0.272	0.238	0.191	0.190
SE		0.010	0.010	0.009	0.005	0.007	0.011
basisphenoid length		0.322	0.209	0.193	0.254	0.235	0.252
SE		0.009	0.010	0.010	0.004	0.009	0.010
basisphenoid width		0.297	0.265	0.269	0.287	0.155	0.205
SE		0.008	0.010	0.010	0.008	0.009	0.009
% Variance	PC1	95.481	93.454	96.686	94.920	91.936	94.152
	PC2	2.424	3.743	1.778	3.083	2.467	3.517

Supplementary Table 3.1: continued

		Rattus rattus	*Rhizomys sumatrensis*	*Tachyorctes splendens*	*Thryonomys swinderianus*
premaxilla ventral length		0.319	0.255	0.228	0.295
SE		0.011	0.010	0.006	0.009
premaxilla width at max suture		0.230	0.192	0.247	0.179
SE		0.007	0.008	0.006	0.009
palatine length		0.268	0.151	0.225	0.325
SE		0.005	0.009	0.006	0.009
palatine width		0.166	0.502	0.234	0.364
SE		0.009	0.009	0.007	0.010
occipital condyles width		0.165	0.173	0.206	0.188
SE		0.010	0.009	0.008	0.009
skull length		0.245	0.249	0.248	0.244
SE		0.008	0.009	0.009	0.009
nasal length		0.309	0.259	0.217	0.285
SE		0.008	0.008	0.007	0.009
nasal width		0.154	0.228	0.274	0.202
SE		0.008	0.007	0.007	0.009
frontal midline length		0.259	0.220	0.218	0.180
SE		0.008	0.008	0.008	0.009
parietal midline length		0.215	0.204	0.352	0.180
SE		0.008	0.009	0.008	0.008
jugal length		0.345	0.225	0.252	0.208
SE		0.008	0.009	0.008	0.010
length of dental diastema		0.293	0.205	0.231	0.263
SE		0.008	0.009	0.009	0.010
max interorbital width		0.194	0.139	0.252	0.261
SE		0.008	0.010	0.007	0.009
basioccipital length		0.220	0.222	0.264	0.332
SE		0.008	0.007	0.009	0.009
basioccipital width		0.223	0.257	0.226	0.209
SE		0.008	0.008	0.010	0.009
basisphenoid length		0.230	0.253	0.209	0.222
SE		0.008	0.007	0.007	0.009
basisphenoid width		0.181	0.175	0.198	0.153
SE		0.009	0.008	0.007	0.009
% Variance	PC1	97.139	97.298	96.007	95.225
	PC2	1.187	1.542	2.373	2.995

		HH	HH	OS	OS	HH	HH	HH	OS	HS	OS	HH	HH	HH	OS	HH	HH	OS
		Arvicola terrestris	*Castor fiber*	*Cricetomys gambius*	*Cricetus cricetus*	*Dicrostonyx torquatus*	*Microtus economus*	*Myopus schisticolor*	*Ondatra zibethicus*	*Pogonomys forbesi*	*Rattus rattus*	*Rhizomys sumatrensis*	*Tachyorctes splendens*	*Apodemus sylvaticus*	*Akodon azarae*	*Myospalax fontanierii*	*Meriones unguiculatus*	*Orzyomys albigularis*
HH	*Arvicola terrestris*		19.43	13.00	14.32	16.25	19.17	17.12	16.38	17.23	17.22	23.31	20.38	20.97	16.26	16.11	17.88	8.83
HH	*Castor fiber*			20.04	19.19	13.12	15.21	15.11	17.18	20.40	20.42	20.17	16.10	7.69	11.11	18.03	13.05	15.70
OS	*Cricetomys gambius*				21.92	15.05	16.87	24.58	18.47	17.28	12.87	21.00	15.72	15.84	20.10	13.16	12.61	18.36
OS	*Cricetus cricetus*					12.82	21.55	22.15	21.53	17.04	24.64	23.53	17.90	17.78	11.48	15.84	8.20	15.66
HH	*Dicrostonyx torquatus*						22.41	20.71	15.14	16.03	17.20	15.38	10.84	19.28	18.16	17.39	14.01	16.34
HH	*Microtus economus*							13.05	14.34	22.14	16.45	20.88	18.38	15.82	15.46	16.80	14.39	15.48
HH	*Myopus schisticolor*								16.93	10.59	10.55	12.13	13.13	19.91	16.57	22.74	11.85	15.17
OS	*Ondatra zibethicus*									18.67	14.55	18.71	17.96	20.20	21.05	19.36	29.64	17.37
HS	*Pogonomys forbesi*										11.11	18.03	13.05	10.96	18.08	20.06	13.83	28.22
OS	*Rattus rattus*											19.87	16.55	17.04	20.75	14.29	18.10	19.42
HH	*Rhizomys sumatrensis*												13.90	10.72	8.72	17.54	16.25	22.11
HH	*Tachyorctes splendens*													16.48	12.18	13.65	19.43	22.25
HH	*Apodemus sylvaticus*														17.67	17.08	15.57	16.42
OS	*Akodon azarae*															10.91	12.56	20.10
HH	*Myospalax fontanierii*																18.92	16.98
HH	*Meriones unguiculatus*																	24.32
OS	*Orzyomys albigularis*																	

Supplementary Table 3.2: Vector angle (degrees) matrix for muroid rodents studied, HH = herbivore hard, HS = herbivore soft, OH = omnivore hard, OS = omnivore soft.

		OH	HH	OH	HH	HS	HH	HS	HS	HS	HH	HH	HS	HH	HS	HH	HS	HH
		A. africanus	*B. suillus*	*C. pilorides*	*C. porcellus*	*C. lanigera*	*C. prehensilis*	*C. paca*	*D. leporina*	*D. patagonum*	*E. dorsatum*	*H. glaber*	*H. hydrochaeris*	*H. africaeaustralis*	*L. maximus*	*M. coypus*	*M. acouchy*	*T. swinderianus*
OH	*Atherurus africanus*		10.72	8.72	22.11	18.07	17.07	12.66	17.11	13.22	19.43	23.40	18.99	20.13	9.11	8.34	23.00	17.23
HH	*Bathyergus suillus*			17.04	18.10	16.87	19.41	16.88	12.89	16.71	21.67	15.79	12.11	19.89	17.33	12.87	13.37	18.05
OH	*Capromys pilorides*				17.84	25.20	14.52	33.14	16.75	22.74	20.58	20.41	15.30	20.11	14.48	11.05	18.31	20.60
HH	*Cavia porcellus*					16.57	11.85	20.22	22.11	32.23	14.57	18.24	13.66	20.96	11.34	18.63	21.06	21.48
HS	*Chinchilla lanigera*						15.12	18.24	19.78	25.32	20.06	29.82	11.90	13.71	12.14	12.00	14.13	11.50
HH	*Coendou prehensilis*							19.17	14.45	27.05	18.62	19.01	14.46	23.37	11.83	14.40	17.36	13.89
HS	*Cunciculus paca*								19.50	21.30	14.10	21.38	20.00	20.48	18.24	25.80	15.29	22.11
HS	*Dasyprocta leporina*									21.95	15.27	14.39	14.70	17.84	15.74	11.59	31.32	22.88
HS	*Dolichotis patagonum*										19.28	18.16	17.39	14.01	16.34	14.49	21.56	16.51
HH	*Erethizon dorsatum*											14.82	15.66	16.95	10.87	13.15	20.79	12.93
HH	*Heterocephalus glaber*												19.70	16.76	12.99	17.85	18.91	15.51
HS	*Hydrochoerous hydrochaeris*													17.78	11.48	8.20	15.66	19.62
HH	*Hystrix africaeaustralis*														15.84	13.16	12.61	12.40
HS	*Lagostomus maximus*															8.27	16.14	16.03
HH	*Myocastor coypus*																16.03	17.93
HS	*Myoprocta acouchy*																	20.04
HH	*Thryonomys swinderianus*																	

Supplementary Table 3.3: Vector angle (degrees) matrix for hystricognath rodents studied, HH = herbivore hard, HS = herbivore soft, OH = omnivore hard, OS = omnivore soft.

		1	2	1	2	2	1	2	2	2	1	2	1	1	1	2	1	1	1
		A. terrestris	*B. suillus*	*C. fiber*	*C. porcellus*	*C. prehensilis*	*D-torquatus*	*E. dorsatum*	*H. glaber*	*H. africaeaustralis*	*M. economus*	*M. coypus*	*M. schisticolor*	*R. sumatrensis*	*T. splendens*	*T. swinderianus*	*A. sylvaticus*	*M. fontanierii*	*M. unguiculatus*
1	*Arvicola terrestris*		12.18	19.43	17.51	22.50	16.25	26.63	21.77	13.78	19.17	18.74	17.12	23.31	20.38	17.81	20.97	16.11	17.88
2	*Bathyergus suillus*			20.75	18.10	19.41	20.88	21.67	15.79	19.89	22.22	12.87	13.35	20.05	10.55	18.05	19.87	20.39	17.27
1	*Castor fiber*				18.08	17.27	13.12	15.74	21.72	14.25	15.21	17.16	15.11	20.17	16.10	17.06	7.69	18.03	13.05
2	*Cavia porcellus*					11.85	19.41	14.57	18.24	20.96	14.83	18.63	16.51	18.23	18.87	21.48	16.93	9.73	10.55
2	*Coendou prehensilis*						12.37	18.62	19.01	23.37	21.01	14.40	20.62	12.95	12.37	13.89	15.45	16.14	16.32
1	*Dicrostonyx torquatus*							14.23	14.40	18.22	22.41	18.05	20.71	15.38	10.84	16.47	19.28	17.39	14.01
2	*Erethizon dorsatum*								14.82	16.95	23.92	13.15	19.49	22.46	19.81	12.93	8.27	15.27	14.39
2	*Heterocephalus glaber*									16.76	19.24	17.85	20.15	15.47	16.05	15.51	19.50	21.30	14.10
2	*Hystrix africaeaustralis*										20.10	13.16	18.36	31.40	10.15	12.40	21.92	17.94	15.05
1	*Microtus economus*											14.69	13.05	20.88	18.38	31.30	15.82	16.80	14.39
2	*Myocastor coypus*												18.17	21.79	15.70	17.93	20.94	16.70	14.23
1	*Myopus schisticolor*													12.13	13.13	20.16	19.91	22.74	11.85
1	*Rhizomys sumatrensis*														13.90	16.03	10.72	17.54	16.25
1	*Tachyorctes splendens*															21.23	16.48	13.65	19.43
2	*Thryonomys swinderianus*																14.12	10.61	13.13
1	*Apodemus sylvaticus*																	17.08	15.57
1	*Myospalax fontanierii*																		18.92
1	*Meriones unguiculatus*																		

Supplementary Table 3.4: Vector angle (degrees) matrix for rodents belonging to the HH group (hard herbivorous diet), 1= muroid, 2 = hystricognath.

Supplementary Table 3.5: Vector angle (degrees) matrix for rodent species classified in group HS (soft herbivorous diet), 1= muroid, 2 = hystricognath.

		2	2	2	2	2	2	2	1
		Chinchilla lanigera	*Cunciculus paca*	*Dasyprocta leporina*	*Dolichotis patagonum*	*Hydrochoerous hydrochaeris*	*Lagostomus maximus*	*Myoprocta acouchy*	*Pogonomys forbesi*
2	*Chinchilla lanigera*		18.24	19.78	25.32	11.90	12.14	14.13	19.24
2	*Cunciculus paca*			19.50	21.30	20.00	18.24	15.29	17.62
2	*Dasyprocta leporina*				21.95	14.70	15.74	31.32	17.29
2	*Dolichotis patagonum*					17.39	16.34	21.56	13.38
2	*Hydrochoerous hydrochaeris*						11.48	15.66	21.05
2	*Lagostomus maximus*							16.14	17.23
2	*Myoprocta acouchy*								17.30
1	*Pogonomys forbesi*								

Supplementary Table 3.6: Vector angle (degrees) matrix for all species classified in group OS (soft omnivorous diet). For the study sample, members of this group are exclusively muroid taxa.

	Cricetomys gambius	*Cricetus cricetus*	*Ondatra zibethicus*	*Rattus rattus*	*Akodon azarae*	*Orzyomys albigularis*
Cricetomys gambius		21.92	18.47	12.87	20.10	18.36
Cricetus cricetus			21.53	24.64	11.48	15.66
Ondatra zibethicus				14.55	21.05	17.37
Rattus rattus					20.75	19.42
Akodon azarae						20.10
Orzyomys albigularis						

CHAPTER 4

Skeletogenesis and sequence heterochrony in rodent evolution, with particular emphasis on the African striped mouse (*Rhabdomys pumilio*)

CHAPTER 4

Skeletogenesis and sequence heterochrony in rodent evolution, with particular emphasis on the African striped mouse (*Rhabdomys pumilio*)

Article submitted to *Organisms Diversity and Evolution* on 19th September 2009, accepted for publication on 20th January 2010

Reference: **Wilson LAB**, Schradin C, Mitgutsch C, Galliari FC, Mess A, Sánchez-Villagra MR. 2010. Skeletogenesis and sequence heterochrony in rodent evolution, with particular emphasis on the African striped mouse (*Rhabdomys pumilio*). *Org. Div. Evol.* 10: 243-258

Abstract

Data documenting skeletal development in rodents, the most species-rich 'Order' of mammals, are at present restricted to a few model species, a shortcoming that hinders exploration of the morphological and ecological diversification of the group. In this study we provide the most comprehensive sampling of rodent ossification sequences to date with the aim of exploring whether heterochrony is ubiquitous in rodent evolution at the onset of skeletal formation. The onset of ossification in 17 cranial elements and 24 postcranial elements was examined for eight muroid and caviomorph rodent species. New data are provided for two non-model species, of these, extended sampling of the African striped mouse, *Rhabdomys pumilio*, was conducted with the study of 53 autopodial elements and examination of intraspecific variation. The Parsimov method to study sequence heterochrony was used to explore the role that changes in developmental timing play in early skeletal formation. Few heterochronies were found to diagnose the muroid and caviomorph clades, suggesting conserved patterning in skeletal development. Mechanisms leading to the generation of the wide range of morphological diversity encapsulated within Rodentia may be restricted to later periods in development than those studied in this work. Documentation of skeletogenesis in *Rhabdomys* indicates intraspecifc variation in ossification sequence pattern is present, though not extensive. Our study suggests that sequence heterochrony is neither pivotal nor prevalent during early skeletal formation in rodents.

KEYWORDS**:** rodent; heterochrony; *Rhabdomys*; skeletogenesis; development; intraspecific variation

INTRODUCTION

The clade Rodentia at present contains 2,277 members representing almost half of all living mammalian species (Wilson and Reeder 2005). There is a relative dearth of data on skeletal development across mammalian clades, and the available information is limited to a few model species (e.g. the house mouse, *Mus musculus*; Kaufman 2008). Since Rodentia is species-rich compared to other mammalian 'orders', the documentation of rodent skeletal development is most markedly understudied. This shortcoming restricts studies exploring the developmental basis for the morphological and ecological diversification of this group, which has proven a rich avenue of research examining other aspects of prenatal development (Kavanagh et al. 2007).

Extant rodents encapsulate an array of differing traits in terms of ecology, life history, body size and locomotory habits. With the exception of Antarctica, rodents inhabit all continents and play fundamental roles in a multitude of ecosystems. Rodentia presents an ideal mammalian group in which to examine the developmental basis associated with organismal diversity (Michaux et al. 2008; Monteiro et al. 2005; Roth 1996). Indeed, within the rodent sample studied here, there are representatives from two clades characterized by contrasting attributes. On the one hand, caviomorph rodents comprise relatively few species (fewer than 13% of rodents; Wilson and Reeder 2005) and yet this South American radiation includes species that differ in body size by several orders of magnitude (Nowak 1999), and possess numerous different adaptations to locomotory style (Weisbecker and Schmid 2007).

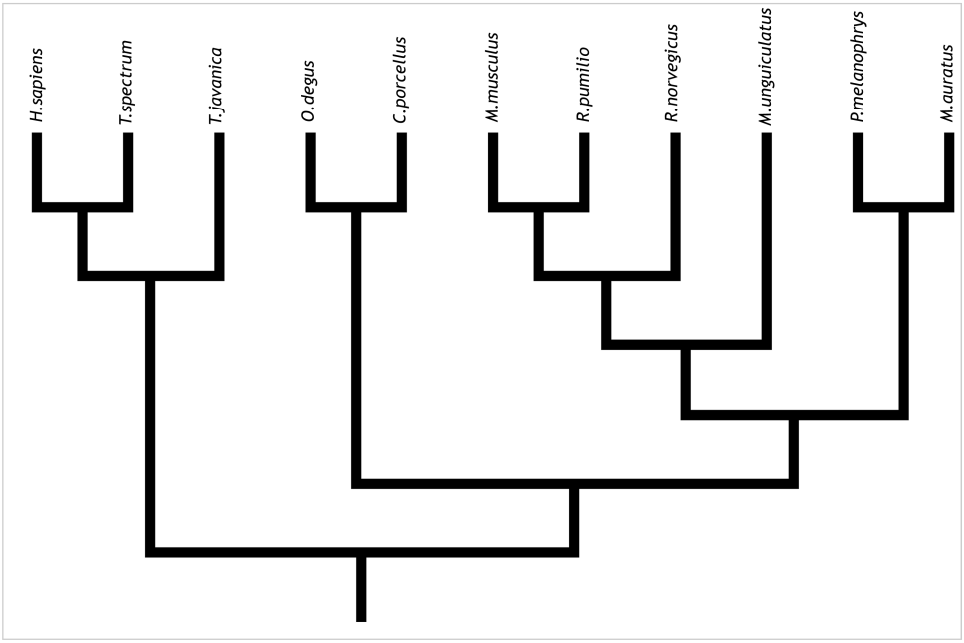

Figure 4.1: Phylogenetic relationships among the species included in this study, reconstructed from Steppan et al. (2004), Bininda-Emonds et al. (2007), and Blanga-Kanfi et al. (2009).

On the other hand, the species-rich muroid clade (1,517 species; Carleton and Musser 2005) contains members that show a comparatively diminished level of anatomical diversity (Steppan et al. 2004).

One process that may be involved in the evolution of morphological traits is heterochrony (Zelditch 2001). Heterochrony, derived from classical approaches to the study of ontogeny and phylogeny (Gould 1977) and subsequently formalized (Alberch et al. 1979), refers to a change in the timing and rate of development. The approach of sequence heterochrony (sensu Smith 2001) provides a methodology to study changes in the timing of developmental events that are not explicitly characterized by size and shape, two parameters that previously governed study for the majority of classical models of heterochrony (Klingenberg 1998). By considering events as discrete and sequentially occurring, the problems inherent to comparing a diverse range of species using size and time are obviated. Studies of heterochronies in ossification sequences at the marsupial/placental dichotomy (e.g. Sánchez-Villagra 2002; Sánchez-Villagra et al. 2008; Sears 2009; Smith 1997; Weisbecker et al. 2008) have yielded critical support for the conclusions from previous comparative studies of morphological diversity in these two clades, that are characterized by extreme differences in life history, especially gestation length (e.g. Lillegraven 1975; Sears 2004). Within Rodentia, postnatal sequence heterochrony examined for cranial suture closure patterning, a late time window in skeletal development, has been reported to play a role in shaping the diversity present among members of the hystricognath clade, which includes South American caviomorphs and African phiomorphs (Wilson and Sánchez-Villagra 2009). Additionally, several studies have concentrated upon the role of growth heterochrony in rodent evolution, using morphometric approaches (e.g. Creighton and Strauss 1986; Hautier et al. 2008, 2009; Monteiro et al. 2005; Wilson and Sánchez-Villagra 2010; Zelditch et al. 2006).

In this study we provide the most comprehensive sampling of rodent ossification sequences to date, with the aim of exploring whether heterochrony is ubiquitous in rodent evolution at the onset of skeletal formation. In doing so, we also help address the problem of the scarcity of data for skeletogenesis in non-model rodents. We present a detailed study of the African striped mouse, *Rhabdomys pumilio*; a small (~50 g) murid rodent with a widespread distribution in southern Africa (Nowak 1999). Found in many habitats, including grassland, desert and forests (Schradin 2005), *R. pumilio* attains approximately twice the body mass of the house mouse, *Mus musculus*. Moreover, unlike the latter model organism, *R. pumilio* is diurnal, and thus lends itself to easy

direct study in its natural habitat (Schradin 2006). Paternal care and communal breeding characterize the desert-living striped mice (Schradin and Pillay 2003, 2004). In addition, we provide the first ossification-sequence data for the degu, *Octodon degus*, a small to medium-sized, diurnal, semi-fossorial and herbivorous caviomorph rodent common to the central region of Chile (Mess 2007; Rojas et al. 1982). Studies of communal breeding in *O. degus* have shown that this rodent lives in groups with polygamous social structure (e.g. Ebensperger et al. 2004). Usually found in open areas, frequently close to human habitation, the degu forms extended family groups and creates complex burrow systems (Fischer 1940; Woods and Boraker 1975).

MATERIALS AND METHODS

Data collection

To the previously largest data set of cranial and postcranial ossification sequences (Sánchez-Villagra et al. 2008; Weisbecker et al. 2008), we add data on postcranial ossification for the degu (*Octodon degus*), on cranial ossifcation for the guinea pig (*Cavia porcellus*), and on cranial, postcranial and autopodial ossification

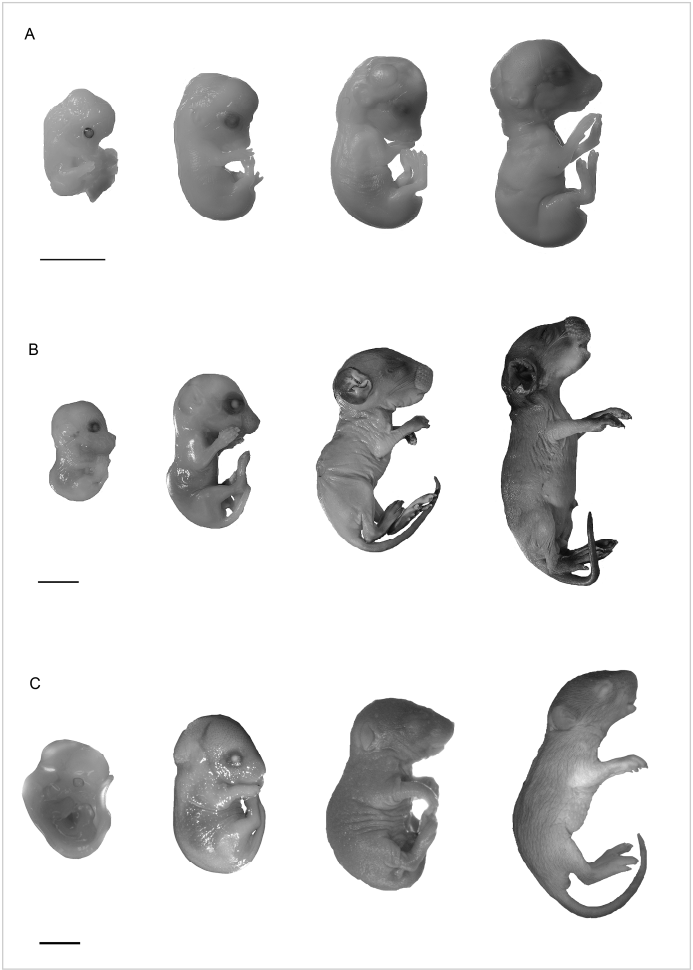

Figure 4.2: A sample of ontogenetic series prepared for this study at the Paläontologisches Institut und Museum, Zürich. A - *Cavia porcellus*. B - *Rhabdomys pumilio*. C - *Octodon degus*. Scales: 2 mm.

for the African striped mouse (*Rhabdomys pumilio*). We examined both prenatal and postnatal specimens, and coded the onset of ossification for 17 cranial and 24 postcranial elements, and also for 53 autopodial elements in *R. pumilio* (26 manus and 27 pes elements). The cranial data set comprised seven rodent species, including five muroids and two caviomorphs. For two species the ossification sequences were examined from specimens collected for this study; data for the remaining five species were taken from the literature. The analysis also included data from the literature for three outgroup species belonging to the Euarchontoglires clade (Tables 4.1–4.3).

Evolutionary relationships among rodent species examined here (Fig. 4.1) were based upon the molecular studies of Steppan et al. (2004) and Blanga-Kanfi et al. (2009). Outgroup species relations were reconstructed from Bininda-Emonds et al. (2007).

We also improve the resolution of ossification sequences for several species previously documented by Sánchez-Villagra et al. (2008) and Weisbecker et al. (2008), using a combination of additional literature sources and specimens held in the collections at the Paläontologisches Institut und Museum, Universität Zürich, Switzerland. The specimens of *Cavia porcellus* (Fig. 4.2A) and *Rhabdomys pumilio* (Fig. 4.2B) were obtained from breeding colonies maintained for research at the Universität Bielefeld (Germany) and the Universität Zürich, respectively (Schradin 2006; Trillmich et al. 2003). The founder individuals of *R. pumilio* originated from the Geogap Nature

Table 4.1: Sources of data for ossification sequences used in this study. Asterisks (*) denote outgroup species N = number of specimens / stages examined.

Taxon	Common name	N	References
Rhabdomys pumilio (Sparrman)	African striped mouse	61 / 12	present study
Rattus norvegicus (Berkenhout)	Norway rat	n.a. / 14	Strong (1925)
Meriones unguiculatus (Milne-Edwards)	Mongolian gerbil	187 / 8	Yukawa et al. (1999)
Peromyscus melanophrys (Coues)	Plateau mouse	13 / 5	Sánchez-Villagra et al. (2008), Weisbecker et al. (2008)
Mesocricetus auratus (Waterhouse)	Golden hamster	168 / 8	Beyerlein et al. (1951)
Mus musculus Linnaeus	House mouse	n.a. / 7	Theiler (1972), Kaufman (2008)
Cavia porcellus (Linnaeus)	Guinea pig	n.a. / 12	Petri (1935), present study
Octodon degus (Molina)	Degu	8 / 5	present study
Tupaia javanica Horsfield*	Horsfield's treeshrew	24 / 6	Nunn and Smith (1998), Zeller (1987), Goswami (2007)
Tarsius spectrum Pallas*	Spectral tarsier	21 / 6	Nunn and Smith (1998)
Homo sapiens Linnaeus*	Human	60 / 15	Mall (1906), Davies and Parsons (1927), Weisbecker et al. (2008)

	Tarsius	*Homo*	*Tupaia*	*Rattus*	*Mus*	*Peromyscus*	*Meriones*	*Mesocricetus*	*Rhabdomys*	*Cavia*
Premaxilla	1	2	1	2	1	1	1	2	2	1
Maxilla	1	1	1	1	1	1	2	1	2	1
Palatine	2	4	4	2	1	2	3	2	1	1
Dentary	?	1	1	1	1	1	1	1	1	1
Frontal	2	3	2	1	1	2	1	2	1	1
Parietal	3	3	2	2	1	2	4	2	1	1
Squamosal	2	3	3	2	3	4	4	2	6	1
Basioccipital	6	6	4	2	1	2	2	3	3	2
Nasal	?	4	4	3	3	4	3	3	5	2
Pterygoid	?	4	5	2	1	2	2	?	1	3
Exoccipital	4	3	3	2	1	3	3	2	4	3
Basisphenoid	6	8	6	4	3	3	4	2	7	4
Jugal	2	3	2	3	2	4	4	5	8	1
Lacrimal	3	7	4	3	4	4	4	6	9	3
Alisphenoid	5	5	4	5	1	4	4	4	10	1
Orbitosphe-noid	?	7	5	6	5	5	5	7	11	5
Periotic	7	4	7	?	6	5	?	?	12	5

Table 4.2: Cranial events ranked according to relative timing of onset of ossification, based on observations from specimens and summaries compiled from the literature.

	Homo	*Rattus*	*Mus*	*Peromyscus*	*Meriones*	*Mesocricetus*	*Rhabdomys*	*Cavia*	*Octodon*
Clavicle	1	1	1	1	1	1	1	1	1
Humerus	2	2	1	2	2	2	1	2	1
Ribs	5	2	1	2	?	2	1	3	1
Femur	2	3	1	2	2	3	1	2	1
Radius	3	2	1	2	2	3	1	2	1
Ulna	1	2	1	2	2	3	1	2	1
Scapula	5	3	1	2	2	3	1	3	1
Cervical v.	7	3	3	2	2	3	1	4	1
Thoracic v.	7	3	3	2	3	3	2	5	2
Tibia	3	3	2	2	2	3	1	2	1
Fibula	5	3	2	2	2	3	2	2	1
Lumbar v.	9	4	3	2	3	3	3	5	2
Sacral v.	11	4	4	2	4	4	5	8	3
Caudal v.	14	4	5	3	6	6	10	10	3
Ilium	6	3	2	2	3	3	2	4	1
Manus phal.	6	7	7	3	5	4	9	6	2
Pes phal.	8	7	7	3	5	4	10	7	3
Ischium	12	5	4	3	5	6	4	5	1
Pubis	15	5	5	3	8	6	7	10	4
Metac.	7	4	5	3	4	4	6	6	3
Metat.	8	4	5	3	5	6	7	7	3
Tarsals	10	6	6	4	7	7	10	11	4
Carpals	16	8	7	4	8	8	11	12	5
Sternum	13	5	5	3	?	5	8	9	3

Table 4.3: Postcranial events ranked according to relative timing of onset of ossification, based on observations from specimens and summaries compiled from the literature.

Reserve in South Africa (29°41.56'S, 18°1.60'E). The specimens of *Octodon degus* (Fig. 4.2C) were part of the personal collection of Andrea Mess and are now deposited at the Universität Zürich. All specimens obtained for this study were prepared using a modified version of standard enzymatic clearing and double staining (Prochel 2006) (Fig. 4.3). Onset of ossification for each element was recorded based upon the earliest uptake of alizarin red. Although data for several sequences of ossification were recorded from published literature, which detailed differing preparation procedures, all embryos for a given species were prepared using the same protocol; hence the resulting ossification sequences are considered to be accurate.

Intraspecific variation in Rhabdomys pumilio

The sample of *R. pumilio* contained multiple specimens from several litters. We used this opportunity to examine intraspecific variation in ossification-event sequences, studies of which are rare, and so far restricted to a limited number of taxa (e.g. Colbert and Rowe 2008; Garn and Rohmann 1960; Mabee et al. 2000; Moore and Townsend 2003). Out of the 61 specimens studied, 55 could be reliably assigned to ten litters as collected at time of death. Each litter contained between three and seven animals. Variation was assessed among siblings within each litter, for each subdivision of the skeleton: cranial, postcranial and autopodial. The latter approach contrasts with that for the ontogenetic sequence of ossification for *R. pumilio*, which was compiled by comparison of individuals across all litters. For each element within a subdivision, we compared the ossification state (ossified or not ossified) across all pups within a litter. We noted the number of litters in which we found a discrepancy in the ossification state of an element. To assess how intraspecific variability (in ossification state) affected the determination of the ossification sequence, we used the quantification methods of Mabee et al. (2000), whereby we calculated the magnitude of rank difference, i.e. the degree to which a bone varied in position in the complete ossification sequence. Rank differences were calculated for all elements in each of the cranial, postcranial and autopodial sequences. The magnitude of rank difference is defined as the number of steps between the maximum and minimum position of an individual bone. We compared variation in position of a bone in relation to a common sequence, which was derived by determining the state (ossified or not ossified) for each element to be that shared by the majority of animals in the litter. For example, if a litter contained four animals, and if three of these displayed an ossified jugal whereas one did not, we determined that for the stage represented by that litter, the jugal was ossified. To generate a common sequence, we then compiled

the information across litters. When deriving ossification sequences for the cranial and postcranial partitions used for Parsimov analyses (Jeffery et al. 2005) and for the autopodial sequence, we took the common, or majority, pattern to be representative of the stage a given litter documented (Mabee et al. 2000).

Analysis of variation in ossification sequence

To examine levels of variation in sequence of a particular ossification event we standardized each rank within a sequence by expressing it as a fraction of the total number of ranks (r_{max}) for a given species, such that the rank sequence for each species falls within the range between $1/r_{max}$ and 1. By scaling ranks in this manner we removed differences in maximum rank between species consequent from differing levels of resolution between species; nonetheless, the small differences in contribution to variance associated with different r_{max} values remain inherent to this methodology. To express variability of a particular element in the ossification sequence, we computed for each cranial and each postcranial bone, from the scaled rank values, a range in rank variation across species examined.

The frequency distribution of ranks, for each of the cranial and postcranial data sets, was calculated, in order to examine the distribution of ossification events within the rank sequence. Maximum documented rank for each species was regressed against number of specimens studied, to test the validity of the expectation that total number of specimens studied does not instigate differences in resolution of ranks.

Figure 4.3: Cleared and double-stained rodents prepared at the Paläontologisches Institut, Zürich. Left: *Octodon degus*. Right: *Rhabdomys pumilio*. Scale: 2 mm.

Event pairing and Parsimov analyses

Two separate data matrices were constructed: one each for the postcranial and cranial data sets. We separated cranial and postcranial data sets, as did previous authors (e.g. Sánchez-Villagra et al. 2008; Weisbecker et al. 2008), because (A) those are two recognized modules, and (B) the resolution and availability of data for these two sets are different (Tables 4.2, 4.3). Because we have separated the skeletal regions, we cannot rule out heterochrony occurring between the cranial and postcranial modules. To identify heterochronies within the sequence of ossification, the timing of each ossification event was assessed by comparing the relative timing of pairs of elements. For each data set an event-pair matrix was produced in which non-redundant pairs of events were compared: each event was coded as having occurred either earlier than (score 0), simultaneous with (1), or later than (2) each other event. The postcranial data matrix contained 276 event pairs, the cranial matrix 136 event pairs. Following the reconstruction of apomorphic character-state changes using PAUP 4.0b10 (Swofford 2002), we analyzed event-pair data using the computer program Parsimov, which reconstructs the least number of event movements that may explain all possible event-pair changes along a given branch

Table 4.4: Detailed heterochronies for non-model species (*R. pumilio* and *O. degus*) analyzed in this study, and major clades.

Clade	Event	Movement	… in relation to …
Muroidea	Nasal	early	Squamosal, Basioccipital
	Ribs	early	Femur, Radius
Rhabdomys	Sternum	late	Pubis, Metatarsals
	Maxilla	late	Palatine, Dentary, Frontal, Parietal
Rhabdomys + *Mus*	Basisphenoid	twins	Orbitosphenoid
	Fibula	late	Femur, Scapula
Octodon	Cervical v.	early	Humerus, Ribs, Fibula
	Sacral v.	early	Pes phal., Metatarsals
	Caudal v.	late	Sacral v., Pes phal., Metatarsals, Sternum
	Ilium	early	Humerus, Ribs
	Manus phal.	early	Thoracic v., Lumbar v.
	Metacarpals	late	Pes phal., Metatarsals
	Pterygoid	early	Premaxilla, Dentary, Jugal

(Jeffery et al. 2005). Optimizations were performed using both ACCTRAN and DELTRAN methods, but only events found in a consensus of the two approaches were interpreted as heterochronic. For instances in which reconstruct-

Figure 4.4: Ossification of elements of the left hand (respective upper row) and foot (lower row), in dorsal views, of *Rhabdomys pumilio*; black = ossified, grey = calcified. Number of specimens examined (N)=1, except at stages a (N=16), f (6), g (2), n (9), y (4), and z (2).

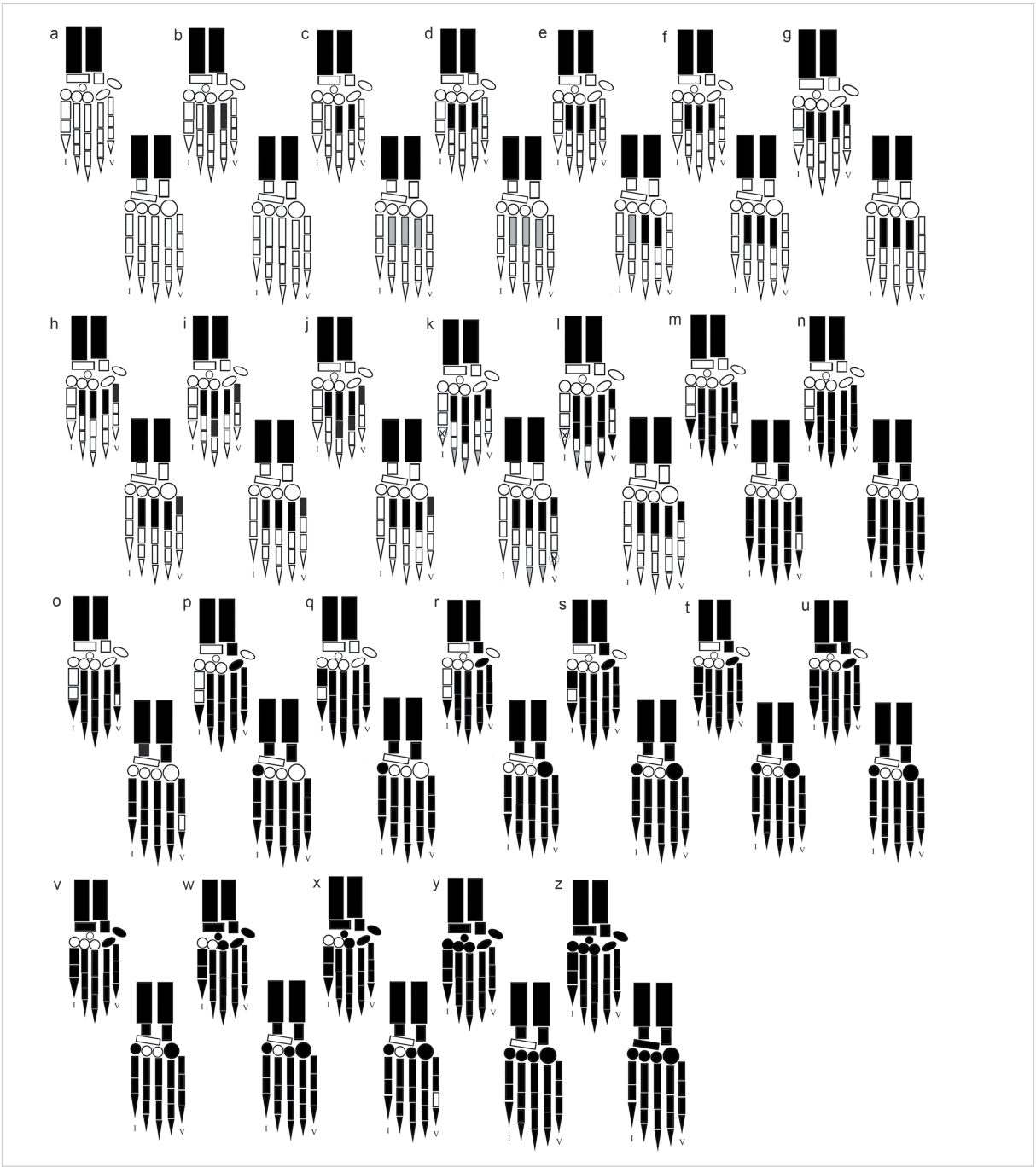

tion of a character is ambiguous, the ACCTRAN optimization assumes early origination of a character and subsequent reversal, whereas the DELTRAN optimization delays a change resulting in parallel origination at a later point. Using a consensus of these two approaches provides the most conservative estimate of heterochronic shifts present in the non-ambiguous events common to both.

RESULTS

Event Pairing and Parsimov analyses

For the cranial data set (Table 4.2), a total of 136 event pairs yielded 79 (58.1%) parsimony-informative pairs and 57 (41.8%) variable pairs that did not provide any informative signal, including 14 pairs (10.2% of total) that were autapomorphic. These autapomorphies include the parietal ossifying before the premaxilla and maxilla in *R. pumilio*, and in *C. porcellus* the pterygoid ossifying after the squamosal and basioccipital, and the jugal before the basioccipital. Of the 276 event pairs in the postcranial data matrix (Table 4.3), 135 (48.9%) were phylogenetically informative, 84 (30.4%) were variable, and 57 pairs (20.7%) possessed the same character state across all species examined. In caviomorphs the metatarsals ossified after the ischium, whereas the manual phalanges ossified before the sacral vertebrae. Among the phylogenetically uninformative event pairs, an autapomorphy concerning the forelimb was distinguishable for *Rattus norvegicus*: both the radius and ulna ossified before the femur. In *C. porcellus* the metacarpals ossified before the sacral vertebrae, and the ribs after the humerus.

The consensus of ACCTRAN and DELTRAN transformations indicates that two early shifts occur within the Muroidea clade, one each in the cranial and postcranial skeleton (Table 4.4). Few heterochronies distinguished different species of muroids: those for *R. pumilio* involve late movements of the sternum and maxilla (Table 4.4). The clade consisting of *M. musculus* and *R. pumilio* is characterized by an early heterochronic shift of the fibula in relation to the femur and scapula, and twinned movement of the basisphenoid and orbitosphenoid (Table 4.4). *Octodon degus* is characterized by several autapomorphic character shifts: six out of seven (85.7%) relate to the postcranium, and specifically three of these six (50%; 42.8% of total) involve the vertebral column (Table 4.4).

Skeletogenesis in Rhabdomys pumilio

Rhabdomys pumilio displays a sequence of ossification in cranial elements that is similar to that of other muroid species studied (Table 4.2), namely ossification of the craniofacial bones and bones in the palatal region followed by the cranial base and then elements

associated with the otic region, and lastly the periotic bone. The largest number of tied ossification events occurs in the earliest stage, with five out of 17 elements (29%) ossifying first: the palatine, dentary, frontal, parietal and pterygoid. The pattern of earliest events having the least resolution is shared with *Cavia porcellus* and *Mus musculus*; the remaining four species (57%) exhibit three or fewer ossification events occurring at the earliest moment (Table 4.2).

The postcranial ossification sequence indicates that *R. pumilio* is characterized by a late ossification of the caudal vertebrae; this region is the penultimate postcranial element to ossify. Similar to *Rattus norvegicus*, ossification of the pubis in *R. pumilio* occurs earlier within the sequence than in the other rodents studied here, with this element ossifying at position seven out of eleven in *R. pumilio,* and at position five out of eight in *R. norvegicus* (Table 4.3). In *R. pumilio* the first elements to ossify in the postcranium account for nine out of 24 events (38%). *Octodon degus* and *Mus musculus* share a similar concentration of relative simultaneity for the earliest events, whereas in the remaining five rodent species (62.5%) the clavicle ossifies first, and a greater number of events ossify in subsequent stages (Table 4.3).

Table 4.5: Ranked sequences of ossification in the autopodial region of the African striped mouse, *Rhabdomys pumilio*.

Manus		Pes	
Metacarpal III	1	Metatarsal III	1
Metacarpal IV	1	Metatarsal IV	1
Metacarpal II	2	Metatarsal II	2
Metacarpal V	3	Metatarsal V	3
Proximal phalanx III	4	Distal phalanx II	4
Proximal phalanx IV	5	Distal phalanx III	4
Distal phalanx II	6	Distal phalanx IV	4
Distal phalanx III	6	Distal phalanx V	5
Distal phalanx IV	6	Proximal phalanx II	5
Proximal phalanx II	7	Proximal phalanx III	5
Distal phalanx V	7	Proximal phalanx IV	5
Proximal phalanx I	8	Proximal phalanx V	5
Proximal phalanx V	8	Proximal phalanx I	5
Medial phalanx II	8	Medial phalanx I	5
Medial phalanx III	8	Medial phalanx II	5
Medial phalanx IV	8	Medial phalanx III	5
Medial phalanx I	8	Medial phalanx IV	5
Medial phalanx V	9	Calcaneus	5
Triquetrum	10	Metatarsal I	5
Distal carpal IV	10	Medial phalanx V	6
Distal carpal V	10	Astragalus	6
Scaphoid	11	Distal tarsal I	7
Metacarpal I	12	Distal tarsal IV	8
Pisiform	13	Distal tarsal V	8
Centrale	14	Distal tarsal III	9
Distal carpal III	14	Distal tarsal II	10
Distal carpal I	15	Navicular	11
Distal carpal II	15		

Both the manus and pes follow similar ossification patterns concerning the spatial autopodial region (Table 4.5), except that the proximal phalanges begin ossification before the distal phalanges in the hand, though in both the hand and foot, distal and proximal phalanges begin to ossify before their intermediate counterparts (Figs. 4.4, 4.5). In all autopods the middle metapodials are the first elements to start ossification. The capitatum (distal carpal III) starts to ossify before the trapezoid (distal carpal II) and the trapezium (distal carpal I), and the pisiform starts to ossify before the capitatum. Among the carpals, the triquetrum and the hamatum (distal carpals IV and V) consistently are the first two carpals to begin ossification (simultaneously). Metatarsal I is the last metatarsal to ossify, and it does so before any of the distal tarsals. In the hand, ossification of metacarpal I partially follows the same regime, also starting ossification later than all other metacarpals, but not before distal carpal ossification begins (Table 4.5). Indeed, the distal carpals are the last elements to begin ossification in the hand, whereas in the foot the navicular is the last to commence ossification (Figs. 4.4–4.6).

Several heterochronic events characterize *R. pumilio*: late movement of the sternum in relation to the pubis and metatarsals, and late movement of the maxilla in relation to the palatine, dentary, frontal and parietal (Table 4.4). *Rhabdomys pumilio* and *Mus musculus* share twinned movement of the basisphenoid and orbitosphenoid, and late movement of the fibula in relation to the femur and scapula (Table 4.4).

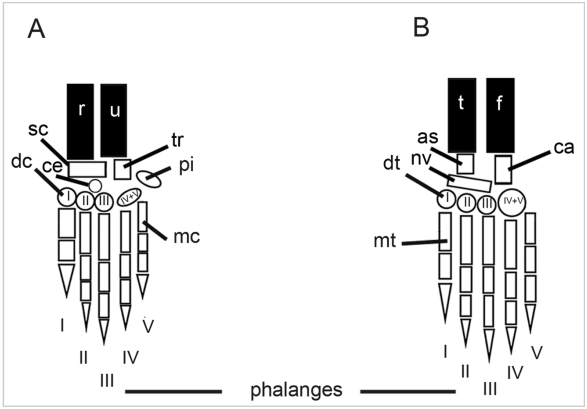

Figure 4.5: Autopodial elements of the left hand (A) and foot (B), in dorsal views, of *Rhabdomys pumilio*. Elements: as = astragalus, ca = calcaneus, ce = centrale, dc = distal carpal, dt = distal tarsal, f = fibula, mc = metacarpal, mt = metatarsal, nv = navicular, pi = pisiform, r = radius, sc = scaphoid, t = tibia, tr = triquetrum, u = ulna.

Intraspecific variation in Rhabdomys pumilio

Intraspecific variation in element ossification is present in all partitions of the skeleton (cranial, postcranial, autopodial). In all ten litters examined, the cranial and postcranial skeletal areas exhibit the most variation. Within the postcranial skeleton, animals in eight out of ten litters displayed variation. Hence, within each of these eight litters at least one of the 24 postcranial elements displayed an

ossification state (ossified or not ossified) opposite to that displayed by the other animals in the litter. Intraspecific variation is found in six out of ten litters for the 17 cranial elements examined. Because the autopodial region contains more than twice the number of elements (53 in total) than either the postcranial or cranial skeletal areas, by sheer chance it would be more probable for intraspecific variation to be detected in this region; therefore, the reported variability among specimens in seven out of ten litters is reduced compared to the postcranial and cranial regions.

The number of different elements that vary intraspecifically is low, with not more than three elements exhibiting variation among members of a litter. Among the cranial elements variation is restricted to the premaxilla, nasal, exoccipital, squamosal and basioccipital, with an average of one element out of 17 (5.8%) exhibiting variation among specimens belonging to a given litter. On average two out of 24 (8.3%) postcranial elements vary between pups from the same litter. Autopodial elements in the manus that exhibit variation in ossification are the metacarpals I, III and IV and the distal phalanx V; in the pes these are the medial phalanx V and metatarsals II, III and IV. When coupled together, variation in the manus and pes is found on average for two out of 53 elements per litter (3.7%).

The effect of intraspecific variation upon ossification sequence was determined using the rank magnitude metric of Mabee et al. (2000); see Appendices 4.1 and 4.2. For the cranial ossification sequence (Appendix 4.1), intraspecific variation resulted in a change in sequence position for nine out of 17 elements (52.9%), though in each case this was restricted to a magnitude rank change of 1. The postcranial results indicate that twelve out of 24 elements (50.0%) altered their position in the ossification sequence, with ten of these exhibiting a rank magnitude difference of 1, and the remaining two (pubis, lumbar vertebrae) a rank difference of 2. For the autopodial region, ten out of 26 elements (38.5%) in the hand, and twelve out of 27 (44.4%) in the foot, exhibited a variation in position (Appendix 4.2). Similar to the cranial and postcranial data sets, the majority of elements that moved position in the autopodial sequences moved by only one place (Appendix 4.2). The exceptions concern the pisiform in the manus and metacarpal V, and the astragalus in the pes, each of which exhibited a magnitude or rank variation of 2.

Rank variability among rodents

For all rodents studied here, the elements in the cranial ossification sequences that exhibit the highest amount of variation in rank position are the parietal and alisphenoid, followed by the squamosal and jugal. The least

variable elements within an ossification sequence are the dentary and the periotic, the latter being the last bone to ossify in all rodents examined (Table 4.2, Fig. 4.7A). In the postcranium, both the ischium and the manual phalanges were found to be most variable in position, whereas the carpals, sternum and clavicle differed least in rank position (Table 4.2, Fig. 4.7B). Across all species studied, the number of ranks extends to a maximum of twelve, and event distributions for cranial and postcranial elements indicate that ossification-event occurrences are predominant in the earliest stages of a sequence (Fig. 4.8). In cranial elements, the frequency of ossification events is highest at the first stage (35; 30.4%) and progressively decreases throughout later stages. By comparison, in postcranial elements the second position in the sequence is characterized by the highest number of ossification-event occurrences (42; 23.4%), and the later stages of the sequence show increased variation in frequency of events (stages 7–12; Fig. 4.8) compared to elements within a cranial sequence. The number of ranks in a sequence, for a given species taken from maximum value, was not significantly correlated with the number of specimens available for study; hence, resolution in a sequence is neither directly improved nor reduced as a consequence of sample size ($r = 0.248$, $p = 0.553$).

DISCUSSION

Sequence heterochrony

Our results indicate that heterochrony does not play a pivotal role in early skeletal formation in rodents, based on comparisons between six muroid and two caviomorph species. The lack of heterochrony recorded here for prenatal and early postnatal stages may

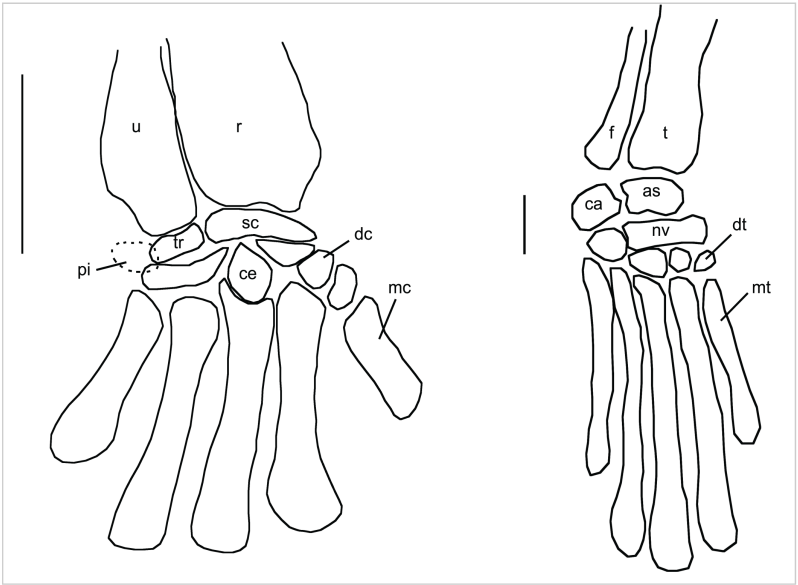

Figure 4.6: Camera lucida drawings of the right hand (shown at left) and foot, in dorsal views, of *Rhabdomys pumilio*. Autopodial elements: as = astragalus, ca = calcaneus, ce = centrale, dc = distal carpal, dt = distal tarsal, f = fibula, mc = metacarpal, mt = metatarsal, nv = navicular, pi = pisiform, r = radius, sc = scaphoid, u = ulna, t = tibia, tr = triquetrum. Scales: 2 mm.

indicate that heterochrony is more prominent in rodent evolution at later postnatal stages of growth (Wilson and Sánchez-Villagra 2009).

We detected few shared heterochronic shifts in the cranial ossification sequence (Table 4.4). Only the early ossification of the nasal in relation to the squamosal and basiocciptal characterizes Muroidea. Similar to the results presented herein, Sánchez–Villagra et al. (2008), in their study of mammalian cranial ossification patterns, also reported few shared shifts while, as in the study by Bininda-Emonds et al. (2003) on mammalian development, several autapomorphic shifts were documented. The lack of shared heterochronic shifts in the species examined in the present study further supports previous findings of conservatism in relative timing of vertebrate cranial developmental events (Schoch 2006).

Similarly, postcranial sequence heterochronies reported here are restricted to a single event for the Muroidea clade (Table 4.4). Weisbecker et al. (2008) found Muroidea to be characterized by early ossification of the scapula and cervical vertebrae in relation to the forelimb and hindlimb elements, based upon the

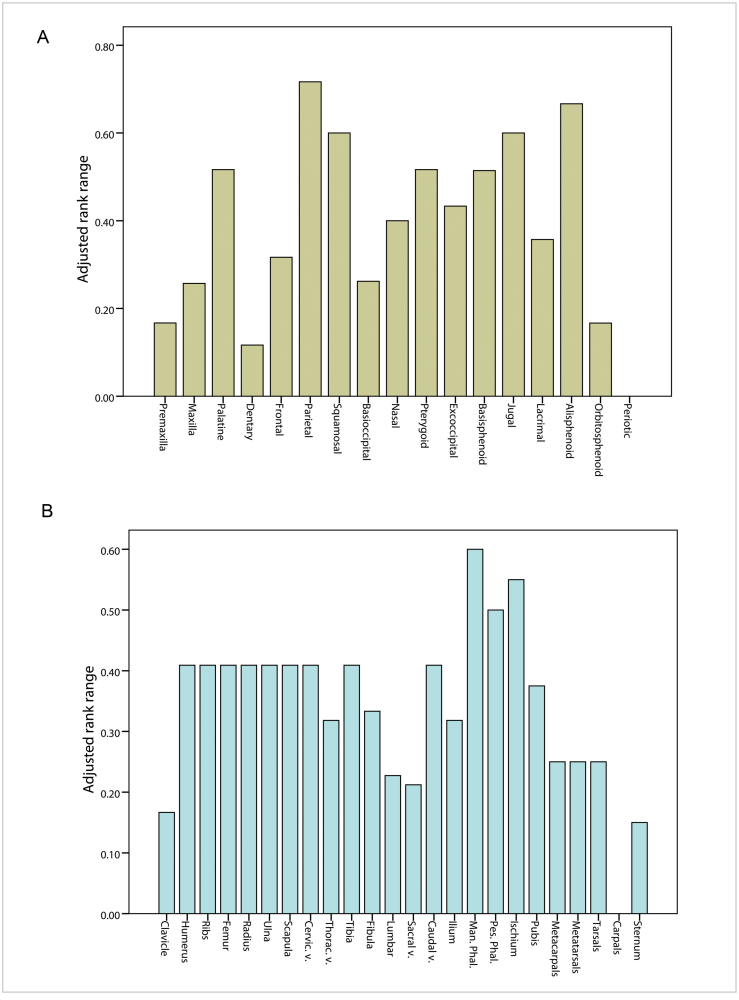

Figure 4.7: Adjusted rank range plots of cranial (A) and postcranial (B) elements for rodents examined in this study.

same species of rodent studied here, except *O. degus*, but using a lizard and alligator outgroup. Our results do not mirror the findings of Weisbecker et al. (2008) but instead yield a shared shift for Muroidea involving an early movement of the ribs in relation to the femur and radius (Table 4.4). A similar earlier movement of the ribs was recorded by Sánchez-Villagra (2002) for *R. norvegicus* and *M. auratus*, although the feature was not shared as a synapomorphy between these two taxa. The discrepancies between our results and those of Weisbecker et al. (2008) and Sánchez-Villagra (2002) may be explained by our relatively expanded rodent sampling, particularly its inclusion of another non-muroid species (*O. degus*), and by the use of more closely related non-rodent outgroups, both of which act to improve the resolution of rodent-specific shifts. Two heterochronic shifts in postcranial ossification sequence were found to characterize caviomorphs: the late ossification of metatarsals in relation to the ischium, and early ossification of the manual phalanges in relation to the sacral vertebrae. Several autapomorphic events are also reported, including those for *Octodon* that relate to early ossification of elements in the posterior skeleton, including the cervical and sacral vertebrae, and the ilium (Table 4.4). A lack of distinguishable heterochronies between the caviomorphs and the muroids may corroborate a recent finding that changes in postnatal growth pattern were equally common during the evolutionary history of both clades (Wilson and Sánchez-Villagra 2010).

The considerable number of autapomorphic shifts found for the species studied here, and the comparative lack of sequence heterochronies towards the root of the phylogeny, are features in common with previous results produced with the Parsimov algorithm (Harrison and Larsson 2008), and have been discussed before, along with issues of character non-independence (Schulmeister and Wheeler 2004). Additionally, our approach of inferring heterochronies common to the consensus of ACCTRAN and DELTRAN is also highly conservative, and may further restrict the identification of heterochronic shifts in our data, an issue previously acknowledged to characterize this method (e.g. Sánchez-Villagra et al. 2008; Werneburg and Sánchez-Villagra 2009). Hence, in the light of methodological limitations and also considering the limited taxon sampling resulting from the difficulty of obtaining developmental sequences for any mammal, the role of sequence heterochrony in rodent evolution cannot be dismissed conclusively. Our study, however, uses a similar conservative approach to quantification of heterochrony comparable to that carried out in recent studies of mammals on a similar time window of development (e.g. Sánchez-Villagra et al. 2008; Weisbecker et

al. 2008) and on embryology of the external morphology (Werneburg and Sánchez-Villagra in press). The pattern of limited heterochrony we found in rodents does not deviate from that reported in those previous studies.

Autopodial ossification

As is the case in almost all placentals, and in contrast to marsupials examined to date (Prochel and Sánchez-Villagra 2003; Prochel et al. 2004), the capitatum (distal carpal III) of *R. pumilio* begins ossification before the trapezoid (distal carpal II) and the trapezium (distal carpal I) (Figs. 4.4, 4.5). *Rhabdomys pumilio* also displays early ossification of the pisiform in relation to the capitatum: this event has been reported by Prochel et al. (2004) to characterize Rodentia. Among the carpals, the triquetrum and the hamatum (distal carpals IV and V) consistently are the first two carpals to start ossification (simultaneously). Within the rodents examined, these two elements develop to be the largest carpals in adulthood, adding support to the notion, proposed by Huxley (1932), that the timing of initiation of an organ in the embryo is related to its size attained at adulthood. The general sequence of manual element ossification for *R. pumilio* follows that reported for *M. musculus* (Prochel et al. 2004), in that ossification begins with the humerus, radia and ulna, after which metacarpal III ossifies, followed sequentially by proximal phalanx III, distal phalanx II and medial phalanx III (Table 4.5). This sequence is a slight depar-

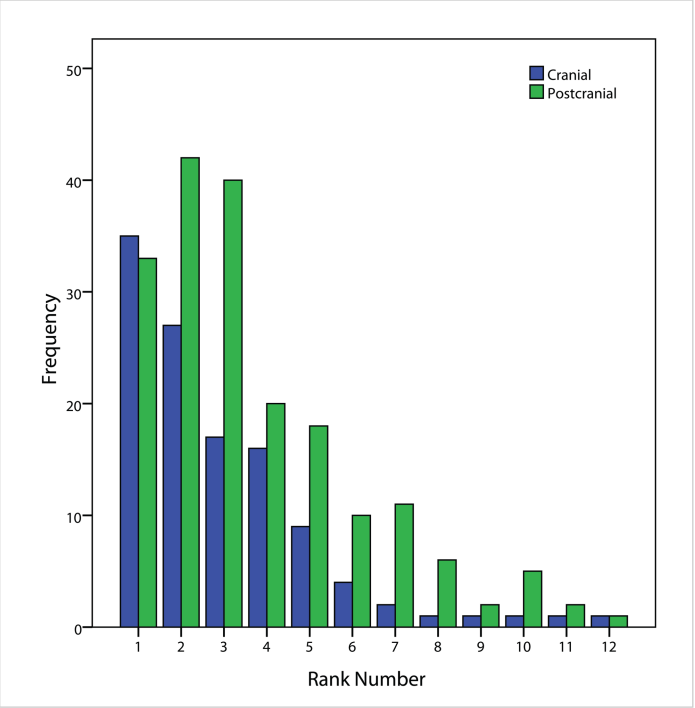

Figure 4.8: Frequency variation plot of cranial and postcranial ossifying events for rodents examined in this study.

ture from that reported for *C. porcellus* (by Petri 1935), *R. norvegicus* (Strong 1925) and *M. auratus* (Beyerlein et al. 1951), where the distal phalanx begins ossification before the proximal phalanx in the aforementioned pattern.

Variability in rank

In their study of mammalian cranial ossification patterns, Sánchez-Villagra et al. (2008) found the most variable cranial elements in an ossification sequence to be the basioccipital, basisphenoid, jugal, parietal, pterygoid and squamosal. In addition to the rodents examined here, the data set of Sánchez-Villagra et al. (2008) included representatives from a number of other clades, including primates, Chiroptera and Soricidae. In comparison, we find the basioccipital to display reduced difference in ossification rank across the rodent species examined, but the squamosal, jugal and basisphenoid all exhibit relatively high levels of rank variability, consistent with the previous findings.

Because the non-rodent species examined by Sánchez-Villagra et al. (2008) represented more than 85% of the sampled species, and since their analysis also encapsulated a greater phylogenetic breadth than that presented here, particularly with more distantly related outgroup taxa, such as turtles, it is highly likely that these factors contributed to mask the aforementioned rodent-specific patterns of rank variability identified herein. The alisphenoid displays the second-highest level of variation in this study, whereas Sánchez-Villagra et al. (2008) do not report elevated variation for this element. The amplified variation in alisphenoid ossification found here is the consequence of the early ossification reported for *C. porcellus* and *M. musculus* (at position one in the sequence) compared to the remaining rodents in the study sample (position four, or later) (Table 4.2). Although neither of these two species has fewer ranks in the ossification sequence compared to the other species sampled, both species do show an increased frequency of events ossifying in the first stage and, hence, reduced resolution at the earliest point of development. This suggests that the pattern may be an artefact attributable to an issue of inadequate resolution that could be remedied by obtaining specimens covering a finer sampling of ontogenetic stages. Elements displaying the least variability in the present study are not confined exclusively to previously reported modules of the mammalian cranium (Goswami 2006). The premaxilla, orbitosphenoid and periotic are found in spatially different areas of the cranium, and other elements contained within the corresponding modules exhibit increased lability. For example, although the periotic does not vary in sequence position in the rodents studied, the other elements defined by Goswami (2006) to

belong to the cranial base module (basioccipital, basisphenoid and exoccipital) exhibit variability comparable to that in elements associated with other modules (Fig. 4.7A). While the aim here is not to explicitly test modularity within sequence heterochrony (Goswami et al. 2009), the labile nature of the cranial elements we present for species within one clade of mammals suggests that developmental timing can be less integrated than previously assumed (Schoch 2006).

Variability in the postcranium is highest for the ischium and both manual and pedal phalanges, and lowest for the clavicle, carpals and sternum (Fig. 4.7B). In agreement with Prochel (2006) and Weisbecker et al. (2008) we find an early ossification of anterior postcranial elements (Table 4.3), and elements of high and low variability are shared with those reported in the former study. The variation we find in the manual and pedal phalanges can be attributed to the late ossification of these elements in *R. pumilio*, *R. norvegicus* and *M. musculus*. Compared to the other species studied, these murids show earliest ossification of phalanges beginning at the second-to-last position in the ossification sequence, whereas among the remaining species sampled ossification of phalanges begins as early as the second stage (*O. degus*) and not later than within the first two-thirds of all events (Table 4.3).

Intraspecific variation in ossification sequence

The incidence and extent of intraspecific variation in the ossification sequence of *R. pumilio* is low and mainly restricted to a few elements per region of the skeleton examined. Similar to work completed on bony fishes, we find that elements involved in intraspecific variation are not exclusively concentrated towards the end of the ossification sequence, a feature that has been cited to suggest an extension or truncation to a linear ancestral ontogeny (Mabee et al. 2000). Indeed, for the autopods variation is mostly found in the first elements to begin ossification: the metacarpals and metatarsals (Figs. 4.5, 4.6; Table 4.5). In contrast, Garn and Rohmann (1960) and Garn et al. (1961a, 1961b, 1966), in their studies of the appendicular and axial skeleton of humans, reported variability in the ossification sequence in the hands and feet to be concentrated to the elements ossifying last; a similar situation was reported by Alberch and Blanco (1996) for sequence variation in the European fire salamander, *Salamandra salamandra*. Nevertheless, consistent with the present findings for *R. pumilio*, the above studies also documented a comparatively low overall level of intraspecific variation.

One might expect intraspecific variation to parallel interspecific variation to the exclusion of non-variable elements that, thus, may exhibit functionally related units reflecting

modular components within the skeleton, or tightly integrated subsets (Goswami et al. 2009; Wagner 1988). We find, however, that elements involved in cases of intraspecific variation did not consistently exhibit the highest levels of interspecific variability. Variation in ossification sequence, like variation in any feature, can be explained by genetic and/or environmental factors (Wagner 1988). Indeed, Garn et al. (1966) proposed the former to provide a strong basis for variations in the human appendicular skeleton. Nevertheless, the particular influence of the genotype, and also that of environmental variables in relation to ossification sequence variations, remains unclear, which impedes development of a direct causal explanation for the variation in *R. pumilio* reported here.

The results of the rank-magnitude calculations (Appendices 4.1 and 4.2) indicate that variation in sequence position was generally low; none of the variable elements changed position by more than two ranks. The low intraspecific variation in *R. pumilio* is not surprising, especially since the sample size (55 individuals) for our study was approximately one quarter that of earlier studies, which also reported low levels of intraspecific variability (e.g. Alberch and Blanco 1996; Moore 1991). Nonetheless, recent works have demonstrated and underlined that it is imperative to consider patterns of embryonic variability when examining developmental time (Colbert and Rowe 2008; de Jong et al. 2009). Consideration of this notion opens a suite of questions in relation to the evolution of developmental sequences. For instance, comparisons between natural and experimentally controlled populations may help identify the respective functions of heritable variation and of environmentally induced developmental variation in the generation of intraspecific variation.

CONCLUSIONS

The present examination of ossification sequences, based upon the largest data set so far compiled for rodents, suggests that sequence heterochrony is neither pivotal nor prevalent during early skeletal formation in this clade. Documentation of skeletogenesis in *R. pumilio* indicates that intraspecifc variation in ossification-sequence pattern is present, though not extensive. Further extension of the ossification data on rodents, especially the collection of information on non-model organisms, will assist our understanding of how important sequence changes are as a raw material for evolution in this species-rich clade of mammals.

ACKNOWLEDGEMENTS

We thank Fritz Trillmich for kindly providing specimens of *Cavia porcellus* for use in this study. This work received support from the Swiss National Fond (3100A0-116013) to

M.R.S.-V., a Forschungskredit (nr. 3771) from the Universität Zürich to L.A.B.W., and from the Consejo de Investigaciones Científicas y Técnicas in Argentina to F.C.G. For insightful comments that helped to improve an earlier version of this paper, we thank Olaf R. P. Bininda-Emonds and two anonymous reviewers.

REFERENCES

Alberch, P., & Blanco, M. J. (1996). Evolutionary patterns in ontogenetic transformation: from laws to regularities. *International Journal of Developmental Biology, 40*, 845–858.

Alberch, P., Gould, S. J., Oster, G. F., & Wake, D. B. (1979). Size and shape in ontogeny and phylogeny. *Palaeobiology, 5*, 296–317.

Beyerlein, L., Hillemann, H. H., & Van Arsdel, W. C., III (1951). Ossification and calcification from postnatal day eight to the adult condition in the golden hamster (*Cricetus auratus*). *Anatomical Record, 111*, 49–65.

Bininda-Emonds, O. R. P., Cardillo, M., Jones, K. E., MacPhee, R. D. E., Beck, R. M. D., Grenyer, R., et al. (2007). The delayed rise of present-day mammals. *Nature, 446*, 507–512.

Bininda-Emonds, O. R. P., Jeffery, J. E., & Richardson, M. K. (2003). Is sequence heterochrony an important evolutionary mechanism in mammals? *Journal of Mammalian Evolution, 10*, 335–361.

Blanga-Kanfi, S., Miranda, H., Penn, O., Pupko, T., DeBry, R. W., & Huchon, D. (2009). Rodent phylogeny revised: analysis of six nuclear genes from all major rodent clades. *BMC Evolutionary Biology, 9, 71*, doi:10.1186/1471-2148-9-71

Carleton, M., & Musser, G. (2005). Order Rodentia. In D. W. Wilson, & D. M. Reeder (Eds.), *Mammal species of the world*, (pp. 745–752). Washington, D.C.: Smithsonian Institution Press.

Colbert, M. W., & Rowe, T. (2008). Ontogenetic sequence analysis: using parsimony to characterize developmental sequences and sequence polymorphism. *Journal of Experimental Zoology, 310B*, 398–416.

Creighton, G. K., & Strauss, R. E. (1986). Comparative patterns of growth and development in cricetine rodents and the evolution of ontogeny. *Evolution, 40*, 94–106.

Davies, D. A., & Parsons, F. G. (1927). The age order of the appearance and union of the normal epiphyses as seen by X-rays. *Journal of Anatomy, 62*, 58–71.

Ebensperger, L. A., Hurtado, M. J., Soto-Gamboa, M., Lacey, E. A., & Chang, A. T. (2004). Communal nesting and kinship in degus (*Octodon degus*). *Naturwissenschaften, 91*, 391–395.

Fischer, G. M. (1940). Contribución a la anatomia de los Octodontidos. *Boletín del Museo Nacional de Historia Natural (Santiago de Chile), 18*, 103–124.

Garn, S. M., & Rohmann, C. G. (1960). Variability in the order of ossification of the bony centers of the hand and wrist. *American Journal of Physical Anthropology, 18*, 219–230.

Garn, S. M., Rohmann, C. G., & Apfelbaum, B. (1961a). Complete epiphyseal union of the hand. *American Journal of Physical Anthropology, 19*, 365–372.

Garn, S. M., Rohmann, C. G., & Blumenthal, T. (1966). Ossification sequence polymorphism and sexual dimorphism in skeletal development. *American Journal of Physical Anthropology, 24*, 101–115.

Garn, S. M., Rohmann, C. G., & Wallace, D. K. (1961b). Association between alternate sequences of hand-wrist ossification. *American Journal of Physical Anthropology, 19*, 361–364.

Goswami, A. (2006). Cranial modularity shifts during mammalian evolution. *American Naturalist, 168*, 270–280.

Goswami, A. (2007). Modularity and sequence heterochrony in the mammalian skull. *Evolution & Development, 9*, 291–299.

Goswami, A., Weisbecker, V., & Sánchez-Villagra, M. R. (2009). Developmental modularity and the marsupial-placental dichotomy. *Journal of Experimental Zoology, 312B*, 186–195.

Gould, S. J. (1977). *Ontogeny and phylogeny*. Cambridge, MA: Belknap Press.

Harrison, L. B., & Larsson, H. C. E. (2008). Estimating evolution of temporal sequence changes: a practical approach to inferring ancestral developmental sequences and sequence heterochrony. *Systematic Biology, 57*, 378–387.

Hautier, L., Fabre, P. H., & Michaux, J. (2009). Mandible shape and dwarfism in squirrels (Mammalia, Rodentia): interaction of allometry and adaptation. *Naturwissenschaften, 96*, 725–730.

Hautier, L., Michaux, J., Marivaux, L., & Vianey-Liaud, M. (2008). Evolution of the zygomasseteric construction in Rodentia, as revealed by a geometric morphometric analysis of the mandible of *Graphiurus* (Rodentia, Gliridae). *Zoological Journal of the Linnean Society, 154*, 807–821.

Huxley, J. S. (1932). *Problems of relative growth*. London: Methuen.

Jeffery, J. E., Bininda-Emonds, O. R. P., Coates, M. I., & Richardson, M. K. (2005). A new technique for identifying sequence heterochrony. *Systematic Biology, 54*, 230–240.

Jong, I. M. L. de, Colbert, M. W., Witte, F., & Richardson, M. K. (2009). Polymor-

phism in developmental timing: intraspecific heterochrony in a Lake Victoria cichlid. *Evolution & Development, 11*, 625–635.

Kaufman, M. H. (2008). *The atlas of mouse development*. London: Elsevier Academic Press.

Kavanagh, K. D., Evans, A. R., & Jernvall, J. (2007). Predicting evolutionary patterns of mammalian teeth from development. *Nature, 449*, 427–433.

Klingenberg, C. P. (1998). Heterochrony and allometry: the analysis of evolutionary change in ontogeny. *Biological Reviews, 73*, 79–123.

Lillegraven, J. A. (1975). Biological considerations of the marsupial-placental dichotomy. *Evolution, 29*, 707–722.

Mabee, P. M., Olmstead, K. L., & Cubbage, C. C. (2000). An experimental study of intraspecific variation, developmental timing, and heterochrony in fishes. *Evolution, 54*, 2091–2106.

Mall, F. P. (1906). On ossification centres in human embryos less than one hundred days old. *American Journal of Anatomy: Developmental Dynamics, 5*, 433–458.

Mess, A. (2007). Development of the chorioallantoic placenta in *Octodon degus*—A model for growth processes in caviomorph rodents? *Journal of Experimental Zoology, 308B*, 371–383.

Michaux, J., Hautier, L., Simonin, T., & Vianey-Liaud, M. (2008). Phylogeny, adaptation and mandible shape in Sciuridae (Rodentia, Mammalia). *Mammalia, 72*, 286–296.

Monteiro, L. R., Bonato, V., & Reis, S. F. dos (2005). Evolutionary integration and morphological diversification in complex morphological structures: mandible shape divergence in spiny rats (Rodentia, Echimyidae). *Evolution & Development, 7*, 429–439.

Moore, M. K. (1991). *Comparative ontogeny of cranial ossification in the spotted salamander, Ambystoma maculatum, and the tailed frog, Ascaphus truei*. M. Sc. thesis. Baton Rouge, LA: Louisiana State University.

Moore, M. K., & Townsend, V. R., Jr. (2003). Intraspecific variation in cranial ossification in the tailed frog, *Ascaphus truei*. *Journal of Herpetology, 37*, 714–717.

Nowak, R. M. (1999). *Walker's mammals of the world, 6th edition*. Baltimore, MD: Johns Hopkins University Press.

Nunn, C. L., & Smith, K. K. (1998). Statistical analyses of developmental sequences: the craniofacial region in marsupial and placental mammals. *American Naturalist, 152*, 82–101.

Petri, C. (1935). Die Skelettentwicklung beim Meerschwein, zugleich ein Beitrag zur vergleichenden Anatomie der

Skelettentwicklung der Säuger. *Vierteljahrsschrift der Naturforschenden Gesellschaft in Zürich, 80*, 157–240.

Prochel, J. (2006). Early skeletal development in *Talpa europaea*, the common European mole. *Zoological Science, 23*, 427–434.

Prochel, J., & Sánchez-Villagra, M. R. (2003). Carpal ontogeny in *Monodelphis domestica* and *Caluromys philander* (Marsupialia). *Zoology, 106*, 73–84.

Prochel, J., Vogel, P., & Sánchez-Villagra, M. R. (2004). Hand development and sequence of ossification in the forelimb of the European shrew *Crocidura russula* (Soricidae) and comparisons across therian mammals. *Journal of Anatomy, 205*, 99–111.

Rojas, M. A., Montenegro, M. A., & Morales, B. (1982). Embryonic development of the degu, *Octodon degus*. *Journal of Reproduction and Fertility, 66*, 31–38.

Roth, V. L. (1996). Cranial integration in the Sciuridae. *American Zoologist, 36*, 14–23.

Sánchez-Villagra, M. R. (2002). Comparative patterns of postcranial ontogeny in therian mammals: an analysis of relative timing of ossification events. *Journal of Experimental Zoology: Molecular Development Evolution, 294*, 264–273.

Sánchez-Villagra, M. R., Goswami, A., Weisbecker, V., Mock, O., & Kuratani, S. (2008). Conserved relative timing of cranial ossification patterns in early mammalian evolution. *Evolution & Development, 10*, 519–530.

Schoch, R. R. (2006). Skull ontogeny: developmental patterns of fish conserved across major tetrapod clades. *Evolution & Development, 8*, 524–536.

Schradin, C. (2005). When to live alone and when to live in groups: ecological determinants of sociality in the African striped mouse (*Rhabdomys pumilio*, Sparrman, 1784). *Belgian Journal of Zoology, 135 (Suppl. 1)*, 77–82.

Schradin, C. (2006). Whole-day follows of striped mice (*Rhabdomys pumilio*), a diurnal murid rodent. *Journal of Ethology, 24*, 37–43.

Schradin, C., & Pillay, N. (2003). Paternal care in the social and diurnal striped mouse (*Rhabdomys pumilio*): laboratory and field evidence. *Journal of Comparative Psychology, 117*, 317–324.

Schradin, C., & Pillay, N. (2004). The striped mouse (*Rhabdomys pumilio*) from the succulent karoo of South Africa: A territorial group living solitary forager with communal breeding and helpers at the nest. *Journal of Comparative Psychology, 118*, 37–47.

Schulmeister, S., & Wheeler, W. C. (2004). Comparative and phylogenetic analy-

sis of developmental sequences. *Evolution & Development, 6*, 50–57.

Sears, K. E. (2004). Constraints on the morphological evolution of marsupial shoulder girdles. *Evolution, 58*, 2353–2370.

Sears, K. E. (2009). Differences in the timing of prechondrogenic limb development in mammals: the marsupial-placental dichotomy resolved. *Evolution, 63*, 2193–2200.

Smith, K. K. (1997). Comparative patterns of craniofacial development in eutherian and metatherian mammals. *Evolution, 51*, 1663–1678.

Smith, K. K. (2001). Heterochrony revisited: the evolution of developmental sequences. *Biological Journal of the Linnean Society, 73*, 169–186.

Steppan, S. J., Adkins, R. M., & Anderson, J. (2004). Phylogeny and divergence date estimates of rapid radiations in muroid rodents based on multiple nuclear genes. *Systematic Biology, 53*, 533–553.

Strong, R. M. (1925). The order, time, and rate of ossification of the albino rat (*Mus norvegicus albinus*) skeleton. *Amererican Journal of Anatomy: Developmental Dynamics, 36*, 313–355.

Swofford, D. L. (2002). PAUP, Phylogenetic Analysis Using Parsimony (and other methods), version 4.0b10. Computer program. Sunderland, MA: Sinauer Associates.

Theiler, K. (1972). *The House mouse: development and normal stages from fertilization to 4 weeks of age*. Berlin: Springer.

Trillmich, F., Bieneck, M., Geissler, E., & Bischof, H.-J. (2003). Ontogeny of running performance in the Wild guinea pig (*Cavia aperea*). *Mammalian Biology, 68*, 214–223.

Wagner, G. P. (1988). The influence of variation and of developmental constraints on the rate of multivariate phenotypic evolution. *Journal of Evolutionary Biology, 1*, 45–66.

Weisbecker, V., Goswami, A., Wroe, S., & Sánchez-Villagra, M. R. (2008). Ossification heterochrony in the therian postcranial skeleton and the marsupial-placental dichotomy. *Evolution, 62*, 2027–2041.

Weisbecker, V., & Schmid, S. (2007). Autopodial skeletal diversity in hystricognath rodents: functional and phylogenetic aspects. *Mammalian Biology, 72*, 27–44.

Werneburg, I., & Sánchez-Villagra, M. R. (2009). Timing of organogenesis support basal position of turtles in the amniote tree of life. *BMC Evolutionary Biology, 9, 82*, doi: 10.1186/1471-2148-9-82

Werneburg, I., & Sánchez-Villagra, M R. (in press). The early development of the

Echidna, *Tachyglossus aculeatus* (Mammalia: Monotremata) and the grundmuster of mammalian development. *Acta Zoologica*.

Wilson, D. E., & Reeder, D. M. (2005). *Mammal species of the world: a taxonomic and geographic reference*. Washington, D.C.: Smithsonian Institution Press.

Wilson, L. A. B., & Sánchez-Villagra, M. R. (2009). Heterochrony and patterns of cranial suture closure in hystricognath rodents. *Journal of Anatomy, 214*, 339–354.

Wilson, L. A. B., & Sánchez-Villagra, M. R. (2010). Diversity trends and their ontogenetic basis: an exploration of allometric disparity in rodents. *Proceedings of the Royal Society of London, B Biological Sciences*, 277, 1227-1234.

Woods, C. A. & Boraker, D. K. (1975). *Octodon degus. Mammalian Species, 67*, 1–5.

Yukawa, M., Hayashi, N., Takagi, K., & Mochizuki, K. (1999). The normal development of Mongolian gerbil foetuses and, in particular, the timing and sequence of ossification centres. *Anatomia Histologia Embryologia, 28*, 319–324.

Zelditch, M. L. (2001). *Beyond heterochrony: the evolution of development*. New York: Wiley-Liss Press.

Zelditch, M. L., Mezey, J., Sheets, H. D., Lundrigan, B. L., & Garland, T., Jr. (2006). Developmental regulation of skull morphology II: ontogenetic dynamics of covariance. *Evolution & Development, 8*, 46–60.

Zeller, U. (1987). Morphogenesis of the mammalian skull with special reference to *Tupaia. Mammalia depicta, 13*, 17–50.

SUPPLEMENTARY MATERIAL

Appendix 4.1

Appendix 4.2

Cranial element	Magnitude of rank variation	Postcranial element	Magnitude of rank variation
Premaxilla	1	Clavicle	0
Maxilla	1	Humerus	0
Palatine	0	Ribs	0
Dentary	0	Femur	0
Frontal	0	Radius	0
Parietal	0	Ulna	0
Squamosal	0	Scapula	0
Basioccipital	0	Cervical v.	0
Nasal	1	Thoracic v.	1
Pterygoid	0	Tibia	0
Exoccipital	1	Fibula	1
Basisphenoid	1	Lumbar v.	2
Jugal	1	Sacral v.	1
Lacrimal	1	Caudal v.	1
Alisphenoid	1	Ilium	1
Orbitosphenoid	1	Manus phal.	1
Periotic	0	Pes phal.	1
		Ischium	1
		Pubis	2
		Metac.	0
		Metat.	1
		Tarsals	1
		Carpals	0
		Sternum	0

Appendix 4.1: Intraspecific variation in ossification of cranial and postcranial elements in *Rhabdomys pumilio*.

Manus	Magnitude of rank variation	Pes	Magnitude of rank variation
Metacarpal III	0	Metatarsal III	1
Metacarpal IV	0	Metatarsal IV	1
Metacarpal II	1	Metatarsal II	1
Metacarpal V	1	Metatarsal V	2
Proximal phal. III	0	Distal phal. II	1
Proximal phal. IV	0	Distal phal. III	1
Distal phal. II	1	Distal phal. IV	1
Distal phal. III	1	Distal phal. V	0
Distal phal. IV	1	Proximal phal. II	0
Proximal phal. II	1	Proximal phal. III	0
Distal phal. V	1	Proximal phal. IV	0
Proximal phal. I	0	Proximal phal. V	0
Proximal phal. V	0	Proximal phal. I	0
Medial phal. II	1	Medial phal. I	0
Medial phal. III	0	Medial phal. II	0
Medial phal. IV	0	Medial phal. III	0
Medial phal. I	0	Medial phal. IV	1
Medial phal. V	0	Calcaneus	1
Triquetrum	1	Metatarsal I	1
Distal carpal IV	0	Medial phal. V	0
Distal carpal V	0	Astragalus	2
Scaphoid	0	Distal tarsal I	0
Metacarpal I	0	Distal tarsal IV	0
Pisiform	2	Distal tarsal V	0
Centrale	0	Distal tarsal III	0
Distal carpal III	0	Distal tarsal II	0
Distal carpal I	0	Navicular	2
Distal carpal II	0		

Appendix 4.2: Intraspecific variation in ossification of autopodial elements in *Rhabdomys pumilio*.

CHAPTER 5

A comparison of prenatal and postnatal ontogeny: cranial allometry in the African striped mouse *Rhabdomys pumilio*

CHAPTER 5

A comparison of prenatal and postnatal ontogeny: cranial allometry in the African striped mouse *Rhabdomys pumilio*

Article submitted to *Journal of Mammalogy*

Reference: **Wilson LAB**. submitted. A comparison of prenatal and postnatal ontogeny: cranial allometry in the African striped mouse *Rhabdomys pumilio*.

Abstract

The relationship between prenatal and postnatal ontogenetic allometry is poorly known, and empirical studies documenting prenatal allometry are few, precluding an understanding of changes in growth patterns during life history and their relation to proximal, physiological, and ultimate evolutionary variables. In this study I compare prenatal and postnatal ontogenetic allometry of the cranium in a cleared and stained developmental series of the African striped mouse *Rhabdomys pumilio*. Eighteen cranial measurements, reflecting the dimensions of individual elements, were analysed using bivariate and multivariate estimates of allometry and methods of matrix comparison. Prenatal allometry is characterised in *R. pumilio* by a relative rapid lengthening of cranial elements, particularly the frontal, parietal, basisphenoid, premaxilla and palatine, as evidenced by larger bivariate allometric coefficients (>30% increase) and, across all variables measured, a greater proportion of cranial elements growing with a positive allometry than in the postnatal period. Growth dynamics are found to shift for measurements of several elements including the parietal, frontal and palatine, indicating a non-linearity of ontogenetic allometry with respect to birth; similar shifts have been found between prenatal and postnatal growth for some regions of the human cranium. Application of common principal component analyses, a generalized extension of principal component analysis, revealed that the prenatal and postnatal matrices shared a highly similar structure, further quantified by high correlations (>0.78) using the random skewers method of matrix comparison. These results indicate a close correspondence between morphological based variance structures over the course of ontogeny in *R. pumilio*.

KEYWORDS**:** prenatal allometry; rodent; cranium; common principal components; ontogeny; ontogenetic allometry

INTRODUCTION

Morphological changes in evolution do not simply happen at the adult stage; ontogenetic pathways evolve too. Stemming from the early 20th Century (see Gayon 2000 for review), an extensive amount of literature has illuminated morphological differences in a development context by the examination of covariation among traits across ontogenetic stages of a given species, commonly termed ontogenetic allometry (Cock 1966; Klingenberg 1998). A recent resurgence in the investigation of ontogenies has been facilitated by the advent and application of analytical techniques and metric methods, which have permitted differences in form to be appreciated quantitatively and intuitively.

Although a vast amount of study has been directed to documenting the variability and evolution of ontogenetic allometry in mammals, for instance detailing the relation of diet to growth patterns (e.g. Beecher and Corrucini 1981; Corrucini et al. 1985), examining how growth patterns are influenced by environmental conditions (e.g. Fadda and Leirs 2009) or exhibit heterochronic patterns (e.g. Weston 2003; Zollikofer and Ponce de León 2004, 2010; Cubo et al. 2006), and investigating growth patterns among species and clades (e.g. Creighton and Strauss 1986; Cardini and O'Higgins 2005; Marroig 2007; Wilson and Sánchez-Villagra 2010), all of these works have dealt with the postnatal period of development. Despite recognition that early ontogenetic stages are an important component of influence to adult morphology (e.g. Viðarsdóttir et al. 2002; Bastir & Rosas 2004; Bulgina et al. 2006; Wilson et al. 2008, 2010a), studies of prenatal allometry in mammals are scarce and, with the exception of a study on the common European mole (Goswami and Prochel 2007), are limited to humans (Latham 1972; Mandarim-de-Lacerda and Alves 1992; Plavcan and German 1995; Vinicius 2005; Sardi et al. 2007; Bastir and Rosas 2009). From the present standpoint it is evident that the relationship between prenatal and postnatal allometry is poorly known, and the role that prenatal allometry plays in providing raw material for morphologic evolution cannot be evaluated. One reason for this is the difficulty in obtaining prenatal developmental series for any mammal in the sample size numbers required to assess allometric relationships (Sánchez-Villagra 2010).

Several studies of skull growth in rodents have indicated that postnatal ontogenetic allometry is non-linear for some species, including model organisms such as the house mouse and cotton rat, and further that ontogenetic trajectories "stabilize" during the postnatal period, around the time of weaning (Zelditch 1988; Zelditch and Carmichael 1989; Hingst-Zaher et al. 2000; Zelditch et al. 2003; Willmore et al. 2006). The adult pattern of cra-

nial integration exhibited by preweaning rats has been shown to reflect the influence of functional and developmental sources of constraint, and experimental studies using rats have revealed that the preweaning period plays a critical role in the development of normal skull shape (Pucciarelli and Oyhenart 1987). Nevertheless, in contrast to these results, several studies in other mammalian species, including rodents (Monteiro et al. 1999), primates (O'Higgins et al. 2001; Singleton 2002) and hippopotamuses (Weston 2003) have suggested that ontogenetic allometry is linear. Complexity is further added to this debate since several works have indicated that during the prenatal period the embryo is not in a forceless environment (e.g. Harris et al. 1981; Tuckett and Morriss-Kay 1985) and throughout later prenatal stages, movements occur which are equivalent to those happening postnatally (Hamburger 1973). Hence, whilst postnatal ontogenies represent at least the possible pathways that may be taken to reach a realisable adult form through development, it remains unclear how early in development these pathways are "fixed". Especially given the complex interactions between genetic and epigenetic factors that control skull morphogenesis (see Herring 1993), with epigenetic factors also influencing prenatal growth, for example in the instance of embryonic muscle-loading (Atchley et al. 1984; Hall 2005), it is clear that framing cranial growth in a more extended context, that incorporates the earliest periods of development, is necessary. Particularly, the finding that life-history and developmental milestones are correlated with alterations to covariance structure during postnatal cranial growth in rats and humans leads to the expectation that birth may also represent a point of significant transition in growth dynamics (Mitteroecker and Bookstein 2009).

The objective of this study is to document prenatal allometry for a non-model rodent species and compare this with postnatal allometry to provide an estimation of the relationship for growth dynamics of cranial elements between the two periods, segmented by birth. A developmental series of cleared and stained specimens of the African striped mouse *Rhabdomys pumilio* is used as subject for investigation. Found from Uganda and Kenya to Angola and South Africa, *R. pumilio* is a diurnal murid rodent that attains approximately twice the body mass of the house mouse *Mus musculus* (Wilson and Reeder 2005). *R. pumilio* has been the subject of several ecological studies because it has a complex and fluid social system, and has been shown to demonstrate parental care in laboratory and desert-living wild populations (e.g. Schradin and Pillay 2003, 2004).

MATERIALS AND METHODS

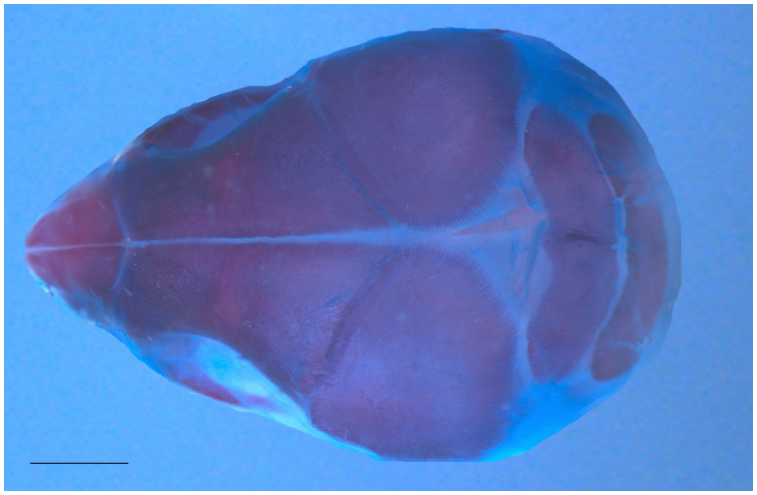

Figure 5.1: Prenatal cleared and stained skull of *Rhabdomys pumilio*. Scale bar = 2mm.

Specimens and preparation

I measured an ontogenetic series of 56 specimens of *Rhabdomys pumilio*, comprising 25 prenatal individuals and 31 postnatal specimens. All of the prenatal specimens, and 16 of the postnatal specimens were obtained from breeding colonies maintained for research at the Universität Zürich (see Schradin 2006), and prepared using a modified version of standard enzymatic clearing and double staining (Prochel 2006). The founder individuals of *R. pumilio* originated from the Geogap Nature Reserve in South Africa (29°41.56'S, 18°1.60'E). The remaining 15 postnatal specimens in the study sample included adult and juvenile crania measured from the osteological collections at the Universität Zürich. For each of the cleared and stained specimens (N = 41), the crown rump length (CRL) was measured from digital photographs taken of the whole animal, before preparation, using a Leica M165C microscope and camera attachment. The CRL ranged from 14.8 to 41.1mm, which equates to approximately 16.5 days p.c. to 2 postnatal days of age (Kaufmann 2008).

Data collection

Eighteen measurements were recorded on each cranium (Table 5.1; Fig. 5.1). These were chosen to record the dimensions of single bones, rather than encapsulating several bones. This approach was adopted to enable the allometry of a single element to be identified, and also because many elements are not completely ossified in prenatal specimens, and hence portions of the skull include cartilaginous regions, which make difficult the recording of measurements spanning across several bones. A reflex microscope was used to record three dimensional landmarks on all cleared and stained specimens. This method was first applied by Goswami and Prochel

(2007), who used reflex microscopy to gather data from cleared and stained common European moles (*Talpa europaea*). Often used in the fields of dentistry and component manufacture, reflex microscopy is especially useful because it affords the possibility to measure small and delicate materials, such as embryos, with a resolution of approximately 1μm. Each specimen was suspended in glycerol in a sampling dish and held in position using pins fixed to a dissection mat. A total of 108 landmarks were digitized in dorsal, ventral and lateral orientations. Measurements were computed from three dimensional coordinates, whilst adult and juvenile osteological specimens were measured with digital callipers. In both instances, measurements were computed from an average of 3 repetitions for each variable. Measurement error was 0.034mm for landmarks obtained using the reflex microscope, and 0.09mm for measurements taken using digital callipers.

Orientation of specimen	Variable	Abbreviation
Lateral	Jugal length	JUL
	Squamosal length	SQL
Ventral	Premaxilla length	PRL
	Premaxilla width	PRW
	Maxilla length	MXL
	Palatine length	PLL
	Palatine width	PLW
	Basioccipital length	BOL
	Basisphenoid length	BSL
	Basioccipital width	BOW
	Basisphenoid width	BSW
Dorsal	Nasal length	NAL
	Nasal width	NAW
	Frontal length	FRL
	Minimum interorbital width	MIW
	Skull length	SKL
	Parietal length	PAL
	Parietal width	PAW

Table 5.1: Osteological measurements recorded in the present study.

Bivariate allometry

Two matrices were constructed: one for the prenatal specimens (N=25) and one for the postnatal specimens (N=31). Bivariate allometry was estimated for each matrix using skull length and CRL (for cleared and stained specimens) as proxies for body size. Skull length and CRL were regressed against one another, since skull length may scale allometrically with true body size, and CRL is a commonly accepted body size metric for embryological specimens. To study the scaling relationships between cranial variables, I used the linear transformation ($\log_{10}$) of the power equation $y = b_0 x^{b1}$ where y is the variable of study, b_0 is the y-intercept, x is a proxy for size, and the coefficient b_1 details the relative magnitude of y vs. x change, thus indicating ontogenetic polarity.

When $b_1 = 1$ the 2 traits under study change only by means of absolute size, that is isometric growth (i.e. $y/x = b_1$). If $b_1 < 1$, y is negatively allometric in respect to x, conversely if $b_1 > 1$, y is positively allometric with respect to x (i.e. with growth there is an increase in the ratio y/x). Two tailed t-tests were used to assess the significance of deviations from isometry, whereby type I error rate (α) was fixed at 0.01 under the null hypothesis of $b_1 = 1$. A relationship was deemed isometric if not significantly different from unity. To improve the reliability of estimates, allometric coefficients (b_1) were calculated using both least squares (LS) and reduced major axis (RMA) regression methods (model I and II). Symmetrical line fitting techniques (model II), such as RMA, are usually preferred (Wolpoff 1985) because error is assumed to be associated equally with both x and y variables, and simulation investigations have indicated these methods provide more stable estimates, especially if sample sizes are small (Riggs et al. 1978). In contrast, LS assumes that the independent x variable is measured without error. When this assumption is violated, LS estimates will consistently underestimate the true slope, since by definition RMA = LS/r with $r \leq 1$, and the magnitude of this error will increase with decreasing correlation between the variables (Harvey and Pagel 1991).

Multivariate allometry

In multivariate allometry (Jolicoeur 1963), an allometric trajectory is represented by the first eigenvector (axis) of a principal component analysis (PCA) using the covariance matrix of natural log transformed measurements. Because PCA requires a complete data set, it was necessary to remove several specimens which had measurements missing for a variable, and hence the prenatal matrix contained 17 specimens and the postnatal matrix contained 25 specimens. To prevent a singular matrix from being produced, only 14 of the 18 measured variables were included in the multivariate analyses. The coefficients of the first principal components (PC1s) for each of the 14 variables were used to identify growth trends by comparison to the isometric vector of length (p): the value at which all PC1 coefficients are equal, calculated as $p^{-1/2}$ (where p = number of measured variables). The bootstrap approach was used to compute standard error (SE) values for PC1 coefficients in comparison with the value expected for isometry; replicates were performed for 1000 iterations for each matrix (Efron and Tisbshirani, 1993). A growth trend was identified to be positively or negatively allometric if the bootstrap confidence interval for the PC1 coefficient did not include the isometric vector.

Vector and matrix comparisons

I used common principal component analysis (CPC) (Flury 1988) and the random skewers method (Cheverud 1996) to compare the structure of the prenatal and postnatal covariance matrices. The two approaches differ fundamentally in that on the one hand CPC considers a null hypothesis of equality among covariance matrices, whilst on the other hand the random skewers method assumes a null hypothesis of no structural similarity. CPC is a generalization of a single PCA to multiple groups and permits the sharing of complex relationships between covariance matrices (Flury 1988). Relationships between matrices are tested following a hierarchy that begins with unrelated structure and ends with equality, and is based upon the understanding that if 2 matrices share 2 principal components, then they necessarily share 1. As such, a number of hypotheses are considered by comparing eigenvectors and eigenvalues; a) equality – matrices share equal eigenvalues and eigenvectors, b) proportionality – matrices share equal eigenvectors and proportional eigenvalues, c) CPC – matrices share common principal components whereby the eigenvectors are equal but the eigenvalues are unequal, and d) unrelated structure – the two matrices have unequal eigenvectors and eigenvalues (see Phillips and Arnold 1999). Because the ontogenetic data in this study are non-normally distributed, the likelihood ratio tests commonly used to evaluate the CPC models are not suitable. Instead, I examined the angular difference between vector PCs of the individual matrices in comparison to CPCs and also the amount of variance encapsulated in the individual PC1s compared to the CPC1s, to estimate the goodness of fit of the CPC model (Klingenberg and Zimmermann 1992). Although the possible number of CPCs that may be generated from analysis of the prenatal and postnatal matrices is 12 (calculated as N-2; where N= number of variables), examination was limited to CPC(7), that is the sharing of the first 7 components, since in both the prenatal and postnatal matrices loadings beyond the sixth component were close to zero.

To assess the significance of angular comparisons, vector angles were computed between 1000 pairs of randomly generated unit length vectors. The angles calculated between these vectors were compiled, and the 1% quantile of this distribution was used to assess significance ($< 27.6^{\circ}$). All CPC analyses of prenatal and postnatal covariance matrices were conducted using CPC software (Phillips 1998).

To gain a clearer insight into the degree of similarity between prenatal and postnatal patterns of covariance, the random skewers method was used in conjunction with CPC. Indeed, the latter has been shown to often diagnose matrices to be completely dissimilar, despite other matrix correlation tests depicting

the opposite result (e.g. Steppan 1997). Simulated tests indicate that relatively restricted changes in causal structure will produce a result of complete matrix dissimilarity (Houle et al. 2002), and it has been recommended that examining how well the constructed matrices match the original ones may yield a more real estimate of model fit (Arnold and Phillips 1999). The random skewers method measures matrix similarity by correlating the selection response between two matrices using a series of random selection vectors, in this case 10,000. Vectors are drawn from a uniform distribution between 0 and 1, assigned positive or negative signs with a probability of 50%, and standardized to unit length. Each selection vector is applied to each matrix and the vector correlations between the paired expected responses are compared. The outputted vector correlations are used to generate an average vector correlation which is a measure of the covariance matrix similarity, and, associated with this, a significance value based upon the distribution of correlation values (see Cheverud 1996; Cheverud and Marroig 2007). The matrix constructed at each stage of the CPC hierarchy was compared to the original matrices using the random skewers method.

RESULTS

For several traits, bivariate and multivariate allometric analyses reveal differences in growth relationships between prenatal and postnatal animals. Matrix comparison tests indicate these differences do not preclude a result of overall similarity in covariance structure between each of the two matrices.

Bivariate results

For both prenatal and postnatal specimens, reduced major axis (RMA) and least squares (LS) regression approaches produced broadly similar allometric trends (Tables 5.2 and 5.3). Consistency between the 2 methods was highest for postnatal specimens, with maxilla length (MXL) being the only variable which differed between RMA and LS. For prenatal specimens, 5 of the variables differed between RMA and LS when skull length was used as a proxy for body size (Table 5.3). Across the variables, considerable differences in correlation with skull length were exhibited by both prenatal and postnatal specimens. Correlations were lower for prenatal specimens, varying between R^2 values of 0.66 for premaxilla width (PRW) and 0.91 for parietal width (PAW) using skull length, and 0.55 for parietal length (PAL) to 0.83 for nasal width (NAW) when using CRL, compared with postnatal specimens (range from 0.70 for PLW to 0.97 for NAL) (Table 5.2). CRL was significantly correlated with skull length for all prenatal specimens ($R^2 = 0.84$; $p<0.001$) and regression results indicate skull length scales isometrically am-

	Prenatal specimens										Postnatal specimens				
	Skull length					Crown rump length					Skull length				
Variable	RMA		LS			RMA		LS			RMA		LS		
	b_1	p^{iso}	b_1	p^{iso}	R^2	b_1	p^{iso}	b_1	p^{iso}	R^2	b_1	p^{iso}	b_1	p^{iso}	R^2
JUL	1.70	0.0002	1.41	0.0181	0.69	1.65	<0.0001	1.43	0.0029	0.75	0.97	0.6366	0.89	0.1224	0.84
SQL	1.50	0.0036	1.24	0.1458	0.68	1.96	<0.0001	1.59	0.0030	0.66	1.32	0.0005	1.25	0.0059	0.89
PRL	1.32	0.0419	1.01	0.9672	0.78	1.17	0.2181	0.88	0.3855	0.57	1.52	<0.0001	1.42	0.0004	0.87
PRW	0.99	0.1530	0.50	0.0028	0.66	0.75	0.0671	0.55	0.0027	0.63	1.13	0.1460	1.03	0.6849	0.85
MXL	1.65	<0.0001	1.49	0.0002	0.82	1.49	0.0005	1.28	0.0371	0.73	1.19	0.0369	1.09	0.2965	0.84
PLL	2.60	<0.0001	2.44	<0.0001	0.88	2.08	<0.0001	1.88	<0.0001	0.81	0.83	0.0304	0.73	0.0014	0.78
PLW	0.73	0.0138	0.44	<0.0001	0.66	0.69	0.0026	0.39	<0.0001	0.62	1.11	0.4392	0.86	0.3265	0.70
BOL	1.05	0.6456	0.88	0.2234	0.70	0.96	0.6899	0.78	0.0257	0.66	1.05	0.4216	1.00	0.9739	0.90
BSL	2.60	<0.0001	2.44	<0.0001	0.88	2.40	<0.0001	2.02	0.0001	0.71	1.70	<0.0001	1.59	<0.0001	0.88
BSW	0.70	0.0059	0.40	<0.0001	0.73	0.70	0.0048	0.41	<0.0001	0.73	2.04	<0.0001	1.96	<0.0001	0.92
BOW	1.29	0.0079	1.14	0.1874	0.78	1.19	0.0599	1.02	0.8172	0.74	0.83	0.0470	0.72	0.0020	0.75
NAL	1.98	<0.0001	1.86	<0.0001	0.89	1.75	<0.0001	1.59	<0.0001	0.82	2.02	<0.0001	1.99	<0.0001	0.97
NAW	0.82	0.0006	0.77	<0.0001	0.90	0.73	<0.0001	0.67	<0.0001	0.83	0.38	<0.0001	0.34	<0.0001	0.78
FRL	1.42	<0.0001	1.31	0.0016	0.85	1.36	0.0018	1.18	0.0973	0.75	0.74	<0.0001	0.71	<0.0001	0.93
MIW	0.76	0.0001	0.68	<0.0001	0.81	0.84	0.0146	0.75	0.0003	0.79	0.25	<0.0001	0.18	<0.0001	0.72
PAL	1.33	0.0253	1.03	0.8112	0.70	1.14	0.2615	0.85	0.2263	0.55	1.50	<0.0001	1.43	<0.0001	0.91
PAW	1.23	0.0013	1.17	0.0121	0.91	1.16	0.1247	0.99	0.9233	0.73	0.37	<0.0001	0.34	<0.0001	0.84

Table 5.2: Results of bivariate allometry analyses. R^2 - adjusted coefficient of determination, b_1 - coefficient of allometry, p^{iso} - P value for null hypothesis of isometry (coefficient of allometry = 1), RMA – Reduced Major Axis, LS – Least squares.

ong the prenatal specimens using both RMA (b_1 = 1.03; p>0.05) and LS (b_1 = 0.95; p>0.05) methods. Hence for the prenatal specimens herein, skull length scales isometric with size.

The distribution of growth trends differed between prenatal and postnatal specimens. For prenatal specimens, 11 out of 17 (65%) variables exhibited significant positive allometry when using RMA, 4 exhibited significant negative allometry (24%), and 2 variables scaled isometrically with skull length (11%) (Table 5.3). When using CRL as a body size proxy, 4 of the 11 aforementioned positive allometric trends (SQL; PRL; BOW; PAL) were instead identified to be isometric, whilst the variables exhibiting negative trends were the same as those when the analysis was performed using skull length (PLW; BSW; NSW; MIW). Positive allometric trends were identified for fewer variables in postnatal specimens (7; 41%); a greater amount of negative (6; 35%) and isometric (4; 24%) trends exist (Table 5.3). Across all variables, the average allometric coefficient for prenatal specimens was 1.39, compared with 1.12 for postnatal specimens, indicating a shift in the relative magnitude of growth rate between the 2 periods (Table 5.2). For several variables, including basisphenoid

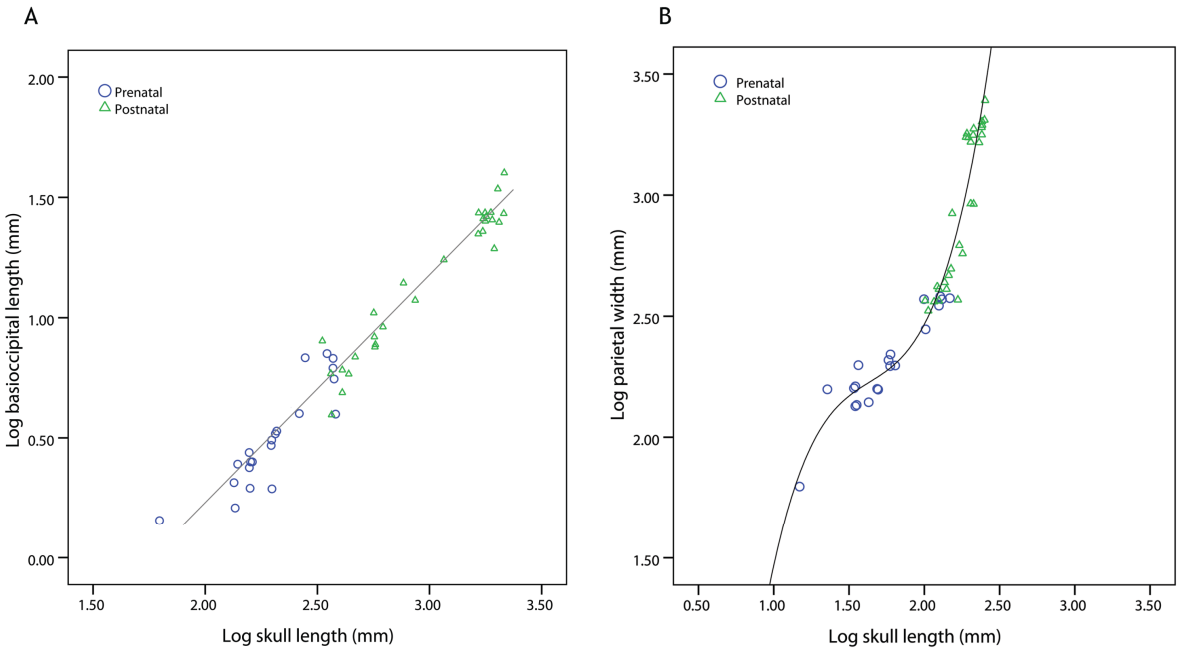

Figure 5.2: Comparison of prenatal and postnatal trajectories for relationships between skull length and (A) basioccipital length using reduced major axis regression (R^2 = 0.913) and (B) parietal width, using a cubic model (R^2 = 0.933).

length (BSL), frontal length (FRL) and parietal width (PAW), coefficients were at least 30% greater for prenatal specimens (Fig 5.2; Table 5.2). When comparing between prenatal and postnatal specimens, the 2 groups share the same growth trends for 59% (10; 6 positive, 2 negative and 2 isometric trends) of the variables, using RMA and skull length (see Fig. 5.2A as example). Of the 7 variables that exhibited different trends between the 2 groups, 5 variables (PLL; BOW; FRL; PAW; JUL) switched from a positive growth relationship with skull length to either a negative or, in the case of jugal length (JUL), isometric trend (Table 5.3). The remaining 2 cases are represented by a prenatal to postnatal shift from negative to positive allometry for basisphenoid width (BSW), and from negative allometry to isometry for palatine width (PLW). Correspondence between prenatal and postnatal trends reduced to only 6 shared variables (35%) when LS results, using skull length, were compared. The 6 shared trends consisted of 3 positive trends, two isometrically scaled variables and 1 negatively allometric trend; in all, reflecting the different growth trend results obtained for squamosal length (SQL), premaxilla length (PRL), premaxilla width (PRW), and palatine length (PLL) when using LS instead of RMA. When comparing the prenatal trends, derived using CRL, with postnatal trends, a similar pattern of more shared traits between prenatal RMA results and postnatal results is found. Eight growth trends are shared between prenatal and postnatal specimens when RMA results are compared; these include 4 positive, 2 negative and 2 isometric trends. Whilst, on the other hand, when LS results are used, only 7 trends are shared with postnatal specimens; the difference being reflecting by the identification of an isometric trend for premaxilla width (PRW) using RMA and a negative trend using LS (Table 5.3). Overall correspondence between RMA results derived from skull length and those derived using CRL is slightly higher (13 variables; 76%) than that between LS results for the same two groups (12 variables; 71%).

Multivariate results

Principal component coefficients for both prenatal and postnatal specimens were fairly robust, as indicated by bootstrapped standard errors ranging from 0.008 (FRL) to 0.022 (BOL) for prenatal analyses and from 0.006 (SQL) to 0.019 (FRL and PAW) for postnatal analyses (Table 5.4). The proportion of variance accounted for by the first principal component (PC1) varied between 64% for the prenatal and 89% for the postnatal specimens (Fig. 5.3). Six isometric trends, 4 positive and 4 negative trends were identified amongst prenatal specimens, whilst among postnatal individuals there were 7 negative trends, 5 positive

	Prenatal specimens				Postnatal specimens	
	Skull length		Crown rump length		Skull length	
Variable	RMA	LS	RMA	LS	RMA	LS
JUL	+	+	+	+	=	=
SQL	+	=	+	+	+	+
PRL	+	=	=	=	+	+
PRW	=	-	=	-	=	=
MXL	+	+	+	+	+	=
PLL	+	+	+	+	-	-
PLW	-	-	-	-	=	=
BOL	=	=	=	=	=	=
BSL	+	+	+	+	+	+
BSW	-	-	-	-	+	+
BOW	+	=	=	=	-	-
NAL	+	+	+	+	+	+
NAW	-	-	-	-	-	-
FRL	+	+	+	=	-	-
MIW	-	-	-	-	-	-
PAL	+	=	=	=	+	+
PAW	+	+	=	=	-	-

Table 5.3: Gross comparison of bivariate results.

and 2 isometric trends (Table 5.4). Prenatal and postnatal specimens shared only 5 out of 14 growth trends (36%), consisting of 3 positive trends (SQL; NAL; PAL) and 2 negative trends (NAW; MIW) (Fig. 5.4) These 5 variables were also found to have the same trends in the prenatal-postnatal comparison of bivariate results (Table 5.3).

For prenatal specimens, 9 out of the 14 (64%) variables analysed using multivariate methods were found to have the same growth trend as indicated in bivariate analyses. The differing growth trends were represented by three isometric trends that were identified as positively allometric under bivariate methods (PRL; FRL; PAW) and 2 negative trends that were instead identified as isometric (PRW) and positive (MXL) (Tables 5.3 and 5.4). Three of the 5 trends that differed between the two estimation methods (PRL; PRW and MXL) were also found to differ between RMA and LS regression approaches (Table 5.3). For postnatal specimens, 10 out of 14 (71%) multivariate growth trends corresponded with their bivari-

ate counterparts. Of the 4 trends that differed (JUL; MXL; BOL; BOW), 2 negative trends were found to be isometric with bivariate methods (JUL and BOL) whilst 1 positive trend was found to have a negative relationship (BOW) and lastly 1 isometric trend was identified to be positively allometric using bivariate methods (MXL) (Tables 5.3 and 5.4). The latter variable, maxilla length, was also the only one to differ between RMA and LS results for bivariate analyses (Table 5.3), with LS results corresponding to the multivariate estimate of isometry (Table 5.4).

Matrix similarity tests and vector comparisons

The comparison of CPC models with prenatal and postnatal matrices using random skewers provides an indication of how well the constrained matrices constructed under CPC fit the actual matrices created from measurements of the prenatal and postnatal specimens. Pairwise comparisons between prenatal and postnatal matrices and the constructed matrices at each level of Flury's hierarchy are significant, indicating a close correspondence with the original data matrices (Table 5.5). The postnatal matrix is slightly more similar to the CPC

	Prenatal		Postnatal	
Variable	PC1 coefficient	GT	PC1 coefficient	GT
JUL	0.404 (0.021)	+	0.201 (0.010)	-
SQL	0.466 (0.019)	+	0.276 (0.006)	+
PRL	0.253 (0.019)	=	0.310 (0.010)	+
PRW	0.148 (0.011)	-	0.249 (0.019)	=
MXL	0.223 (0.009)	-	0.276 (0.010)	=
BOL	0.252 (0.022)	=	0.247 (0.018)	-
BOW	0.250 (0.018)	=	0.414 (0.011)	+
NAL	0.367 (0.008)	+	0.461 (0.009)	+
NAW	0.140 (0.009)	-	0.082 (0.011)	-
FRL	0.270 (0.008)	=	0.141 (0.019)	-
MIW	0.157 (0.020)	-	0.053 (0.018)	-
SKL	0.261 (0.017)	=	0.252 (0.011)	-
PAL	0.300 (0.009)	+	0.339 (0.010)	+
PAW	0.256 (0.019)	=	0.184 (0.019)	-

Table 5.4: Results of multivariate allometry analyses detailing principal component (PC) coefficients, bootstrap standard error (in parentheses), and corresponding growth trend (GT) considering an isometric vector of 0.267 applicable to all variables (see materials and methods). Symbols indicate isometry ("="), positive allometry ("+"), and negative allometry ("-").

matrices, on average (0.87), than the prenatal matrix (0.85), and both are most dissimilar in structure to CPC(1), with an average correlation of 0.859 (Table 5.5). The greatest discrepancies between the 2 original matrices and the CPC results are associated with the equality and proportionality models, with the postnatal matrix exhibiting a higher correlation to both models (0.968 and 0.981; Table 5.5) than the prenatal matrix (0.806 and 0.780; Table 5.5). This result is more marked when considering the vector angles between the first principal components of the matrices: when comparing the proportionality and equality matrices with the prenatal matrix, angular comparisons are 21◦ and 19◦, respectively, whilst for postnatal matrix these values drop considerably to 3◦ and 4◦, respectively. The result of overall similarity in patterns of covariance structure between the prenatal and postnatal matrices is further indicated by a significant correlation (0.69, *p* 0.008) between the two matrices using a random skewers test, and an angle measurement of 22.7◦ between the two PC1 vectors, which is smaller than expected between two random vectors (27.6◦). The first principal component (CPC1) encapsulated the greatest amount of variance in the constructed CPC matrix (67%; Fig. 5.3). This was expected since both prenatal and postnatal PCAs yielded similar results, nevertheless it may be the case in CPC analysis, unlike PCA, that the largest proportion of variance may not be associated with the largest eigenvalue. To evaluate how much variance was associated with isometric and allometric variation, the square of the inner product of the isometric vector and CPC1 vector was calculated. The proportion of isometric variation was 0.87 and hence the remaining 0.13 was due to allometry. The amount of variance expressed by CPC1 resulting from allometry (38%) was thus calculated by multiplying 0.13 by each of the eigenvectors of the CPC matrix and calculating a percentage for the first component. CPC1 variance for the equality matrix, which was the CPC model with the highest correlations to prenatal and postnatal matrices, was associated with nasal length (21%; NAL) and basisphenoid length (23%; BSL), whilst squamosal length (SQL) contributed the greatest proportion of variance to the CPC2 axis. NAL and BSL also both exhibited positive allometric trends under bivariate analyses (RMA and LS) in both prenatal and postnatal specimens (Table 5.3).

DISCUSSION

Two broad conclusions can be reached from this study. First, prenatal and postnatal ontogenetic allometry differs, with the former being characterised by a comparatively increased rate of bone growth among several cranial variables, as evidenced by larger allometric coefficient values and a greater num-

ber of positive allometric trends. Second, the overall manner in which traits co-vary among prenatal and postnatal specimens is structurally similar, as indicated by high matrix correlations using random skewers tests at each stage of the CPC hierarchy.

Prenatal allometry is characterised in *Rhabdomys pumilio* by a relative rapid lengthening of cranial elements, especially the frontal, parietal, basisphenoid, premaxilla and palatine (see Table 5.3). Particularly, bivariate coefficients for parietal, palatine and basisphenoid lengths were more than 30% greater for prenatal compared to postnatal specimens. The magnitudes of the prenatal coefficients in this study were comparable with the only other study of mammalian prenatal cranial allometry to date, that examines similar measurements to those taken herein, on the skull of the common European mole (0.7 – 4.5; Goswami and Prochel 2007). Coefficients for postnatal specimens were largely consistent with the range of values previously reported among allometry studies of other mammalian taxa, including rodents (0.2 – 2.3; Leamy and Bradley 1982, Leamy and Atchley 1984) and marsupials (0.4 – 1.5; Abdala et al. 2001, Flores et al. 2003). Notably, elements exhibiting a positive allometric trend are mostly those belonging to the neurocranial, as opposed to the facial, skeleton. Bivariate analyses indicate positive allometries are found for 6 out of 8 neurocranial variables

	Prenatal	Postnatal	Average
Equality	0.806	0.968	0.887
Proportionality	0.780	0.981	0.881
CPC	0.851	0.872	0.862
CPC(7)	0.848	0.873	0.861
CPC(6)	0.849	0.872	0.861
CPC(5)	0.851	0.871	0.861
CPC(4)	0.851	0.871	0.861
CPC(3)	0.876	0.855	0.866
CPC(2)	0.899	0.842	0.870
CPC(1)	0.856	0.861	0.859

Table 5.5: Vector correlations from random skewers analysis for each pairwise comparison for the reconstructed covariance matrices at each step in the CPC hierarchy: CPC = sharing of all principal components between the prenatal and postnatal matrices; CPC(1) – CPC(7) = sharing of a number of components, as denoted in the parentheses. All vector correlations are significant ($p<0.008$).

among postnatal specimens and of these, frontal length and parietal width shift to display a negative allometry during postnatal ontogeny, indicating an alteration to a relatively reduced rate of bone growth in association with body size (Fig. 5.2). This overall trend of positive prenatal allometry supports the notion that during the prenatal period the brain is expanding rapidly and the neurocranial elements are thus growing quickly to encase and protect this organ (e.g. Herring 1993). Subsequently, postnatal growth of the neurocranium is typically isometric or negatively allometric to compensate for rapid prenatal growth and prevent distortion of the cranium in adulthood (Emerson and Bramble 1993), with neurocranial bone growth proceeding at sutural margins (Wilson and Sánchez-Villagra 2009). Another aspect of relevance is the timing of onset of ossification of the skeletal elements. This begins only around 4 days prior to birth in the house mouse *Mus musculus* (Kaufmann 2008). A similar timing is expected for *Rhabdomys* pumilio, based upon its close phylogenetic relatedness to *M. musculus* (Steppan et al. 2004) and since *R. pumilio* has a similar sequence of ossification in cranial elements to other muroid rodents (Wilson et al. 2010b). The accelerated growth of several prenatal elements herein is thus foreseeable given the short period of time before birth for skeletal elements to grow.

With a more limited sample than presented here, Goswami & Prochel (2007) were also able to detect rapid prenatal bone growth in several elements, including the basisphenoid, frontal and squamosal, as exhibited here for *R. pumilio*. The authors also noted that prenatal and postnatal growth trends for facial elements were more consistent with one another than for neurocranium elements. A similar trend is found among the variables analysed herein, and particularly for the nasal bone, which lengthens with positive allometry and widens with negative allometry throughout prenatal and postnatal ontogeny. The former feature is also consistent with nasal length allometric estimates for *Talpa europaea* (Goswami and Prochel 2007), whilst postnatal estimates of nasal length allometry in several marsupials, including *Didelphis albiventris* (Abdala et al. 2001), *Dromiciops gliroides* (Giannini et al. 2004), and *Caluromys philander* (Flores et al. 2010), also indicate a positive trend. Though, in 2 other studies conducted by the same authors, negative and isometric trends for nasal growth have also been found for *Lutreolina crassicaudata* (Flores et al. 2003) and *Dasyurus albopunctatus* (Flores et al. 2006), respectively.

The shifts between prenatal and postnatal trends for some variables point to a non-linearity of ontogenetic allometry in *Rhabdomys pumilio*. Several authors have proposed postnatal ontogenetic allometry to be non-linear in

other rodent species (e.g. Zelditch et al. 1992; Hingst-Zaher et al. 2000). Particularly, Zelditch et al. (2003) have shown that both the house mouse *Mus musculus domesticus* and the cotton rat *Sigmodon fulviventer* have complex non-linear trajectories, though these have been shown to stabilize shortly after weaning. The time of weaning represents a milestone in development (Humphrey 2010) that is associated with a major shift in dietary composition, and has been suggested to exert an epigenetic impact on craniofacial morphology during growth (Helm and German 1996). Phenotypic variance has been shown to decrease at around 35 days in mice (Atchley 1984; Riska et al. 1984; Willmore et al. 2006) and a broadly similar result has been found for the common rat (Nonaka and Nakata 1984), thus suggesting that the effects of epigenetic influences have already been determined by this point and have little effect on patterning variance in skull morphology (Willmore et al. 2006). The timing of development may play a role in the latter hypothesis, and hence Zelditch et al. (2003) suggested that stabilization of allometries may occur earlier in highly precocial mammals, and perhaps even before birth. The young of eutherian mammals differ in their degree of neonatal development and are normally described to be either poorly developed (altricial) or well developed (precocial) (Derrikson 1992), though the dichotomy inferred by the use of these two

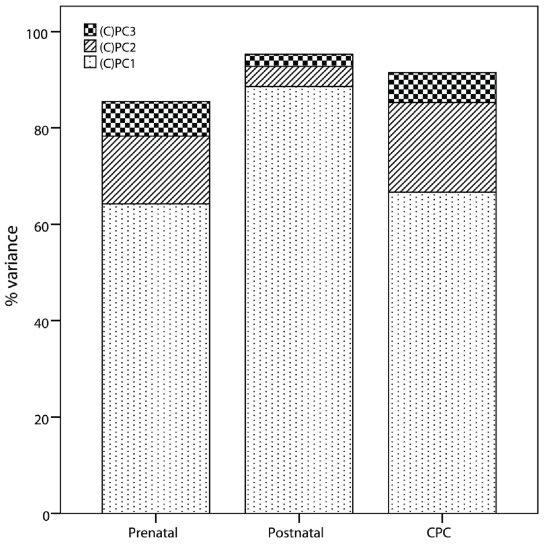

Figure 5.3: Eigenvalues, expressed as percentages of total variance, of principal component analysis of prenatal and postnatal matrices, and of the CPC matrix, following the Flury hierarchy produced from common principal component analysis of prenatal and postnatal matrices.

terms is commonly recognised rather as a continuum (Starck and Ricklefs 1998; Sánchez-Villagra and Sultan 2002). Based upon factors frequently used to ascribe either altricial or precocial development, such as birth weight and length of gestation period (e.g. Martin and MacLarnon 1985; Derrickson 1992), *Rhabdomys pumilio* is considered, similar to many other muroids, to produce altrical neonates, and these wean at 16 days (Brooks 1982). Notably, though, in comparison to other muroids that are described as altricial, for instance the house mouse, *R. pumilio* weans around 5 days sooner. Similarly, the young of *R. pumilio* open their eyes after around 7 days, which represents a

half-way point between the time taken for young of *M. musculus* (14 days; Nowak 1999) and those of *Sigmodon* (0-1 days; Nowak 1999), an atypically precocial group of muroid rodents. Hence it would be most probable that allometry stabilization occurs during postnatal development for *R. pumilio*, and most likely slightly earlier than the timing indicated by Zelditch et al. (2003) for the house mouse, given the discrepancy in life history attributes between the two. Nevertheless, the data presented herein suggest birth represents a key point of transition for the growth dynamics of several cranial elements, especially the palatine, frontal and parietal, whilst other elements such as the basisphenoid appear to display constant growth relationships across ontogeny (see Fig. 5.2 as example). In a comparison of late prenatal and early postnatal ontogenetic allometry of the cranium in humans, Sardi et al. (2007) found some parts, such as the vault, exhibited differences in shape during ontogeny, whilst others, such as the facial region, did not. Examination of middle and late prenatal cranial ontogeny in humans and pigtailed macaques also revealed some regions exhibit alterations to growth dynamics whilst others do not (Zumpano and Richtsmeier 2003). The latter two studies, coupled with the results herein, suggest that morphological differentiation of some traits in the mammalian cranium is established during the prenatal period. Experimental studies have demonstrated that external stimuli can alter cranial form (e.g. Moore 1967; Bouvier and Hylander 1981; Smith 1981), indicating morphogenesis of the skull is affected by epigenetic factors as well as genetic factors. The shift in growth dynamics at birth for several of the elements measured herein promotes epigenetic control of bone growth, since if an exclusively genetic programme was followed then one would not anticipate a shift at birth, which marks the point when epigenetic factors, assumed here to be defined as all stimuli affecting skull growth as per Hall (1983), are likely to begin asserting a greater degree of regulation on skull growth (e.g. Rayne and Crawford 1972). A complex organisation of cranial growth is evident and further consideration of the role birth plays in cranial growth dynamics is clearly warranted.

In a broad study of postnatal growth for muroid and hystricognath species, Wilson and Sánchez-Villagra (2010) showed that changes in covariance structure, as denoted by alterations to PC1 axes, are common among rodents. The inter-trajectory angle of 22.7° found herein between prenatal and postnatal stages of *R. pumilio* falls within the range of vector angles that Wilson and Sánchez-Villagra (2010) reported between species (7.7° to 33.1°), suggesting ontogenetic allometric variation is of a similar magnitude to evolutionary allometric variation. Whilst the sample size of Goswami

and Prochel (2007) did not permit a vector comparison between prenatal and postnatal allometry, the results of Zelditch et al. (2003) indicated large and statistically significant differences in vector angles between successive stages during the postnatal ontogenies of *M. m. domesticus* (up to 73.5°) and *S. fulvivienter* (up to 84.6°). In comparison to the latter study, the closer correspondence between prenatal and postnatal specimens may be due to the effects of a "general size" factor as previously suggested by Cheverud (1982) in relation to concordance between static and ontogenetic allometry. The latter may be further excerbated since all the measurements herein are either lengths or widths of elements, whereas in the work of Zelditch et al. (2003), geometric morphometric landmarks were recorded on the rodent crania under study. Comparison of geometric morphometric and distance measurement methods of data collection has indicated that the amount of allometric variation identified within a sample differs between the two approaches, largely reflecting their differing capacity to separate size from shape, though allometric pattern estimations have been shown to be in agreement (Swiderski 2003).

Despite the differences between prenatal and postnatal allometry trends identified in the bivariate analyses, the overall structure of the two covariance matrices is indicated to be significantly similar as shown by the correlations between the original and CPC matrices using random skewers. CPC analysis partitions variance in the same manner as PCA, onto orthogonal axes, and hence if the factor causing

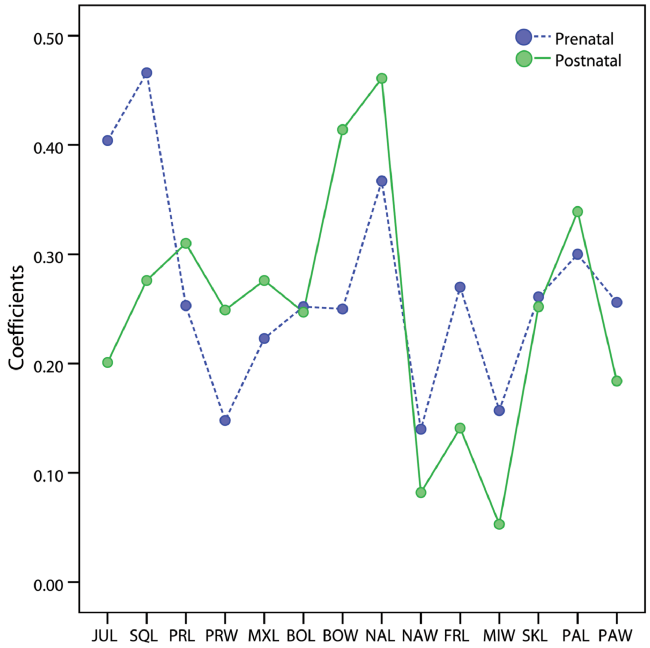

Figure 5.4: Comparison of prenatal and postnatal multivariate allometry estimated by principal component coefficients.

covariation structure is largely limited to a similar orthogonal axis, for instance in the case here of multivariate allometry where the first principal component reflects a "general size" axis to which other variables are highly correlated, then it is likely that CPC analysis will result in the construction of a shared matrix that is significantly correlated with the originals. One consideration to bear in mind with this scenario is the biological reality of orthogonal structure, particularly Houle et al. (2000) have cautioned against the interpretation of CPC results in terms of biological causation. Nevertheless this point is also a relevant criticism of PCA, which assumes uncorrelated orthogonal axes, and since PC1 here reflects "general size", PC2 represents a contrast of two ways to attain size, and thus by definition is correlated to PC1 (see Mitteroecker et al. 2005 for discussion of PCA). Using an analogous approach to that applied herein, in their study of Neotropical primates, Cheverud and Marroig (2007) also found high pairwise correlations between CPC constructed matrices at each stage of the hierarchy, these ranged from 0.943 to 0.990 for matrices with sample sizes of 79 and 92 individuals. CPC has also been used in studies of several non-mammalian taxa and has indicated shared structure between and within types of allometry among species (e.g. Klingenberg and Zimmermann 1992; Klingenberg 1996) and also within species (Cuzin-Roudy 1975). Studies on differences in postnatal covariance structure of cranial variables among rodents have yielded some results of similarity among populations of muroid rodents, including between members of the genus *Zygodontomys* (Voss et al. 1990) and also *Phyllotis* (Steppan 1997), whilst differences have been found between static and ontogenetic allometries for *Mus musculus* (Leamy and Bradley 1982), within stages of ontogenetic allometry for the hystricognath rodent *Thrichomys apereoides* (Monteiro et al. 1999), and for the muroid rodent *Mastomys natalensis* (Fadda and Leirs 2009). Evaluating the significance of the highly similar prenatal and postnatal matrix structure herein is difficult since the aforementioned studies of rodents all examined postnatal growth, and further since methodological limitations have been noted in association with CPC. It has been shown that small sample sizes do influence CPC results, mostly in favour of accepting a similar structure between matrices (Marroig and Cheverud 2001; Houle et al. 2002). The use of a random skewers test in this study, which is less affected by sample size, because randomization is achieved through the application of random selection vectors to each matrix rather than the randomization of the columns and rows of the original matrices, removes any sample size bias that may influence the statistical significance of the outcome. But it should be noted

that matrices containing well separated eigenvalues tend to have more influence on CPC analysis than do those with eigenvalues that are almost equal to one another (Airoldi and Flury 1988). This may explain why the postnatal matrix corresponds more closely in structure to the CPC constructed matrices than the prenatal matrix, as indicated by much narrower vector angles and higher random skewers correlations in relation to the equality and proportionality models (Table 5.5). Since the age range encapsulated within the postnatal sample exceeds that of the prenatal one, and since PC1, in accordance with multivariate allometry, largely accounts for size variation, the relative magnitude of the first eigenvector in relation to the succeeding ones is greater for the postnatal matrix than the prenatal matrix, and as such instigates a greater influence upon CPC analyses.

CONCLUSIONS

This study compared prenatal and postnatal ontogenetic allometry in the African striped mouse *Rhabdomys pumilio*. Results indicate that the prenatal period is characterized by rapid bone growth, as evidenced by larger bivariate allometric coefficients and a greater proportion of cranial elements growing with a positive allometry than in the postnatal period. Growth dynamics are found to shift for measurements of several elements including the parietal, frontal and palatine, indicating a non-linearity of ontogenetic allometry with respect to birth. CPC and random skewers results indicate that overall the prenatal and postnatal matrices are structurally highly similar, indicating covariance structure is conserved over ontogeny. Further empirical study to unravel the role prenatal allometry plays in the generation of adult form will undoubtedly yield greater insight into the dynamics of ontogenetic allometry.

ACKNOWLEDGEMENTS

Random skewers analyses were performed using software written by Liam J. Revell (available at: http://anolis.oeb.harvard.edu/~liam/). I thank Carsten Schradin (Universität Zürich) for kindly providing the *Rhabdomys pumilio* specimens that were cleared and stained for this study, and Marianne Haffner (Zürich) for access to osteological collections. I am especially grateful to Marcelo R. Sánchez-Villagra for support and thoughtful discussion during the preparation of this manuscript. For useful comments and discussion, I also thank Anjali Goswami (London), Ingmar Werneburg (Zürich) and Hauke Koch (Zürich). This work was supported by a Forschungskredit of the Universität Zürich (Nr. 3771).

REFERENCES

ABDALA, F., D. A. FLORES, AND N. P. GIANNINI.

2001. Post-weaning ontogeny in the skull in *Didelphis albiventris*. Journal of Mammalogy 82 (1):190-200.

AIROLDI, J. P., AND B. D. FLURY. 1988. An application of common principal component analysis to cranial morphometry of *Microtus californicus* and *M. ochrogaster* (Mammalia, Rodentia). Journal of Zoology 216: 21-36.

ARNOLD, S. J., AND P. C. PHILLIPS. 1999. Hierarchical comparison of genetic variance-covariance matrices. II. Coastal-inland divergence in the garter snake, *Thamnophis elegans*. Evolution 53: 1516-1527.

ATCHLEY, W. R. 1984. Ontogeny, timing of development, and genetic variance-covariance structure. American Naturalist 123: 519–540.

ATCHLEY, W. R., S.W. HERRING, B. RISKA, AND A. A. PLUMMER. 1984. Effects of the muscular dysgenesis gene on developmental stability in the mouse mandible. Journal of Craniofacial Genetics and Developmental Biology 4: 179-189.

BASTIR, M., AND A. ROSAS. 2004. Facial heights: evolutionary relevance of postnatal ontogeny for facial orientation and skull morphology in humans and chimpanzees. Journal of Human Evolution 47: 359-381.

BASTIR, M., AND A. ROSAS. 2009. Mosaic evolution of the basicranium in *Homo* and its relation to modular development. Evolutionary Biology 36: 57-70.

BEECHER, R. M., AND R. S. CORRUCCINI. 1981. Effects of dietary consistency on craniofacial and occlusal development in the rat. Angle Orthodontist 51: 61-69.

BOUVIER, M., AND W. L. HYLANDER. 1981. Effect of bone strain on cortical bone structure in macaques (*Macaca mulatta*). Journal of Morphology 167: 1-12.

BROOKS, P. M. 1982. Aspects of the reproduction, growth and development of the four striped mouse, *Rhabdomys pumilio* (Sparrman, 1784). Mammalia 46: 53–64.

BULYGINA, E., P. MITTEROECKER, AND L. AIELLO. 2006. Ontogeny of facial dimorphism and patterns of individual development within one human population. American Journal of Physical Anthropology 131: 432-443.

CARDINI, A., AND P. O'HIGGINS. 2005. Postnatal ontogeny of the mandible and ventral cranium in *Marmota* species (Rodentia, Sciuridae): allometry and phylogeny. Zoomorphology 124: 189-203.

CHEVERUD, J. M. 1982. Relationships among ontogenetic, static, and evolutionary allometry. American Journal of Physical Anthropology 59: 139-149.

CHEVERUD, J. M. 1996. Quantitative genetic analysis of cranial morphology in the cotton-top (*Saguinus oedipus*) and

saddle-back (*S. fuscicollis*) tamarins. Journal of Evolutionary Biology 9: 5–42.

CHEVERUD, J. M., AND G. MARROIG. 2007. Comparing covariance matrices: Random skewers method compared to the common principal components model. Genetics and Molecular Biology 30(2): 461-469.

COCK, A. 1966. Genetical aspects of metrical growth and from in animals. Quarterly Review of Biology 41: 131-190.

CORRUCCINI, R. S., L. D. WHITLEY, S. S. KAUL, L. B. FLANDER, AND C. A. MORROW. 1985. Facial height and breadth relative to dietary consistency and oral breathing in two populations (North India and U.S.). Human Biology 57: 151-161.

CREIGHTON, G. K., AND R. E. STRAUSS. 1986**.** Comparative patterns of growth and development in Cricetine rodents and the evolution of ontogeny. Evolution 40: 94–106.

CUBO, J., J. VENTURA, AND A. CASINOS. 2006. A heterochronic interpretation of the origin of digging adaptations in the Northern water vole, *Arvicola terrestris* (Rodentia: Arvicolidae). Biological Journal of the Linnean Society. 87: 381-391.

CUZIN-ROUDY, J. 1975. Étude de la variabilité et de l'allométrie de taille chez *Notonecta maculata* Fabricius (Insectes, Hétéroptè res), par les méthodes classiques et par la méthode des composantes principales. Archives de Zoologie Expérimentale et Générale 116: 173-227.

DERRIKSON, E. M. 1992. Comparative reproductive strategies of altricial and precocial eutherian mammals. Functional Ecology 6: 57-65.

EFRON, B., AND R. J. TIBSHIRANI. 1993. An introduction to the bootstrap. Chapman and Hall, New York.

EMERSON, S. B., AND D. M. BRAMBLE. 1993. Scaling, allometry and skull design. Pp384-416 in The skull Vol.3 (J. Hanken and B. K. Hall, eds.). The University of Chicago Press, Chicago, Illinois.

FLORES, D. A., F. ABDALA, AND N. P. GIANNINI. 2010. Cranial ontogeny of *Caluromys philander* (Didelphidae, Caluromyinae): a qualitative and quantitative approach. Journal of Mammalogy. In press

FLORES, D. A., N. P. GIANNINI, AND F. ABDALA. 2003. Cranial ontogeny of *Lutreolina crassicaudata* (Didelphidae): a compare son with Didelphis albiventris. Acta Theriologica 48(1): 1-9.

FLORES, D. A., N. P. GIANNINI, AND F. ABDALA. 2006 Comparative postnatal ontogeny of the skull in the australidelphian metatherian Dasyurus albopunctatus (Marsupialia: Dasyuromorpha: Dasyuridae). Journal of Morphology 267: 426-

440.

FADDA, C., AND H. LEIRS. 2009. The role of growth stop as a morphogenetic factor in *Mastomys natalensis* (Rodentia: Muridae). Biological Journal of the Linnean Society 97: 791-800.

FLURY, B. D. 1988. Common principal components and related multivariate models. Wiley, New York.

GAYON, J. 2000. History of the concept of allometry. American Zoologist 40: 748-758.

GIANNINI, N. P., D. A. FLORES, AND F. ABDALA. 2004. Comparative postnatal ontogeny of the skull in *Dromiciops gliroides* (Marsupialia: Microbiotheriidae). American Museum Novitates 3460: 1-17.

GOSWAMI, A., AND J. PROCHEL. 2007. Ontogenetic morphology and allometry of the cranium in the common European mole (*Talpa Europaea*). Journal of Mammalogy 88(3): 667-677.

HALL, B. K. 1983. Epigenetic control in development and evolution. Pp. 353-379 in Development and Evolution (B. C. Goodwin, N. Holder and C. G. Wylie, eds.). Cambridge University Press, Cambridge.

HALL, B. K. 2005. Bones & Cartilage: Developmental and Evolutionary Skeletal Biology. Elsevier Academic Press, London.

HAMBURGER, V. 1973. Anatomical and physiological basis of embryonic motility in birds and mammals. Pp. 51-76 in Studies in the Development of Behaviour and the Nervous System (G. Gottlieb, ed.). Academic Press, New York.

HARRIS, A. K., D. STOPAK, AND P. WILD. 1981. Fibroblast traction as a mechanism for collagen morphogenesis. Nature 290: 249-251.

HARVEY, P. H., AND M. D. PAGEL. 1991. The comparative method in evolutionary biology. Oxford University Press, Oxford.

HELM, J. W., AND R. Z. GERMAN. 1996. The epigenetic impact of weaning on craniofacial morphology during growth. The Journal of Experimental Zoology 276: 243-253.

HERRING, S. W. 1993. Epigenetic and functional influences in skull growth. Pp 153-206 in The skull Vol. 1 (J. Hanken and B. K. Hall, eds.). The University of Chicago Press, Chicago, Illinois.

HINGST-ZAHER, E., L. F. MARCUS, AND R. CERQUERIA. 2000. Application of geometric morphometrics to the study of postnatal size and shape changes in the skull of *Calomys expulsus*. Hystrix 11: 99-114.

HOULE, D., J. MEZEY, AND P. GALPERN. 2002. Interpretation of the results of common principal components analyses. Evolution 56(3): 433-440.

HUMPHREY, L. T. 2010. Weaning behaviour in

human evolution. Seminars in Cell and Developmental Biology 21(4): 463-451.

JOLICOEUR, P. 1963. The multivariate generalization of the allometry equation. Biometrics 19: 497-499.

KAUFMAN, M. H. 2008. The Atlas of Mouse Development. Elsevier Academic Press, London.

KLINGENBERG, C. P. 1996. Individual variation of ontogenies: a longitudinal study of growth and timing. Evolution 50(6): 2412-2428.

KLINGENBERG, C. P. 1998. Heterochrony and allometry: the analysis of evolutionary change in ontogeny. Biological Reviews 73: 79-123.

KLINGENBERG, C. P., AND M. ZIMMERMANN. 1992 Static, ontogenetic, and evolutionary allometry: A multivariate compare son in nine species of water striders. American Naturalist 140: 601-620.

LATHAM, R. A. 1972. The different relationship of the sella point to growth sites of the cranial base in fetal life. Journal of Dental Research. 51: 1646-1650.

LEAMY, L., AND W. R. ATCHLEY. 1984. Static and evolutionary allometry of osteometric traits in selected lines of rats. Evolution 38: 47-54.

LEAMY, L., AND D. BRADLEY. 1982. Static and growth allometry of morphometric traits in randombred house mice. Evolution 36: 1200-1212.

MANDARIM-DE-LACERDA, C. A., AND M. U. ALVES. 1992. Human mandibular prenatal growth: bivariate and multivariate growth allometry comparing different mandibular dimensions. Anatomy and Embryology (Berlin) 186: 537-541.

MARROIG, G. 2007. When size makes a differ ence: allometry, life-history and morphological evolution of capuchins (*Cebus*) and squirrels (*Saimiri*) monkeys (Cebinae, Platyrrhini). BMC Evolutionary Biology 7: 20.

MARROIG, G., AND J. M. CHEVERUD. 2001 A comparison of phenotypic variation and covariation patterns and the role of phylogeny, ecology, and ontogeny during cranial evolution of New World monkeys. Evolution 55: 2576-2600.

MARTIN, R. D., AND A. M. MACLARNON. 1985. Gestation period, neonatal size and maternal investment in placental mammals. Nature 313: 220-223.

MITTEROECKER, P., AND F. L. BOOKSTEIN. 2009. The ontogenetic trajectory of the phenotypic covariance matrix, with examples from craniofacial shape in rats and humans. Evolution 63(3): 727-737

MITTEROECKER, P., P. GUNZ, AND F. L. BOOKSTEIN. 2005. Heterochrony and geometric morphometrics: a comparison of cranial growth in *Pan paniscus* versus

Pan troglodytes. Evolution and Development 7(3): 244-258.

MOORE, W. J. 1967. Muscular function and skull growth in the laboratory rat (*Rattus norvegicus*). Journal of Zoology 152: 287-296.

MONTEIRO, L. R., L. G. LESSA, AND A. S. ABE. 1999. Ontogenetic variation of skull shape in *Thrichomys aperoides* (Rodentia: Echimyidae). Journal of Mammalogy 80: 102-111.

NONAKA, K., AND M. NAKATA. 1984. Genetic variation and craniofacial growth in inbred rats. Journal of Craniofacial Genetics and Developmental Biology 4: 271-302.

NOWAK, R. M. 1999. Walker's Mammals of the World, 6th Edition. The John Hopkins University Press, Baltimore.

O'HIGGINS, P., P. CHADFIELD, AND N. JONES. 2001. Facial growth and the ontogeny of morphological variation within and between the primates *Cebus apella* and *Cercocebus torquatus*. Journal of Zoology (London) 254: 337-357.

PHILLIPS, P. C. 1998. CPC: Common Principal Components Analysis. University of Oregon, Eugene, OR. [Software available at:dawrkwing.oregon.edu/~pphil/software.html]

PHILLIPS, P. C., AND S. J. ARNOLD. 1999. Hierarchical comparison of genetic variance-covariance matrices. I. Using the Flury hierarchy. Evolution 53: 1506-1515.

PLAVCAN, J., AND R. GERMAN. 1995. Quantitative evaluation of craniofacial growth in the third trimester human. The Cleft-Palate-Craniofacial Journal. 32(5): 394-404.

PROCHEL, J. 2006. Early skeletal development in *Talpa europaea*, the common European mole. Zoological Science. 23: 427–434.

PUCCIARELLI, H. M., AND E. E. OYHENART. 1987. Effects of maternal food restriction during lactation on craniofacial growth in weanling rats. American Journal of Physical Anthropology 72: 67-75.

RAYNE, J., AND G. N. C. Crawford. 1972. The growth of the muscles of mastication in the rat. Journal of Anatomy 113:391-408.

RIGGS, D. S., J. A. GUARNIERI, AND S. ADDEL MAN. 1978. Fitting straight lines when both variables are subject to error. Life Sciences 22:1305-1360.

RISKA, B., W. R. ATCHLEY, AND J. J. RUTLEDGE. 1984. A genetic analysis of targeted growth in mice. Genetics 107: 79–101.

SÁNCHEZ-VILLAGRA, M. R. 2010. Developmental palaeontology in synapsids: the fossil record of ontogeny in mammals and their closes relatives. Proceedings of the Royal Society B 277: 1139-1147

SÁNCHEZ-VILLAGRA, M. R., AND F. SULTAN. 2002. The cerebellum at birth in therian

mammals, with special reference to rodents. Brain, Behaviour and Evolution 59: 101-113.

SARDI, M. L., F. VENTRICE, AND F. RÁMÍREZ ROZZI F. 2007. Allometries throughout the late prenatal and early postnatal human craniofacial ontogeny. The Anatomical Record 290: 1112-1120.

SCHRADIN, C., AND N. PILLAY. 2003. Paternal care in the social and diurnal striped mouse (*Rhabdomys pumilio*): laboratory and field evidence. Journal of Comparative Psychology. 117: 317-324.

SCHRADIN, C., AND N. PILLAY. 2004. The striped mouse (*Rhabdomys pumilio*) from the succulent karoo of South Africa: A territorial group living solitary forager with communal breeding and helpers at the nest. Journal of Comparative Psychology. 118: 37-47.

SCHRADIN, C. 2006. Whole-day follows of striped mice (*Rhabdomys pumilio*), a diurnal murid rodent. Journal of Ethology. 24 (1): 37-43.

SINGLETON, M. 2002. Patterns of cranial shape variation in the Papionini (Primates: Cercopithecinae). Journal of Human Evolution 42: 547-578.

SMITH, D. W. 1981. Mechanical forces and patterns of deformation. Pp. 215-223 in Morphogenesis and Pattern Formation (T. G. Connelly, L.L Brinkley and B. M. Carlson, eds.). Raven Press, New York.

STARCK, J. M., AND R. E. RICKLEFS. 1998. Patterns of Development: the altricial-precocial spectrum. Pp. 3-29 in Avian Growth and Development. Evolution within the altricial precocial spectrum. (J. M. Starck and R E. Ricklefs, eds.). Oxford University Press, New York.

STEPPAN, S. J. 1997. Phylogenetic analysis of phenotypic covariance structure. II: Reconstructing matrix evolution. Evolution 51: 587-594.

STEPPAN, S. J., R. M. ADKINS, AND J. ANDERSON. 2004. Phylogeny and divergence date estimates of rapid radiations in muroid rodents based on multiple nuclear genes. Systematic Biology 53: 533-553.

SWIDERSKI, D. L. 2003. Separating size from allometry: analysis of lower jaw morphology in the fox squirrel *Sciurus niger*. Journal of Mammalogy 84(3): 861-876.

TUCKETT, F., AND G. M. MORRISS-KAY. 1985. The ontogenesis of cranial neuromeres in the rat embryo. II. A transmission electron microscopy study. Journal of Embryology and Experimental Morphology 88: 231-247.

VINICUS, L. 2005. Human encephalization and developmental timing. Journal of Human Evolution 49: 762-776.

VIÐARSDÓTTIR, U. S., P. O'HIGGINS, AND C.

STRINGER. 2002. A geometric morphometric study of regional differ ences in the ontogeny of the modern human facial skeleton. Journal of Anatomy 201: 211-229

VOSS, R. S., L. F. MARCUS, AND P. P. ESCA LANTE. 1990. Morphological evolution in muroid rodents I. Conservative patterns of craniometric covariance and their on togenetic basis in the Neotropical genus *Zygodontomys*. Evolution 44(6): 1568–1587.

WESTON, E. M. 2003. Evolution of ontogeny in the hippopotamus skull: using allometry to dissect developmental change. Biological Journal of the Linnean Society 80: 625-638.

WILLMORE, K. E., L. LEAMY, AND B. HALL GRIMSSON. 2006. The effects of developmental and functional interactions on mouse cranial variability through late ontogeny. Evolution and Development 8: 550-567.

WILSON, D. E., AND D. M REEDER. 2005. Mammal species of the world: a taxonomic and geographic reference. Smithsonian Institution Press, Washington DC.

WILSON, L. A., N. MACLEOD, AND L. T. HUMPHREY. 2008. Morphometric criteria for sexing juvenile human skeletons using the ilium. Journal of Forensic Sciences 53 (2): 269-278.

WILSON, L. A. B., H. F. V. CARDOSO, AND L. T. HUMPHREY. 2010a. On the reliability of a geometric morphometric approach to sex determination: a blind test of six criteria of the juvenile ilium. Forensic Science International In press

WILSON, L. A. B., AND M. R. SÁNCHEZ-VILLAGRA. 2009. Heterochrony and patterns of cranial suture closure in hystricognath rodents. Journal of Anatomy 214: 339-354.

WILSON, L. A. B., AND M. R. SÁNCHEZ-VILLA GRA. 2010. Diversity trends and t h e i r ontogenetic basis: an exploration of al lometric disparity in rodents. Proceed ings of the Royal Society of London, B Biological Sciences 277: 1227-1234.

WILSON, L. A. B., C. SCHRADIN, C. MITGUTSCH, F. C. GALLIARI, A. MESS, AND M. R. SÁNCHEZ-VILLAGRA. 2010b. Skeletogenesis and sequence heterochrony in rodent evolution, with particular emphasis on the African striped mouse, *Rhabdomys pumilio* (Mammalia). Organisms Diversity and Evolution 10: 243-248.

WOLPOFF, M. H. 1985. Tooth size-body scaling in a human population. Theory and practice of an allometric analysis. Pp. 273-318 in Size and scaling in primate biology (W. L. Jungers, ed.). Plenum Press, New York.

ZELDITCH, M. L. 1988. Ontogenetic variation in patterns of phenotypic integration in the laboratory rat. Evolution 42:28-41.

ZELDITCH, M. L., F. L. BOOKSTEIN, AND B. L. LUNDRIGAN. 1992. Ontogeny of integrated skull growth in the cotton rat *Sigmodon fulviventer*. Evolution 46: 1164-1180.

ZELDITCH, M. L., AND A. C. CARMICHAEL. 1989. Ontogenetic variation in patterns of developmental and functional integration in skulls of *Sigmodon fulviventer* Evolution 43(4): 814-824.

ZELDITCH, M. L., B. L. LUNDRIGAN, D. SHEETS, AND T. GARLAND JR. 2003. Do precocial mammals develop at a faster rate? A comparison of rates of skull development in *Sigmodon fuliviventer* and *Mus musculus domesticus.* Journal of Evolutionary Biology 16: 708-720.

ZOLLIKOFER, C. P. E., AND M. S. PONCE DE LEÓN. 2004. Kinematics of cranial ontogeny: heterotopy, heterochrony, and geometric morphometric analysis of growth models. Journal of Experimental Zoology 302B: 322-340.

ZOLLIKOFER, C. P. E., AND M. S. PONCE DE LEÓN. 2010. The evolution of hominin ontogenies. Seminars in Cell and Developmental Biology 21: 441-452.

ZUMPANO, M. P., AND J. T. RICHTSMEIER. 2003. Growth-related shape changes in the fetal craniofacial complex of humans (*Homo sapiens*) and pigtailed macaques (*Macaca nemestrina*): a 3D-CT comparative analysis. American Journal of Physical Anthropology 120: 339-351

CHAPTER 6

Conclusions and future perspectives

As an organism progresses along its ontogenetic pathway to reach adult form, a multitude of interwoven processes act to shape the outcome. The examination of morphological evolution can thus be enriched by studies providing insights into the evolution of ontogenies and the role these changes play in contributing to the generation of adult form. However, the temporal continuum of growth is unequally sampled and studied, in terms of both the range of taxa and the point in ontogeny examined. Broad-scale comparisons of morphologically diverse taxa, as presented through the chapters of this thesis, provide information about developmental dynamics, contributing to our understanding of how morphological diversity evolves.

The chapters of this thesis, as a whole, present the first exploration of the developmental basis for the contrasting levels of morphological diversity in two parallel radiations of mammals. In chapters 2 and 4, the evolutionary importance of heterochrony is examined at two different points during growth: the closure of sutures during a late stage of postnatal growth and the ossification of skeletal elements, beginning prenatally. In complement, chapters 3 and 5 focus upon allometry. Allometric evolution, estimated from postnatal growth, is examined in chapter 3, whilst chapter 5 documents prenatal ontogenetic allometry.

The first detailed study of cranial suture closure patterns in hystricognath rodents (chapter 2) reveals that numerous heterochronies have occurred during the evolution of this clade. From an evolutionary perspective, this study shows that suture closure patterning can be used to document changes in growth patterns, and that these changes may be associated with life history and functional correlates. In complement to this finding, based upon the largest data set so far compiled for ossification onsets in rodents, chapter 4 shows that sequence heterochrony is neither pivotal nor prevalent during this comparatively earlier point in development. Taken together, it appears that the evolutionary importance of heterochrony in rodents is restricted to postnatal modifications. Since a heterochronic shift requires a dissociation between two events, this may reflect the incapacity of modular organization to permit evolutionary modifications during ossification of the skeletal elements; the data collected for chapter 4 could be used as a platform to assess whether developmental modularity in rodents is recoverable in a comparable manner to that demonstrated for evolutionary modularity, on a broader scale, across therian mammals (Goswami 2006). Leading on from chapter 4, a further application of interest would be the extension of these methods to interface with a genetic approach. Through the study of mice that possess genetic

mutations which directly, or indirectly affect skeletogenesis (e.g. null mutations in myogenin; Rot-Nikcevic et al. 2006) it would be possible to examine the affects that developmental anomalies have upon recorded heterochrony. Adding a mutant strain as a comparative to the developmental series studied in chapter 4, would enable one to test the hypothesis that genetic alterations affect heterochronic pathways, and define how these lead to discrepancies in size and/or shape between normal and mutant mice.

At present, the understanding of allometric evolution is limited by a lack of empirical clade-wide studies. Chapter 3 provides the first estimation of allometric evolution for rodents, focussing on a clade-wide comparison of hystricognaths and muroids. We show that phylogenetic relatedness and anatomical diversity do not constrain allometric patterning, since both clades of rodents are found to occupy comparable amounts of morphospace and their distributions in this space overlap. The comparatively increased amount of morphological diversity displayed by hystricognaths is thus not achieved primarily by a more extensive variability in allometric patterns. We find that diet plays a crucial role in the evolution of allometric patterns, hence underlining the importance of convergent morphology in the evolution of ontogenies, and demonstrating that the evolution of allometry has an adaptive basis. Burgeoning attempts to bridge the gap between microevolutionary processes and macroevolutionary patterns have resulted in a wealth of study directed towards the evolution of covariance structure, and in particular much attention has focused upon the fields of morphological integration (e.g. Cheverud 1995, 1996) and **P** (phenotype) matrix evolution (e.g. Roff and Mousseau 2005). Allometric evolution is a field of enquiry that directly parallels these lines of research, and as such equally warrants attention since it also yields the potential to illuminate our knowledge about the evolution of covariance structure. A recent study using carnivorans has shown *Runx2* to be a candidate for regulating heterochronic changes in allometric growth, and has further demonstrated that links between phenotype and genotype may be related to allometry (Sears et al. 2007). Further clade-wide studies, are required in extension to chapter 3 to provide a clearer understanding of how morphologies are generated, since logic confers that over a long enough time scale **P** and **G** (genotype) matrices will alter, otherwise all organisms would have morphologies of approximately the same form (Lofsvold 1986). The methods used in chapter 3 lead innately to the possibility of empirically testing whether the unequal distribution of morphological diversity among muroids and hystricognaths is a result of differing magnitudes of evolution (e.g. Cooper

and Purvis 2009) or differing modes of evolution (e.g. Harmon et al. 2003). Given the robust and well-studied phylogenetic frameworks available for rodents, as used throughout this thesis, the mapping of a phylogenetic framework into allometric space accompanied with calculations of lineage densities would present a worthwhile extension to this dataset.

Whilst chapter 3 indicates that postnatal modifications to allometries occurred commonly during rodent evolution, the lack of developmental series available for any mammal currently precludes the evaluation of this finding in the context of prenatal allometries. Though, with the advent of non-destructive imaging techniques (e.g. CT shadow imaging; Weisbecker et al. 2008) that permit the fast throughput of developmental series, the outlook is likely to change in the near future. Crucially acting as a base for further comparative studies of prenatal ontogeny, chapter 5 provides the first comparison of prenatal and postnatal ontogenetic allometry for a rodent and supplies insights into the dynamics of prenatal development. The findings that ontogenetic allometry shifts between the prenatal and postnatal period and that localized variation in growth relationships occurs among cranial elements need to be assessed through the examination of additional taxa, to develop an understanding of how common this pattern is among rodents.

are now extinct. The archive of information recorded in fossilized ontogenies has the potential to yield insights into the evolution of ontogeny. Whilst the recovery of fossilized ontogenies is rare and incomplete, recent studies, in some cases using similar methods to those herein, have highlighted the fundamental importance of coupling development in the present and past (e.g. Schoch 2006; Guenther 2009; Delfino and Sánchez-Villagra 2010). In addition to growth series (Vucetich et al. 2005), the rodent fossil record also includes forms of extreme size (Sánchez-Villagra et al. 2003), which surely provide a rich subject of study for future work. In this regard, examination of the rodent fossil record will undoubtedly shed light upon the evolutionary questions that provided the impetus for undertaking this work.

REFERENCES

Cheverud JM. 1995. Morphological integration in the saddleback tamarin (*Saguinus fuscicollis*) cranium. *American Naturalist* 145: 63-89.

Cheverud JM. 1996. Developmental integration and the evolution of pleiotropy. *American Zoologist* 36:44-50.

Cooper N, Purvis A. 2009. What factors shape rates of phenotypic evolution? A comparative study of cranial morphology of four mammalian clades. *Journal of Evolutionary Biology* 22: 1024-1035

Delfino M, Sánchez-Villagra MR. 2010. A survey of the rock record of reptilian ontogeny. *Seminars in Cell & Developmental Biology* 21(4): 432-440

Goswami A. 2006. Morphological integration in the carnivoran skull. *Evolution* 60: 169-183

Guenther MF. 2009. Influence of sequence heterochrony on hadrosaurid dinosaur postcranial development. *The Anatomical Record* 292: 1427-1441

Harmon LJ, Schulte JA, Larson A, Losos JB. 2003. Tempo and mode of evolutionary radiation in iguanian lizards. *Science* 301: 961-964

Lofsvold D. 1986. Quantitative genetics of morphological differentiation in *Peromyscus*. I. Test of the homogeneity of genetic covariance structure among species and subspecies. *Evolution* 40: 559-573

Roff DA, Mousseau T. 2005. The evolution of the phenotypic covariance matrix: evidence for selection and drift in *Melanopus*. *Journal of Evolutionary Biology* 18: 1104-1114

Rot-Nikcevic I, Reddy T, Downing KJ, Belliveau AC, Hallgrimsson B, Hall BK, Kablar B. 2006. Myf5$^{-/-}$:MyoD$^{-/-}$ amyogenic fetuses reveal the importance of early contraction and static loading by striated muscle in mouse skeletogenesis. *Development Genes and Evolution* 216: 1-9

Sánchez-Villagra MR, Aguilera O, Horovitz I. 2003. The anatomy of the world's largest extinct rodent. *Science* 301: 1708-1710

Schoch RR. 2006. Skull ontogeny: developmental patterns of fishes conserved across major tetrapod clades. *Evolution and Development* 8(6): 524-536

Sears KE, Goswami A, Flynn JJ, Niswander LA. 2007. The correlated evolution of *Runx2* tandem repeats, transcriptional activity and facial length in Carnivora. *Evolution and Development* 9: 555-565

Vucetich MG, Deschamps CM, Olivares AI, Dozo MT. 2005. Capybaras, size, shape, and time: a model kit. *Acta Palaeontologica Polenica* 50(2): 259-272

Weisbecker V, Goswami A, Wroe S, Sánchez-Villagra MR. 2008. Ossification heterochrony in the mammalian postcranial skeleton and the marsupial-placental dichotomy. *Evolution* 62: 2027-2041

APPENDIX I

The evolution and phylogenetic signal of growth trajectories: the case of chelid turtles

APPENDIX I
The evolution and phylogenetic signal of growth trajectories: the case of chelid turtles

Article submitted to *Journal of Experimental Zoology Part B* on 2nd February 2010, accepted for publication on 7th July 2010

Reference: **Wilson LAB**, Sánchez-Villagra MR. 2010. The evolution and phylogenetic signal of growth trajectories: the case of chelid turtles. *J. Exp. Zool (Mol Dev Evol)* In press

Abstract

Morphological and molecular data yield incongruent hypotheses concerning the interrelationships of chelid side-necked turtles, neither of which is widely accepted. Molecular studies recognise monophyletic South American and Australasian clades, whereas morphological characters distinguish a long-necked clade and a short-necked clade. We take a developmental approach to exploring chelid interrelationships. None of the nine species studied have the same growth pattern for all measurements examined, indicating changes in ontogenetic scaling of cranial characters was common during chelid evolution. The variability in scaling relationships precludes overwhelming support for either hypothesis. Scaling patterns are most similar between the geographically separate clades promoted by molecular analyses, and hence our data favour an independent origin of the long neck in South American and Australasian species. A close relationship between *Hydromedusa* and *Chelus*, rather than *Chelodina*, is supported by scaling patterns associated with a relative widening of the cranium.

KEYWORDS**:** ontogeny; heterochrony; allometry; development; skull; Chelidae; Pleurodira

INTRODUCTION

The growth trajectories that characterize species evolve, and with that the morphological space that is occupied during growth and the resulting adult morphology (Weston, 2003; Giannini et al., 2004; Wilson and Sánchez-Villagra, 2010). Growth trajectories are most easily studied in post-hatching stages. These can in many cases be studied in fossils, providing information to solve taxonomic issues and/ or understand the developmental patterns that result in diverse adult skeletal anatomies (Delfino and Sánchez-Villagra, 2010).

Whilst allometry has long been a focus of study (Huxley, '32; Reeve and Huxley, '45; Jolicoeur, '63), there is a relative dearth of work that documents growth allometry in turtles. The existing literature on turtle growth focuses upon early postnatal and late embryonic specimens, and specifically the onset of cranial ossification or the development of cartilaginous and ossified structures (e.g. Kuratani, '87; Rieppel, '93; Sheil, 2003, 2005; Sánchez-Villagra et al., 2009; Werneburg et al., 2009). The detailed studies of Dalrymple ('77) on the North American soft-shelled turtle *Apalone ferox* and Bever (2008) on the Texas river cooter *Pseudemys texana* are a notable exception. Both studies concentrate on cryptodire species and pleurodires remain in this respect, as much else in evolutionary studies, largely unstudied (Gaffney et al., 2006). Here we focus upon cranial ontogeny in chelids, to explore the evolution of allometries in this group, and its relation to the competing molecular and morphological phylogenetic hypotheses.

Living chelid turtles are restricted in distribution to South America and Australasia (Australia and New Guinea). These semi-aquatic side-necked turtles (Pleurodira) are presently represented by 55-60 species (Bickham et al., 2007; Fritz and Havaš, 2007), and their fossil record reflects a geographic distribution consistent with that of present day, supporting a Gondwanan origin of the clade, with ample records in the late Cretaceous of South America (de Broin, '87; Fuente et al., 2001) and the Miocene of Australia (Gaffney et al., '89).

Morphological and molecular data yield incongruent hypotheses concerning the interrelationships of chelids; the phylogeny of these turtles is a subject of ongoing contention in the literature. After the pioneering cladistic work of Gaffney ('77) on the skulls of several species, chelids have been largely separated into two clades irrespective of their geographic distribution. Accordingly, one clade has been proposed to contain all South American and Australasian taxa with short necks (*Phrynops*, *Platemys*, *Elseya* and *Emydura*) whilst the other clade includes long-necked species found in South America (*Chelus*, *Hydromedusa*) and Australasia (*Chelodina*), so called because the neck is typi-

cally as long as, or longer than, the carapace. A large expansion of Gaffney's ('77) data matrix including new morphological characters from different skeletal parts and fossil taxa supported those conclusions (Bona and Fuente, 2005). In contrast, molecular studies suggested the parallel evolution of long-necks and distinguish two monophyletic clades: one containing all taxa from Australasia, and the other all South American species (Seddon et al., '97; Shaffer et al., '97; Georges et al., '98; Fujita et al., 2004). However, so far the molecular studies have been limited in terms of the scope of genes and taxa examined, resulting in clades with weak bootstrap support values. Examples of this are the monophyly of the Australasian chelids, for example in the analyses of Seddon et al. ('97) (64%), Shaffer et al. ('97) (58-69%) and Georges et al. ('98) (52-66%), though the latter study, using mitochondrial and nuclear genes, placed *Hydromedusa tectifera* among the monophyletic South American chelids. Taking a functional approach to the problem, Pritchard ('84) discounted the morphological grouping of Gaffney ('77) by proposing that the overall similarity in skull shape between the long-necked species of *Hydromedusa* and *Chelodina* is independently derived as a response to a piscivorous diet, and particularly a spear-fish feeding technique that can be accomplished by a great elongation of the neck to allow prey to be seized with a faster forward movement than would be possible if the entire body had to be moved. More recently Scheyer (2009) tested the two competing hypotheses using the microstructures of the shell bones of seven chelid taxa, and did not find unambiguous support for either hypothesis. In this study we take a developmental approach to exploring chelid interrelationships by examining cranial ontogenetic trajectories.

MATERIALS AND METHODS

We measured 11 characters on 141 crania from nine extant species, these are: *Chelodina longicollis*, *Chelodina reimanni, Chelus fimbriatus*, *Elseya novaguineae*, *Emydura macquarii*, *Hydromedusa tectifera*, *Phrynops hilarii*, *Platemys platycephala*, and *Podocnemis expansa* (Fig. 6.1). Additionally, we examined specimens from two species of *Pelusios*, which we treated together in this study. Calliper measurements were recorded to 0.1mm, and the average from three repetitions was used for each character. We measured both juvenile and adult crania to obtain a postnatal growth series for each species. The cranial measurements mostly follow Bever (2008), and are as listed: (1) *cranial height*; the vertical distance between basioccipital/basisphenoid suture and the highest point as the parietal/supraoccipital suture, (2) *greatest width of aperture narium externa*, (3) *minimum interorbital width*, (4) *greatest length of orbit*, (5) *palatal width*; distance between medial

margin of left and right foramen palatinum posterius, (6) *minimum width of pterygoid waist*, (7) *width between lateral margins of right and left processus trochlearis pterygoidei*, (8) *least length across dorsal surface of otic chamber*; measured between the medial margin of the jaw condyle in the quadratum to the posterior-most border of the basioccipital where an indentation at the skull base is formed, (9) *intersquamosal width*, (10) *condylobasal length*; measured from the tip of the snout to the posterior end of the occipital condyle, and (11) *maximum skull width* (see Fig. 6.2).

Bivariate allometry

We analysed nine measurements with bivariate allometric methods, using a geometric mean of condylobasal length and maximum skull width as a proxy for size (characters 10 and 11; Fig. 6.2). To study the scaling relationships between cranial characters we used the linear transformation ($\log_{10}$) of the power equation $y = b_0 x^{b1}$ where y is the variable of study, b_0 is the y-intercept, x is a proxy for size,

Figure 6.1: Dorsal view of specimens measured in this study, including (a) *Pelusios sinuatus*, (b) *Hydromedusa tectifera*, (c) *Emydura macquarii*, (d) *Podocnemis expansa*, (e) *Platemys platycephala*, (f) *Elseya novaguineae*, (g) *Phrynops hilarii*, (h) *Chelodina reimanni*, (i) *Chelus fimbriatus*. Scale bar represents 2cm.

and the coefficient b_1 details the relative magnitude of y vs. x change, thus indicating ontogenetic polarity. When $b_1 = 1$ the two characters under study change only by means of absolute size, that is isometric growth (i.e. $y/x = b_1$). If $b_1 < 1$, y is negatively allometric in respect to x, conversely if $b_1 > 1$, y is positively allometric with respect to x (i.e. with growth there is an increase in the ratio y/x). Two tailed t-tests were used to assess the significance of deviations from isometry, whereby we fixed type I error rate (α) at 0.01 under the null hypothesis of $b_1 = 1$. A relationship was deemed isometric if not significantly different from unity. To increase reliability we calculated allometric coefficients (b_1) using both least squares (LS) and reduced major axis (RMA) regression methods (model I and II). Symmetrical line fitting techniques (model II), such as RMA, are usually preferred (Wolpoff, '85) because LS assumes that the independent x variable is measured without error. When this assumption is violated, LS estimates will consistently underestimate the true slope, since by definition RMA = LS/r with $r \leq 1$, and the magnitude of this error will increase with decreasing correlation between the variables (Harvey and Pagel, '91).

Multivariate allometry

Following the multivariate generalization of simple allometry, using principal component analysis (PCA) (Jolicoeur, '63), we iden-

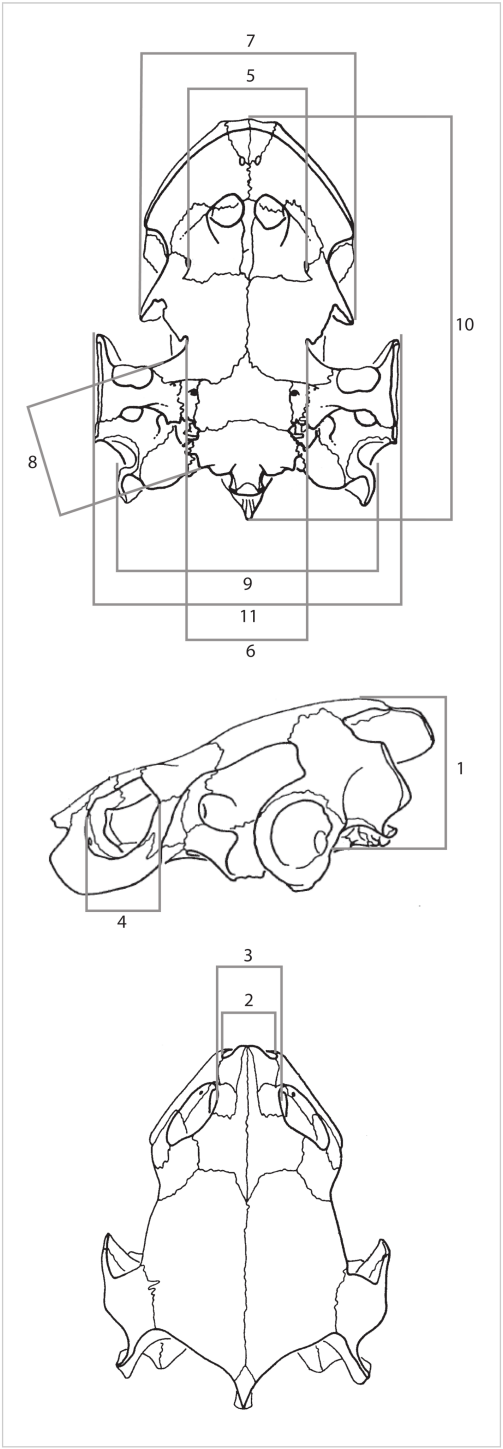

Figure 6.2: Dorsal, ventral (*Emydura macquarii*) and lateral (*Elseya novaguineae*) view of the cranium, illustrating measurements recorded in this study. See Materials and Methods for detail.

tified the patterns of multivariate allometry for seven of the ten species studied; *Chelodina reimanni, Emydura macquarii*, and *Platemys platycephala* had to be excluded because of small sample size. In multivariate allometry, an allometric trajectory is represented by the first eigenvector (axis) of a PCA using the covariance matrix of natural log transformed measurements. The coefficients of the first principal components (PC1s) for each of the 11 variables were used to identify growth trends by comparison to the isometric vector of length (p): the value at which all PC1 coefficients are equal, calculated as $p^{-1/2}$ (where p = number of measured variables). The bootstrap approach was used to compute standard error (SE) values for PC1 coefficients in comparison with the value expected for isometry; replicates were performed for 1000 iterations for each species (Efron and Tisbshirani, '93). A growth trend was identified to be positively or negatively allometric if the bootstrap confidence interval for the PC1 coefficient did not include the isometric vector.

Test of phylogenetic signal

Although the allometric coefficients derived from the analyses herein violate the assumptions of phylogenetic analysis, and thus cannot be used for such purpose, we considered an alternate approach to quantify the phylogenetic signal that may be present in these data. Several studies have revealed that data shown to possess a strong phylogenetic signal, for example through the use of a permutation test, cannot be used to successfully reconstruct phylogenetic relationships among the taxa under study (e.g. Caumul and Polly, 2005; Klingenberg and Gidaszewski, 2010 and references within). Laurin (2004) proposed a permutation method, which is the proper null hypothesis of a test for presence or absence of phylogenetic signal through the use of random swapping of characters on terminal branches. Underlying this method is the notion that randomly changing the characters among the tips of the phylogeny should not alter the amount of change recorded along the branches (step length) since a rearrangement is equally likely to produce, overall, a greater or lesser amount of change than documented on the original phylogenetic framework. Thus, if the characters possessed phylogenetic signal, swapping them on the phylogeny would likely result in trees of a longer length.

Because each coefficient has an associated standard deviation of error, reflected by the range generated by bootstrap computations of b_1, we did not simply use the absolute value of b_1 as a continuous character. Doing so would prevent cognizance of this aspect, and thus artificially inflate the amount of trends identified to be positively or negatively allometric, since coefficients whose confidence

intervals overlapped with isometry would not be recognized to be isometric when adopting such an approach. Instead, the reduced major axis bivariate growth trends documented in S-Tables 6.1 through 6.10, which were based upon two tailed *t*-tests results (as described above), were transformed to character states of 0, 1, and 2; representing negative allometry, isometry, and positive allometry, respectively. Positive or negative allometric trends identified as marginally significant (i.e. $0.05 > p > 0.01$) were coded as either 2 or 0, respectively. The distribution of character states upon the molecular and morphological phylogenies were compared with those on 100 randomly generated trees, using the Treefarm package of modules of Mesquite (Maddison and Maddison, 2009). The number of steps for each character on each of the randomly generated trees was compared with the number of steps for that character on the molecular phylogeny and the morphological phylogeny (Laurin, 2004). A character was considered to possess phylogenetic signal if it had fewer steps on either chosen phylogeny than in at least 95% of the randomly generated trees. A significant result indicates phylogenetic structure is present in relation to the chosen framework; because the null hypothesis is a total absence of phylogenetic signal, it is important to note that a close association cannot be inferred but rather that the importance of accounting for phylogeny when conducting analyses can be underlined.

Phylogenetic framework

The phylogenetic framework taken for the taxa studied herein (Fig. 6.3) is a composite based on the work of Seddon et al. ('97), Georges and Adams ('92), and the supermatrix analysis of Thomson and Shaffer (2010). Recent phylogenetic analyses involving pleurodires, both molecular and morphological, have been restricted in terms of the taxa studied (Shaffer et al., '97; Georges et al., '98; Fujita et al., 2004; Krenz et al., 2005), hence it was necessary to construct a composite reflecting the existing information for the taxa studied herein.

Study specimens

Specimens were measured and examined from the following institutions: AM: Australian Museum, Reptiles, Sydney; AMNH: American Museum of Natural History, New York; MACN: Museo Argentino de Ciencias Naturales Bernardino Rivadavia, Buenos Aires; MNKB: Museum für Naturkunde Berlin; MTKD: Museum für Tierkunde, Dresden; NMB: Naturhistorischesmuseum Basel; NMW: Naturhistorischesmuseum Wien; PCHP: Chelonian Research Institute, Oviedo, Florida (Peter C. H. Pritchard collection); SAM: South Australian Museum, Adelaide; SMF: Senkenberg Museum Frankfurt; ULP-FCN: Universidad de La Plata, Facultad de Ciencias Natu-

	Pelusios sp.		*P.expansa*		*E.novaguineae*		*E.macquarii*		*C.reimanni*		*C.longicollis*		*H.tectifera*		*P.platycephala*		*P.hilarii*		*C.fimbriatus*	
	LS	RMA	LS	RMA	LS	RMA	LS	RMA	LS	RMA	LS	RMA	LS	RMA	LS	RMA	LS	RMA	LS	RMA
1	=	=	+	+	=	=	=	=	-	-	-	-	-	-	-	-	=	=	+	+
2	=	=	+	+	(-)	(-)	=	=	(-)	(-)	=	=	-	-	=	=	=	=	(-)	(-)
3	=	=	=	=	+	+	+	+	+	+	=	(+)	=	(+)	=	=	+	+	(-)	(-)
4	-	-	-	-	-	-	-	-	-	-	-	-	-	-	=	=	-	-	-	-
5	=	=	(-)	(-)	(+)	(+)	=	=	=	=	+	+	(+)	(+)	=	=	=	=	+	+
6	(-)	(-)	=	=	-	-	=	=	=	=	=	=	=	(+)	=	=	(+)	(+)	+	+
7	=	=	=	=	=	=	=	=	=	=	=	=	(+)	(+)	(+)	(+)	(+)	(+)	+	+
8	(-)	(-)	-	(-)	-	-	=	=	(+)	(+)	=	=	(+)	(+)	(+)	(+)	-	-	(+)	(+)
9	(-)	(-)	(-)	(-)	=	=	-	-	=	(+)	=	=	=	=	+	+	(+)	+	+	+

Table 6.1: Growth trends for each species measured in this study. Regression modes: RMA – reduced major axis, LS – least squares. See Fig. 6.2 for description of the nine measurements.

rales; and ZSM: Zoologische Staatssammlung München.

RESULTS

Bivariate analyses

The correlation of the variables with a size proxy, the mean of characters 10 and 11, is evaluated using R^2 coefficient values. Across all species examined, R^2 values range from 0.726 to 0.999 with an average fit of 0.954, indicating a high correlation with size (S-Tables 6.1-6.10). All R^2 values exceed 0.832, with the exception of character 2 (greatest width of aperture narium externa) for *Hydromedusa tectifera* (0.726) (S-Table 6.5) and for *Platemys platycephala* (0.738) (S-Table 6.7). Across all species the characters exhibiting the highest correlations with size (0.985) are the minimum width of the pterygoid (character 6), and the width between the lateral margins of the right and left processus trochlearis pterygoidei (character 7).

Cranial height (character 1), greatest width of the aperture narium externa (character 2) and the greatest length of the orbit (character 4) exhibited the most strongly negative relationships with size, for eight out of nine studied species, with b_1 values ranging from 0.588 for *H. tectifera* (character 2; S-Table 6.5) to 0.891 for *Pelusios* sp. (character 4; S-Table 6.10). The outgroup taxon, *Podocnemis expansa*, in contrast to the other species examined herein, displays the most strongly negative relationship between size and least length across the dorsal surface of the otic chamber (0.808; character 8) and intersquamosal width (0.819; character 9) (S-Table 6.8). On the other hand, the strongest positively allometric relationships are associated with minimum interorbital width (character 3) and palatal width (character 5) for six out of ten species, with b_1 values ranging from a minimum of 1.250 for *Chelodina longicollis* (S-Table 6.1) to a maximum value of 1.668 for *Phrynops hilarii* (S-Table 6.4). The greatest width of the aperture narium externa exhibits the most variability in significant growth trend across the studied species (range of b_1 = 0.690), with *P. expansa* and *P. platycephala* both exhibiting a positive allometric trend for this character (1.148-1.278) while other species, such as *H. tectifera*, exhibit a negative allometric scaling with size. In contrast, the greatest length of the orbit (character 4) exhibits the least variability in significant growth trend patterns (b_1 range of 0.375), showing an overall negative allometric relationship to size.

There is not a single character measured here that exhibits the same growth trend for all species examined (Table 6.1). The most similar growth trends across all species studied are found for the greatest length of the orbit (character 4) with nine out of ten taxa exhibiting negative allometric growth for this meas-

urement, the exception being an isometric trend recorded for *P. platycephala* (Table 6.1). Additionally, six out of ten taxa share a positive growth trend for minimum interorbital width (character 3), with only *C. fimbriatus* exhibiting a negative allometry for this character.

Table 6.2: Results of multivariate allometry detailing allometric coefficients, bootstrap standard error (in parentheses), and corresponding growth trend (GT) considering an isometric vector of 0.3015 applicable to all variables (see Materials and Methods). Symbols indicate isometry ("="), positive allometry ("+"), and negative allometry ("-"). Marginally significant trends are denoted with parentheses.

Variable		*Pelusios* sp.	*P.expansa*	*E.novaguineae*	*C.longicollis*	*H.tectifera*	*P.hilarii*	*C.fimbriatus*
1		0.297 (0.0070)	0.336 (0.0080)	0.307 (0.0200)	0.213 (0.0124)	0.227 (0.0108)	0.308 (0.0214)	0.312 (0.0049)
	GT	=	+	=	-	-	=	+
2		0.306 (0.0048)	0.334 (0.0083)	0.265 (0.0200)	0.293 (0.0111)	0.219 (0.0101)	0.260 (0.0212)	0.263 (0.0045)
	GT	=	+	-	=	-	-	-
3		0.298 (0.0070)	0.346 (0.0078)	0.391 (0.0165)	0.357 (0.0210)	0.357 (0.0122)	0.459 (0.0200)	0.269 (0.0058)
	GT	=	+	+	+	+	+	-
4		0.257 (0.0143)	0.256 (0.0080)	0.215 (0.0160)	0.225 (0.0091)	0.218 (0.0134)	0.204 (0.0200)	0.235 (0.0058)
	GT	-	-	-	-	-	-	-
5		0.293 (0.0150)	0.264 (0.0082)	0.350 (0.0178)	0.369 (0.0090)	0.342 (0.0139)	0.309 (0.0251)	0.358 (0.0060)
	GT	=	-	+	+	+	=	+
6		0.286 (0.0098)	0.298 (0.0083)	0.278 (0.0178)	0.297 (0.0100)	0.342 (0.0136)	0.327 (0.0250)	0.329 (0.0053)
	GT	(-)	=	(-)	=	+	+	+
7		0.299 (0.0192)	0.334 (0.0082)	0.292 (0.0165)	0.311 (0.0111)	0.361 (0.0132)	0.332 (0.0245)	0.329 (0.0053)
	GT	=	+	=	=	+	(+)	+
8		0.264 (0.0354)	0.287 (0.0083)	0.262 (0.0165)	0.309 (0.0113)	0.304 (0.0114)	0.219 (0.0255)	0.302 (0.0052)
	GT	(-)	-	-	=	=	-	=
9		0.290 (0.0090)	0.284 (0.0083)	0.309 (0.0164)	0.305 (0.0121)	0.303 (0.0116)	0.318 (0.0253)	0.316 (0.0053)
	GT	(-)	-	=	=	=	=	+
10		0.303 (0.0210)	0.299 (0.0082)	0.297 (0.0176)	0.300 (0.0156)	0.302 (0.0139)	0.305 (0.0255)	0.300 (0.0053)
	GT	=	=	=	=	=	=	=
11		0.299 (0.0091)	0.305 (0.0081)	0.305 (0.0181)	0.302 (0.0112)	0.308 (0.0114)	0.302 (0.0221)	0.306 (0.0051)
	GT	=	=	=	=	=	=	=

Species with the most similar growth trends are *C. longicollis* and *E. macquarii*, which exhibit analogous relationships for seven out of nine characters (Fig. 6.3, Table 6.1). Additionally, *H. tectifera* and *C. fimbriatus* share the same relationship for six out of nine characters; particularly these long-necked South American turtles share positive allometric trends for characters 5 to 8. In contrast, species that share the fewest growth trends are *C. fimbriatus* and *E. macquarii*, and also *C. fimbriatus* and outgroup taxon *Pelusios* sp. In both instances only a negative growth relationship for greatest length of the orbit (character 4) is shared between the species, and this is the character for which growth trends are most conserved across all taxa studied here. Australasian taxa have the same growth trends for three out of nine characters whilst taxa that inhabit South America do not all exhibit the same growth trend for any character measured here.

In terms of growth trends for specific characters, there are no clear differences that serve to characterise the two geographically distinct groups or the two morphologically distinct groups, with one exception: the width between the lateral margins of the right and left processus trochlearis pterygoidei grows isometrically in relation to body size among Australasian taxa, whilst this character exhibits positive allometry for all South American taxa, excluding outgroup species *P. expansa* and *Pelusios* sp. (Table 6.1).

Across all species, the two regression techniques produced identical growth trends for the majority of variables (Table 6.1), providing additional support to conclusions about cranial allometry trends for the species under study. Differing growth trends were reported in two cases for *H. tectifera* (characters 3 and 6), and in one case each for *C. longicollis* (character 3), *P. expansa* (character 8), and *C. reimanni* (character 9) making a total of five from a possible 81 comparisons (6.2%). Four out of these five cases involved a marginally significant positive growth trend for RMA (denoted "(+)") whilst LS indicated an isometric relationship between the variable in question and size (denoted "=") (see Table 6.1). In the case of *P. expansa*, a significant negative allometric trend under LS regression is found to be marginally significant with RMA methods. These results are to be expected since RMA slopes are always equal or higher than LS slopes (RMA = LS/r where $r \leq 1$, see Materials and Methods).

Multivariate analyses

Overall, growth trends detected with the multivariate analyses are in agreement with those reported using bivariate methods (Table 6.2). Six growth trends differed between the two methods with three marginally significant allometric trends under bivariate methods

Character No.	% of random trees	
	Morphological phylogeny	Molecular phylogeny
1	64	**99**
2	**98**	83
3	72	**98**
4*	-	-
5	77	77
6	93	93
7	**99**	**99**
8	81	**99**
9	**100**	**100**

Table 6.3: Percent (%) of random trees with a greater number of steps for a given character than on either the morphological or molecular phylogenies: see Materials and Methods for detail. Both chosen trees, and all random trees had 1 step for character 4 - marked with an asterisk (*). Characters with values > 95% are considered to possess phylogenetic signal (Laurin, 2004), and are denoted by bold type.

being reported as isometric under multivariate analyses, and conversely three trends reported to be isometric with bivariate analyses were found to be either positively (two cases) or negatively (one case) allometric when analysed using multivariate methods. Multivariate allometry methods are normally preferred over bivariate analyses because in the former, size is considered a latent variable that affects all measurements simultaneously. Nonetheless, the usefulness of bivariate methods is underlined because the coefficients produced are more directly interpretable in the context of size-dependent functional relationships (Jungers and German, '81), and these methods are less sensitive to incomplete matrices. Here, for a size proxy we used a mean of two characters to improve the stability of bivariate analyses: the allometric coefficients produced from PCA for both characters chosen (10 and 11) were found to be the closest to the isometric vector (0.3015) for each of the six species upon which multivariate analyses were conducted hence providing further confidence that these were the best possible measurements to use as a proxy for body size in the bivariate analyses (Table 6.2).

Test for phylogenetic signal

Of the nine characters used for bivariate analyses, five possessed a significant phylogenetic signal on the molecular phylogeny whilst a phylogenetic signal was detected for three characters when using the morphological phylogeny as a chosen comparative (Table 6.3). The greatest length of the orbit (character 4) had an invariant number of steps on all random trees and both chosen phylogenies, and

hence was deemed to be phylogenetically uninformative. Characters 5, 6, 7, and 9 yielded, on the molecular and morphological phylogenies, overall identical numbers of random topologies with greater numbers of steps (Table 6.3). Discrepancies between the two chosen topologies were found for characters 1-3, and 8. Differences were most marked for character 1, with 64% of the random trees having a greater number of steps than the morphological phylogeny, compared to 99% for the molecular phylogeny (Table 6.3).

DISCUSSION

Growth trends among the chelid taxa studied here are variable, suggesting considerable modifications to scaling relationships have occurred during chelid evolution. Shared growth relationships beteween *H. tectifera* and *C. fimbriatus* provide support for the hypothesis that promotes an independent origin of the long neck in chelids. Whilst mapping of growth trends reveals the ontogenetic data herein favour the molecular hypothesis by a single character and hence do not yield unequivocal support for either competing hypothesis, the role of these data in further elucidating patterns during turtle evolution should not be discounted. Wide-scale comparisons of growth data represent a potentially rich record of information that has barely been mined for turtles, particularly in relation to further understanding the plasticity of allometries, their propensity to exact evolutionary change and the polarity of such change.

None of the species studied here have the same growth pattern for all measurements examined. We find the growth trends for only one character differ between the Australasian species on the one hand, and the South American taxa on the other, attesting the geographical relationships depicted in the molecular typology (Fig. 6.3). The width between the lateral margins of the right and left processus trochlearis pterygoidei (character 7; Fig. 6.2) scales isometrically with body size amongst the Australasian taxa, and, in contrast, exhibits a positively allometric trend amongst all South American taxa measured herein. The processus trochlearis pterygoidei is a unique feature of pleurodire turtles. The function of the trochlea in turtles is to alter the line of action of the main adductor tendon, and it varies in position between pleurodires and cryptodires. Instead of being on the pterygoid as in pleurodires, the trochlea is located on the otic chamber in cryptodires. The size and orientation of the processus trochlearis pterygoidei has been recognized to be variable among pleurodire species (Gaffney, '79). The extreme opposites of the spectrum of morphological variability present in this structure are cited to be represented by *Podocnemis* and *Chelus*. *Podocnemis* displays a large and laterally directed processus whilst in

Chelus it is reduced, and directed posteriorly (Gaffney, '79). These differences have been proposed to be related to the relative stress borne by the pterygoid during feeding (Bramble, '71). In the latter work, a correlation was detected between the degree of lateral pro-

Figure 6.3: Competing phylogenetic hypotheses of the interrelationships of South American and Australasian Chelidae. Long and short bars represent long- and short-necked species. Growth relationships for each character (Fig. 6.2) are based on bivariate analyses, indicating positive ("+"), negative ("-") and isometric ("=") relationships with size. Parentheses denote marginal positive or negative allometric growths (i.e. $0.05 > p > 0.01$). Phylogenetic hypothesis based on molecular data, adapted from the single most parsimonious tree based on mitochondrial 12S rRNA sequence data presented by Seddon et al. (1997, Fig. 2), and the phylogeny of Thomson and Shaffer (2010, Fig. 5).

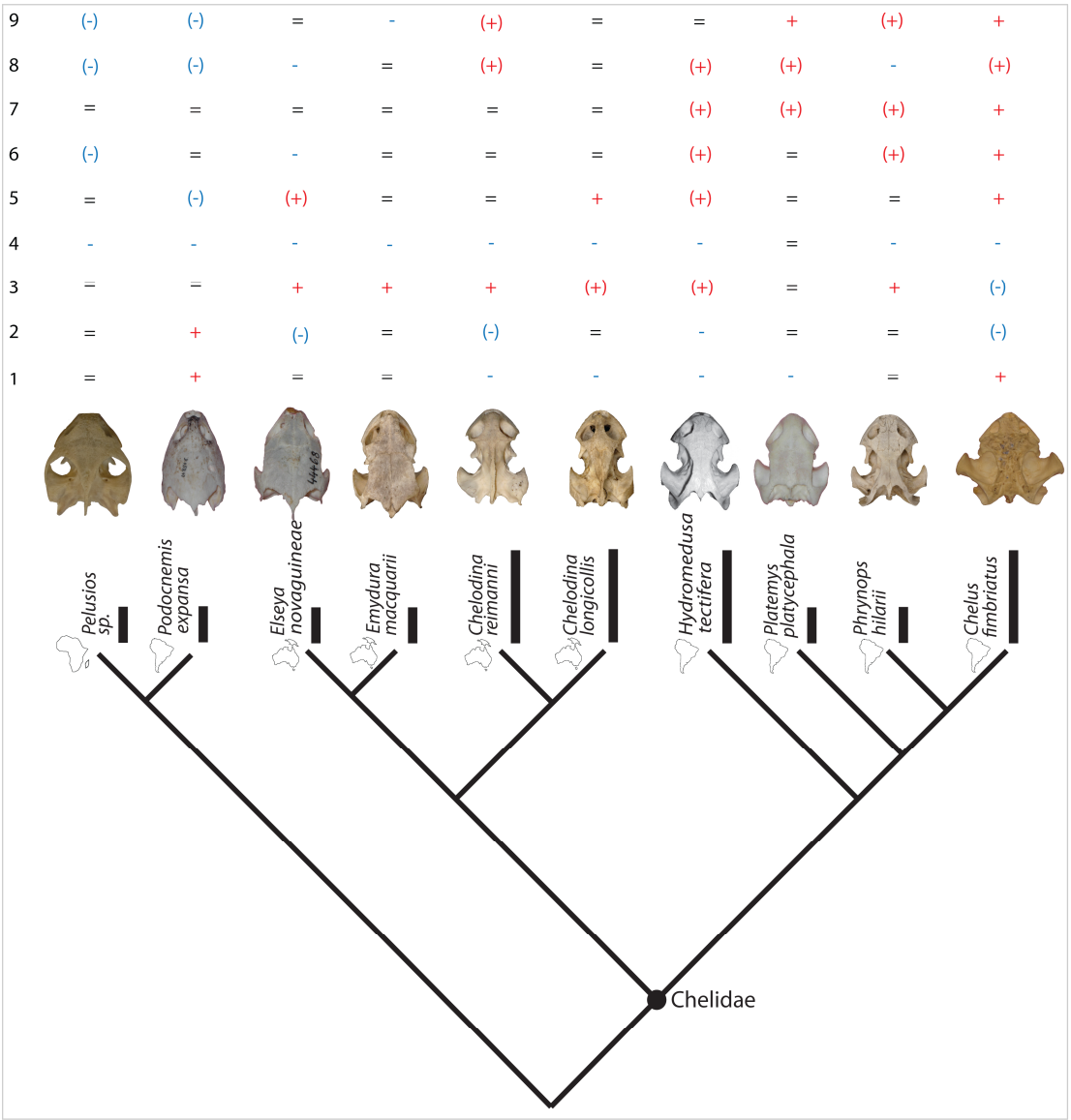

jection of the processus and extent of buttressing for the pterygoid, provided by the joining of the basisphenoid and quadrate (Bramble, '71). Hence the broad contact between the basisphenoid and quadrate in *Podocnemis* is thought to provide additional surface area to support the pterygoid, which is subject to comparatively high levels of stress, associated with the mainly herbivorous diet of these turtles (Ojasti, '71). Whilst, in contrast, the highly carnivorous diet of *Chelus*, consisting of materials more tractable to processing by the masticatory apparatus, is considered to confer less stress onto the pterygoid and thus in these turtles the processus projects posteriorly and the quadrate-basisphenoid articulation is reduced (Bramble, '71; Gaffney, '77, '79). Although the diets of *Chelus* and *Podocnemis* differ sharply, this is not the case among the other species examined herein, and even though feeding habits of many of these turtles are not well documented or systematically investigated, most members from the molecularly identified South American and Australasian clades are assumed to feed upon fish, invertebrates and in some instances molluscs (e.g. *Phrynops hilarii*) (see Ernst and Barbour, '92, and references therein), hence the contrasting growth trends between these two groups cannot simply be related to dietary preference, and its purported role in quadrate-basisphenoid and pterygoid morphology.

Comparative growth allometry data for turtles are scarce. Nonetheless, our findings correspond partly with the most comprehensive studies published to date, namely, those on cryptodire species *Pseudomys texana* (Bever, 2008) and *Apalone ferox* (Dalrymple, '77). Similar to Bever (2008), we find that the cranial measurements for the species examined here exhibit a high correlation with size: 80% of cranial characters measured by Bever (2008) displayed R^2 values of greater than 0.90, while across the nine species we examined this value was minimally 78%. Hence for the pleurodire species studied here, a large amount of the variation in postnatal growth can be explained by size and not shape changes and thus juvenile form is retained in adulthood, though the prevalence of positive and negative scaling across taxa (Table 6.1) means the retention of juvenile shape should be interpreted as partial. In comparison, Dalrymple ('97) reported considerably more shape change during ontogeny in trionychid species *A. ferox*, with the growth of less than 40% of characters being highly correlated with size.

Bever (2008) found that overall the skull of *P. texana* scaled negatively with size, though here, similar to Dalrymple ('77), we report a much greater variability in growth trends across measured characters than did Bever (2008). Characters 1 and 4 exhibit the most

number of negative trends across all pleurodire taxa (Table 6.1), and thus are most comparable with growth relationships reported for *P. texana*. In particular, orbit length (character 4) grows with a negative allometry for nine out of ten examined species, a relationship further found for *A. ferox* (Dalrymple, '77), and a feature consistent with the plesiomorphic vertebrate growth pattern. Only *P. expansa* shares a relative widening of the aperture narium with *A. ferox*, while *C. fimbriatus*, *P. hillari* and *H. tectifera* share a widening of the pterygoid waist with this cryptodire taxon (Dalrymple, '77). The complex and variable patterns of growth trends in *A. ferox* are interpreted by Dalrymple ('77) to be indicative of a trophic apparatus that is loosely integrated and highly plastic, with the corresponding capacity to respond to the homeostatic needs of individuals. Previously, in relation to feeding, the extremely flattened skull of *C. fimbriatus* has been compared with that of several trionychids, and its streamlined shape has been suggested to be adaptive to ambush predation (Legler, '81, '89). Nevertheless, direct interpretations of plasticity in cranial morphology among turtles are difficult in light of the highly derived nature of the Trionychidae (Delfino et al., 2010), and also the highly variable growth patterns reported here for pleurodire taxa.

In their broad-scale study of morphological variation in adult testudinoidae skulls, Claude et al. (2004) showed a relationship between skull shape and lifestyle, proposing that morphotype was closely correlated with ecological factors, irrespective of phylogenetic relationships. While several studies have indicated that lifestyle (aquatic vs. terrestrial) plays a fundamental role in adopted feeding habits (e.g. Bels et al., '97; Summers et al., '98; Lemell et al., 2000), it has also been shown that phylogenetic constraint may preclude the occurrence of certain feeding modes in given lineages and thus act to shape cranial evolution (Collin and Janis, '97). The role of shared morphological features in relation to feeding habits is a point of contention for the taxa examined in this study. Particularly, Pritchard ('84) has proposed the morphological topology presented by Gaffney ('77) that indicates a close relationship between *Hydromedusa* and *Chelodina*, to be incorrect. Aspects of the similarity in skull shape between the two genera include a marked cranial flattening, narrowing and elongation, and anterior placement of the eyes. These features, Pritchard ('84) suggested, reflect simply a sharing of characters common among piscivorous turtles that spear-fish. Accordingly, Pritchard ('84) hypothesized the independent acquisition of exceptionally long necks and attenuated strike and suction mode of feeding during chelid evolution.

Our growth data appear to concur in part with the functional interpretations of

Pritchard ('84), who proposed that *Hydromedusa* is actually more closely related to *Chelus* than to *Chelodina*. We find *H. tectifera* and *C. fimbriatus* share six out of nine growth trends for the measurements examined here, and notably a positive allometric relationship for characters 5-8, largely reflecting a relative widening of the skull and lengthening of the otic chamber (see Fig. 6.2). The growth trends for the two species of *Chelodina* we measured differ from one another, though both share fewer growth trends with *H. tectifera*, and neither share the positive allometries mentioned above for characters 5-8. Indeed, characters 6 and 7 grow isometrically for both species of *Chelodina* while these exhibit a positive allometric scaling for *C. fimbriatus* and *H. tectifera*. The relative widening of the skull, displayed particularly by the South American taxa studied (Fig. 6.3; characters 5-7), has recently been associated with the emergence of piscivory among turtles (Herrel et al., 2002). Several authors have proposed that the flattened skull shape of piscivorous turtles is an adaptation to reduce hydrodynamic drag, allowing these species to extend the head-neck system at high speeds (e.g. Van Damme and Aerts, '97; Lemell et al., 2002). However, Herrel et al. (2002) suggested there is no a priori reason for this to be the case and the results of their broad-scale study of bite performance, which included several of the species examined herein, instead promote an increase in the frontal area of the head to be pivotal for successful feeding on fast, elusive prey.

Giannini and colleagues (e.g., Giannini et al., 2004) have presented a series of papers which provide data on the allometric relations among parts of the marsupial skull. In their comparisons of different marsupial species, some patterns supporting some monophyletic clades are apparent, although much more extended sampling is needed. Our findings similarly indicate that the evolution of several allometrically influenced characters can be significantly associated with phylogenetic relationships. Indeed, the importance of considering allometry when conducting phylogenetic analyses has recently been underlined by Gilbert et al. (2009). These authors showed that when correcting for allometry it was possible to find congruence between previously conflicting morphological and molecular hypotheses for papionin (Primates) interrelationships, demonstrating that the effects of allometry are largely responsible for the appearance of homoplasy in the cranium of primates belonging to this group (Gilbert and Rossie, 2007; Gilbert et al., 2009). At present, the study of cranial growth in turtles remains in its infancy, a situation which, given the growing fossil record of chelids (Fuente et al., 2001; Bona and Fuente, 2005) that makes any morphological study of recent forms more desirable as way of comparison, requires resolution through active ef-

forts to expand comparative ontogenetic approaches, such as those presented herein.

ACKNOWLEDGEMENTS

We are indebted to curators for access to, and help with, specimens: Robert Pascocello (AMNH), Mark Hutchison (SAM), Ross Sadlier (AM), Fredy Carlini, Diego Verzi and Leandro Alcalde (ULP-FCN), Daiana Ferraro and Julian Faviovich (MACN), Frank Tiedemann (NMW), Uwe Fritz (MTKD-Senckenberg), Peter C. H. Pritchard and Sybille Pritchard (CRI. Oviedo), Mark-Oliver Rödel (MNKB), Michael Franzen (ZSM), Loïc Costeur (NMB), Linda Acker (SMF). For help with photographs we thank Christian Mitgutsch and Torsten Scheyer (Zürich). We thank an anonymous reviewer for insightful comments to an earlier version of this paper and for constructive discussion we thank Ingmar Werneburg (Zürich) and Michel Laurin (Paris). M.R.S.-V. thanks Peter and Sybille Pritchard for hospitality. This work received support from the Swiss National Fond (3100A0-116013) to M.R.S.-V., and a Forschungskredit (nr. 3771) from the Universität Zürich to L.A.B.W.

REFERENCES

Bels VL, Davenport J, Delheusy V. 1997. Kine matic analysis of the feeding behaviour in the turtle *Terrapene carolina* (L.), (Reptilia: Emydidae). J Exp Zool 277: 198-212.

Bever GS. 2008. Comparative growth in the postnatal skull of the extant North American turtle *Pseudemys texana* (Testudinoidea: Emydidae). Acta Zool (Stockh) 89(2): 107-131.

Bickham JW, Iverson JB, Parham JF, Philippen HD, Rhodin AGJ, Shaffer BS, Spinks PQ, Van Dijk PP. 2007. An annotated list of modern turtle terminal taxa with comments on areas of taxonomic instability and recent change. Chelonian Conservation and Biology Research Monographs 4: 173-199.

Bona P, de la Fuente MS. 2005. Phylogenetic and paleobiogeographic implications of *Yaminuechelys maior* (Staesche, 1929) new comb., a large long-necked chelid turtle from the early Paleocene of Patagonia, Argentina. J Vertebr Paleontol 25(3): 569-582.

Bramble DM. 1971. Functional morphology, evolution, and paleontology of gopher tortoises. Ph.D. Thesis. University of California, Berkeley, 341 pp.

Caumull R, Polly PD. 2005. Phylogenetic and environmental components of morphological variation: skull, mandible, and molar shape in marmots (Marmota, Rodentia). Evolution 59(1): 2460-2472.

Claude J, Pritchard PCH, Tong HY, Paradis E, Auffray JC. 2004. Ecological correlates

and evolutionary divergence in the skull of turtles: a geometric morphometric assessment. Syst Biol 53(6): 933-948.

Collin R, Janis CM. 1997. Morphological constraints on tetrapod feeding mechanisms: Why were there no suspension-feeding marine reptiles? In: Callaway JM, Nicholls EL, editors. Ancient Marine Reptiles. San Diego, California: Academic Press. p 451-465

Dalrymple GH. 1977. Intraspecific variation in the cranial feeding mechanism of turtles of the genus *Trionyx* (Reptilia, Testudines, Trionychidae). J Herp 11: 255-285.

de Broin F. 1987. The late Cretaceous fauna of Los Alamitos, Patagonia, Argentina. Part IV. Chelonia. Revista del Museo Argentino de Ciencias Naturales, Bernardino Rivadavia, Paleontologia 3(3): 131-139.

de Broin F, Fuente M. 1993. Les tortees fossiles d'Argentine: Synthèse. Annales de Paleontologie 79: 169- 232.

Delfino M, Sánchez-Villagra MR. 2010. A survey of the rock record of reptilian ontogeny. In: Sánchez-Villagra MR, editor. Developmental Vertebrate Palaeontology. Sem Cell Dev Biol 21(4) 432-440.

Delfino M, Scheyer TM, Fritz U, Sánchez-Villagra MR. 2010. An integrative approach to examining a homology question: shell structures in soft-shell turtles. Biol J Linn Soc 99: 462-476.

Efron B, Tibshirani RJ. 1993. An introduction to the bootstrap. New York: Chapman & Hall.

Ernst CH, Barbour RW. 1992. Turtles of the world. Washington: Smithsonian Institution Press.

Fritz U, Havaš P. 2007. Checklist of chelonians of the world. Vertebrate Zoology 57(2): 149-368.

Fuente M de la, Lapparent de Broin F de, Manera de Bianco T. 2001. The oldest and first nearly complete skeleton of a chelid, of the Hydromedusa sub-group (Chelidae, Pleurodira), from the Upper Cretaceous of Patagonia. Bulletin de la Societe Geologique de France 172(2): 237-244. doi: 10.2113/172.2.237.

Fujita MK, Engstrom TN, Starkey DE, Shaffer BS. 2004. Turtle phylogeny: insights from a novel nuclear intron. Mol Phyl Evol 31: 1031-1040.

Gaffney ES. 1977. The side-necked turtle family Chelidae: A theory of relationships using shared derived characters. Am Mus Novit 2620: 1-28.

Gaffney ES. 1979. Comparative cranial morphology of recent and fossil turtles. Bull Am Mus Nat Hist 164 (2): 65-376.

Gaffney ES, Archer M, White A. 1989. Chelid turtles from the Miocene freshwater limestones of Riversleigh Station, North

western Queensland, Australia. Am Mus Novit 2959: 1-10.

Gaffney ES, Eugene S, Tong H, Meylan PA. 2006. Evolution of the side-necked turtles: the families Bothremydidae, Euraxemydidae, and Araripemydidae. Bull Am Mus Nat Hist 300: 1-698.

Georges A, Adams M. 1992. A phylogeny for Australian chelid turtles based on allozyme electrophoresis. Aust J Zool 40 (5): 453-476.

Georges A, Birrell J, Saint KM, McCord W, Donnellan SC. 1998. A phylogeny for side necked turtles (Chelodina: Pleurodira) based on mitochondrial and nuclear gene sequence variation. Biol J Linn Soc 67: 213-246.

Giannini NP, Flores DA, Abdala F. 2004. Coparative postnatal ontogeny of the skull in *Dromiciops gliroides* (Marsupialia: Microbiotheriidae). Am. Mus. Novit 3460:1-17.

Gilbert CG, Frost SR, Strait DS. 2009. Allometry, sexual dimorphism, and phylogeny: A cladistic analysis of extant African papionins using craniodental data. J Hum Evol 57: 298-320

Gilbert CG, Rossie JB. 2007. Congruence of molecules and morphology using a narrow allometric approach. Proc Natl Acad Sci USA 104(29): 11910-11914.

Harvey PH, Pagel MD. 1991. The comparative method in evolutionary biology. Oxford: Oxford University Press.

Herrel A, O'Reilly JC, Richmond AM. 2002. Evolution of bite performance in turtles. J Evol Biol 15: 1083-1094.

Huxley JS. 1932. Problems of relative growth. London: John Hopkins Univ. Press.

Jolicoeur P. 1963. The multivariate generalization of the allometry equation. Biometrics 19: 497-499.

Jungers WL, German R. 1981. Ontogenetic and interspecific skeletal allometry in nonhuman primates: Bivariate vs. multivariate analysis. Am J Phys Anthropol 55: 195-202.

Klingenberg CP, Gidaszewski NA. 2010. Testing and quantifying phylogenetic signals and homoplasy in morphometric data. Syst Biol 49(3): 245-261.

Krenz JG, Naylor GJP, Shaffer BS, Janzen FJ. 2005. Molecular phylogenetics and evolution of turtles. Mol Phyl Evol 37: 178-191.

Kuratani S. 1987. The development of the orbital region of *Caretta caretta* (Chelonia, Reptilia). J Anat 154: 187-200.

Laurin M. 2004. The evolution of body size, Cope's rule and the origin of amniotes. Syst Biol 53(4): 594-622.

Legler JM. 1989. Diet and head size in Australian chelid turtles, genus *Emydura.* Annales de la Société royale Zoologique de

Belgique 119: 10.

Legler JM. 1981. The taxonomy, distribution and ecology of Australian turtles (Testudines: Pleurodira: Chelidae). National Geographic Society Research Re ports 13: 391-404

Lemell P, Beisser CJ, Weisgram J. 2000. Morphology and function of the feeding apparatus of *Pelusios castaneus* (Chelonia; Pleurodira). J Morphol 244: 127-135.

Lemell P, Lemell C, Snelderwaard P, Gumpenberger M, Wöcheslander R, Weisgram J. 2002. Feeding patterns of *Chelus fimbriatus* (Pleurodira: Chelidae). J Exp Zool 205: 1495-1506.

Maddison WP, Maddison DR. 2009. Mesquite: a modular system for evolutionary analysis. Version 2.72 http://mes quiteproject.org

Ojasti J. 1971. La tortuga arrau del Orinoco. Defensa de la Naturaleza 1(2): 3-10.

Pritchard PCH. 1984. Piscivory in turtles, and evolution of the long-necked Chelidae. Symp Zool Soc Lond 52: 87-110.

Reeve ECR, Huxley JS. 1945. Some problems in the study of allometric growth. In: le Gros Clark WE, Medawar PB, editors. Essays on growth and form. Oxford: Claredon Press. p 121-156.

Rieppel O. 1993. Studies on skeleton formation in reptiles. Patterns of ossification in the skeleton of *Chelydra serpentina* (Reptilia: Chamaeoleoninae). J Zool (Lond) 231: 487-509.

Sánchez-Villagra MR, Müller H, Sheil CA, Scheyer TM, Nagashima H, Kuratani S. 2009. Skeletal Development in the Chinese soft-shelled turtle Pelodiscus sinensis (Reptilia: Testudines: Trionychidae). J Morphol 270: 1381–1399.

Scheyer TM. 2009. Conserved bone mircro structure in the shells of long-necked and short-necked chelid turtles (Testudinata, Pleurodira). Fossil Record. 12(1): 47-57.

Seddon JM, Georges A, Baverstock PR, McCord W. 1997. Phylogenetic relation ships of chelid turtles (Pleurodira: Chelidae) based on mitochondrial 12S rRNA gene sequence variation. Mol Phyl Evol 7(1): 55-61.

Shaffer HB, Meylan P, McKnight ML. 1997. Tests of turtle phylogeny: molecular, morphological, and paleontological approaches. Syst Biol 46: 234-268.

Sheil CA. 2003. Osteology and skeletal development of *Apalone spinifera* (Reptilia: Testudines: Trionychidae). J Morphol 256: 42-78.

Sheil CA. 2005. Skeletal development of *Macrochelys temminckii* (Reptilia: Testudines: Chelydridae). J Morphol 263: 71-106.

Summers AP, Darouian KF, Richmond AM, Brainerd EL. 1998. Kinematics of aquatic

and terrestrial prey capture in *Terrapene carolina*, with implications for the evolution of feeding in cryptodire turtles. J Exp Zool 281: 280-287.

Thomson RC, Shaffer HB. 2010. Sparse super matrices for phylogenetic inference: taxonomy, alignment, rogue taxa, and the phylogeny of living turtles. Syst Biol 59 (1): 42-58.

Van Damme J, Aerts P. 1997. Kinematics and functional morphology of aquatic feeding in Australian snake- necked turtles. J Morphol 233: 113-125.

Werneburg I, Hugi J, Müller J, Sánchez-Villagra MR. 2009. Embryogenesis and ossification of *Emydura subglobosa* (Testudines, Pleurodira, Chelidae) and the Grundmuster of turtle development. Dev Dyn 238: 2770-2786.

Weston EM. 2003. Evolution of ontogeny in the hippopotamus skull: using allometry to dissect developmental change. Biol J Linn Soc 80: 625-638.

Wilson LAB, Sánchez-Villagra MR. 2010. Diversity trends and their ontogenetic basis: an exploration of allometric disparity in rodents. Proc Roy Soc B 277: 1227-1234.

Wolpoff MH. 1985. Tooth size-body scaling in a human population. Theory and practice of an allometric analysis. In: Jungers WL, editor. Size and scaling in primate biology. New York: Plenum Press. p 273-318.

SUPPLEMENTARY MATERIAL

S-Tables 6.1 - 6.10

S-Table 6.1: Results of bivariate allometry analyses. R^2 - adjusted coefficient of determination, b_1 - coefficient of allometry, p^{iso} - P value for null hypothesis of isometry (coefficient of allometry = 1), "=" - isometry, "+" - positive allometry, "-" - negative allometry, SE - standard error for b_1, GT – growth trend. Marginal positive or negative allometric growth trend denoted with parentheses for $0.05 > p > 0.01$. Refer to Fig. 6.2, Material and Methods for further detail.

Chelodina longicollis	R^2	Reduced major axis				Least squares			
Character		b_1	SE	p^{iso}	GT	b_1	SE	p^{iso}	GT
1	0.985	0.718	0.028	<0.001	-	0.712	0.028	<0.001	-
2	0.998	0.991	0.037	0.806	=	0.985	0.037	0.685	=
3	0.930	1.237	0.103	0.044	(+)	1.193	0.103	0.091	=
4	0.982	0.758	0.032	<0.001	-	0.751	0.032	<0.001	-
5	0.972	1.250	0.066	0.003	+	1.232	0.066	0.005	+
6	0.985	1.019	0.039	0.637	=	1.012	0.040	0.776	=
7	0.990	1.046	0.032	0.186	=	1.041	0.032	0.235	=
8	0.988	1.043	0.036	0.265	=	1.037	0.036	0.339	=
9	0.992	1.026	0.029	0.381	=	1.022	0.288	0.455	=

S-Table 6.2

Elseya novaguineae	R^2	Reduced major axis				Least squares			
Character		b_1	SE	p^{iso}	GT	b_1	SE	p^{iso}	GT
1	0.990	0.975	0.030	0.425	=	0.970	0.030	0.347	=
2	0.950	0.849	0.060	0.031	(-)	0.828	0.599	0.017	(-)
3	0.985	1.240	0.049	<0.001	+	1.231	0.049	<0.001	+
4	0.996	0.768	0.018	<0.001	-	0.767	0.018	<0.001	-
5	0.982	1.119	0.048	0.031	(+)	1.109	0.048	0.045	(+)
6	0.976	0.851	0.029	<0.001	-	0.847	0.029	<0.001	-
7	0.974	0.923	0.018	0.134	=	0.911	0.181	0.088	=
8	0.966	0.835	0.035	0.007	-	0.821	0.032	0.004	-
9	0.979	1.046	0.024	0.095	=	1.044	0.024	0.107	=

S-Table 6.3: Results of bivariate allometry analyses. R^2 - adjusted coefficient of determination, b_1 - coefficient of allometry, p^{iso} - P value for null hypothesis of isometry (coefficient of allometry = 1), "=" - isometry, "+" - positive allometry, "-" - negative allometry, SE - standard error for b_1, GT – growth trend. Marginal positive or negative allometric growth trend denoted with parentheses for $0.05 > p > 0.01$. Refer to Fig. 6.2, Material and Methods for further detail.

Emydura macquarii	R^2	Reduced major axis				Least squares			
Character		b_1	SE	p^{iso}	GT	b_1	SE	p^{iso}	GT
1	0.996	0.973	0.029	0.407	=	0.971	0.029	0.380	=
2	0.999	1.028	0.023	0.347	=	1.060	0.023	0.348	=
3	0.988	1.509	0.074	<0.001	+	1.500	0.074	<0.001	+
4	0.984	0.737	0.054	0.003	-	0.731	0.054	0.002	-
5	0.954	1.058	0.079	0.556	=	1.033	0.079	0.734	=
6	0.986	0.963	0.050	0.495	=	0.956	0.050	0.426	=
7	0.991	0.942	0.045	0.262	=	0.938	0.045	0.234	=
8	0.984	1.061	0.032	0.288	=	1.054	0.032	0.348	=
9	0.908	0.620	0.077	0.003	-	0.591	0.077	0.002	-

S-Table 6.4

Phrynops hilarii	R^2	Reduced major axis				Least squares			
Character		b_1	SE	p^{iso}	GT	b_1	SE	p^{iso}	GT
1	0.982	1.091	0.051	0.113	=	1.082	0.051	0.151	=
2	0.986	0.915	0.049	0.143	=	0.908	0.049	0.120	=
3	0.949	1.668	0.132	0.001	+	1.622	0.133	0.002	+
4	0.993	0.718	0.023	<0.001	-	0.716	0.023	<0.001	-
5	0.988	1.068	0.042	0.138	=	1.062	0.042	0.174	=
6	0.995	1.097	0.035	0.040	(+)	1.094	0.035	0.044	(+)
7	0.996	1.068	0.022	0.011	(+)	1.066	0.022	0.013	(+)
8	0.991	0.803	0.030	<0.001	-	0.800	0.030	<0.001	-
9	0.941	1.172	0.063	0.034	(+)	1.162	0.063	0.042	(+)

S-Table 6.5: Results of bivariate allometry analyses. R^2 - adjusted coefficient of determination, b_1 - coefficient of allometry, p^{iso} - P value for null hypothesis of isometry (coefficient of allometry = 1), "=" - isometry, "+" - positive allometry, "-" - negative allometry, SE - standard error for b_1, GT – growth trend. Marginal positive or negative allometric growth trend denoted with parentheses for $0.05 > p > 0.01$. Refer to Fig. 6.2, Material and Methods for further detail.

Hydromedusa tectifera	R^2	Reduced major axis				Least squares			
Character		b_1	SE	p^{iso}	GT	b_1	SE	p^{iso}	GT
1	0.867	0.706	0.086	0.008	-	0.658	0.086	0.003	-
2	0.726	0.588	0.109	0.005	-	0.502	0.108	0.002	-
3	0.942	1.206	0.092	0.040	(+)	1.170	0.092	0.095	=
4	0.970	0.744	0.039	<0.001	-	0.733	0.039	<0.001	-
5	0.956	1.310	0.103	0.020	(+)	1.281	0.103	0.030	(+)
6	0.951	1.199	0.084	0.039	(+)	1.169	0.084	0.072	=
7	0.953	1.202	0.079	0.027	(+)	1.172	0.079	0.050	(+)
8	0.993	1.108	0.388	0.032	(+)	1.104	0.039	0.037	(+)
9	0.966	1.101	0.083	0.268	=	0.966	0.083	0.359	=

S-Table 6.6

Chelus fimbriatus	R^2	Reduced major axis				Least squares			
Character		b_1	SE	p^{iso}	GT	b_1	SE	p^{iso}	GT
1	0.988	1.103	0.029	0.002	+	1.096	0.029	0.003	+
2	0.935	0.888	0.050	0.039	(-)	0.858	0.051	0.011	(-)
3	0.969	0.918	0.034	0.028	(-)	0.904	0.034	0.011	(-)
4	0.940	0.804	0.041	<0.001	-	0.780	0.041	<0.001	-
5	0.991	1.114	0.022	<0.001	+	1.109	0.022	<0.001	+
6	0.991	1.129	0.023	<0.001	+	1.107	0.022	<0.001	+
7	0.986	1.127	0.021	<0.001	+	1.119	0.021	<0.001	+
8	0.991	1.050	0.022	0.031	(+)	1.046	0.022	0.048	(+)
9	0.986	1.084	0.021	0.002	+	1.077	0.020	0.005	+

S-Table 6.7: Results of bivariate allometry analyses. R^2 - adjusted coefficient of determination, b_1 - coefficient of allometry, p^{iso} - P value for null hypothesis of isometry (coefficient of allometry = 1), "=" - isometry, "+" - positive allometry, "-" - negative allometry, SE - standard error for b_1, GT – growth trend. Marginal positive or negative allometric growth trend denoted with parentheses for $0.05 > p > 0.01$. Refer to Fig. 6.2, Material and Methods for further detail.

Platemys platycephala	R^2	Reduced major axis				Least squares			
Character		b_1	SE	p^{iso}	GT	b_1	SE	p^{iso}	GT
1	0.979	0.743	0.048	0.003	-	0.735	0.048	0.003	-
2	0.738	1.148	0.095	0.496	=	0.986	0.096	0.536	=
3	0.996	1.057	0.039	0.238	=	1.055	0.039	0.253	=
4	0.989	0.998	0.060	0.980	=	0.855	0.060	0.999	=
5	0.982	0.960	0.058	0.522	=	0.951	0.058	0.439	=
6	0.996	1.054	0.031	0.139	=	1.502	0.031	0.152	=
7	0.999	1.047	0.017	0.048	(+)	1.046	0.017	0.050	(+)
8	0.991	1.124	0.038	0.012	(+)	1.118	0.038	0.014	(+)
9	0.960	1.359	0.096	0.006	+	1.332	0.096	0.009	+

S-Table 6.8

Podocnemis expansa	R^2	Reduced major axis				Least squares			
Character		b_1	SE	p^{iso}	GT	b_1	SE	p^{iso}	GT
1	0.989	1.221	0.045	0.001	+	1.214	0.045	0.001	+
2	0.984	1.278	0.065	0.006	+	1.268	0.066	0.007	+
3	0.847	1.241	0.171	0.197	=	1.142	0.171	0.431	=
4	0.961	0.853	0.057	0.018	(-)	0.820	0.057	0.010	(-)
5	0.969	0.897	0.044	0.037	(-)	0.883	0.044	0.020	(-)
6	0.997	1.014	0.029	0.661	=	1.013	0.003	0.689	=
7	0.990	1.069	0.038	0.101	=	1.065	0.037	0.125	=
8	0.955	0.808	0.061	0.014	(-)	0.790	0.061	0.009	-
9	0.948	0.819	0.066	0.025	(-)	0.797	0.066	0.015	(-)

S-Table 6.9: Results of bivariate allometry analyses. R^2 - adjusted coefficient of determination, b_1 - coefficient of allometry, p^{iso} - P value for null hypothesis of isometry (coefficient of allometry = 1), "=" - isometry, "+" - positive allometry, "-" - negative allometry, SE - standard error for b_1, GT – growth trend. Marginal positive or negative allometric growth trend denoted with parentheses for $0.05 > p > 0.01$. Refer to Fig. 6.2, Material and Methods for further detail.

Chelodina reimanni	R^2	Reduced major axis				Least squares			
Character		b_1	SE	p^{iso}	GT	b_1	SE	p^{iso}	GT
1	0.980	0.787	0.042	0.001	-	0.779	0.042	0.001	-
2	0.969	0.860	0.058	0.045	(-)	0.846	0.058	0.032	(-)
3	0.981	1.508	0.078	0.001	+	1.494	0.078	0.001	+
4	0.904	0.663	0.084	0.007	-	0.630	0.084	0.005	-
5	0.979	0.967	0.053	0.549	=	0.957	0.053	0.439	=
6	0.832	1.452	0.059	0.170	=	1.291	0.059	0.313	=
7	0.971	1.122	0.078	0.170	=	1.105	0.078	0.226	=
8	0.976	1.272	0.087	0.027	(+)	1.257	0.087	0.032	(+)
9	0.987	1.109	0.048	0.043	(+)	1.101	0.048	0.073	=

S-Table 6.10

Pelusios sp.	R^2	Reduced major axis				Least squares			
Character		b_1	SE	p^{iso}	GT	b_1	SE	p^{iso}	GT
1	0.987	0.970	0.033	0.367	=	0.963	0.033	0.277	=
2	0.967	1.060	0.058	0.321	=	1.043	0.058	0.477	=
3	0.894	1.112	0.105	0.305	=	1.051	0.105	0.633	=
4	0.891	0.869	0.050	0.006	-	0.817	0.050	0.003	-
5	0.972	0.954	0.048	0.357	=	0.940	0.048	0.240	=
6	0.990	0.929	0.030	0.038	(-)	0.924	0.030	0.029	(-)
7	0.958	0.896	0.055	0.086	=	0.877	0.055	0.048	=
8	0.960	0.848	0.060	0.036	(-)	0.831	0.060	0.023	(-)
9	0.954	0.881	0.050	0.033	(-)	0.861	0.050	0.015	(-)

APPENDIX II

On the reliability of a geometric morphometric approach to sex determination: a blind test of six criteria of the juvenile ilium

APPENDIX II

On the reliability of a geometric morphometric approach to sex determination: a blind test of six criteria of the juvenile ilium

Article submitted to *Forensic Science International* on 13th Novemeber 2009, accepted 13th June 2010

Reference: **Wilson LAB**, Cardoso HFV, Humphrey LT. 2010. On the reliability of a geometric morphometric approach to sex determination: a blind test of six criteria of the juvenile ilium. *Forensic Sci. Int.* In press

Abstract

Despite the attention of many studies, researchers still struggle to identify criteria with which to sex juvenile remains at levels of accuracy and reproducibility comparable with those documented for adults. This study uses a sample of 82 juvenile ilia from an identified Portuguese population (Lisbon collection) to test the cross applicability of a new approach by Wilson et al. (2008) that uses geometric morphometric methods to sex the subadult ilium. Further, we evaluate the wider applicability of these methods for forensic casework, extending the age range of the original study by examining an additional 19 juvenile ilia from the St. Brides and Spitalfields collections, housed in London. Levels of accuracy for the Portuguese sample (62.2-89.0%) indicate that the methods can be used to document dimorphism in another sample. Discriminant functions are sample-specific, indicated by not better than average classification using cross validation. We propose a methodological update, whereby we recommend disuse of the auricular surface morphology criterion, based upon reduced success rates and inadequate accuracy of female identification. We show, in addition to population differences, differences in the ontogeny of dimorphism may lead to differing degrees of success for female identification using some criteria. The success rates are highest between the ages of 11.00 and 14.99 years (93.3% males, 80.0% females).

KEYWORDS**:** forensic science; sex determination; ilium; geometric morphometrics; ontogeny

INTRODUCTION

In the analysis of juvenile skeletal remains, one of the greatest problems is the difficulty in reliably identifying the sex of an individual [1]. If the sex of an individual is unknown, only an incomplete profile can be obtained during the identification process of a forensic case. Additionally, in bioarchaeological studies, the rich record of information that may be disclosed through sex specific studies profiling growth patterns, mortality and morbidity rates, and response to disease stress, cannot be revealed.

Consequently, to address this issue, much work has focused upon attempting to identify sexually diagnostic non-metric and metric traits in juvenile remains [2] (and references within). The investigation of pelvic indicators in subadults has an extensive history in the literature, with sexually distinctive features having been noted in fetal and neonatal pelvic bones [e.g. 3-8]. The greater sciatic notch region may provide a reliable basis for sex determination. Schutkowski [9-10] suggested that the greater sciatic notch was narrower and deeper for males than females, and identified morphological features that enabled individuals to be identified with a success of 71.4–95.0%. His methods, originally developed on an 18th–19th century population from London (Christ Church, Spitalfields), were later tested by Sutter [11] on a Chilean population of immature mummies and revealed a comparatively consistent result (79.0-80.7% success). Nonetheless, more recent tests on a different population have placed doubt upon the reliability of the criteria proposed by Schutkowski [9], suggesting that the general applicability of his methods is hampered by a lack of precision in the definition of features and the subjective nature of the scoring procedures [12-13].

Besides the subjectivity associated with morphological scoring, differences in the pattern and degree of sexual dimorphism between populations, resulting from population variation in shape, size and robustness and the influence of differences in lifestyle and living conditions, may act to confound the universal applicability of any technique. The poor success of many morphological methods when applied to a population other than the one used to originally develop the technique, serves to highlight this issue. For instance, Loth & Henneberg [14] used an African population (Dart Collection) to develop methods to sex juvenile remains using mandibular morphology, reporting an average accuracy of 81%. Subsequently Scheuer [15] tested this technique independently on a set of individuals from a London population, and reported a reduced accuracy of 64%. Similarly, Hunt [7] and Mittler and Sheridan [16] failed to replicate the accuracy levels reported by Weaver [6] (75-91%) when applying his methods, based on

differences in morphology of the sacro-iliac joint, to another sample.

In contrast to previous metric methods, eigenshape analysis is an outline-based technique for testing explicit shape based hypotheses [17-18] that, given recent advances in data acquisition and imaging methods, represents an important tool for the study of morphological variation. Eigenshape analysis is based upon the definition of additional points of reference, or so called semilandmarks [19] that are used to fill landmark-depleted regions, and in doing so enable the shape difference located in-between landmarks to be sampled, and the global aspect of a boundary outline to be evaluated. The ilium is suited to the use of semilandmarks because its curved nature precludes the identification of a sufficient number of biologically meaningful, homologous, landmark points, required to provide an accurate description of shape if a landmark-based approach were to be used (e.g. generalised procrustes analysis). Eigenshape methods may be applied to both open and closed outlines and thus are used herein rather than other outline methods such as Elliptical Fourier Analysis [20]. Outline-based approaches have been criticised because semilandmarks are not homologous to one another across outlines; that is, the point-to-point homology that characterises landmark-based approaches is absent [21]. This issue, though valid, is of limited concern unless biological variables are one-to-one mapped to individual points, and in most instances this is not the case, but rather the entire outline itself represents a biologically homologous or functionally meaningful form (e.g. [18, 22]). One solution is to slide semilandmarks along an outline until they reach correspondence with one another [19], thus removing tangential variation and enabling the resulting points to be treated with the methods commonly used for landmark approaches. We do not slide the semilandmarks in our analyses because the use of equidistant semilandmarks constrained by homologous points (e.g. greater sciatic notch outline constrained by landmarks A and C; [23]) effectively achieves the same result, and further avoids the necessity to consider between sliding algorithms, many of which yield disparate outcomes (see [24]).

The first application of eigenshape analysis to the problem of sex determination of juvenile remains by Wilson et al. [23] aimed to develop the methods described by Schutkowski [9] for sex determination of the juvenile ilia in a quantitative and objective manner. Six morphological criteria were evaluated, and these achieved an accuracy of 64.0-96.0% for subadaults aged between 6 months and 8 years. This high level of success indicates that the objective shape based methods yield a marked improvement over previous simple metric or categorical methods, and a more

visually intuitive approach compared to an earlier geometric morphometric study that used convex hulls to mathematically construct landmarks [8].

The shape based approach developed by Wilson et al. [23] using an 18th-19th century British population has not been tested on another population. The aims of this study are to test whether this technique can achieve a comparable level of successful identification when using another population. Further, to enable cross applicability to be evaluated, we extended the London sample originally presented by Wilson et al. [23] to include older individuals, and thus provide an expanded model sample to update understanding about the wider applicability, and thus practical use, of these methods to forensic cases. Since it is possible to extract biologically meaningful representations from any given point in eigenshape space, we use this platform to illustrate pelvic shape difference between populations. As a test subject, we use juveniles from a collection of identified Portuguese skeletons.

MATERIALS AND METHODS

Osteological samples

We examined 101 juvenile skeletons for this study. These comprised 82 individuals from the Lisbon osteological collection, curated at the National Museum of Natural History in Lisbon, Portugal; 11 individuals from the St. Brides crypt in London; and eight individuals belonging to the Christ Church Spitalfields collection, held at the Natural History Museum, London. The 19 juveniles from London collections were added to the data set of Wilson et al. [23] to provide an extension to the age range and enable direct comparison with the Lisbon sample (Table 7.1). The total sample from both populations comprised 126 individuals (see Table 7.1).

The St. Brides sample comprises individuals interred in the crypt of St Brides Church between 1740 and 1852, and excavated in the 1950s prior to rebuilding of the church [25]. Individual skeletons could be identified from an associated coffin plate, detailing the name, date of death, and age at death of the deceased. In total 227 individuals have been reliably identified, including 12 individuals aged less than 15 years, of which 11 were suitable for this study. The Lisbon osteological collection comprises individuals interred in temporary graves between the late 19th century and early 20th century in local cemeteries of the city of Lisbon [26]. The remains of these individuals were subsequently exhumed and re-interred in secondary burial niches, where they were abandoned by their relatives and eventually collected by the Museum in the 1980s and 1990s, under a special permit by the City Hall [26]. Detailed biographic informa-

tion, including name, date of death, and age at death was obtained from coffin plates and associated burial records. The collection contains approximately 1700 individuals, but only 742 are fully identified, including 82 individuals aged less than 15 years used in this study.

Quantification of inter– and intra-observer error

To quantify error inherent from landmark acquisition, we chose a single specimen and retook photographs once per day for three days. The collection of landmarks from each of these photographs, for each trait, was replicated three times over the space of a week, with at least 1.5 days between each collection period. In all cases, two observers performed the collection of landmark data separately, and the deviations between their measurements were used as quantification of inter-observer error.

Because all the criteria defined by Wilson et al. [23] are measured with outline data that are constrained by homologous landmark points, we assess the error in placing the homologous landmark points and also the error associated with the shape variables derived from the outline data. The latter point is necessary because the tertiary statistic methods used

Table 7.1: Age and sex distribution for London and Lisbon samples used in this study (N=126).

Age	Auricular surface and Greater sciatic notch				Curvature of the iliac crest			
	London		Lisbon		London		Lisbon	
	Male	Female	Male	Female	Male	Female	Male	Female
0 – 0.99	9	3	6	7	7	3	6	5
1.00 – 1.99	3	4	11	4	2	4	10	4
2.00 – 2.99	3	1	5	2	3	0	4	2
3.00 – 3.99	0	2	4	0	0	2	4	0
4.00 – 4.99	4	0	3	5	4	0	3	4
5.00 – 5.99	1	0	2	2	1	0	2	2
6.00 – 6.99	2	0	1	2	2	0	1	2
7.00 – 7.99	2	0	3	1	2	0	3	1
8.00 – 8.99	1	0	0	2	0	0	0	2
9.00 – 9.99	1	0	2	1	0	0	1	1
10.00 – 10.99	1	0	2	3	0	0	1	2
11.00 – 11.99	0	0	5	3	0	0	5	3
12.00 – 12.99	0	1	2	1	0	0	2	0
13.00 – 13.99	0	0	0	0	0	0	0	0
14.00 – 14.99	1	2	2	1	1	0	2	1
15.00 -	1	2	0	0	0	0	0	0
Total	29	15	48	34	22	9	44	29

herein are based upon shape variables, not individual landmarks, and more importantly the link between individual landmark repeatability and shape variable repeatability is typically obscure. We assess error associated with individual homologous landmarks by calculating residual landmark standard deviations (see [27]). The methodology of Arnqvist and Martensson [28] is used to assess the impact of error on shape variables: the outlines interpolated for the error repeats were added to the original data set and eigenshape analysis was used to obtain shape variables. The resultant variables were then subject to a one-way ANOVA to detect whether the among-individual variance was greater than the within-individual (repeated) variance [28]. The repeatability (R) value scales between 0 and 1. An R value of 0 would represent a sample in which all variance is found within individuals, whilst an R value of 1 would indicate all the variance in a sample to be between individuals.

Outline data collection and analysis

The left ilium was preferentially selected, though in 24 cases where this bone was poorly preserved or absent, the right ilium was used. Three individuals from the London sample were excluded from analysis of the greater sciatic notch because the ilium had begun to fuse with the ischium and pubis, thus making difficult the precise placement of landmarks required to record notch shape. All samples were photographed in two dimensions using a digital camera, following a consistent orthogonal orientation scheme. To record the notch and auricular surface shapes, the ilium was laid on a flat surface each time, aligning the base of the bone with the horizontal plane. For the iliac crest criteria, the ilium was oriented such that the crest outline was horizontal and, at maximal height, perpendicular to the photographic surface (see [23]; Figs. 1 and 2).

Landmark data were collected for six traits of the ilium, as defined by Wilson et al. [23]. All landmarks were collected using TPS dig [29]. A resample script was written using R [30] to generate equally spaced semi-landmarks to characterise a set of corresponding outlines from preliminary sample files (script available from LABW, upon request). Cartesian *x-y* coordinates were converted into the phi (ϕ) form of the Zahn & Roskies [31] shape function, required for eigenshape analysis. Because the points are equally spaced, they can be represented completely by the vector of tangent angles produced as one circumscribes the outline. The tangent angles contain only geometric information about shape because non-shape differences in location, orientation and geometric scale are either removed by explicit standardization, or are not relevant to the tangent-angle descriptor. The covariances between shape functions are used as a basis for a

singular value decomposition resulting in set of vectors (eigenshapes) that express variance-maximized composite shape variation trends. Eigenshape analysis was performed using FORTRAN routines written by N. MacLeod [32].

The eigenscores outputted from eigenshape analysis were used to perform discriminant function analyses for both samples, and for a combined sample from London and Lisbon to assess classification accuracy for each criterion. To test the cross validation of the morphometric techniques initially described by Wilson et al. [23] and used herein, discriminant functions derived from the London sample were used to classify individuals from the Lisbon sample, and visa-versa. Additionally, to explore the relation between age and shape change for each criterion, the Lisbon collection was subdivided into four age groups (years): 0.00 – 1.99, 2.00 – 6.99, 7.00 – 10.99, and 11.00 – 14.99. For each age group, eigenshape analysis was performed for each trait, as above, and classification accuracies were compared through ontogeny. We applied Bayes' theorem [33] of conditional probability to compute the chance of an individual being male, given a discriminant test that indicates male, or the chance of an individual being female, given a discriminant test that indicates female [34]. We use the true prevalence for each sex in a population (0.5), rather than the sample prevalence, because this provides a more accurate representation of the probability of an unknown being correctly assigned in general forensic casework [34-35]. The posterior odds are computed to be equal to the product of the prior odds of correct identification (sample prevalence) multiplied by the likelihood ratio. For osteological data, the likelihood ratio is calculated using the following formula [35]:

$$\text{Likelihood ratio} = P(\text{“}M\text{”} \mid M) \,/\, P(\text{“}M\text{”} \mid M)*P(M) + P(\text{“}M\text{”} \mid F)*P(F)$$

Whereby "*M*" denotes the probability of assessing male sex if an individual is male (*M*). *P*(*M*) and *P*(*F*) denote the probabilites of getting a male or female, respectively. Since there are only two sexes, the likelihood ratio falls between the interval of 0 and 2. The latter, maximal, value reflects the instance whereby there are no misclassifications (i.e. [*P*("*M*" | *M*) = 1 and *P*("*M*" | *F*) = 0]) and hence the greater the likelihood ratio the lower the misclassification probability (see supplementary data Tables S7.1 – S7.4).

Because eigenshape analysis derives a set of shape functions from those produced by analysis of the original observations, the resulting orthogonal axes define a shape space in which geometric relationships among the original shape functions can be represented by computing covariances between each original

Criterion	% correctly identified (% chance of correct identification)								
	Full sample			Male			Female		
	London	Lisbon	Combined	London	Lisbon	Combined	London	Lisbon	Combined
Auricular surface morphology	67.4	62.2	65.2	100.0 (53.3)	87.5 (88.0)	88.3 (55.3)	12.5 (100)	26.5 (68.4)	28.6 (70.7)
Greater sciatic notch	78.1	89.0	84.1	100.0 (59.1)	91.7 (86.8)	88.3 (80.0)	30.8 (100)	85.3 (91.3)	77.6 (86.7)
Iliac crest (complete)	93.6	82.2	85.6	95.5 (89.6)	86.4 (77.4)	90.9 (79.1)	88.9 (95.8)	75.9 (84.0)	76.3 (89.4)
Iliac crest (upper plane)	87.1	67.1	70.2	95.5 (74.2)	48.3 (71.8)	87.9 (59.5)	66.7 (93.1)	79.5 (60.6)	39.5 (76.9)
Iliac crest (lower plane)	87.1	80.8	74.0	90.9 (81.3)	90.9 (72.8)	89.4 (62.9)	77.8 (90.5)	65.5 (88.0)	47.5 (77.0)

Table 7.2: Identification success for each criterion for the Lisbon and London samples and the combined sample. London: N = 44; males =29, females =15. Lisbon: N = 82; males = 48, females = 34. Combined: N = 126; males = 77, females = 49. Chance of correct identification noted in parentheses. Calculations based upon equal priors of 0.5 using Bayes' theorem. See text for details.

shape function and each latent eigenshape function [17]. Hence it is possible to produce an outline model for any point in eigenshape space, and for any subset of outlines (meanshape). Thus rather than coordinate points on a graph, patterns of shape variation can be visualized in their true form – the outline originally recorded. To visualize differences between male and female shape we generated meanshape models for the greater sciatic notch criterion for both samples, since this criterion had previously been shown to be the most sexually dimorphic of those studied here [23].

Angle data collection and analysis

The angle of the greater sciatic notch was measured for each individual using the dot product, calculated from three landmark points, following Wilson et al. [23]. The angle measurement for each individual was based upon the geometric mean of three replicates for each landmark point. Angle data were analysed using circular scale methods (see [36]): for each of the four age groups defined above and for the entire sample, mean angle measurements were calculated for males and females and Watson's U^2 test, a two sample non-parametric test, was used to test the null hypothesis that male notch angles do not differ significantly from female notch angles for a given sample. The relation between angle measurement and age was determined for males and females from each sample using ANCOVAs.

RESULTS

Quantification of inter– and intra-observer error

Intra-observer error was lower than inter-observer error for all homologous landmark replications (Appendix 7.1). Observers 1 and 2 both had greatest difficulty identifying landmark D for the auricular surface. This point had a high inter-observer error value of 4.2% (Appendix 7.1). Similarly, observers experienced some difficulties capturing the position of landmark B, the maxima of curvature of the greater sciatic notch, which had an inter-observer error of 3.7%. Landmarks 1 and 2 of the iliac crest criteria were most accurately recaptured with inter and intra-observer error measuring not more than 2.2%. The error results for the outlines indicate that repeatability for the auricular surface suffers most from inter-observer error for the first two shape variables (ES-1, ES-2; Appendix 7.2). Repeatability (R) of the axes accounting for the most variance (ES-1) ranged from 0.93 to 0.97, when discounting the auricular surface. Inter-observer concordance was typically highest for the first two axes (ES-1 and ES-2) with R values differing by not more than 0.02 between observers, hence indicating inter-observer differences do not destabilise these axes. Axes contributing to

smaller portions of the shape variance had lower R values and inter-observer error was also higher for these axes, with a maximum difference of 0.12 between observers for outlines of the auricular surface morphology (ES-3; Appendix 7.2). Such a trend is expected because eigen analysis will tend to recover true structure from the earlier axes, leaving the later ones containing larger portions of error. The lower repeatability values for ES-3 and ES-4 indicate the robustness of these axes is considerably reduced and thus interpretations based on axes representing small portions of variance (<3%) should be evaluated carefully.

Classification success

Identification success across all criteria ranged from 62.2-89.0% for the Lisbon sample and 67.4-93.6% for individuals from the London collection (Table 7.2). Lisbon individuals were most successfully identified using the greater sciatic notch criterion (89.0%, Table 7.2, Fig. 7.1), whilst shape differences in the iliac crest (93.6%, Table 7.2) resulted in the largest number of accurate identifications in the London sample. Shape of the auricular surface was the most concordant between the sexes, and thus the least successful criterion for discriminating individuals from both samples (62.2-67.4%, Table 7.2). Across all the criteria examined, shape divergence, and thus discriminatory capacity, was marginally greater between the sexes for the London sample (average 82.7%; Lisbon, average 76.3%).

Table 7.3: Cross validation of discriminant functions using learning samples.

Criterion	% correctly identified (% chance of correct identification)			
	Learning sample - London		Learning sample - Lisbon	
	Male	Female	Male	Female
Auricular surface morphology	58.3 (50.0)	50.0 (69.2)	48.3 (45.0)	60.0 (53.7)
Greater sciatic notch	50.0 (50.0)	50.0 (50.0)	54.0 (48.0)	54.0 (48.0)
Iliac crest (complete)	68.2 (49.7)	27.6 (47.6)	63.6 (74.4)	77.8 (68.4)
Iliac crest (upper plane)	72.7 (54.3)	41.4 (60.4)	59.1 (42.0)	66.7 (62.0)
Iliac crest (lower plane)	59.1 (55.1)	51.7 (56.1)	45.5 (58.9)	66.7 (55.1)

For both samples, a greater percentage of males (average 88.7%) compared to females (average 60.9%) were correctly identified. Lisbon males were less well classified (average 81.0%) than London males (average 96.4) whereas classification of Lisbon females (average 66.5%) was better than that of females from London (average 55.3%). Bayesian probabilities reveal that the chance of correct identification for males (average 75.4%) is lower than for females (average 87.2%) reflecting the reduced specificity of male classification, namely an increased number of false positives relative to false negatives. Chances of correctly identifying a male or female were, on average, similar for individuals from the Lisbon sample (males: 79.4%, females: 78.5%) whereas London males had a lower chance of being correctly identified (71.5%) than females (95.9%). Differences between the sexes in the chance of correct identification were most marked for the auricular surface and the greater sciatic notch criteria (Table 7.2, supplementary material Table S7.1).

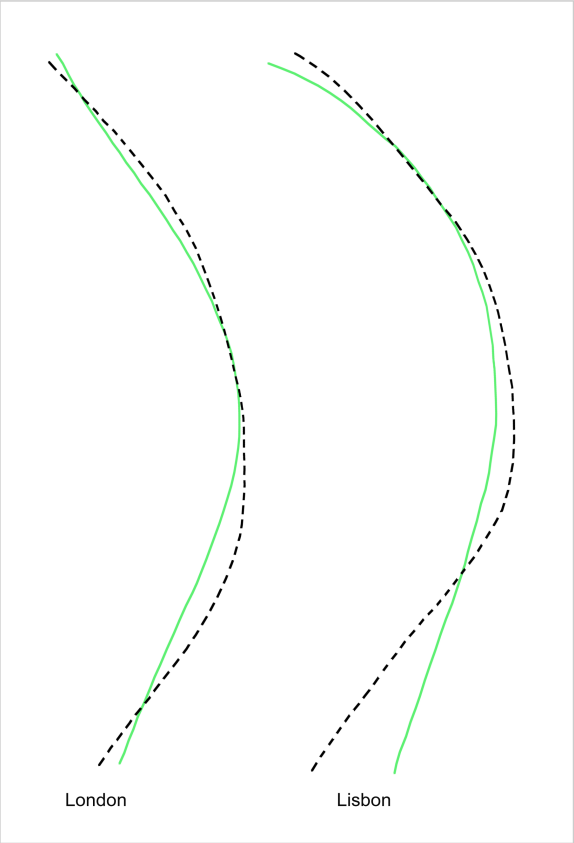

Figure 7.1: Meanshape models of the greater sciatic notch criterion calculated from eigenshape analysis of semilandmark data, detailing male shape (dashed line) and female shape (solid line).

Cross applicability of technique

When conducting a single discriminant analysis on individuals from both samples, shape differences between populations confound those exhibited between the sexes (Table 7.2, Table 7.3). Reduction in classification success for the combined sample, when compared with the analyses performed on each separate sample (see Table 7.2), ranged from 2.2% for the auricular surface to 16.9% for the upper plane of the iliac crest when using the full sample. Males in the combined sample were less well identified than London males by between 1.5% and 11.7%, whilst the identification of Lisbon males improved for three out of five criteria by between 0.8% (auricular surface) and 39.6% (upper plane). The successful identification of females improved for the auricular

surface in the combined sample when compared to both other samples (2.1-16.1% improvement), and also the greater sciatic notch exhibited improvement in the combined sample compared to the London sample (46.8% increase). For the remaining criteria, there was a reduction of between 7.7% and 40% in female classification. The average classification success for the combined sample is 75.8%; lower than that for either sample considered separately (Table 7.2).

Application of the discriminant functions generated from the Lisbon sample to the London sample, and visa-versa, results in a reduction in the number of correctly classified cases, irrespective of sex or sample, for the majority of criteria (Table 7.3). One exception is the increased success associated with London females for two of the criteria. Classification for the auricular surface morphology and greater sciatic notch criteria improves from poor (12.5% and 30.8%, respectively) to values one would expect by chance (60% and 54%, respectively). This may imply that sex differences for these two traits are obscured in the London sample by the heavily biased sex ratio in favour of males (2:1, see Table 7.1). When using discriminant functions generated from the Lisbon sample, London males are less well identified (average 54.1%) than London females (average 65.0%) whilst in reverse Lisbon males show marginal improvement in classification success (average 61.7%) over Lisbon females (average 44.1%) when using functions developed from the London sample (Table 7.3).

Classification success for age groups

The division of Lisbon individuals into age categories reveals differing levels of divergence in shape during ontogeny between males and females. Classification success fluctuates across the age categories most for the iliac crest and greater sciatic notch criteria among males (range 40.0% and 28.6%, respectively), whilst identification of females at different age ranges fluctuated for the greater sciatic notch, which, with the exception of the youngest group, provided the lowest level of correct identification for females. Similar, inconsistency in classification success for females was also achieved when using the upper plane of the iliac crest (range 40.0%). Across all criteria, shape differences are most distinct between the ages of 11.00 to 14.99 years, with 93.3% of males and 80.0% of females being correctly identified, on average (Table 7.4). For four out of five criteria, males exhibit a decreased level of identification success between the ages of 2.00 and 10.99 years, most markedly at the age of 7.00 and 10.99 whilst females exhibit a decrease in success from 2.00 to 6.99 years followed by a continual increase from 7.00 to 14.99 years (Table 7.4). The oldest age category (10.00-14.99 years) exhibits the most consistent

Table 7.4: Identification success for each criterion tested on divisions of the Lisbon sample. Sample size and distribution detailed in parentheses.

Age	Criterion	% correct identification (% chance of correct identification)	
		Male	Female
0 – 1.99 (N=28; M:17, F:11)	Auricular surface Likelihood	88.2 (61.5)	45.5 (78.9)
	Greater sciatic notch	88.2 (71.6)	59.1 (84.2)
	Iliac crest (complete)	100.0 (75.2)	66.7 (98.5)
	Iliac crest (upper plane)	77.8 (92.9)	93.8 (81.0)
	Iliac crest (lower plane)	87.5 (77.9)	66.7 (82.7)
2.00 – 6.99 (N=26; M:15, F:11)	Auricular surface	73.3 (57.0)	45.5 (76.3)
	Greater sciatic notch	93.3 (59.2)	36.4 (83.7)
	Iliac crest (complete)	90.0 (92.8)	92.9 (90.3)
	Iliac crest (upper plane)	85.7 (68.3)	60.0 (81.1)
	Iliac crest (lower plane)	100.0 (62.5)	80.0 (100.0)
7.00 – 10.99 (N=15; M:8, F:7)	Auricular surface	71.4 (71.7)	71.4 (71.7)
	Greater sciatic notch	71.4 (62.3)	57.1 (54.8)
	Iliac crest (complete)	60.0 (100.0)	100.0 (71.4)
	Iliac crest (upper plane)	100.0 (85.5)	83.3 (100.0)
	Iliac crest (lower plane)	80.0 (74.1)	83.3 (80.6)
11.00 – 14.99 (N=14; M:9, F:5)	Auricular surface	88.9 (69.5)	60.0 (84.5)
	Greater sciatic notch	100.0 (62.5)	40.0 (100)
	Iliac crest (complete)	88.9 (100.0)	100.0 (90.1)
	Iliac crest (upper plane)	100.0 (100.0)	100.0 (100.0)
	Iliac crest (lower plane)	88.9 (100.0)	100.0 (90.1)

levels of accuracy across traits for males (range 11.1%) but the reduced accuracy of the greater sciatic notch (40.0%) in females results in greater variability in this age category. Females aged 7.00 to 10.99 years were more consistently correctly identified.

Angle data

The angle of the greater sciatic notch is significantly narrower in males than in females (p <0.001) for both samples (Table 7.5). Notch angles measured between 94.1◦ and 133.6◦ for Lisbon males and between 97.4◦ and 142.0◦ for London males, implying that notch angles were both wider and more variable (44.6◦ compared to 39.5◦) in London males. For both samples, female angle measurements were concentrated within a narrower range than males: Lisbon females measured between 113.0◦ and 141.7◦ (range 28.7◦) and London females had on average wider notch angles of between 123.4◦ and 141.5◦ (range 18.1◦). Division of each sample into age groups reveals male notch angles to be significantly narrower than females at all four age ranges analysed, for both samples. London males exhibit a downward trend in mean notch angle, from 124.5◦ in the youngest individuals to 107.9◦ in the oldest, while Lisbon males display a similar trend (121.1◦ to 108.6◦; Table 7.5), though the narrowest angle is measured between the ages of 7.00 and 10.99 (106.97◦; Table 7.5). In contrast, females from both samples have mean angles which alter less markedly during ontogeny, especially difference in mean angle among London females is maximally 2.2◦, compared with 16.6◦ among males.

ANCOVA results indicate males from the Lisbon sample exhibit a trend toward a narrower greater sciatic notch through ontogeny (F 8.523, p 0.005), and a similar trend was also exhibited for London males though this was not significant (F 2.259, p 0.1). There was no relationship between notch angle and age in females from either sample.

DISCUSSION

A fundamental aspect to determining the sex of skeletal remains is the ability to apply a technique successfully developed on one population to another population, and achieve comparable levels of accuracy. Our results demonstrate that the methods of Wilson et al. [23] do not achieve levels of success concordant with those originally reported when tested on a Portuguese sample (see Table 7.3). The use of discriminant functions developed on the London sample for sex determination on the Lisbon sample, and visa-versa, does not result in levels of success greater than would be expected by chance in most cases (see Table 3). The percentage classification success was reduced by an average of between 2.2% to 16.9% when conducting a single discriminant

analysis on individuals from both samples compared to results obtained from separate analyses. Nevertheless, these shape based methods result in comparatively similar levels of success for each sample, confirming that these criteria do reliably document a degree of sexual dimorphism. Wilson et al. [23] reported between 64% and 96% accuracy for their original sample. Similar success levels are achieved for both the extended London sample (67.4-93.6%) and for the Lisbon sample (62.2-89.0%). The average classification success for the combined samples also falls within a comparable range (65.2-85.6%).

Several factors impede the success of cross application. These include, most basically, the difficulty that researchers experience when attempting to follow a described technique (inter-observer error), for example highlighted by Cardoso & Saunders [12] in relation to the work of Sutter [11]. This problem is inherent in the qualitative studies that have dominated the literature on sex determination of juvenile remains, reflecting the subjectivity of qualitative approaches and the initial, logical, transposition of qualitative techniques that are successful for adults (e.g. [37]), to juveniles. The advent and application of metric techniques has acted to subvert some of the errors linked to qualitative coding, particularly for those techniques that require the development of appropriate expertise for correct identification of traits [38], and has additionally enabled the appraisal of shape differences through the use of geometric morphometrics [8, 23]. Nonetheless, a more complex factor, namely differ-

Table 7.5: Greater sciatic notch angle measurements, generated by circular distribution analyses (Zar, 1999). Watson-Williams test statistic (U^2) values and associated probability values detail differences between mean angles for males and females within each age group, and the full sample.

Age	London			Lisbon		
	Mean angle (degrees)		U^2	Mean angle (degrees)		U^2
	Male	Female		Male	Female	
0 – 1.99	124.53	134.62	0.35*	121.10	131.75	0.79**
2.00 – 6.99	120.45	134.47	0.33*	113.57	125.39	0.47**
7.00 – 10.99	-	-	-	106.97	130.73	0.74**
11.00 – 14.99	107.90	132.42	0.33*	108.62	133.47	0.72**
Full sample	122.01	134.19	1.08**	114.33	129.73	2.56**

* $0.02 > p > 0.001$ ** $p < 0.001$

ences among populations, remains pertinent in influencing levels of replication success for metrical approaches (e.g. [13, 39, 40]), as the cross validation of discriminant functions reported here further demonstrates (Table 7.3).

Access to adequate nutrition, the availability of treatment or care, and the standard of living conditions can also influence skeletal growth and hence, the size and shape of skeletal elements. These factors commonly differ among populations, and may be exacerbated by cultural practices such as preferential treatment of male or female children [41]. Thus the degree and patterning of sexual dimorphism present in one population may differ from another; illustrated here when comparing the mean shape of the greater sciatic notch between the Lisbon and London samples used for this study (Fig. 7.1). Males belonging to the London sample have a shallower greater sciatic notch than Portuguese males, with the deepest portion located closer to the site of fusion with the ischium and pubis. Deepening of the male notch for the Lisbon sample is more pronounced and most exaggerated towards the centre (Fig. 7.1), a feature further exemplified by an average notch angle measurement of 114.33◦ for Lisbon males compared with 122.01◦ for London individuals (Table 7.5).

Although the discriminant functions generated here do not result in identification success better than chance when cross validated thus precluding the correct identification of sex in isolated cases, our results do indicate this geometric approach documents dimorphism in another sample. Individuals from the Lisbon sample are successfully identified at a level of 62.2-89.0% which is comparable to that of 64.0-96.0% reported by Wilson et al. [23] and the extended London sample here (67.4%-93.6%). This consistent level of success has not been reported for recent direct tests of Schutkowski's [10] methods for sex determination. Vlak et al. [13] reported 54.0-59.0% accuracy compared to 80.0-82.0% achieved by Schutkowski [10]. Further, the combined analyses using individuals from both samples result in an identification success of 65.2-85.6%, which falls within the success range first reported by Wilson et al. [23]. When comparing the analyses for either sample with the combined result, identification success was reduced by not more than 16.9% for the full sample and thus less than the reduction in classification reported by Vlak et al. [13] and further Cardoso & Saunders [12], whose test of Schutkowski's [10] arch criterion resulted in accuracies of 26.7-50.5% overall. Considering that the combined sample incorporates inter-population differences which may swamp more subtle shape differences between males and females in a given sample, it is encouraging that these results remain within the range of those for the individual samples. Similarly, when combining all

criteria, except the auricular surface morphology which had poor levels of accuracy (see Table 7.2), and using a majority outcome to determine the sex of an individual we find 89.2% of the London sample and 95.6% of the Lisbon sample can be correctly identified, indicating the combined strength of these traits as a useful set of criteria for documenting dimorphism in these samples.

The low levels of success associated with classifying females [6, 10, 14] have been attributed to differential growth among females and lack of female-trait expression [11, 39]. Consistent with previous work, the criteria tested here are less successful in identifying females and these differences are most marked for the London sample (Table 7.2) with particularly poor accuracy reported for the auricular surface and greater sciatic notch (12.5% and 30.8%, respectively, Table 7.2). Molleson et al. [42] previously noted the shortcomings of the London sample used here, especially the lack of females that may mask an accentuated bias of a technique to identify males in a sample. Whilst this is a fundamental concern, it is important to note the limited availability of identified juvenile material. Since the sex ratio of the Lisbon sample is less biased than that of the London sample, and females from the Lisbon sample were identified with a much higher level of success (85.3%) using the greater sciatic notch, it seems unlikely that this criterion is biased to identifying males in a given sample. Rather the reduced success may be due to a less marked difference between male and female notch shape in older children from London, such that females exhibit a shape that is more analogous to males. Hence shape ontogeny of dimorphism differs considerably between samples for the greater sciatic notch. The reduced success of the auricular surface for both London and Lisbon females (12.5% and 26.5%, Table 7.2) in comparison to that achieved previously (62.5%; [23]) suggests that the practical applicability of this criterion is questionable and, if at all useful, at least restricted to the age range previously documented by Wilson et al. [23] (6 months to 8 years).

Division of the Lisbon sample into age ranges reveals a broadly similar level of identification accuracy between the sexes when averaging success across all traits. There is an absolute, and continual, increase in success from birth to 14.99 years for both males and females with the exception of age group 7.00 to 10.99 in males and 2.00 and 6.99 in females: within each sex, identification success for these age groups is on average lower than for any other age range. Whilst it has been suggested that the concentration of testosterone in male foetuses reaches sufficient levels between 16 and 24 weeks to result in sexual dimorphism [2], and this may contribute to elevated levels of suc-

cess during the youngest age range, it appears here that the level of success is less marked during this period than the level achieved in the older age ranges. Nonetheless, the reduced accuracy between 2.00 and 6.99 years (females) and 7.00 to 10.99 years (males) partially reflects a suggestion that sexual dimorphism among diagnostic characteristics would be comparatively reduced later in development when these features may be masked by growth [6]. The oldest age range comprises subadults who are closer to attainment of their size and adult morphology therefore it is not surprising that success levels are comparatively reduced at earlier stages in development, when sex specific traits have not manifested. The degree of dimorphism in the infant pelvis has been shown to be slight compared with that found in adults, for instance Hager [43] reported a 22% difference between adult male and female greater sciatic notch depth to width ratios, whilst Fazekas & Kósa [44] report a 4% difference for the same measurement in juveniles. Despite this, intrinsic factors that influence sexual dimorphism such as differences in the rate and duration of male and female growth [45], are in some instances difficult to tease apart from extrinsic factors, such as disease or malnutrition, with the absence of complete information about the life of an individual or past population. Therefore further exploration and quantification of the shape ontogeny of dimorphism in the ilium, particularly in relation to extrinsic factors, represents a useful avenue to extend the practical potential of these results, and may lead to a clearer understanding of the wider applicability of the criteria tested here.

In light of the results presented here, we propose an update of the technique Wilson et al. [23] developed on a London sample of limited size. Based upon the success of the greater sciatic notch criterion in the Lisbon sample (89.0%, Table 7.2), we suggest that this criterion should still be considered useful for sex determination, but it should be noted that the success of female identification in the extended London sample is poor and much lower than for the Lisbon sample (30.8% compared to 85.3%, Table 7.2). This implied that the ontogeny of sexual dimorphism in the greater sciatic notch may vary considerably between populations. The consistent, and large, reduction in reliable classification of females when using the auricular surface morphology (12.5-26.5%, Table 7.2) and the inter-observer error associated with identifying landmarks leads us to propose that this criterion may be of limited wider applicability and at least caution should be taken when using this criterion to sex the remains of children under the age of 8 years. The curvature of the iliac crest (complete, upper, and lower), based upon the original qualitative method of Schutkowski [10], is more

successful in the extended London sample used in this study (87.1-93.6%, Table 7.2) than in the original sample (64.0-72.0%, [19]) , and similarly, though less pronounced, in the Lisbon sample (67.1%-82.2%, Table 7.2). Female identification accuracy also remains overall high for these criteria, especially in the oldest children (83.3-100%, for 7.00-14.99 years) .This suggests that sexual dimorphism in iliac curvature develops during later ontogeny and that the reduced accuracy of the original study [23] reflected the younger age distribution of juveniles in that study. The significant difference between male and female greater sciatic notch angles for both samples and across age groups considered here (p <0.01, Table 7.5) indicates, similar to previous tests [11, 13], that this criterion documents dimorphism within a population, though in the latter study a significant trend with age was reported such that only juveniles from 11 to 15 years expressed differences leading to the attainment of accuracy levels comparable to Schutkowski [10]. Similar to Vlak et al. [13] we note an ontogenetic trend to a narrower greater sciatic notch angle for males in the Lisbon sample, but our results also reveal significant differences between males and females at earlier stages in ontogeny (Table 7.5). For each of the four age groups analysed, differences between mean angle among males and females were significant, suggesting differences in notch morphology between the sexes are at least present from birth, and continue to remain distinct during later ontogeny. Nonetheless, the overlapping distribution of angle measurements between males and females from either the London or Lisbon samples act to preclude the wider application of this criterion to determining the sex of individuals from other populations.

CONCLUSION

The shape based approach to sex determination of juvenile ilia developed by Wilson et al. [23] on a identified juvenile sample from London was used to produce a new set of discriminant functions for an identified sample of juveniles from Lisbon. The high level of accurate identification achieved for the Lisbon sample demonstrates the wider applicability of this approach. This study also highlights the confounding effect of population differences on sex determination of juvenile ilia since discriminant functions developed on each of the samples resulted in a substantial reduction in the proportion of successful identifications when applied to the other series. Disciminant functions developed on the combined series also resulted in a lower success rate. The accuracy of sex determination for isolated individuals using these shape based methods is therefore reduced if population affinity is unknown. Nevertheless, 89.2% of the London sample and 95.6% of the Lisbon sample were correctly

identified using the majority outcome of five criteria based on the total sample to determine the sex of an individual. Based on the results of this broader study we recommend disuse of the auricular surface morphology criterion for sex determination of juvenile ilia. The differing ontogeny of dimorphism among populations may lead to differing degrees of success for some criteria, and we recommend study directed to documenting the ontogeny of dimorphism in the ilium, which may provide clarity for assessing the wider applicability of pelvic criteria for sex determination in juveniles.

ACKNOWLEDGEMENTS

Norm MacLeod is especially thanked for the impetus and encouragement to approach outline-based methods. We are also grateful to Morana Mihaljević for her participation in this project. An anonymous reviewer is thanked for helpful comments, which improved an earlier version of this paper. This work was supported by a Forschungskredit of the Universität Zürich (Nr. 3771) granted to LABW. HFVC was partially funded by Fundação para a Ciência e Tecnologia (Grant#SFRH/BPD/22142/2005) and the Synthesys Project, financed by European Community Research Infrastructure Action under the FP6 Programme (GB-TAF-4686).

REFERENCES

[1] L. Scheuer, S. Black, Developmental Juvenile Osteology, London Academic Press, London, 2000.

[2] S. R. Saunders, Juvenile Skeletons and Growth-Related Studies, in: M. A. Katzenberg, S. R. Saunders (Eds.), Biological Anthropology of the Human Skeleton, Wiley-Liss, Hoboken, NJ, 2008, pp. 117-147.

[3] H. Fehling, Die Form des Beckens beim Fötus und Neugeborenen und ihre Bezierhung zu der beim Erwaschsenen, *Arch. Gynäk.* 10 (1876) 1-80.

[4] A. Thompson, The sexual differences of the foetal pelvis, *J. Anat. Physiol.* 33 (1899) 359-380.

[5] B. J. Boucher, Sex differences in the foetal sciatic notch, *J. Forens. Med.* 2 (1955) 51-54.

[6] D. S. Weaver, Sex differences in the ilia of a known sex and age sample of fetal and infant skeletons, *Am. J. Phys. Anthropol.* 52(2) (1980) 191-195.

[7] D. R. Hunt, Sex determination in the subadult ilia: an indirect test of Weavers non-metric sexing method, *J. Forensic. Sci.* 35 (1990) 881-885.

[8] S. M. C. Holcomb, L. W. Konigsberg, Statistical study of sexual dimorphism in the human fetal sciatic notch, *Am. J. Phys. Anthropol.* 97 (1995) 113-125.

[9] H. Schutkowski, Geschlechtsdifferente Merkmale an kindlichen Skeletten, Kentnisstand und diagnostische Beduetung, *Zeitschrift für Morphologie und Anthropologie* 76 (1986) 149-168.

[10] H. Schutkowski, Sex determination of infant and juvenile skeletons: I. Morphognostic features, *Am. J. Phys. Anthropol.* 90 (1993) 199-205.

[11] R. C. Sutter, Nonmetric subadult skeletal sexing traits: I. A blind test of the accuracy of eight previously proposed methods using prehistoric known sex mummies from Northern Chile, *J. Forensic. Sci.* 48(5) (2003) 1-9.

[12] H. F. V. Cardoso, S. R. Saunders, Two arch criteria of the ilium for sex determination of immature skeletal remains: A test of their accuracy and an assessment of intra- and inter-observer error, *Forensic Sci. Int.* 178 (2008) 24-29.

[13] D. Vlak, M. Roksandic, M. A. Schillaci, Greater sciatic notch as a sex indicator in juveniles, *Am. J. Phys. Anthropol.* 137(3) (2008) 309-315.

[14] S. R. Loth, M. B. Henneberg, Sexually dimorphic mandibular morphology in the first few years of life, *Am. J. Phys. Anthropol.* 115 (2001) 179-186.

[15] L. B. Scheuer, Brief communication: a blind test of mandibular morphology for sexing mandibles in the first few years of life, *Am. J. Phys. Anthropol.* 119 (2002) 189-191.

[16] D. M. Mittler, S. G. Sheridan, Sex determination in subadults using auricular surface morphology: a forensic science perspective, *J. Forensic Sci.* 37(4) (1992) 1068-1075.

[17] G. P. Lohmann, P. N. Schweitzer, On eigenshape analysis, in: F. J. Rohlf, F. L. Bookstein (Eds.) Proceedings of the Michigan morphometrics workshop, The University of Michigan Museum of Zoology, Special Publication No. 2, Ann Arbour, Michigan, 1990, pp.145-166.

[18] N. MacLeod, Generalizing and extending the eigenshape method of shape space visualization and analysis, *Paleobiology* 25 (1999) 107-138.

[19] F. L. Bookstein, Landmark methods for forms without landmarks: localizing group differences in outline shape, *Med. Image Anal.* 1 (1997) 225-243.

[20] F. P. Kuhl, C. R. Giardina, Elliptic Fourier features of a closed contour, *Comp. Graph. Imag. Proc.* 18 (1982) 236-258.

[21] M. L. Zelditch, W. L. Fink, D. L. Swiderski, Morphometrics, homology and phylogenetics: quantified characters as synapomorphies, *Syst. Biol.* 44 (1995) 179-189.

[22] A. M. Lawing, P. D. Polly, Geometric morphometrics: recent applications to

the study of evolution and development, *J. Zool.* 280 (2009) 1-7.

[23] L. A. Wilson, N. MacLeod, L. T. Humphrey, Morphometric criteria for sexing juvenile human skeletons using the ilium, *J. Forensic Sci.* 53 (2008) 269-278.

[24] S. I. Perez, V. Bernal, P. N. Gonzalez, Differences between sliding semi-landmarks in geometric morphometrics, with an application to human craniofacial and dental variation, *J. Anat.* 208 (2006) 769-784.

[25] J. L. Scheuer, S. M. Black, The St. Bride's documented skeletal collection, University of Glasgow, 1995.

[26] H. F. V. Cardoso, Brief communication: The collection of identified human skeletons housed at the Bocage Museum (National Museum of Natural History), Lisbon, Portugal, *Am. J. Phys. Anthropol.* 129(2) (2006) 173-176.

[27] N. von Cramon-Taubadel, B. C. Frazier, M. M. Lahr, The problem of assessing landmark error in geometric morphometrics: theory, methods, and modifications, *Am. J. Phys. Anthropol.* 134 (2007) 24-35.

[28] G. Arnqvist, T. Martensson, Measurement error in geometric morphometrics: empirical strategies to assess and reduce its impact on measures of shape, *Acta Zoologica Academiae Scentiarum Hungarica* 44 (1998) 73-96.

[29] F. J. Rohlf, tpsDig, digitize landmarks and outlines, Version 2.0, Department of Ecology and Evolution, State University of New York at Stony Brook, New York, 2004.

[30] R Development Core Team, R: A Language and Environment for Statistical Computing, R Foundation for Statistical Computing, Vienna, Austria, 2008.

[31] C. T. Zahn, R. Z. Roskies, Fourier shape descriptors for closed plane curves, *IEEE Trans. Comput.* 21 (1972) 269-281.

[32] N. MacLeod, Eigenshape 2.1, Natural History Museum, London, U. K.

[33] T. Bayes, An essay towards solving a problem in the doctrine of chances. *Biometrika* 45 (1958) 296-315.

[34] L. Klepinger, E. Giles, Clarification or confusion: statistical interpretation in forensic anthropology, in: K. J. Reichs (Ed.), Forensic Osteology: Advance in the Identification of Human Remains, Charles C. Thomas, Springfield, IL, 1998, pp. 435-439.

[35] D. W. Steadman, B. J. Adams, L. W. Konigsberg, Statistical basis for positive identification in forensic anthropology, *Am. J. Phys. Anthropol.* 131 (2006) 15-26.

[36] J. H. Zar, Biostatistical Analysis 4th Edition, Prentice Hall, Upper Saddle River, New Jersey, 1999, pp. 310–326.

[37] T. W. Phenice, A newly developed visual method of sexing the os pubis, *Am. J. Phys. Anthropol.* 30 (1969) 297-302.

[38] J. Bruzek, A method for visual determination of sex, using the human hip bone, *Am. J. Phys. Anthropol.* 117 (2002) 157-168.

[39] T. Rogers, S. Saunders, Accuracy of sex determination using morphological traits of the human pelvis, *J. Forensic Med.* 39 (1994) 1047-1056.

[40] H. F. V. Cardoso, Sample-specific (universal) metric approaches for determining the sex of immature human skeletal remains using permanent tooth dimensions, *J. Archaeol. Sci.* 35 (2008) 158-168.

[41] S. Stinson, Sex differences in environmental sensitivity during growth and development, *Yearb. Phys. Anthropol.* 28 (1985) 123-147.

[42] T. Molleson, K. Cruse, S. Mays, Some sexually dimorphic features of the human juvenile skull and their value in sex determination in immature skeletal remains, *J. Archaeol. Sci.* 25 (1998) 719-728.

[43] L. Hager, Sex differences in the sciatic notch of great apes and modern humans, *Am. J. Phys. Anthropol.* 99 (1996) 287-300.

[44] I. G. Fazekas, F. Kósa, Forensic Foetal Osteology, Academiai Kiado, Budapest, 1978.

[45] L. T. Humphrey, Patterns of growth in the modern human skeleton, *Am. J. Phys. Anthropol.* 105 (1998) 57-72.

SUPPLEMENTARY MATERIAL

Appendix 7.1

Appendix 7.2

Tables S7.1—S7.4

R code for outline interpolation

Appendix 7.1: Percentage residual standard deviations of individual landmarks used for angle measurement (dot product) and to constrain outlines.

Criterion		Landmark acquisition		
		observer 1	observer 2	inter-observer
Auricular surface morphology	LM1 (A)	2.362	3.254	3.662
	LM2 (D)	3.814	3.362	4.181
Greater sciatic notch	LM1 (A)	2.554	2.112	2.771
	LM2 (C)	1.987	2.741	3.024
Iliac crest	LM1	1.653	1.874	1.997
	LM2	1.998	2.039	2.200
Greater sciatic notch angle	LM1 (A)	2.033	2.516	2.663
	LM2 (B)	2.881	3.642	3.718
	LM3 (C)	1.443	2.326	2.441

Appendix 7.2: Assessment of shape variable repeatability (R) for variables explaining up to 95% of the variation in shape for each criterion. R_1 and R_2 are calculated from repeated measures taken from separate images of the same specimen by two (numbered) different observers.

Criterion	% variance	% cumulative variance	R_1	R_2
Auricular surface morphology				
ES-1	45.3	45.3	0.93	0.90
ES-2	42.7	89.0	0.92	0.83
ES-3	11.9	99.9	0.84	0.72
Greater sciatic notch				
ES-1	79.2	79.2	0.94	0.96
ES-2	12.6	90.8	0.88	0.90
ES-3	2.2	93.0	0.87	0.86
ES-4	1.8	95.8	0.81	0.77
Iliac crest (complete)				
ES-1	86.6	86.6	0.97	0.96
ES-2	7.8	94.4	0.92	0.92
ES-3	1.5	95.9	0.83	0.79
Iliac crest (upper plane)				
ES-1	54.7	54.7	0.93	0.94
ES-2	34.8	89.5	0.84	0.82
ES-3	6.5	96.0	0.77	0.69
Iliac crest (lower plane)				
ES-1	67.0	67.0	0.96	0.96
ES-2	16.8	83.8	0.91	0.90
ES-3	10.0	93.8	0.83	0.89
ES-4	2.9	96.7	0.71	0.76

Table S7.1: Bayesian inference statistics for identification success values reported in Table 7.2.

Criterion			Male		Female	
			London	Lisbon	London	Lisbon
Auricular surface morphology						
		likelihood	1.06	1.09	2.00	1.52
		posterior	0.81	0.64	0.47	0.63
		prior	0.76	0.59	0.24	0.41
Greater sciatic notch						
		likelihood	1.18	1.68	2.00	1.82
		posterior	0.81	0.98	0.63	0.76
		prior	0.68	0.59	0.32	0.41
Iliac crest (complete)						
		likelihood	1.79	1.56	1.90	1.70
		posterior	1.00	0.94	0.55	0.67
		prior	0.71	0.60	0.29	0.40
Iliac crest (upper plane)						
		likelihood	1.48	1.40	1.87	1.21
		posterior	1.00	0.56	0.54	0.73
		prior	0.71	0.40	0.29	0.60
Iliac crest (lower plane)						
		likelihood	1.61	1.45	1.79	1.76
		posterior	1.00	0.87	0.52	0.70
		prior	0.71	0.60	0.29	0.40

Table S7.2: Bayesian inference statistics for identification of combined sample, reported in Table 7.2.

Criterion			Male	Female
Auricular surface morphology				
		likelihood	1.11	1.42
		posterior	0.68	0.55
		prior	0.61	0.39
Greater sciatic notch				
		likelihood	1.59	1.74
		posterior	0.97	0.68
		prior	0.61	0.39
Iliac crest (complete)				
		likelihood	1.59	1.79
		posterior	1.00	0.65
		prior	0.63	0.37
Iliac crest (upper plane)				
		likelihood	1.18	1.53
		posterior	0.75	0.56
		prior	0.63	0.37
Iliac crest (lower plane)				
		likelihood	1.26	1.63
		posterior	0.80	0.60
		prior	0.63	0.37

Table S7.3: Bayesian inference statistics for identification success values reported in Table 7.3.

			Learning sample - London		Learning sample - Lisbon	
Criterion			Male	Female	Male	Female
Auricular surface morphology						
		likelihood	1.08	1.09	1.09	1.07
		posterior	0.63	0.45	0.72	0.37
		prior	0.59	0.41	0.66	0.34
Greater sciatic notch						
		likelihood	1.00	1.00	1.09	1.09
		posterior	0.59	0.41	0.72	0.37
		prior	0.59	0.41	0.66	0.34
Iliac crest (complete)						
		likelihood	0.97	0.93	1.48	1.36
		posterior	0.59	0.37	1.00	0.40
		prior	0.60	0.40	0.71	0.29
Iliac crest (upper plane)						
		likelihood	1.11	1.21	1.28	1.24
		posterior	0.67	0.48	0.91	0.36
		prior	0.60	0.40	0.71	0.29
Iliac crest (lower plane)						
		likelihood	1.10	1.06	1.15	1.10
		posterior	0.66	0.42	0.82	0.32
		prior	0.60	0.40	0.71	0.29

Table S7.4: Bayesian inference statistics for identification success values reported in Table 7.4.

Age	Criterion			Male	Female
0 to 1.99	Auricular surface morphology		likelihood	1.24	1.59
			posterior	0.75	0.62
			prior	0.61	0.39
	Greater sciatic notch		likelihood	1.32	1.67
			posterior	0.80	0.66
			prior	0.61	0.39
	Iiliac crest (complete)		likelihood	1.50	2.00
			posterior	0.98	0.69
			prior	0.65	0.35
	Iliac crest (upper plane)		likelihood	1.85	1.60
			posterior	1.12	0.63
			prior	0.61	0.39
	Iliac crest (lower plane)		likelihood	1.45	1.68
			posterior	0.93	0.61
			prior	0.64	0.36
2.00 to 6.99	Auricular surface morphology		likelihood	1.15	1.26
			posterior	0.66	0.53
			prior	0.58	0.42
	Greater sciatic notch		likelihood	0.93	1.69
			posterior	0.54	0.72
			prior	0.58	0.42
	Iliac crest (complete)		likelihood	1.85	1.81
			posterior	1.08	0.75
			prior	0.58	0.42
	Iliac crest (upper plane)		likelihood	1.36	1.62
			posterior	0.80	0.67
			prior	0.58	0.42
	Iliac crest (lower plane)		likelihood	1.67	2.00
			posterior	0.97	0.83
			prior	0.58	0.42
7.00 to 10.99	Auricular surface morphology		likelihood	1.43	1.43
			posterior	0.76	0.67
			prior	0.53	0.47
	Greater sciatic notch		likelihood	1.25	1.33
			posterior	0.67	0.62
			prior	0.53	0.47
	Iliac crest (complete)		likelihood	2.00	1.43
			posterior	0.91	0.78
			prior	0.45	0.55
	Iliac crest (upper plane)		likelihood	1.71	2.00
			posterior	0.78	1.00
			prior	0.45	0.55
	Iliac crest (lower plane)		likelihood	1.66	1.61
			posterior	0.75	0.88
			prior	0.45	0.55

Table S7.4: continued

Age	Criterion				Male	Female
11.00 to 14.99	Auricular surface morphology			likelihood	1.38	1.69
				posterior	0.89	0.60
				prior	0.64	0.36
	Greater sciatic notch			likelihood	1.25	2.00
				posterior	0.80	0.71
				prior	0.64	0.36
	Iliac crest (complete)			likelihood	2.00	1.80
				posterior	1.38	0.55
				prior	0.69	0.31
	Iliac crest (upper plane)			likelihood	2.00	2.00
				posterior	1.00	0.71
				prior	0.64	0.36
	Iliac crest (lower plane)			likelihood	2.00	1.80
				posterior	1.38	0.55
				prior	0.69	0.31

R CODE FOR OUTLINE INTERPOLATION

N.B. written in R v. 2.7.1

```
library(ape)
library(paleoTS)
library(rimage)
read.jpeg(file.choose())
read.pnm(file.choose())

#generating an outline
outlinegenrt<-function(x, imagematrix)
{I<-imagematrix
x<-rev(x)
x[1]<-dim(I)[1]-x[1]
while (abs(I[x[1],x[2]]-I[x[1],(x[2]-1)])<0.1){x[2]<-x[2]-1}
a<-1
M<-matrix(c(0,-1,-1,-1,0,1,1,1,1,1,0,-1,-1,-1,0,1),
2,8,byrow=T)
M<-cbind(M[,8],M,M[,1])
X<-0; Y<-0;
x1<-x[1]; x2<-x[2]
SS<-NA; S<-6
while ((any(c(X[a],Y[a])!=c(x1,x2))| length(X)<3))
{if (abs(I[x[1]+M[1,S+1],x[2]+M[2,S+1]]-I[x[1],x[2]])<0.1)
{a<-a+1;X[a]<-x[1];Y[a]<-x[2];x<-x+M[,S+1]
SS[a]<-S+1; S<-(S+7)%%8}
else if (abs(I[x[1]+M[1,S+2],x[2]+M[2,S+2]]
-I[x[1],x[2]])<0.1)
{a<-a+1;X[a]<-x[1];Y[a]<-x[2];x<-x+M[,S+2]
SS[a]<-S+2; S<-(S+7)%%8}
else if (abs(I[x[1]+M[1,(S+3)],x[2]+M[2,(S+3)]]
-I[x[1],x[2]])<0.1)
{a<-a+1;X[a]<-x[1];Y[a]<-x[2];x<-x+M[,(S+3)]
SS[a]<-S+3; S<-(S+7)%%8}
else S<-(S+1)%%8}
list(X=(Y[-1]), Y=((dim(I)[1]-X))[-1])}

start<-locator(1)
Rc<-outlinegenrt(c(round(start$x),round(start$y)),y@grey), imagematrix(y, type=NULL,ncol=dim(y)
[1], nrow=dim(y)[2], noclipping=FALSE)
lines(Rc$X, Rc$Y, lwd=4)
arrows(0,Rc$Y[1],Rc$X[1],Rc$Y[1],length=0.1)
start<-locator(1)
Rc<-outlinegenrt(c(round(start$x),round(start$y)),z@grey)
lines(Rc$X, Rc$Y, lwd=4)
#with pnm image
```

```
z<- as(z, "pixmapGrey")
z@grey[which(z@grey>=0.9)]<-1
z@grey[which(z@grey<0.9)]<-0.7
par(mar=c(1,1,1,1))
plot(z)
trial = outlinegenrt(x=start, imagematrix = z)
layout(matrix(c(1,2), 1,2))
Rc32x<-(Rc$X[seq(1,length(Rc$X),length=33)])[-1]
Rc32y<-(Rc$Y[seq(1,length(Rc$Y),length=33)])[-1]
plot(Rc$X, Rc$Y, type="l", lwd=1.5, asp=1, axes=F, main = "curvilinear")
points(Rc32x, Rc32y)

#grey scale the image and then check the pixel threshold using pmn file in pixmap only
par(mar=c(1,3,2,1))
Y<-z1
layout(matrix(1:4, 2,2))
plot(z, main="Gray-scale image")
z1[which(Y>=0.1)]<-1
z1[which(Y<0.1)]<-0
plot(z, main="Bin image, threshold=0.1")
z1[which(Y>=0.3)]<-1
z1[which(Y<0.3)]<-0
plot(z, main="Bin image, threshold=0.3")
z1[which(Y>=0.9)]<-1
z1[which(Y<0.9)]<-0
plot(z, main="Bin image, threshold=0.9")
length(z1[which(Y<0.9)])

z1[which(Y>=2)]<-1
z1[which(Y<2)]<-0
plot(z, main="Bin image, threshold=2")

#TPS to R
SB49auric<-read.table("H:/SB49auric.txt", header=TRUE, sep="", na.strings="NA", dec=".",
strip.white=TRUE)
library(sp)
lineSB49=Line(SB49auric)
#step three
psuedoSB49=spsample(lineSB49,50,type="regular",offset=c(0,1))@coords    #50 can be substituted...
psuedoSB49
write.table(psuedoSB49,"clipboard",sep="\t",col.names=NA)
```

CURRICULUM VITAE

Laura Anne Balfour Wilson

Date of Birth: 9 June 1984, Preston (United Kingdom)
Nationality: British
Office address: Paläontologisches Institut und Museum, Karl Schmid-Strasse 4, CH-8006, Zürich, Switzerland
Current address: Brandschenkestrasse 163, CH-8002, Zürich, Switzerland
Phone: Handy: +41 (0)789209063/ Office: +41 (0)44 634 24 47
Email: laura.wilson@pim.uzh.ch/ laura.a.b.wilson@gmail.com
Personal webpage: http://www.pim.uzh.ch/de/Institut/Mitarbeitende/index.php?show=70

Education

Sept 2007 – Sept 2010	PhD Student, Paläontologisches Institut und Museum, Universität Zürich Thesis title: *'The evolution of morphological diversity in rodents: patterns of cranial ontogeny'*
Oct 2006 – Sept 2007	MRes DIC Biosystematics (Distinction), Imperial College London, NHM London
Sept 2002 – June 2005	BSc Palaeobiology (1st class honours), University College London
Sept 2000 – June 2002	Runshaw College, Leyland, Lancashire (UK) 5 A-Levels at grade A; Geology, Biology, Geography, English Literature and General Studies.
Sept 1995 – June 2000	Priory High School, Penwortham, Lancashire (UK) 10 GCSE's – A* (7 subjects), A (3 subjects)

Papers under review

7. **Wilson LAB**. A comparison of prenatal and postnatal ontogeny: cranial allometry in the African striped mouse *Rhabdomys pumilio*. *Journal of Mammalogy*

Papers in peer reviewed journals

6. **Wilson LAB**, Sánchez-Villagra MR. 2010. The evolution and phylogenetic signal of growth trajectories: the case of chelid turtles. *Journal of Experimental Zoology* In press
5. **Wilson LAB**, Cardoso HFV, Humphrey LT. 2010. On the reliability of a geometric morphometric approach to sex determination: a blind test of six criteria for the juvenile ilium. *Forensic Science International* In press
4. **Wilson LAB**, Sánchez-Villagra MR. 2010. Diversity trends and their ontogenetic basis: an exploration of allometric disparity in rodents. *Proceedings of the Royal Society of London, B* **227**: 1227-1234
3. **Wilson LAB**, Schradin C, Mitgutsch C, Galliari FC, Mess A, Sánchez-Villagra MR. 2010. Skele togenesis in the African Striped mouse (Rhabdomys pumilio) and a study of sequence heterochrony in rodent evolution. *Organisms Diversity and Evolution* **10**: 243-258
2. **Wilson LAB**, Sánchez-Villagra MR. 2009. Heterochrony and patterns of cranial suture closure

in hystricognath rodents. *Journal of Anatomy* **214**: 339–354

1. **Wilson LAB**, MacLeod N, Humphrey LT. 2008. Morphometric criteria for sexing juvenile human skeletons using the ilium. *Journal of Forensic Sciences* **53(2)**: 269–278.

Conference presentations (talks, posters, published abstracts)

Wilson LAB. Patterns of cranial ontogeny in a diverse clade of mammals (Rodentia). 84th Annual Meeting Deutsche Gesellschaft für Säugetierkunde, 12-16.09.2010 Berlin, Germany
Wilson LAB. The evolution of morphological diversity in rodents. 9th International Congress of Vertebrate Morphology (ICVM), 26-31.07.2010 Punte del Este, Uruguay
Wilson LAB, Sánchez-Villagra MR. Diversity trends and their ontogenetic basis: an exploration of allometric disparity in rodents. 69th Annual Meeting Society of Vertebrate Paleontology, 22-26.09.2009 Bristol, UK
Wilson LAB, Galliari FC, Schradin C, Sánchez-Villagra MR. Skeletogenesis in the African striped mouse *Rhabdomys pumilio*. 10th International Mammalogical Congress, 10-14.08.2009 Mendoza, Argentina
Wilson LAB, Sánchez-Villagra MR. Sequence heterochronies in cranial suture closure patterns: Hystricognath rodents. 101st Jahresversammlung der Deutschen Zoologischen Gesellschaft, 19-22.09.2008 Jena, Germany
Wilson LAB, Sánchez-Villagra MR. Sequence heterochronies in cranial growth. 82nd Annual Meeting Deutsche Gesellschaft für Säugetierkunde, 14-17.09.2008 Wien, Austria
Wilson LAB, Sánchez-Villagra MR. Heterochrony and the evolution of sutures in rodents. 2nd Evo Devo meeting, 29.07-01.08.2008 Ghent, Belgium

Invited talks

Wilson LAB. The role of heterochrony during postnatal growth in rodents. Museum and Institute of Zoology Polish Academy of Sciences, 17.10.2008 Warsaw, Poland
Wilson LAB. Cranial ontogeny in a diverse clade of mammals (hystricognath rodents). Naturhistoriska riksmuseet, 09.09.2008 Stockholm, Sweden

Grants

2010 Japanese Society for the Promotion of Science (JSPS) Postdoctoral grant (25,600CHF)
2010 Forschungskredit Postdoctoral grant (24,800CHF)
2009 Auslands Kurz Mentorate: travel grant to Argentina (2000CHF)
2009 VAUZ Antrag Tagungsfond: travel grant to Italy (550CHF)
2008 Synthesys visit to Warsaw (930CHF)
2008 Synthesys visit to Stockholm (1615CHF)
2008 Travel grant to attend Paleobiology Database Summer School (June – July) in California, USA (1355CHF)
2007 Forschungskredit (Nr. 3771) for two years (97,812CHF)
2006 NERC (Natural Environment Research Council) funding for research masters based at the Natural History Museum (10,900CHF)

Press

Uni Magazin; Evolutionär erfolgreiche Nager, February 2010
Tierwelt; Auch für Meerschweinchen und Mäuse gilt: Man ist, was man isst,15th January 2010
20 Minuten; Man ist, was man isst,8th January 2010
Tages Anzeiger; Formenreichtum durch Futtervorlieben,18th December 2009
UZH Mediadesk and uni-protokolle.de, 17th December 2010